SEISMIC DESIGN AND EVALUATION OF MULTISTORY BUILDINGS USING YIELD POINT SPECTRA

Mid-America Earthquake Center

prepared by:

Edgar F. Black
and
Mark Aschheim

Civil and Environmental Engineering
University of Illinois at Urbana-Champaign
Urbana, Ilinois

July, 2000

ABSTRACT

SEISMIC DESIGN AND EVALUATION OF MULTISTORY BUILDINGS
USING YIELD POINT SPECTRA

Constant ductility response spectra are presented for 15 recorded earthquakes ground motions using the Yield Point Spectra (YPS) representation. Yield Point Spectra are used for analysis and design of SDOF structures. The spectra were computed for bilinear and stiffness degrading load-deformation models, for displacement ductilities equal to 1, 2, 4 and 8.

A methodology for the performance-based seismic design of regular multistory buildings using Yield Point Spectra is described. The methodology is formulated to make use of current code approaches as much as possible while allowing the design engineer to limit the peak displacement response and, to some extent, the peak interstory drift to user-specified values. To achieve this objective, the design methodology makes use of an equivalent SDOF model of the building.

A method to estimate peak displacement response and interstory drift indices of multistory buildings using YPS and establish SDOF formulations is also presented. The method may be considered a new nonlinear static procedure (NSP). Interstory drift indices (IDIs) are estimated using deformed shapes of the building based on the first mode shape and combinations of the first and second mode shapes.

ACKNOWLEDGMENTS

This report was prepared as a doctoral dissertation by the first author in partial fulfillment of the requirements for the Ph.D. degree in Civil and Environmental Engineering at the University of Illinois, Urbana. The research was supervised by the second author.

This research was partially supported by the Mid-America Earthquake Center under National Science Foundation Grant EEC-9701785.

The authors would like to thank Professors William J. Hall, Douglas A. Foutch and Daniel P. Abrams for their helpful comments and suggestions.

Appreciation is expressed to the faculty and staff of the Department of Civil Engineering of University of Illinois ar Urbana-Champaign for their support.

Special gratitude is expressed to Professors Timothy D. Stark, Sharon Wood, and Neil M. Hawkins, as well as to the Department of Civil and Environmental Engineering of the University of Illinois for the support provided.

TABLE OF CONTENTS

LIST OF TABLES

LIST OF FIGURES

CHAPTER 1

INTRODUCTION

1.1 Statement of the Problem

For many years the primary objective of most earthquake structural design provisions, such as the Uniform Building Code (International Conference of Building Officials, 1997), has been to safeguard against major structural failures and loss of life. Others objectives such as maintaining function, limiting damage or providing for easy repair were not explicitly addressed in these provisions.

One major development in seismic design during the last 10 years has been increased emphasis worldwide in performance-based seismic design, as a result of damage and economic losses in the Loma Prieta (1989), Northridge (1994) and Hyogo-Ken Nambu (1995) earthquakes.

Recent provisions require, in addition to the traditional life safety objective, "to increase the expected performance of structures having a substantial public hazard due to occupancy or use as compared to ordinary structures, and to improve the capability of essential structures to function during and after the design earthquake" (FEMA-302/303, 1998).

The seismic performance of buildings is generally associated with structural and nonstructural damage due to ground motions. For example, in the FEMA-273 and the Vision 2000 (SEAOC-1995) documents, performance is expressed in terms of an anticipated limiting level of damage, termed a performance level, for a given intensity of ground motion (Hamburger, 1997).

The importance of drift control is revealed when it is accepted that interstory drift constitutes an acceptable measure of damage. Provisions such as FEMA-302/303 recognize that drift control is needed to restrict damage to partitions, shaft and stairs enclosures, glass, and other nonstructural elements.

However building codes still use strength as the main parameter and have placed the computation of forces as the centerpiece of earthquake-resistant design, relegating drift calculations to the end of the design process. No realistic quantification of the nonlinear

displacement response of the structure during the design earthquake is done, nor of the associated structural and nonstructural damage that is likely to occur (Lepage, 1997).

In this work a new representation of earthquake spectra is introduced, known as Yield Point Spectra (YPS). The construction of Yield Point Spectra and their application to analysis and design of SDOF systems is discussed. It is shown that YPS can be used to reliably determine combinations of lateral strength and stiffness that are effective to limit drift and displacement ductility demands to arbitrary values such as those required to achieve a desired performance. Yield Point Spectra can also be used to estimate the peak displacement and the displacement ductility demands of structures responding to a given earthquake.

The use of the equivalent Single Degree of Freedom (SDOF) analogy plays a central role in the procedures that are presented for using YPS in the design and approximate analysis of multistory buildings.

For design, YPS are used to obtain the minimum lateral strength required to limit peak roof displacement to arbitrary values for a design earthquake. Contrary to current design methods, the proposed design methodology uses an estimate of the yield displacement of the building rather than its fundamental period at the start of the design process. For analysis, YPS are used to establish the peak roof displacement of a building during response to a ground motion. Techniques to estimate interstory drift more accurately than conventional approaches are also discussed.

The design and analysis methodologies introduced here are applied only to four case study examples. However, it is expected that these methodologies may be generally used to design buildings that meet current prescribed limits for interstory drift, and to meet the performance limits that are currently being defined by the profession for use in future performance-based seismic design codes and guidelines.

1.2 Historical Perspective

One of the major and most challenging objectives in modern structural analysis has been to predict the response of structures (buildings) subjected to the action of earthquakes. Considerable effort has been made in the last 30 to 40 years to try to understand the main parameters influencing the response of structures under ground motions, and to understand

the main characteristics of the ground motion itself. Current recommendations and code provisions for seismic design are based largely on work done during the last several decades.

1.2.1 Evolution of Design Philosophies

1.2.1.1 Life Safety

The objective to design structures to respond in a predictable way under different types of earthquake excitation that the structure may experience during its life is not new. The 1967 commentary of the Structural Engineers Association of California (SEAOC) Blue Book introduced a general philosophy for the design of earthquake resistant buildings other than essential and hazardous facilities. This philosophy identifies three design objectives:

(1) Prevent nonstructural damage in minor earthquake ground shaking which may occur frequently during the service life of the structure;

(2) Prevent structural damage and minimize nonstructural damage during moderate earthquakes ground shaking which may occasionally occur; and

(3) Avoid collapse or serious damage during severe earthquake ground shaking which may rarely occur.

This earthquake-resistant design philosophy is also contained in the ATC 3-06 (1978) document; however, this document focuses on life safety in the event of a severe earthquake as "the paramount consideration in design of buildings." In practice, design for life safety has and continues to be the main focus of routine design

Given the relatively small amount of life lost in U.S. earthquakes, existing design procedures may be considered to be successful. However, the extent of damage to structures, the cost of repair, and economic consequences to the areas affected by the Loma Prieta (1989), Northridge (1994) and Hyogo-Ken Nambu (1995) earthquakes, have lead to a broadening of the design philosophy towards what is now known as Performance-Based Seismic Design.

1.2.1.2 Performance-Based Seismic Design

In this new philosophy, attention is focused on explicitly controlling the performance of a structure over varied intensities of ground motions. Although the concepts associated with performance-based seismic design are still in development, one criteria to control the performance of a structure is limiting its level of damage. The perspective adopted in this study is that damage in structures can be reduced by limiting peak roof displacement (as a mean to indirectly limit interstory drift) and system displacement ductility to specified values.

1.3 Objectives and Scope

1.3.1 Objectives

This study has three main objectives:

1) To explore the utility of a new representation of constant ductility response spectra, named Yield Point Spectra, for the analysis and design of single-degree-of-freedom systems.
2) To outline and validate a methodology for the seismic design of regular multistory buildings using Yield Point Spectra in conjunction with establish equivalent SDOF formulations.
3) To use Yield Point Spectra and established equivalent SDOF formulations to develop improved estimates of peak displacement and interstory drift indices of regular multistory buildings responding to earthquake ground motions.

The goodness of the YPS design and analysis methodologies is assessed with respect to the results obtained from nonlinear dynamic analyses and by using the simplified analysis methods known as the Displacement Coefficient Method and the Capacity Spectrum Method. Comparisons are made for four case study example frames consisting of two 4-story and two 12-story moment-resistant steel frames.

1.3.2 Scope and Limitations

The proposed Yield Point Spectra methods are intended for the seismic analysis and

design of regular low and medium-rise frame buildings. The displacement response of all structural elements is assumed to be dominated by flexural deformations and influenced by seismic motions in the plane of the frame. Effects of torsional behavior and vertical ground motions effects are not addressed.

The design methodology is restricted to obtain and distribute the strength (base shear) required for a building to limit its peak displacement response to a prescribed value. Established methods are relied upon for proportioning members sizes and strength; these methods are not cover in this study.

1.4 Organization

Chapter 2 introduces Yield Point Spectra (YPS) and describes their main characteristic, use, and potential applications. Yield Point Spectra for 15 ground motion records and two load-deformation models are shown. An example describing the use of YPS for the performance-based seismic design of a SDOF structure is included.

Chapter 3 presents a formulation that extends the use of Yield Point Spectra to the analysis and design of buildings. The formulation relies on conventional equivalent single-degree-of freedom models used to represent the response of multistory buildings.

Chapter 4 introduces a methodology for the design of regular multistory buildings. The methodology is intended to directly limit the roof displacement and maximum interstory drift index to user-selected values. The methodology relies on Yield Point Spectra to account for nonlinear behavior of the multistory system.

An analysis method to estimate the peak displacement of multistory systems using Yield Point Spectra is introduced in Chapter 5. The method is a new Nonlinear Static Procedure (NSP). Peak roof displacement estimates obtained with the proposed method and also with other procedures are shown and compared. The analysis method is also used to obtain interstory drift using one deformed shape and combinations of two deformed shapes. Finally, a special case in which the second mode causes significant yielding in one of the frames was identified and discussed.

The summary and conclusions are presented in Chapter 6 along with recommendations for future research.

CHAPTER 2

YIELD POINT SPECTRA REPRESENTING SDOF RESPONSE

2.1 Introduction

Traditional seismic response spectra plots the maximum response (displacement, velocity, acceleration or any other quantity of interest) to a specific ground motion as function of the system's natural period or frequency of vibration. Seismic response spectra can be classified as elastic and inelastic response spectra. Constant ductility response spectra (CDRS) belong to the inelastic response spectra class. CDRS plot a strength-related coefficient corresponding to a constant displacement ductility (μ) as a function of period or frequency.

The Yield Point Spectra (YPS) representation is a CDRS in which the strength-related coefficient is defined as the ratio of the yield strength of the system to its weight, denoted the yield strength coefficient (C_y) throughout this work. Contrary to other CDRS, in the YPS representation the constant ductility curves are formed by plotting the yield strength coefficient as a function of the system's yield displacement. Therefore, each point within one of the curves, denoted yield point, corresponds to the yield displacement and strength required by a SDOF oscillator to have the displacement ductility represented by the curve.

This chapter illustrates the main characteristics of YPS and their application to analysis and design of SDOF systems. Subsequent chapters develop procedures to use YPS for the analysis and design of multistory systems.

A set of YPS were computed for representing different earthquake motions and load-deformation models. These were generated using PCNSPEC (Boroschek, 1991), a modified version of NONSPEC (Mahin and Lin, 1983), and are presented at the end of this chapter in Figure 2.18 to Figure 2.20.

2.2 Description of Yield Point Spectra Representation

Yield Point Spectra are graphs plotting curves corresponding to constant displacement ductility demand for a specific excitation, such as the caused by an earthquake. They represent the response of a SDOF system in terms directly useful in the design,

evaluation, and rehabilitation of structures for seismic loading. These graphs are directly used for design and analysis of SDOF structures. For design, Yield Point Spectra may be used to determine combinations of strength and stiffness sufficient to limit drift and/or displacement ductility demands to prescribed values. For analysis, when the period and strength of a SDOF structure are known, YPS may be used to estimate the structure's displacement ductility demands and, therefore, its ultimate displacement. In general, these graphs help to understand the seismic demands imposed on SDOF systems.

Since Yield Point Spectra represent the response of SDOF oscillators, having a specific load-deformation curve and viscous damping ratio, to an individual earthquake, different earthquakes, load-deformation models (bilinear, stiffness degrading etc.), and/or damping ratios result in different YPS.

Figure 2.1 shows Yield Point Spectra for oscillators having a bilinear load-deformation curve, shown in Figure 2.2, subjected to the 1940 record at El Centro. Viscous damping was equal to 5% of critical damping and the post yield stiffness was 10% of the initial elastic stiffness.

Curves representing constant displacement ductility of 1 (elastic), 2, 4, and 8 are shown. Each point along any of the curves represents an oscillator having the yield displacement and strength required to respond with the indicated ductility. For Figure 2.1, each curve was generated for 45 initial periods, from 0.05 to 10.0 sec. In the format used on that figure, lines representing initial periods radiate from the origin. Initial period of 0.5, 1.0, 1.5, 2.0, and 3.0 seconds are explicitly identified on Figure 2.1. The range of periods, displacement ductilities, and the load-deformation model were chosen arbitrarily.

Yield Point Spectra are able to represent elastic and inelastic response of SDOF systems. Any system having a yield point (yield displacement and strength) that lies beyond the curve representing constant displacement ductility equal to one will respond elastically. On the other hand, if the yield point of the system lies below the curve of constant displacement ductility equal to one its response will be inelastic.

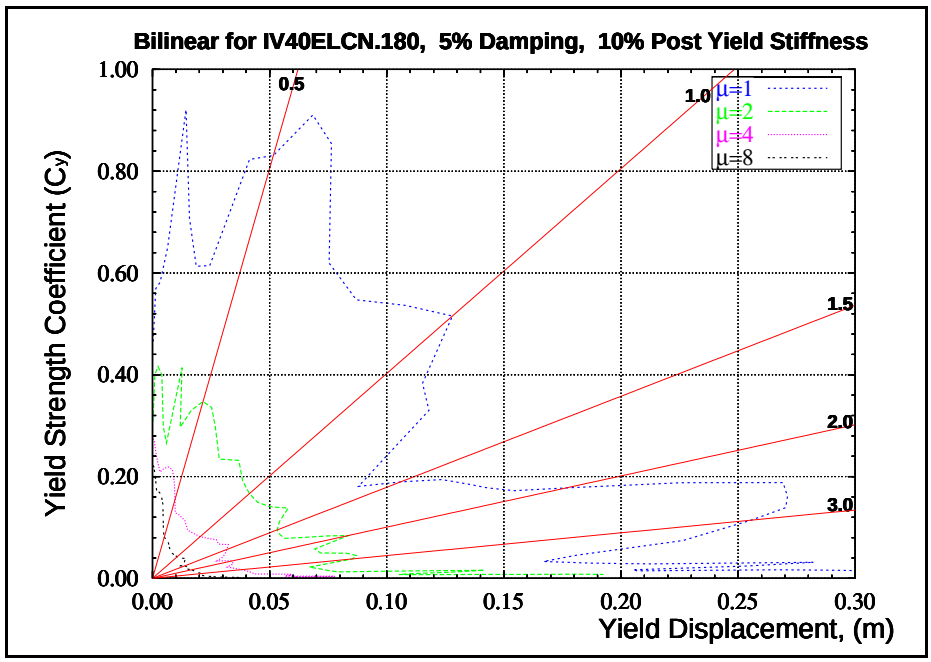

Figure 2.1 Yield Point Spectra

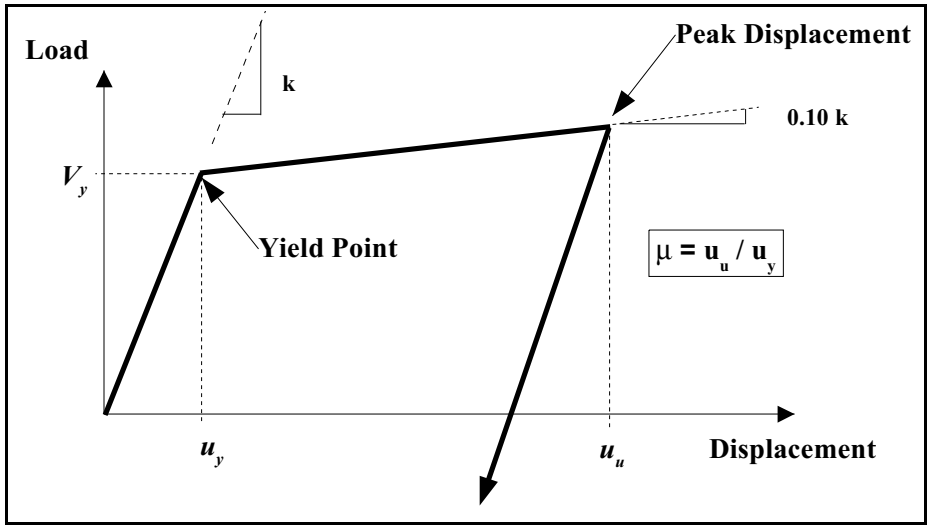

Figure 2.2 Bilinear Load-Deformation Model

It is important here to point out that although smaller values for the yield strength coefficient generally imply largest values for the displacement ductility, it is known the relationship between these two parameters is not monotonic. For those cases when more than one value of the yield strength coefficient results in the specified displacement ductility, the procedure implemented in PCNSPEC (the computer program used to generate the constant ductility curves) identifies and reports the largest yield strength coefficient, as illustrated schematically in Figure 2.3.

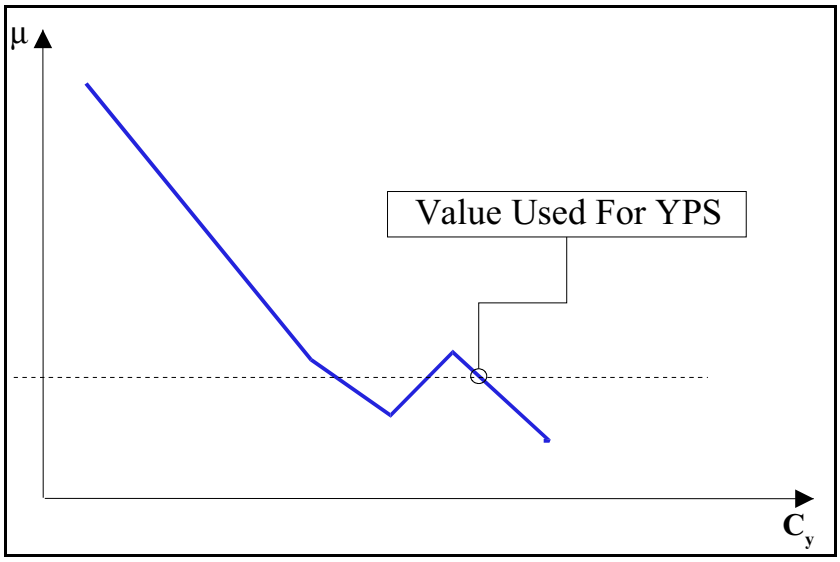

Figure 2.3 Relationship Between Yield Strength Coefficient (C_y) and Displacement Ductility (μ)

The principal axes used to plot YPS are similar to those used in the Capacity Spectrum Method (Freeman, 1978) in the sense that both use the abscissa to represent displacement and the ordinate to represent strength. Nevertheless, the information differs because in the Capacity Spectrum Method the displacement and the strength correspond to an ultimate state, while in the YPS displacement and strength correspond to yield.

Simple manipulations of fundamental relations provide some useful expressions for use with YPS. The yield strength coefficient (C_y), the yield strength (V_y) and the initial period of the oscillator are defined as:

$$V_y = C_y \cdot W = C_y \cdot m \cdot g \tag{2.1}$$

$$T = 2 \cdot \pi \cdot \sqrt{\frac{m}{k}} = 2 \cdot \pi \cdot \sqrt{\frac{m\,u_y}{V_y}} = 2 \cdot \pi \cdot \sqrt{\frac{u_y}{C_y \cdot g}} \tag{2.2}$$

$$C_y = \frac{4 \cdot \pi^2 \cdot u_y}{T^2 \cdot g} \tag{2.3}$$

where:

- C_y is the yield strength coefficient,
- W is the oscillator weight,
- m is the oscillator mass,
- V_y is the base shear strength,
- u_y is the yield displacement,
- k is the initial stiffness,
- T is the initial period, and
- g is the acceleration of gravity.

2.3 Application of Yield Point Spectra

Considerable economic losses resulting from structural damage in the Loma Prieta (1989), Northridge (1994), and Hyogo-Ken Nambu (1995) earthquakes have focused attention explicitly on design to control the performance of a structure over varied intensities of ground shaking, in what is now known as performance-based seismic design.

Under this design philosophy, it is necessary for engineers to be able to accurately estimate the peak displacement of structures responding to strong ground motions. Additionally, it would be very desirable to have tools and procedures to determinate the structural properties necessary to limit peak displacement response and/or displacement ductility demands of buildings to prescribed values.

Yield Point Spectra can be applied to perform both of these operations. For the first one, or analysis application, YPS are use to obtain accurate estimates of peak displacement response of SDOF systems. For the second one, or design application, YPS are used to determine the structural properties required to control peak displacement and displacement ductility demands to specified limits. The ability to perform both operations, analysis and design, make YPS particularly amenable to performance-based design.

2.3.1 Analysis Application: Estimation of Peak Displacement

Several procedures to estimate peak displacement have been promoted recently and are beginning to be used by the engineering community. Among the procedures, known as Nonlinear Static Procedures (NSPs) in the *NEHRP Guidelines for the Seismic Rehabilitation of Buildings* (FEMA-273/274; 1997), there are two methods for estimating peak displacement response under the action of seismic loads: the Displacement Coefficient Method and the Capacity Spectrum Method[1]. These methods determine displacement estimates based on elastic response quantities, and their use require a number of steps, approximations and assumptions. The precision of these methods has been subject of recent discussion (Chopra et al., 1999; Aschheim et al., 1998; and Tsopelas et al., 1997).

Contrary to the two NSPs mentioned above, Yield Point Spectra contain data directly based on inelastic response of SDOF oscillators, allowing them to provide good accuracy for estimating the peak displacement response of SDOF systems. Their use is direct; assumptions as the "equal displacement rule" are needed.

To illustrate how YPS are used to estimate peak displacement, consider an oscillator having a bilinear load-deformation relationship with post-yield stiffness equal to 10% of the initial stiffness, as shown in Figure 2.2. Assume a yield displacement of about 2.0 cm. (0.02 m), an initial period of 0.5 seconds, and viscous damping equal to 5% of critical damping. This yield point plots right over the curve representing a displacement ductility of 2 in Figure 2.4. The resulting peak displacement for this oscillator will, therefore, be equal to twice its yield displacement, as indicated in the figure. This ability to directly obtain peak displacement from known yield points is a valuable feature of the YPS.

2.3.2 Design Application: Control of Peak Displacement and Ductility Demands

The Displacement Coefficient Method and the Capacity Spectrum Method are intended for estimating the peak displacement response of existing structures. They do not readily lend themselves to the reverse operation: determining the strength and stiffness required for a structure in order to limit its peak displacement or its displacement ductility to a specified value.

---

1 The Displacement Coefficient Method and the Capacity Spectrum Method are described in Chapter 5.

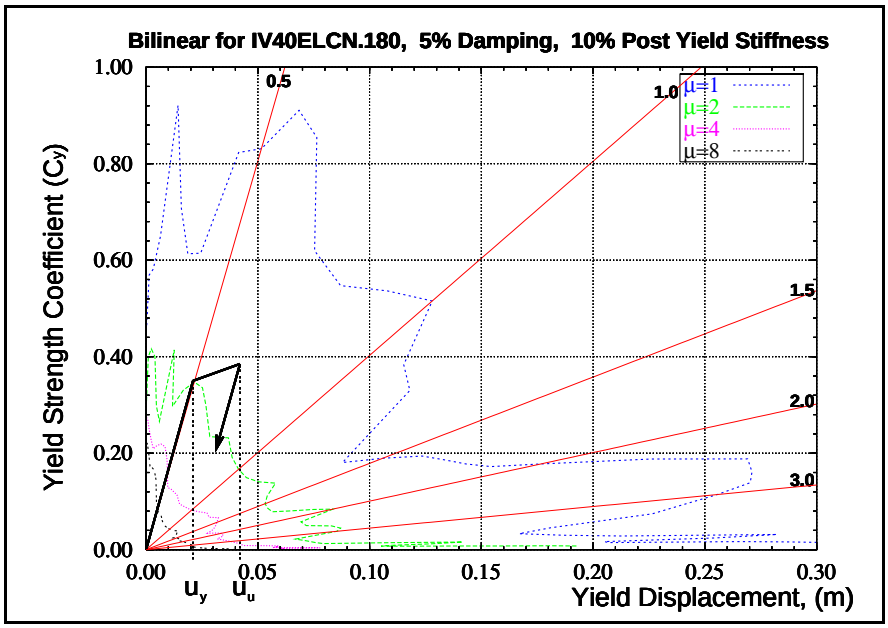

Figure 2.4 Using YPS to Estimate Peak Displacement

Yield Point Spectra, on the other hand, can be used, not only as a analysis tool to estimate peak displacement (Figure 2.4), but also as a design tool to determine combinations of strength and stiffness needed to limit the peak displacement and ductility demands responses to user-prescribed values.

Figure 2.5 shows a curve defining approximate combinations of strength and yield displacement required to limit peak displacement response to 8 cm. This curve has two parts, representing elastic and inelastic response. The part of the curve representing inelastic response (for $\mu > 1$) is constructed through a family of yield points. Each yield point within the family has the property that the product of its yield displacement and its ductility demand equals the limit displacement of 8 cm. The curve is approximate between yield points; greater precision can be had by plotting additional constant ductility curves. The part of the curve representing elastic response (points beyond the constant ductility curve equal to one) is defined by the period (radial line) of an oscillator having a yield displacement equal to the limit displacement (8 cm.). Any oscillator having a yield point that lies in the elastic part of the curve will have a peak displacement equal to the limit displacement regardless of its strength.

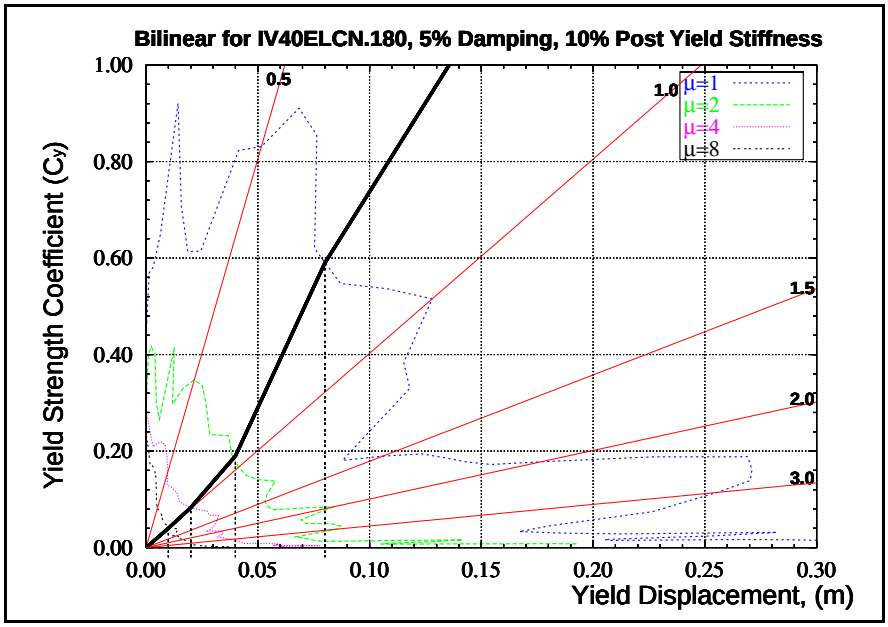

Figure 2.5 Curve Defining Strength and Stiffness Combination to Limit u_u to 8 cm

Yield Point Spectra also provide a way to easily combine peak displacement and displacement ductility limits. Suppose it is desired to limit simultaneously the peak displacement of an oscillator to 8 cm. or less and its displacement ductility to 4 or less. The construction of Figure 2.5 defines a boundary that helps to identify the area of admissible combinations of strength and stiffness that result in an approximate peak displacement less than or equal to 8 cm. Figure 2.6 shows the inadmissible region shaded by vertical lines.

Displacement ductility demands can be controlled by simply choosing a yield point located on or beyond the constant ductility curve representing the prescribed ductility limit. Figure 2.7 identifies the area of inadmissible combinations of strength and stiffness that result in a displacement ductility demand of 4 or more shaded by horizontal lines.

Superposition of Figures 2.6 and 2.7 results in the admissible design region, shown unshaded in Figure 2.8, which represents combinations of strength and stiffness that satisfy constraints on both peak displacement and displacement ductility demands.

Section 2.3.1 and 2.3.2 establish that Yield Point Spectra can be used for both analysis and design operations: estimating peak displacement (analysis) and determining the required combinations of strength-stiffness to limit peak displacement of SDOF to prescribed values (design).

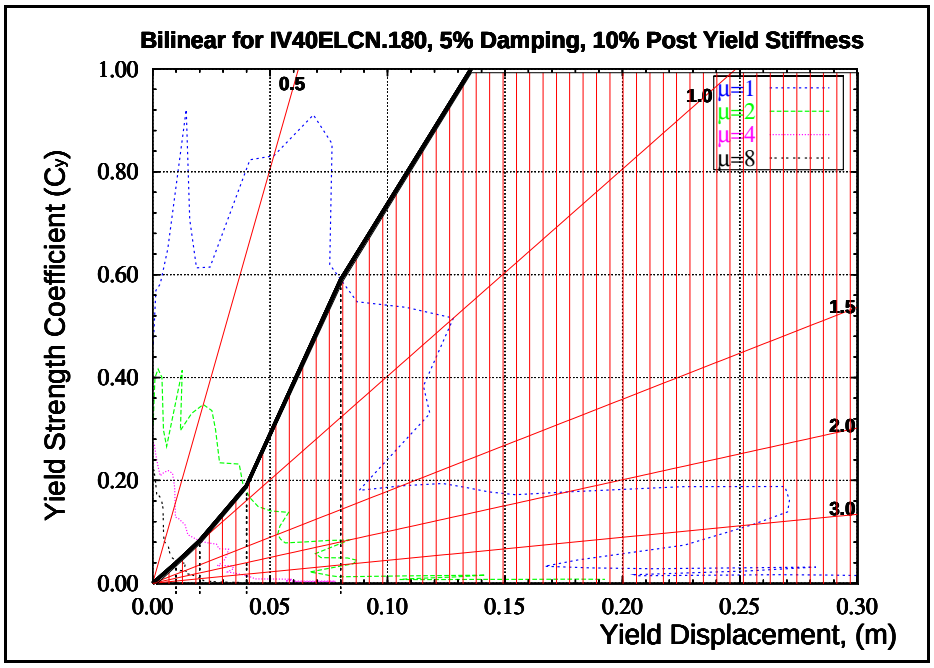

Figure 2.6 Admissible Design Region (Unshaded) for $u_u \leq 8$ cm

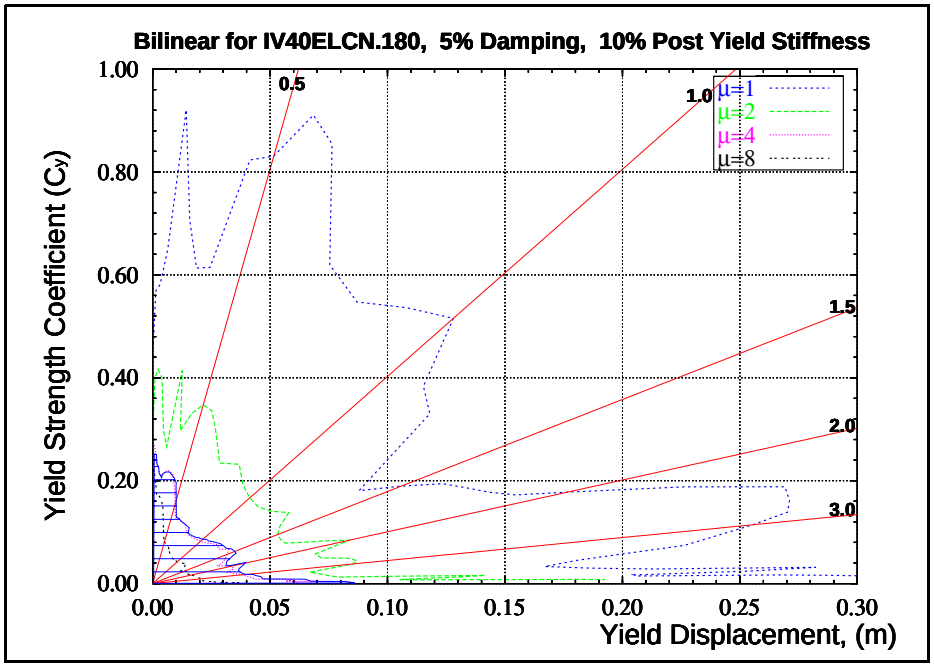

Figure 2.7 Admissible Design Region (Unshaded) for $\mu \leq 4$

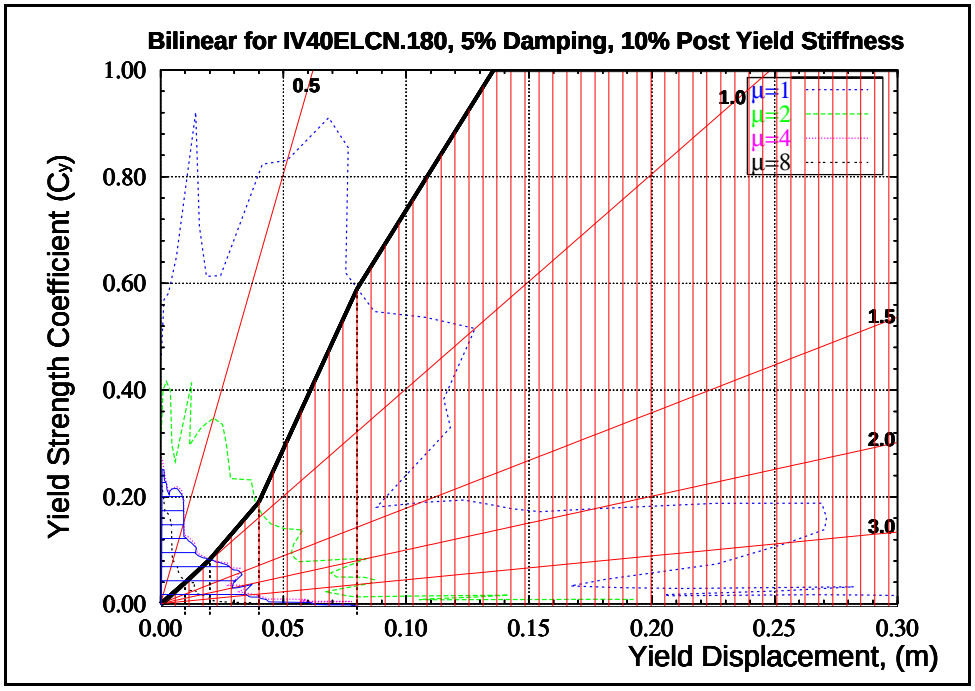

Figure 2.8 Admissible Design Region (Unshaded) for $\mu \leq 4$ and $u_u \leq 8$ cm

2.3.3 Application to Performance-Based Design

Performance-based design provides a framework to control structural performance over a range of contemplated ground shaking intensities. Under this framework, a performance level is described in terms of the degree of damage or functionality of the structure for a specific intensity or likelihood of ground shaking. A performance objective is defined as a performance levels associated with a ground motion intensity. Performance objectives in Vision 2000 (1995) are shown in Figure 2.9.

Performance levels can be associated with numeric values of roof drift and qualitative description of damage to components of the gravity and lateral force resisting systems. Constraints on inter-story drift indices and system displacement ductility can be related to limits on peak displacement response. Similarly, qualitative descriptions of damage can be associated with local member ductility demands and those can be related to system ductility. This allows a performance level to be expressed as a constraint on peak displacement response and system ductility demand.

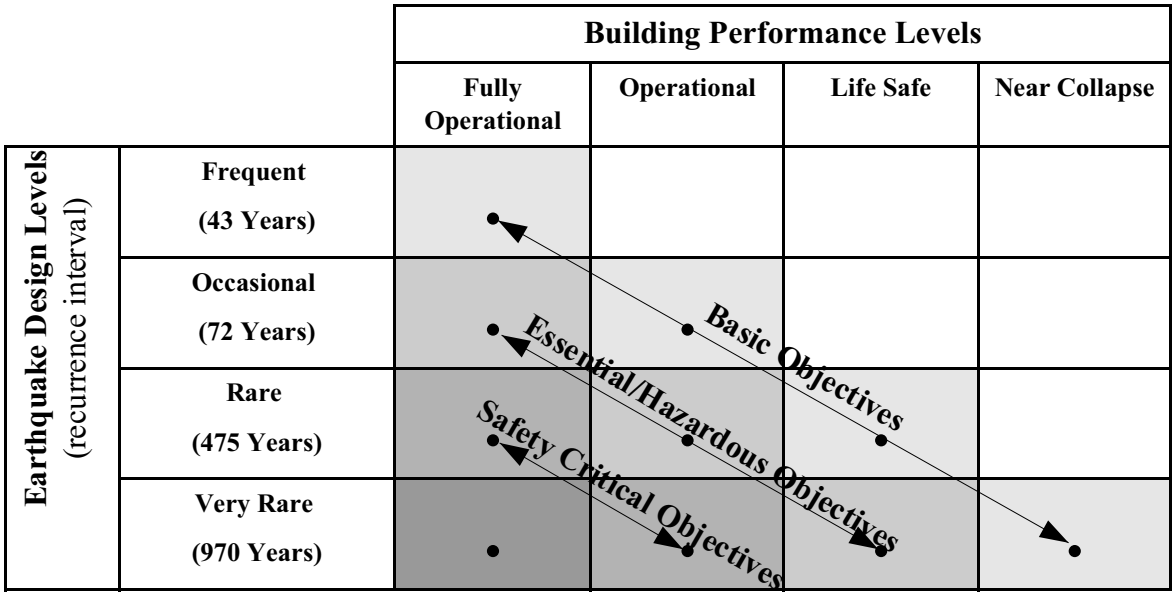

Figure 2.9 Seismic Performance Design Objective Matrix
SEAOC Vision 2000 [1995]

In section 2.3.2 YPS were used to determine an admissible design region that limited peak displacement and ductility demands to arbitrary values that may be associated with a performance level and shaking intensity. This process can be repeated for a set of performance levels and associated shaking intensities corresponding to a series of performance objectives. An admissible design region that satisfies the performance objectives is constructed by superposing the inadmissible design regions determined for each combination of performance levels and shaking intensities. A yield point that lies within the admissible design region satisfies the series of performance objective.

Section 2.6.2 contains a numerical example that helps to illustrate the potential use of Yield Point Spectra in performance-based design.

2.4 Yield Point Spectra and Design Procedures

2.4.1 Conventional Design Procedures

Most seismic design at present is done by elastic methods using equivalent static design lateral forces. In this conventional seismic design procedure, the period of vibration is the key parameter to start the design process. Code provisions allow the fundamental period to be approximated using formulas that depend only on the building height and the type of lateral force resisting system employed. Once the period has been estimated, the required

base shear strength is calculated using strength coefficients obtained from a smooth elastic response spectrum reduced by a strength-reduction factor (R). The design base shear force is distributed vertically along the building height as lateral forces. These lateral forces are used to determine members sizes and strengths.

In general, the fundamental period calculated for the final design of the building will be different from the approximate period used to start the design. Ideally, an iterative process should be used to obtain a new estimate of the required strength determined using the current fundamental period of the building. The iterations would end when the required lateral strength is stable. This iterative process is not done in routine practice; instead codified estimations of periods are used regardless of actual strength and stiffness.

2.4.2 Yield Displacement as Key Parameter For Design

In many practical design situations, changes in lateral strength are achieved by changing member cross sections. These changes in strength induce changes in stiffness and hence in periods of vibration. Only in unusual cases, such as when the grade of steel is changed, can strength be changed without a change in stiffness.

Members depths are commonly established early in the design process and usually change little. If changes in lateral strength are achieved by holding member depths constant while wide flange area (steel) or steel reinforcement content (concrete) are adjusted, the yield displacement remains nearly constant. This is because yield displacements are kinematically determined by the properties of the constituents material(s) and the member geometry. A simple case is a stocky column under axial load. An increase in the cross-sectional area of the column will increase both strength and stiffness, but the yield displacement remains unchanged. In a similar way, for predominantly flexural members, yield displacement is determined by material properties and section depth. This observation is general and, if member depths, materials (e.g. grade of steel), and the relative distribution of strength and stiffness remain nearly constant, can be extended to structures having multiple members.

To illustrate the idea that changes in lateral strength influence stiffness and hence periods, but have little effect on yield displacement, two capacity curves are presented in Figure 2.6. The capacity curves were determined applying a displacement pattern

proportional to the first mode shape in a nonlinear static analysis of the frame. A regular 4-story moment-resistant steel frame with 3-bays was analyzed using DRAIN-2DX (Powell et al., 1993). In one case W21X44 sections were used for all the beams and W14X74 sections were used for all the columns. In a second case W21X68 and W14X145 sections were used for the beams and columns respectively. Figure 2.10 shows that a considerable change in strength accompanies a large change in stiffness (and consequently in period). The periods were 1.13 and 0.81 sec. for the weak and strong frame, respectively (a 28% reduction), while the yield displacements were 0.120 and 0.117 m., respectively (a 2.5% reduction)[2].

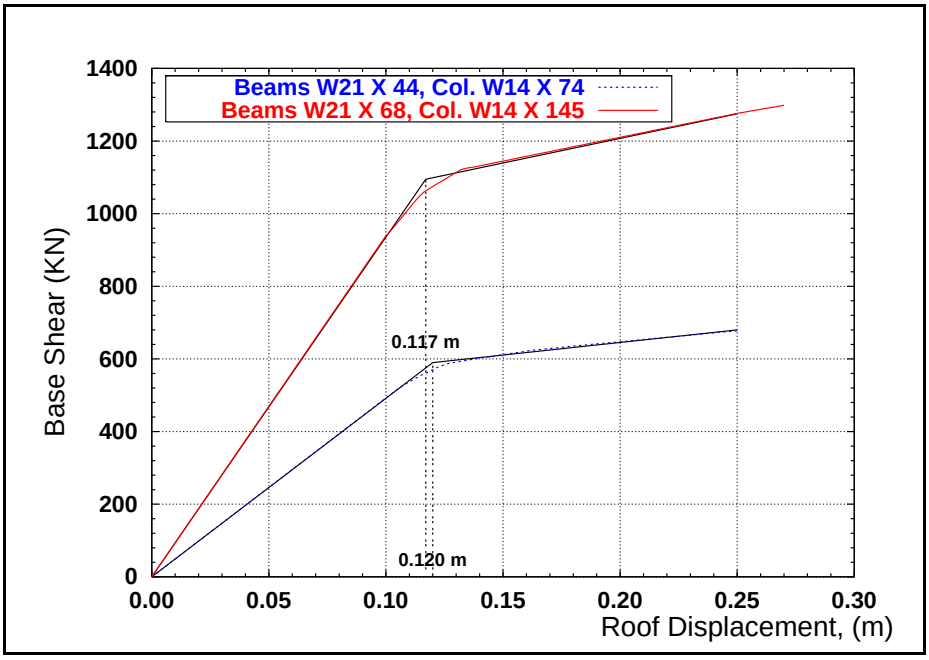

Figure 2.10 Push-over Analysis of 4-Story 3-Bay Building

This observation makes yield displacement a potential substitute for period to start the design process. If the yield displacement can be estimated based on knowledge of the framing configuration and member depth determined in preliminary design, the required system strength can be determined by simply "reading off " the required strength from a Yield Point Spectra. Because the effects of strength on stiffness and period are accounted for directly and implicitly, no iteration is needed, provided that the materials, relative distributions of strength, and member depths do not change significantly.

2 The observation that, under common design situations yield displacement remains nearly constant is convenient for using YPS in design. This observation holds for SDOF and multistory systems. Although this chapter is devoted to SDOF systems, a more general example, using a multistory building, helps to better support this observation. Chapters 4 and 5 discuss multistory systems in more details.

2.5 Strength Demands and Strength-Reduction (R) Factors

Current seismic design approaches have developed from the perspective that a structure may have less than the strength required for elastic response if it is provided with sufficient ductility capacity. Perhaps because of this perspective, it is common for design procedures to relate the strength of the inelastic structure to an elastic spectrum using strength-reduction factors (R). While the traditional strength-reduction factor is a single-valued relationship for a given structural system, many researchers (e.g. Miranda and Bertero 1994; Nassar and Krawinkler, 1991; Newmark and Hall, 1982) have expressed strength-reduction factors as a function of period of vibration (T).

The strength-reduction factor is defined as the ratio of the force that would develop under the specified ground motion if the structure had an entirely linear elastic response, to the prescribed design forces. In typical cases the strength-reduction factor is larger than 1.0; thus, typically structures are designed for forces smaller than those the design earthquake would produce in a completely linear-elastic responding structure (FEMA 303; 1997). Consequently, the design base shear strength is often expressed as a function of the elastic spectral acceleration divided by a strength-reduction factor.

In conventional design procedures, the strength-reduction factor and the elastic response spectra are positive for all periods. Therefore, some lateral strength is required regardless of the period of the structure. Additionally, it is accepted that the larger the strength-reduction factor is the larger the ductility demands.

Yield Point Spectra allow one to identify two consistent trends, derived from the use of yield displacement as primary variable for assessing strength requirements (Section 2.4.2), that question these common views. These trends will be explained using Figure 2.11, and are supported by the YPS prepared for 15 ground motions for both bilinear and stiffness degrading load-deformation models (Figures 2.18-2.20). These ground motions and the load-deformation models are described in Section 2.7.

In Figure 2.11, the Yield Point Spectra for the N-S 1940 El Centro record is shown in log-log format. Using this format, lines of constant period plot as paralel diagonal lines. Data supporting conventional period-based formulations can be recovered by reading the YPS along these lines of constant periods.

There is a region in which ductility demands are a function of the yield strength coefficient (C_y), such as for the yield displacement shown by path **A**. Within this region, decreases in strength produce significant increases in ductility demand and thus in peak displacement response. This trend is consistent with conventional views.

On the other hand, there is another region in Figure 2.11, indicated by path **B**, where if the yield displacements are large enough, response is elastic regardless of strength. While lateral strength affects stiffness and thus period, deformation remains elastic for any value of strength. Path **B** illustrates that those structures with large enough yield displacement will respond elastically independently of strength. Therefore, the strength-reduction factor is undefined in this region. Design of these structures may be governed by stiffness requirements to control ultimate displacement.

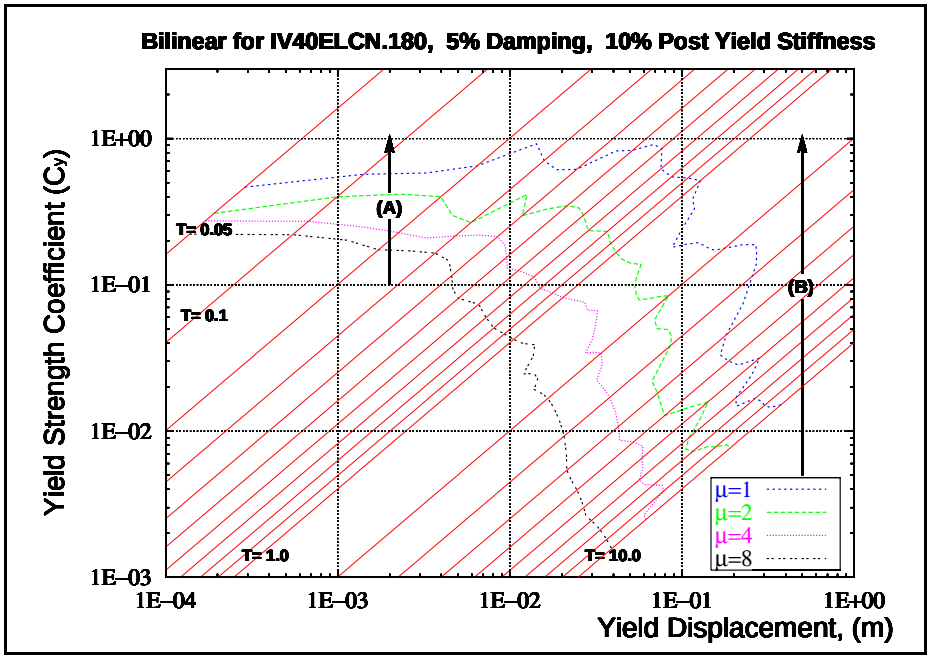

Figure 2.11 Common Trends Identified in Yield Point Spectra

Path A: Ductility Demand depends on Yield Strength Coefficient.

Path B: Ductility Demand does not depend on Yield Strength Coefficient.

An approach to design using YPS would consider the elastic response curve ($\mu = 1$) as incidental rather than as the primary basis for deriving the inelastic response characteristics for the structure. Additionally, and perhaps importantly, the strength-reduction factor is implicit and could become transparent to the designer.

2.6 Numerical Examples

To better support the ideas discussed in this chapter, two numerical examples are presented in this section. The first is intended to show accuracy in peak displacement and displacement ductility estimates made using YPS. The second example illustrates how Yield Point Spectra can be used in performance-based design.

2.6.1 Example 1. Accuracy of YPS Estimates

The peak displacement and displacement ductility responses of three SDOF oscillators are estimated using Yield Point Spectra computed for the N-S 1940 El Centro record. The oscillators have a bilinear load-deformation model with post-yield stiffness equal to 10% of the initial stiffness; damping was to 5% of critical damping.

The yield displacement for the first oscillator is 2 cm. (0.02 m), the second has a yield displacement of 1.5 cm. and the third has a yield displacement of 3.0 cm. One additional parameter, either the initial period or the strength ($\boldsymbol{C_y}$) of the system, is needed to read ductility demands from the Yield Point Spectra of Figure 2.12. For illustration purposes only, the initial period of the first two oscillators is set to 1.0 sec, and for the third oscillator the yield strength coefficient was assumed equal to 3%.

Figure 2.12 shows that for the first oscillator, an arrow representing a yield displacement of 2 cm. intersects the 1.0 sec. period line (diagonal lines represent initial periods) at the curve corresponding to a ductility demand of 4. Therefore, this oscillator will respond to this earthquake with a ductility demand approximately equal to 4 and sustain a peak displacement equal to 4 times its yield displacement (~ 8 cm.).

For the second oscillator, Figure 2.12 shows that the arrow representing its yield displacement (1.5 cm.) intersects the 1.0 sec. period line between the curves corresponding to ductility demand of 4 and 8. Here, it is important to notice that these constant ductility curves are powers of two (2^0, 2^1, 2^2, 2^3) and that they are approximately evenly spaced in the log-log format of Figure 2.12. Then, for this oscillator the ductility should be read for a point that is approximately at 45% of the distance measured from the curve of a ductility of 4 (2^2) toward the curve of a ductility of 8 (2^3). The displacement ductility demand can therefore be estimated as $2^{2.45} = 5.46$. Thus, the peak displacement is approximately (1.5) (5.46) = 8.2 cm.

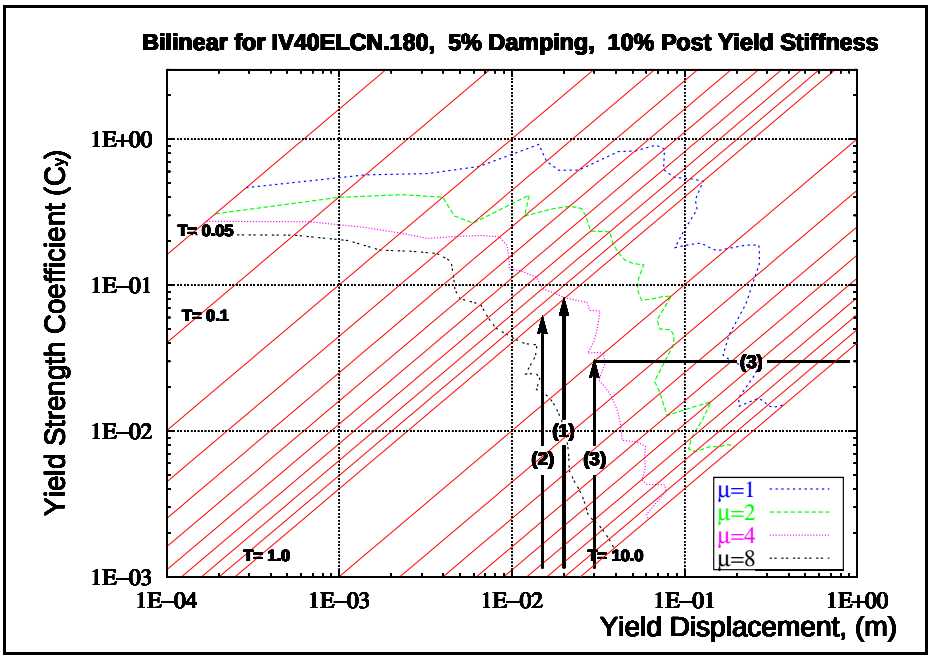

Figure 2.12 Estimating Ductility and Peak Displacement from YPS

For the third oscillator, the arrow representing a yield displacement of 3 cm. intersects the line representing 3% strength in a point that is approximately at 15% of the distance measured from the curve of a ductility of 4 (2^2) toward the curve of a ductility of 8 (2^3). The value of the ductility for this oscillator is estimated as $2^{2.15} = 4.44$. Thus, the peak displacement for this oscillator may be estimated approximately as (3) (4.44) = 13.3 cm.

Figure 2.13 shows displacement response histories computed for the three oscillators using nonlinear dynamic analysis. It can be seen that the peak displacement estimates (and, therefore, the displacement ductility demands) were accurate for all.

2.6.2 Example 2. Admissible Design Regions for Performance-Based Design

Assume that a one-story building has to be designed to meet the performance objectives of a performance-based seismic design code. For example, assume the structure must satisfy performance objectives consisting of two performance levels, named "Operational" and "Life-Safe", each having its own earthquake design level.

Suppose that the Operational performance level requires that the structure remains elastic under its design earthquake, with a drift ratio no larger than 0.5%. The design earthquake level that accompanies this performance level is selected as one that has an

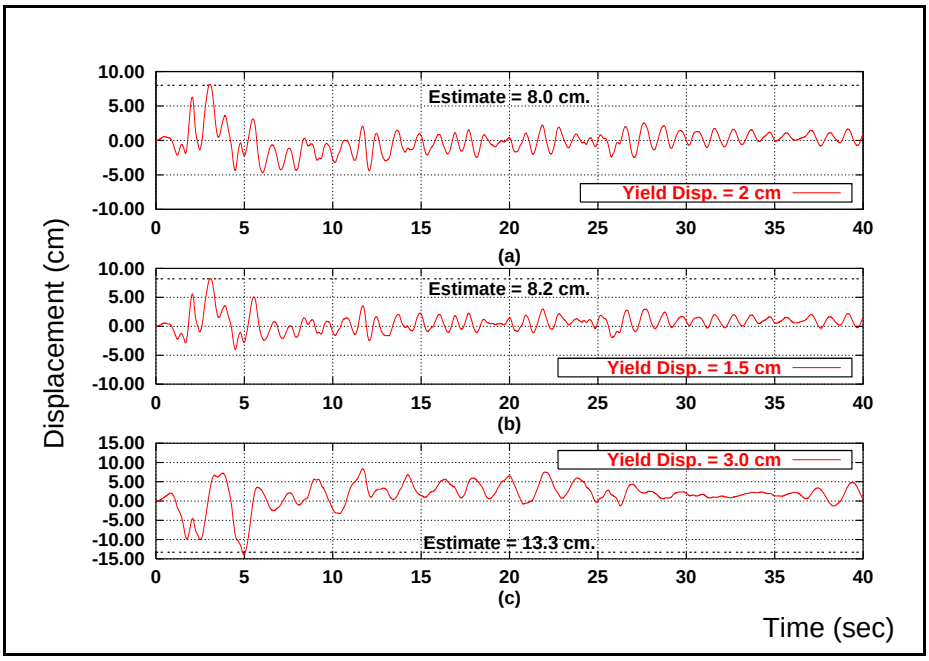

Figure 2.13 Time History to Compare Accuracy

"occasional" (72 years) recurrence interval. Now, assume that the Life-Safe performance level requires the structure to have a ductility no larger than 4 and a drift ratio no larger than 1.5%. The design earthquake level that accompanies this performance level was selected to have a "rare" (475 year) recurrence interval.

For purposes of illustration, the N-S 1988 Spitak at Gukasyan record and the E-W 1994 Northridge at Sylmar record were selected as representative of the earthquake design levels for the Operational and Life-Safe performance levels, respectively. These records were chosen arbitrarily for this example.

In addition to the data already described, assume that the building has a mass of 44 metric Tons, and a height of 4.00 m. Viscous damping was set equal to 5% of critical damping and a bilinear load-deformation model was used with a post-yield stiffness equal to 10% of the initial elastic stiffness.

Admissible Design Region for Operational Performance Level

Using the drift constraint given for the Operational performance level, the maximum allowed roof displacement can be calculated as

$$\text{Roof displacement limit} = (0.5\ \%)\ (400\ \text{cm.}) = 2.0\ \text{cm.} \qquad (2.4)$$

Figure 2.14 shows combinations of strength and stiffness that satisfy both ductility and drift constraints for this performance level. Notice that Figure 2.14 is similar to Figure 2.8 in the sense that both displacement and ductility constraints are shown. The inadmissible region is shaded by vertical lines.

The point having a yield displacement equal to the roof displacement limit (2.0 cm.) and the minimum strength required by the structure to have an elastic response is marked with a dark dot on Figure 2.14. This point divides the border between the admissible and inadmissible regions into two branches. To the left of the dot is the ductility controlled branch; any yield point below this branch represents a system that will have a ductility demand greater than one regardless of peak displacement. To the right of the dot is the drift controlled branch; any yield point below this branch represents a system having peak displacement greater than the roof limit regardless of ductility demand.

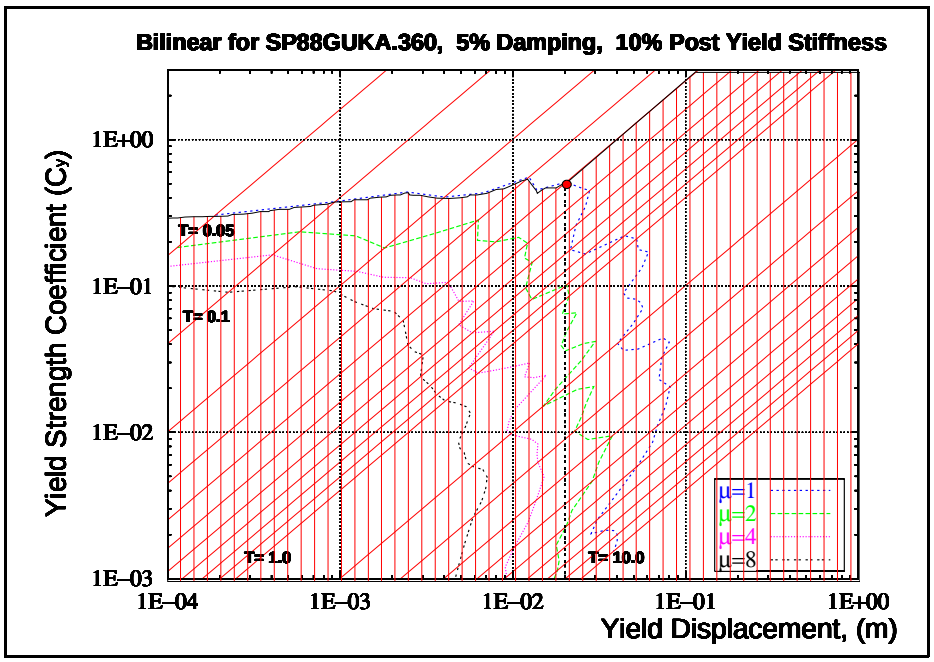

Figure 2.14 Admissible Design Region for Operational Performance Level

- ***Admissible Design Region for Life-Safe Performance Level***

Again, using the drift constraint for this performance level, 1.5%, the maximum allowable roof displacement is found.

Roof displacement limit = (1.5 %) (400) = 6.0 cm. (2.5)

In this case the structure is allowed to have a displacement ductility as high as 4. Some combinations of yield displacement and displacement ductilities that satisfy the roof displacement limit are shown in Table 2.1. They help to define the Admissible Design Region for this performance level.

Table 2.1 Solution Set for Life-Safe Performance Level

u_y (cm)	μ
1.5	4
3.0	2
6.0	1

Figure 2.15 shows combinations of strength and stiffness that satisfy both ductility and drift constraints for this performance level. The inadmissible region is shadowed by a horizontal grid. In this case, the yield point corresponding to the maximum allowed ductility (4) separates the ductility controlled branch from the drift controlled branch. This point is marked with a dark dot on Figure 2.15.

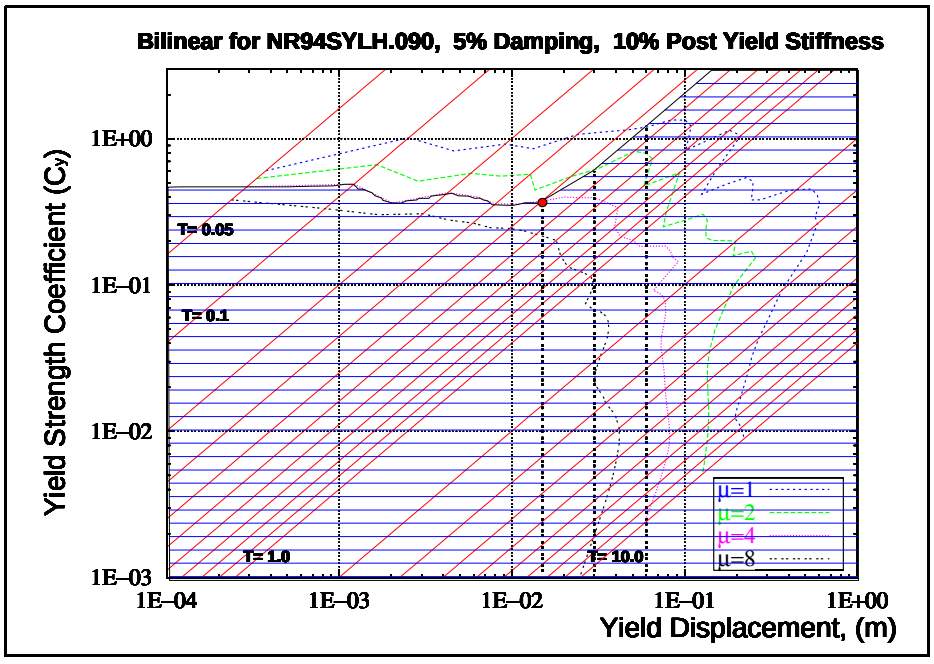

Figure 2.15 Admissible Design Region for Life-Safe Performance Level

Admissible Design Region for Performance Objective

Figure 2.16 shows the combined inadmissible regions for both performance levels over the YPS corresponding to Northridge at Sylmar record. It can be seen that the Admissible Design Region (unshaded area) has been further constrained. The area shown with a vertical grid does not comply with the Operational performance level while area shown with a horizontal lines does not comply with the Life-Safe performance level. The area having both horizontal and vertical grid does not comply with either performance level. Any point within the admissible area (unshaded) is a solution for this design problem.

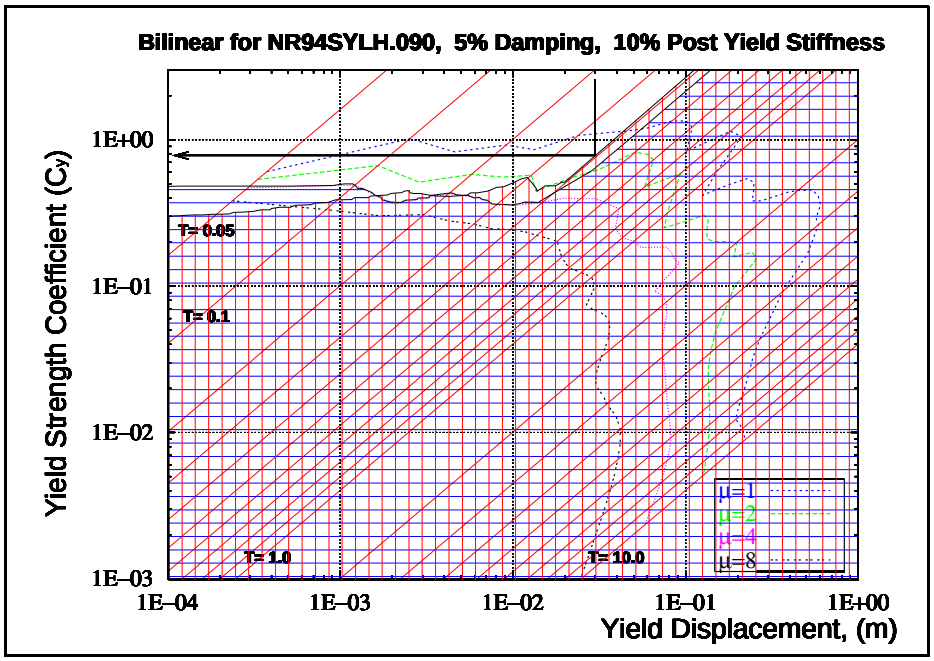

Figure 2.16 Admissible Design Region for Performance Objectives

Final Design

For illustration assume that, from preliminary design, the yield displacement is estimated to be equal to 3 cm. (0.75% of the building height). Figure 2.16 shows that the smallest admissible yield strength coefficient corresponding to a yield displacement of 3 cm. is slightly less than 0.8. A value equal to 0.78 will be assumed for design.

Several observations can be pointed out looking at Figure 2.16. First, notice that this design was controlled by the operational performance level (vertical lines). Second, the design point is on the drift controlled branch of Admissible Design Region. Therefore,

ductility demand will be less than the maximum allowed. Finally, observe that the design point lies approximately over the 0.4 sec. period line.

The final structure will have the following characteristics:

$$C_y = 0.78 \text{ and } u_y = 0.03 \text{ m.}$$

The required yield strength can be found using equation 2.1,

$$V_y = (C_y)\,(m)\,(g) = (0.78)\,(44)\,(9.807) = 337 \text{ kN.} \tag{2.6}$$

The period, obtained using equation 2.2, is 0.39 sec.

The final structure should have a peak displacement not larger than 2 cm (drift equal to 0.5%) responding to the occasional earthquake, and not larger than 6 cm. (drift equal to 1.5%) under the action of the rare earthquake.

Figure 2.17 shows displacement response histories corresponding to the SDOF building designed using Yield Point Spectra for the two performance levels. From the figure it can be seen that both performance objectives (elastic response with peak displacement not exceeding 2 cm. under Spitak at Gukasyan record, and no more than 6 cm. of displacement under the Sylmar record) were satisfied.

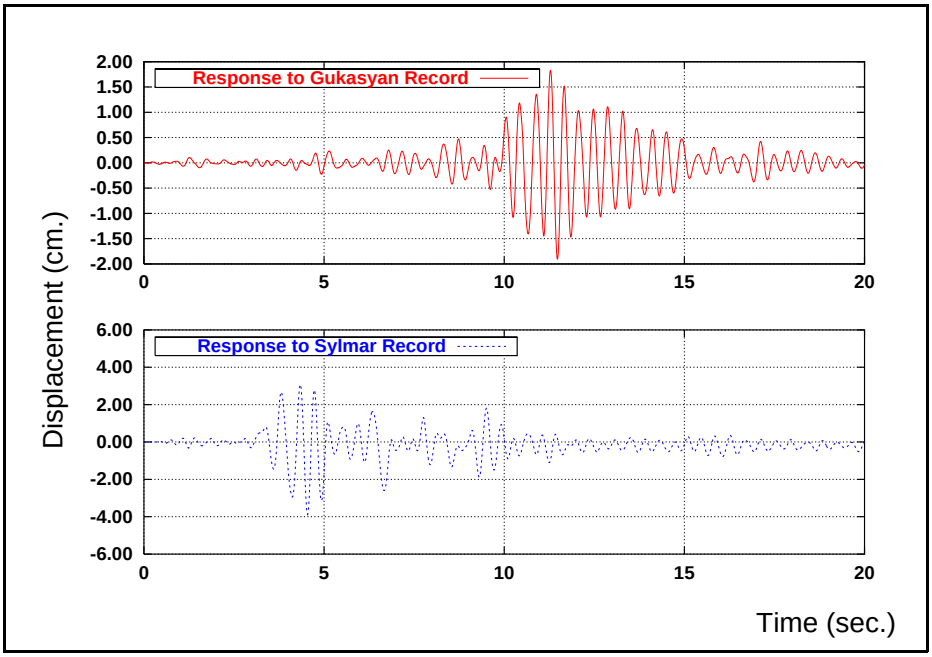

Figure 2.17 Time History For Numerical Example 2

2.7 Sample Yield Point Spectra

Samples of Yield Point Spectra for 15 recorded ground motions and two load-deformation models, plotted in logarithmic format, are shown in Figures 2.18 to 2.20. Viscous damping was assumed equal to 5% of critical damping and the post yield stiffness was 10% of the initial stiffness.

The ground motions and load-deformation models are described in the following subsections.

2.7.1 Ground Motions

A collection of recorded ground motions, representing a broad range of frequency characteristics, magnitude, duration, and the presence or absence of near field-forward directivity effects were selected for this study. In order to separately identify possible effects of duration and forward directivity, ground motions were organized into three categories; Short Duration (SD), Long Duration (LD) and Forward Directive (FD). Record duration was judged qualitatively in order to sort them into the Short and Long duration categories. Ground motions selected for the Forward Directive category were identified as containing near field pulses (Somerville, 1997).

It was intended for each category to represent a broad range of frequency content, to include records familiar to the research community, and to include records from the Loma Prieta, Northridge and Kobe earthquakes. The response characteristics of several hundred ground motion records were considered in detail in order to select the records used within each category.

Table 2.2 identifies the ground motions that compose each category, sorted by characteristic period. The peak ground accelerations (PGA) shown in Table 2.2 are normalized by the acceleration of gravity. Identifiers in this table are formulated using two characters representing the earthquake name, followed by two digits associated with the year of the earthquake, followed by four characters related to the station name at which the ground motion was recorded, followed by three digits representing the compass bearing of the ground motion record.

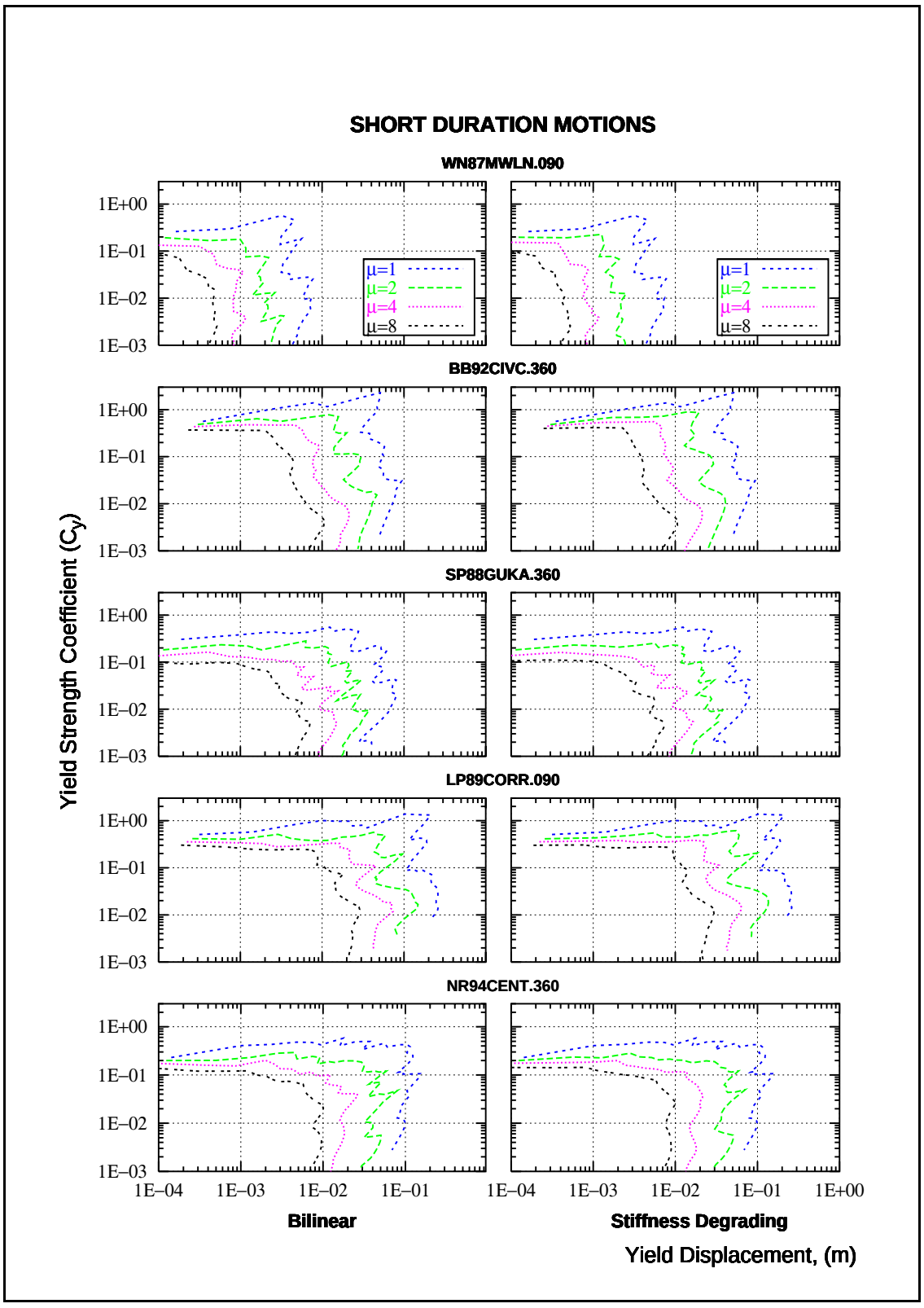

Figure 2.18 Yield Point Spectra for Short Duration Ground Motions

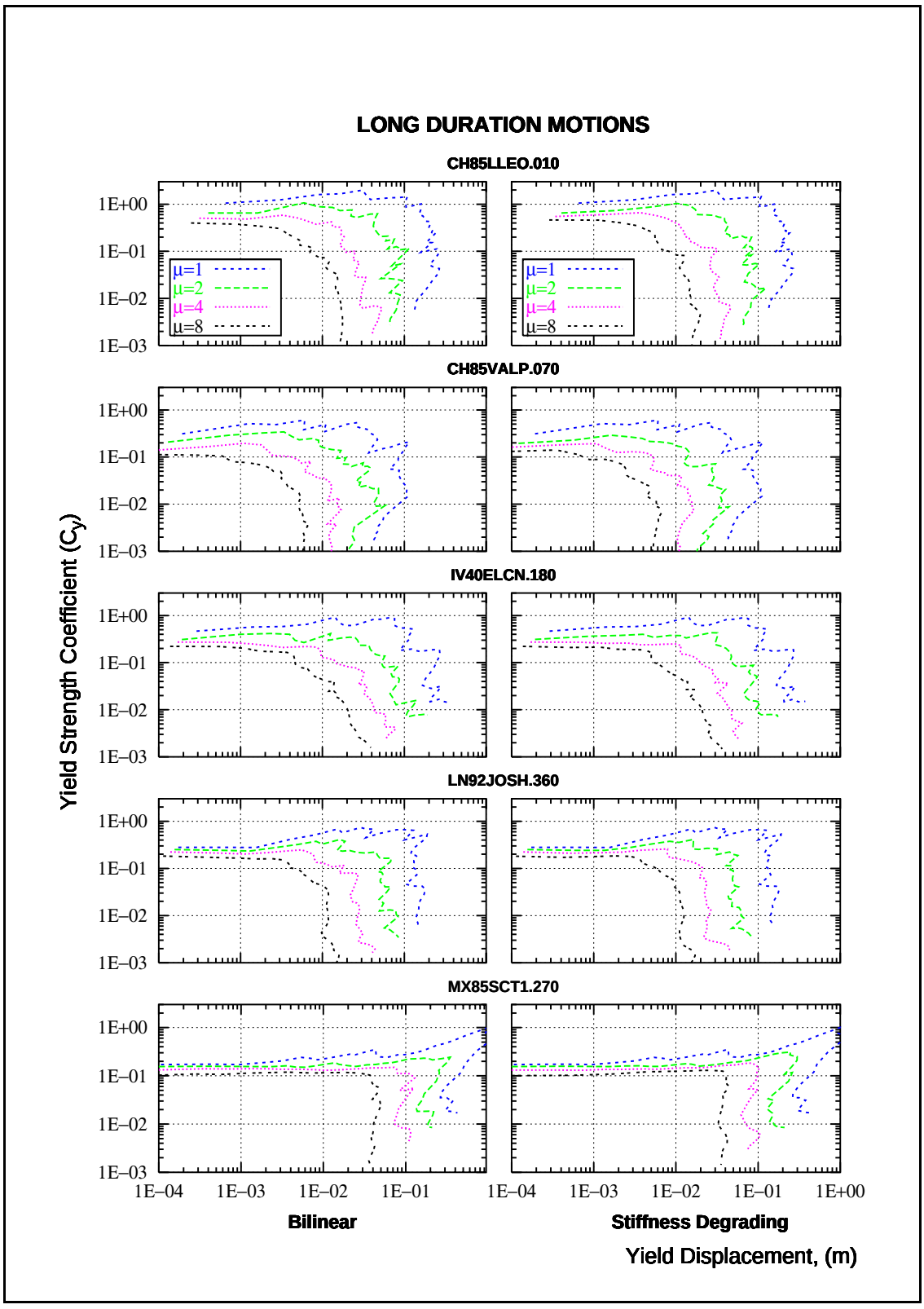

Figure 2.19 Yield Point Spectra for Long Duration Ground Motions

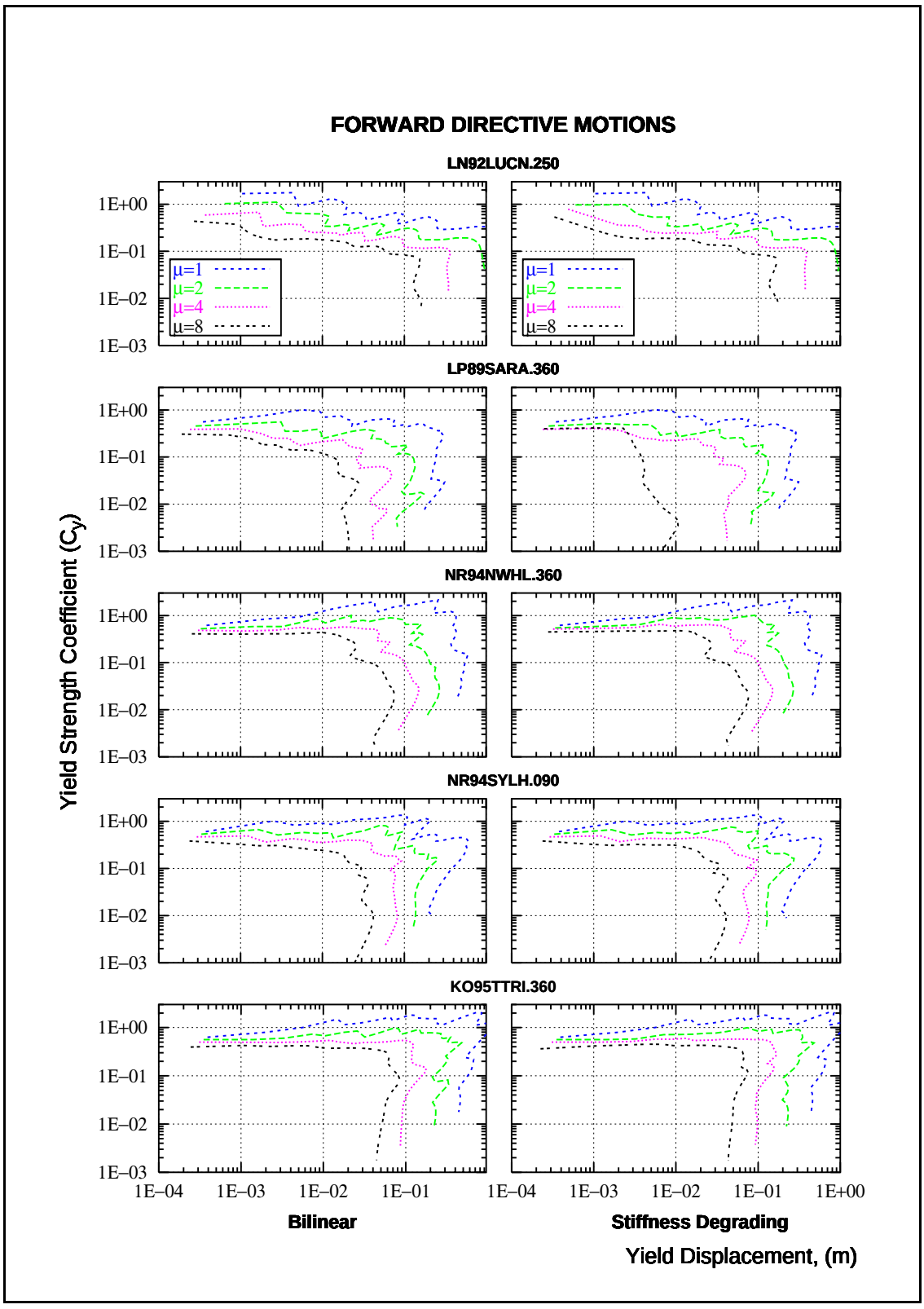

Figure 2.20 Yield Point Spectra for Forward Directive Ground Motions

Various magnitude measures are reported in the literature and are repeated here for reference: M_L is the traditional local or Richter magnitude, M_w is moment magnitude, and M_S is the surface wave magnitude.

Table 2.2 Ground Motions Used for the Yield Point Spectra of Figures 2.18 to 2.20

Identifier	*Earthquake & Station*	*Mag.*	*Component*	*PGA/ g*	*Char. Period (sec.)*
Short Duration Motion (SD)					
WN87MWLN.090	**Whittier Narrows, at Mount Wilson**	**M_L = 6.1**	**90**	**0.175**	**0.20**
BB92CIVC.360	**Big Bear, at Civic Center**	**M_S = 6.6**	**360**	**0.544**	**0.40**
SP88GUKA.360(*)	**Spitak, at Gukasyan-Armenia**	**M_S = 6.9**	**360**	**0.207**	**0.55**
LP89CORR.090	**Loma Prieta, at Corralitos**	**M_S = 7.1**	**90**	**0.478**	**0.85**
NR94CENT.360	**Northridge, at Century City**	**M_W = 6.6**	**360**	**0.221**	**1.20**
Long Duration Motion (LD)					
CH85LLEO.010	**Central Chile, at Llolleo**	**M_S = 7.8**	**10**	**0.711**	**0.30**
CH85VALP.070	**Central Chile, at Valparaiso**	**M_S = 7.8**	**70**	**0.176**	**0.55**
IV40ELCN.180	**Imperial Valley, at El Centro**	**M_L = 6.3**	**180**	**0.348**	**0.65**
LN92JOSH.360	**Landers, at Joshua Tree**	**M_W = 7.5**	**360**	**0.274**	**1.30**
MX85SCT1.270	**Michoacan, at SCT1-Mexico City**	**M_S = 8.1**	**270**	**0.171**	**2.00**
Forward Directive Motion (FD)					
LN92LUCN.250(*)	**Landers, at Lucerne**	**M_W = 7.5**	**250**	**0.733**	**0.20**
LP89SARA.360	**Loma Prieta, at Saratoga**	**M_L = 6.6**	**315**	**0.504**	**0.35**
NR94NWHL.360	**Northridge, at Newhall**	**M_W = 6.7**	**360**	**0.589**	**0.80**
NR94SYLH.090	**Northridge, at Sylmar County**	**M_W = 6.7**	**90**	**0.604**	**0.90**
KO95TTRI.360(*)	**Hyogo-Ken Nambu, at Takatori-kisu**	**M_L = 7.2**	**360**	**0.617**	**1.40**

An asterisk (*) indicates that informal integration procedures were used to calculate the velocity and displacement histories in Figures A.1 through A15 contained in Appendix A

The characteristic period of each ground motion was established considering equivalent velocity spectra and pseudo-acceleration spectra for linear elastic oscillators having 5% damping. The equivalent velocity, V_m, is related to input energy, E_m, and to ground acceleration and velocity response by:

$$\frac{1}{2}\cdot m\cdot V_m^2 \;=\; E_m \;=\; m\int \ddot{x}_g\, \dot{u}\, dt \tag{2.7}$$

where: m is the mass of the oscillator,

$\ddot{x}_g$ is the ground acceleration, and

$\dot{u}$ is the relative velocity of the oscillator mass.

The characteristic periods were identified using judgment to correspond approximately to the first (lowest period) peak of the Equivalent Velocity Spectrum, and, at the same time, the period at which the transition occurs between the constant acceleration and constant velocity portions of a smooth design spectrum fitted to the 5% damped elastic spectrum, following guidance given by Shimazaki (1984), Qi and Moehle (1991), and Lepage (1997).

Detailed plots of the ground motions listed in Table 2.3 are presented in Appendix A.

2.7.2 Selected Load-Deformation Models

Two well known non-linear load-deformation models were used to construct the Yield Point Spectra used throughout this research; the bilinear model and the stiffness-degrading model. These load-deformation models are implemented in PCNSPEC (Boroschek, 1991), and are described as follows.

- **Bilinear Model.** The bilinear model is defined by three parameters: yield strength, initial stiffness and post-yield stiffness. Bilinear models are frequently used in modeling structures that exhibit stable and full hysteretic loops.
- **Stiffness Degrading Model.** The stiffness degrading model is also defined by three parameters: yield strength, initial stiffness, and post-yield stiffness. Just like the bilinear model, the stiffness degrading model unloads with the initial elastic stiffness; however, the stiffness degrading model softens when the force changes sign. After crossing the axis, the model loads towards the previous point of maximum strength and displacement. The stiffness degrading model is commonly used to represent reinforced concrete structures that do not exhibit substantial degradation and/or bond deterioration.

Figure 2.21 shows the load-deformation response of two oscillators having a period of vibration of 1.0 seconds to the 1940 N-S component of El Centro record. One plot illustrate the bilinear model and the other illustrate the stiffness degrading model. The first five seconds in the response of the oscillators are shown.

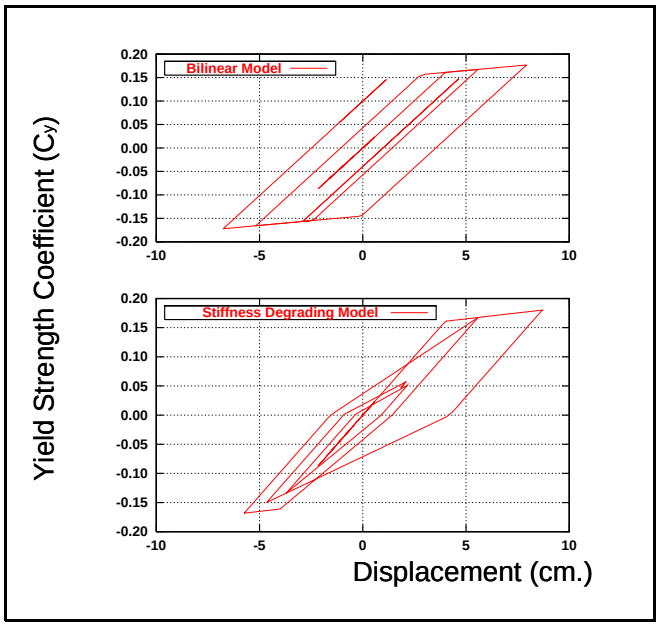

Figure 2.21 Load-Deformation Relationship Used to Construct Yield Point Spectra

2.8 **Summary**

Yield Point Spectra (YPS), a type of Constant Ductility Response Spectra were introduced. Their main characteristics and potential applications were described. Yield Point Spectra for 15 ground motion records and two load-deformation models were presented.

Yield Point Spectra may be used in the analysis and design of SDOF systems. For analysis YPS allow the peak displacement response and displacement ductility demand to be estimated with good accuracy. In design applications, YPS permit the designer to determine the strength and stiffness required to limit peak displacement and ductility demands to arbitrary values. A detailed example describing the use of YPS in a performance-based seismic design was included.

The idea of using the yield displacement of a structure instead of its period of vibration as a key parameter to start seismic design was introduced.

CHAPTER 3

EQUIVALENT SDOF MODEL OF MULTISTORY BUILDINGS

3.1 Introduction

The previous chapter discussed the representation of single-degree-of-freedom (SDOF) systems using Yield Point Spectra (YPS). Yield Point Spectra were used to estimate peak displacement response of SDOF systems and also to determine the strength and stiffness needed to limit peak displacement response and ductility demands to arbitrary values.

The peak displacement response of buildings under ground motion excitations, ideally should be obtained using a nonlinear dynamic analysis of the whole structure. Even though, for structures governed mainly by one mode of vibration, some investigators have proposed that the response of multistory buildings can be approximated using an equivalent SDOF system combined with an incremental nonlinear static analysis (pushover) as an alternative to the more complex nonlinear dynamic analysis. This simplification is the basis for methods such as the Displacement Coefficient Method and the Capacity Spectrum Method, generally known as Nonlinear Static Procedures (NSPs).

The objective of this chapter is to provide a formulation that permits the use of Yield Point Spectra for analysis and design of multistory buildings. Since Nonlinear Static Procedures have used an equivalent single-degree-of-freedom modeling technique for a similar objective, this technique is retained for use with Yield Point Spectra.

Buildings often are modeled as multi-degree-of-freedom (MDOF) systems in which the distribution of mass, stiffness, and strength throughout the structure determines the response of the various degrees of freedom to a base excitation. In this study, the degrees of freedom considered for MDOF systems are the lateral displacements at each floor level in a planar structure.

3.2 Equivalent Single-Degree-of-Freedom Modeling Technique

Representing the response of MDOF systems using an equivalent SDOF system has been routinely used in the past and continues to be widely used. Over the last 40 years

numerous seismic codes have allowed buildings to be designed, either directly or indirectly, using this technique. The methods proposed for design (Chapter 4) and analysis (Chapter 5) of buildings using YPS rely upon the goodness of this technique.

The development of the equivalent SDOF modeling technique can be traced to the early 60's (Biggs, 1964). Some later development can be found in the work by Saiidi and Sozen (1981), and Qi and Moehle (1991). Most recently it has formed the basis for the Nonlinear Static Procedures described in ATC-40 (1996) and in FEMA-273/274 (1997).

Even though various investigators have used different formulations for the technique, all the formulations share two main assumptions. The first one postulates that response of the MDOF system can be represented by a single deformed shape, while the second considers that this deformed shape remains constant during the response.

Although it is known that both assumptions are not completely correct, the technique has provided reasonable predictions of maximum displacement response of an MDOF building, for structures when response is predominantly in the fundamental mode.

3.2.1 Displacement of Equivalent SDOF From MDOF Equation of Motion

The equivalent SDOF modeling technique describes the displacement response at some representative point of a MDOF structure using an equivalent SDOF system. In this work, as in ATC-40 and in FEMA-273/274, the representative point is taken at the top of the MDOF system.

The best estimate of the displacement response of a multistory building is obtained by solving the equation of motion for MDOF systems (Equation 3.1). Multistory buildings are usually modeled as an MDOF system having mass lumped at each story level. For multistory buildings responding elastically to a base excitation $\ddot{u}_g(t)$, the equation of motion can be expressed as:

$$\boldsymbol{M}\{\ddot{u}(t)\}+\boldsymbol{C}\{\dot{u}(t)\}+\boldsymbol{K}\{u(t)\}=-\boldsymbol{M}\{1\}\ddot{u}_g(t) \tag{3.1}$$

where: $\boldsymbol{M}$ is the diagonal mass matrix of the system,
$\boldsymbol{C}$ is the damping matrix of the system,
$\boldsymbol{K}$ is the stiffness matrix of the system,
$\ddot{u}_g(t)$ is the ground acceleration history, and
$\boldsymbol{u(t)}$ is the relative displacement vector of the MDOF system.

If the two assumptions of the equivalent SDOF technique are accepted, the lateral displacement of the building at each level, $\{u(t)\}$, is a vector that can be expressed as a function of some deformed shape vector $\{\phi\}$ times a scalar displacement amplitude, *Y(t)*

$$\{u(t)\} = \{\Phi\}\ Y(t) \tag{3.2}$$

Notice that if the deformed shape vector $\{\phi\}$ is normalized with respect to the displacement at the top of the MDOF system, *Y(t)* represents the displacement at the top of the building.

Pre-multiplying both sides of Equation 3.1 by the transpose of the deformed shape vector $\{\phi\}$ and substituting Equation 3.2 into this expression results in

$$\boldsymbol{M}_{eq}\ddot{Y}(t)+\boldsymbol{C}_{eq}\dot{Y}(t)+\boldsymbol{K}_{eq}Y(t)=-\boldsymbol{L}_{eq}\ddot{u}_g(t) \tag{3.3}$$

or

$$\ddot{Y}(t)+\frac{\boldsymbol{C}_{eq}}{\boldsymbol{M}_{eq}}\dot{Y}(t)+\boldsymbol{w}_{eq}^2 Y(t)=-\frac{\boldsymbol{L}_{eq}}{\boldsymbol{M}_{eq}}\ddot{u}_g(t) \tag{3.3a}$$

where: $\boldsymbol{M}_{eq} = \{\phi\}^T\boldsymbol{M}\{\phi\}$,
$\boldsymbol{C}_{eq} = \{\phi\}^T\boldsymbol{C}\{\phi\}$,
$\boldsymbol{K}_{eq} = \{\phi\}^T\boldsymbol{K}\{\phi\}$, and
$\boldsymbol{L}_{eq} = \{\phi\}^T\boldsymbol{M}\{1\}$.

The scalar quantities $\boldsymbol{M}_{eq}$, $\boldsymbol{C}_{eq}$, $\boldsymbol{K}_{eq}$ denote the mass, damping, and stiffness of the equivalent SDOF system respectively. The factor $\boldsymbol{L}_{eq}$ has been called earthquake-excitation factor and represents the extent to which the ground motion tends to excite response in the assumed deformed shape $\{\phi\}$ (Clough and Penzin, 1993).

The term $\boldsymbol{w}^2_{eq}$ is the circular frequency squared, but also represents the stiffness per unit of mass of the equivalent SDOF system. Notice that the closer the assumed deformed shape vector ($\{\phi\}$) is to the i^{th} natural elastic mode shape of the MDOF system ($\{\psi_i\}$), the

closer the circular frequency squared of the equivalent SDOF (ω^2_{eq}) will be to the i^{th} natural circular frequency squared (ω^2_i) of the MDOF system.

Equation 3.3a is the equation of motion of a unit mass SDOF system subjected to a factored earthquake, where the factor, given by L_{eq}/M_{eq}, is generally known as the participation factor. In this equation *Y(t)* still represents the displacement at the top of the building provided that the deformed shape vector is normalized with respect to the top displacement of the MDOF system.

Multiplying Equation 3.3a by M_{eq}/L_{eq}, a new displacement coordinate may be defined as

$$u^{sdof}(t) = \frac{M_{eq}}{L_{eq}} Y(t) \tag{3.4}$$

and Equation 3.3a can be modified to

$$\ddot{u}^{sdof}(t) + \frac{C_{eq}}{M_{eq}} \dot{u}^{sdof}(t) + \omega^2_{eq} u^{sdof}(t) = -\ddot{u}_g(t) \tag{3.5}$$

Equation 3.5 describes the displacement response of a unit mass SDOF system under an unfactored earthquake. Here, u^{sdof} is the displacement of the equivalent SDOF, and the product ($\omega_{eq}^2 u^{sdof}$) is the force per unit of mass acting on the equivalent system.

Since, in general, Yield Point Spectra and others types of response spectra are usually determined using unfactored ground motions, response displacements obtained from such spectra correspond directly to solutions of Equation 3.5.

3.2.2 Yield Strength of the Equivalent SDOF System

The force per unit of mass acting on the equivalent system ($\omega_{eq}^2 u^{sdof}$) can be used to obtain the force acting on the equivalent SDOF at yield (its yield strength). For the instant when the displacement of the equivalent SDOF system is equal to its yield displacement ($u^{sdof} = u_y^{sdof}$), the yield strength for a unit mass equivalent SDOF system can be expressed as

$$V_y^{sdof} = w_{eq}^2 \cdot u_y^{sdof} \tag{3.6}$$

The yield strength for a unit mass equivalent SDOF may be also expressed, using Equation 2.1, as

$$V_y^{sdof} = C_y \cdot g \tag{3.7}$$

where: V_y^{sdof} is the yield strength per unit of mass of equivalent SDOF,
C_y is the yield strength coefficient,
w^2_{eq} is the circular frequency squared of the equivalent system. It is equal to the stiffness per unit of mass of the system,
u_y^{sdof} is yield displacement of SDOF system, and
g is acceleration of gravity.

3.2.3 Displacement of the MDOF System

The displacement response of the MDOF system can be obtained from the displacement of the equivalent SDOF rearranging equation 3.4 as

$$Y(t) = \frac{\boldsymbol{L}_{eq}}{\boldsymbol{M}_{eq}} \cdot u^{sdof}(t) \tag{3.8}$$

3.2.4 Yield Strength of MDOF System

The yield strength of the MDOF system, also known as base shear strength, can be obtained as

$$V_y = \{1\}^T \cdot \{F_y\} \tag{3.9}$$

where $\{F_y\}$ is a vector of story forces that when applied laterally to the MDOF system causes it to yield. This vector of forces can be expressed as the product of the stiffness matrix, $\boldsymbol{K}$, and the yield displacement vector, $\{u_y\} = \{\phi\} Y_y$ (Eq. 3.2). Now, Eq. 3.9 can be restated as

$$V_y = \{1\}^T \cdot \boldsymbol{K} \cdot \{\phi\} \cdot Y_y \tag{3.10}$$

Here Y_y is the displacement amplitude at the top of the MDOF system corresponding to yield.

Replacing $\boldsymbol{K}$ with $\boldsymbol{w^2_{eq}}\,\boldsymbol{M}$, and substituting Equation 3.8 into Equation 3.10 gives

$$V_y = \{1\}^T \boldsymbol{M} \{\phi\} \frac{\boldsymbol{L_{eq}}}{\boldsymbol{M_{eq}}} w_{eq}^2 u_y^{sdof} = \frac{\boldsymbol{L_{eq}^2}}{\boldsymbol{M_{eq}}} w_{eq}^2 u_y^{sdof} \tag{3.11}$$

substituting Eq. 3.6 and Eq. 3.7 into Eq. 3.11

$$V_y = \frac{\boldsymbol{L_{eq}^2}}{\boldsymbol{M_{eq}}} \cdot C_y \cdot g \tag{3.12}$$

The quantity $(\boldsymbol{L_{eq}})^2 / \boldsymbol{M_{eq}}$ has dimensions of mass and is sometimes called the *effective modal mass*.

The ratio of the effective modal mass to the total mass of the building, is termed effective modal mass coefficient, α,

$$\alpha = \frac{\boldsymbol{L_{eq}^2}}{\boldsymbol{M_{eq}} \cdot \boldsymbol{M_t}} \tag{3.13}$$

where $\boldsymbol{M_t}$ is the total mass of the MDOF system.

Finally, the yield strength of the MDOF system can be expressed as

$$V_y = \alpha \cdot C_y \cdot \boldsymbol{M_t} \cdot g = \alpha \cdot C_y \cdot \boldsymbol{W_t} \tag{3.14}$$

where $\boldsymbol{W_t}$ is the total weight of the building.

3.3 Application of the Equivalent SDOF Technique in Analysis and Design

The equivalent SDOF modeling technique can be applied to the analysis and design of multistory buildings. It is particularly effective when response is dominated by a single mode of deformation. Often this is the case for low and medium height buildings having uniform mass and stiffness distributions. Therefore, it is reasonable to use an approximation to the fundamental mode shape to apply the technique for analysis and design of this type of buildings.

3.3.1 Selecting the Appropriate Deformed Shape Function {φ}

Under analysis situations, in which engineers want to check an existing design, response simulations conducted in this study lead to recommend the first elastic mode shape as the deformed shape to assume in applying the equivalent SDOF technique.

For design situations, where the exact elastic mode shapes can not yet be determined, it is necessary to generate adequate shapes to apply the technique. Shapes having a distribution of lateral deflections resembling the fundamental mode shape, for example, inverted triangular or parabolic shapes, are generally sufficiently precise.

For many buildings, the distribution of mass is nearly uniform; then, the participation factor (L_{eq}/M_{eq}), and the effective modal mass coefficient (α) are functions of the deformed mode shape {φ} only. Following Abrams (1985), these two parameters were determined for three deformation shape functions: one triangular and two parabolic shapes, given by formulas 3.15 to 3.17. The parabolic shapes represent reasonable bounds of likely shapes for well-proportioned buildings.

$$\{\phi\} = \{\frac{h_i}{H}\} \tag{3.15}$$

$$\{\phi\} = \{1 - \frac{(H - h_i)^2}{H^2}\} \tag{3.16}$$

$$\{\phi\} = \{\frac{h_i^2}{H^2}\} \tag{3.17}$$

where: h_i is the height of the i^{th} story, and H is the building total height.

Table 3.1 presents values for these parameters as a function of the number of stories.

Table 3.1 Participation Factors and Effective Modal Mass Coefficients as a Function of Number of Stories

	Shape: Triangular		Shape: Parabolic Shear		Shape: Parabolic Flexure	
No. of Stories	L_{eq} / M_{eq}	α	L_{eq} / M_{eq}	α	L_{eq} / M_{eq}	α
1	1.00	1.00	1.00	1.00	1.00	1.00
2	1.19	0.92	1.12	0.98	1.19	0.78
3	1.28	0.88	1.16	0.95	1.30	0.71
4	1.33	0.86	1.19	0.93	1.37	0.67
5	1.36	0.84	1.20	0.91	1.41	0.64
6	1.38	0.83	1.21	0.90	1.45	0.63
7	1.40	0.82	1.21	0.89	1.47	0.62
8	1.41	0.81	1.22	0.89	1.49	0.61
9	1.42	0.81	1.22	0.88	1.51	0.60
10	1.43	0.80	1.23	0.88	1.52	0.60
11	1.43	0.78	1.23	0.87	1.53	0.59
12	1.44	0.79	1.23	0.87	1.54	0.59
15	1.45	0.78	1.23	0.86	1.57	0.58
20	1.46	0.78	1.24	0.86	1.59	0.58

Figure 3.1 plots the three shapes used to obtain the values presented on Table 3.1.

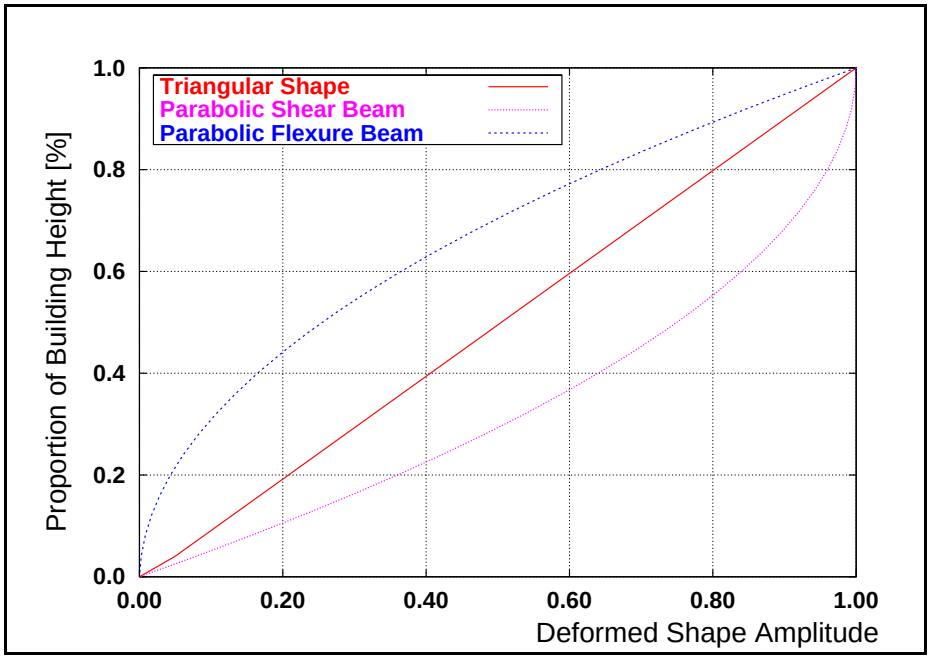

Figure 3.1 Triangular and Parabolic Deformed Shapes

3.4 Summary

A formulation that permits the use of Yield Point Spectra for the analysis and design of multistory buildings was described. The formulation is based on the equivalent single-degree-of freedom modeling technique.

The technique requires that an assumption be made with respect to the deformed shape of the building. For analysis, it is recommended to assume the fundamental mode shape of the building as the deformed shape to define the properties of the equivalent SDOF system. For design, deformed shapes resembling the fundamental mode shape are generally sufficiently precise.

Participation factors and modal mass coefficients were evaluated and tabulated for three deformed shapes as function of the number of stories for the case in which the story height and weight are uniform.

CHAPTER 4

DESIGN METHODOLOGY USING YIELD POINT SPECTRA

4.1 Introduction

Most seismic design codes in the U.S. and around the world allow structures to undergo inelastic deformations in the event of the design earthquake. However, in most practical situations, design is carried out using a set of equivalent static lateral forces in conjunction with linear elastic analysis methods. Typically, explicit checks using inelastic analysis are not required to determine the available strength and the ultimate deformation the structure would experience responding to the design earthquake.

This chapter describes a methodology for the seismic design of regular multistory buildings. The methodology is similar to the ones currently in use in the sense that a minimum strength or design base shear force is determined for use in design. However, this required minimum strength, which is obtained from Yield Point Spectra, is based on constraints intended to directly limit the peak roof displacement of the building to user-specified values. The objective of this limit imposed on the roof displacement is to try to indirectly control interstory drift. Additionally this roof limit could also be used to control the displacement ductility of the building. As in conventional seismic design methods, the design base shear is vertically distributed over the height of the structure as a set of lateral forces. This set of lateral forces is used for sizing structural members of the lateral force resisting system, and also to estimate peak displacement and interstory drift indices.

The effectiveness of the Yield Point Spectra design methodology in limiting peak displacement and system ductility demands is validated using numerical case study examples. The case studies used to illustrate the proposed methodology consist of 4 moment-resistant steel frames (two 4-story and two 12-story) designed to resist recorded strong ground motions. Nonlinear static and dynamic analyses of each design were done to verify if the proposed design methodology achieves the design objectives.

Although a procedure to select the members size and strength is not part of the proposed methodology, in each of the examples a strong column-weak beam plastic hinge mechanism was enforced through the selection of members sizes and strengths.

4.2 Design Philosophy

Structural deformation have been recognized as the centerpiece in evaluating performance and damage state of structures (Algan, 1982). Under seismic excitations, this performance is related to the displacement response of the structure. If satisfactory response of the building under ground motions excitation is desired, displacement control of such structures should be the main objective in earthquake resistant design (Qi and Moehle, 1991).

The idea of designing for displacement and checking strength rather than designing for strength and checking displacement has been discussed before (Moehle, 1992). Even so, the factor that has obstructed the adoption of displacement as the main parameter for seismic design has been the difficulties involved in determining the maximum displacement that develops during nonlinear response (Sozen and Lepage, 1996).

The objective of the design methodology introduced in this chapter is to limit the maximum interstory drift index (IDI) of the multistory system, for a given intensity of ground motion, to an arbitrary value. This objective is achieved indirectly, by establishing a limit to the building's maximum roof displacement. The methodology mighty be easily extended or modified to control the system displacement ductility demand, which in turn may serve to indirectly control local ductility demands in the structure.

4.2.1 Design Premises

The design methodology combines the use of Yield Point Spectra with the equivalent single degree of freedom formulation, presented in Chapter 3, for the design of multistory systems. The methodology is based in the following premises: (1) the use of yield displacement as an alternative to period as fundamental parameter for seismic design. (2) The assumption that the nonlinear behavior of the multistory system is completely accounted for in the SDOF responses represented in the YPS. Furthermore, the displacement ductility of the building is assumed to be equal to the ductility of the equivalent SDOF system.

An implicit assumption inherent to the equivalent SDOF technique is also made here; the deformed shape assumed to apply the equivalent SDOF formulation is a suitable representation of the displacement profile of the multistory building responding to the design ground motion.

4.2.2 Yield Displacement as Fundamental Parameter for Seismic Design

The yield displacement of the multistory system is established during preliminary design, and varies little as member strengths are refined in final design (Section 2.4.2). This parameter is then transformed, using Equation 3.4, to the yield displacement of an equivalent SDOF system in order to obtain the minimum required strength from a Yield Point Spectra.

Common yield displacement values for moment-resistant steel frames, associated with displacement profiles that resemble the fundamental mode of deformation, appear to generally be in the range of 0.6% - 0.9% of the building height, with more typical values toward the middle of this range. Precise values, if needed, may be determined by nonlinear static analysis (pushover) of the preliminary design.

4.2.3 Control of Peak Displacement

The objective of the design methodology introduced here is to indirectly control the peak interstory drift index of multistory buildings by imposing a limit on the peak roof displacement of the building.

The limit in peak roof displacement may be established based on the need to restrict damage to nonstructural elements such as partitions, shafts and stairs, enclosures, glass and other fragile elements.

Alternatively, the peak roof displacement may be established based on the need to restrict damage to structural elements of the lateral force resisting system. In this case a limit may be imposed on the system ductility demand in order to minimize local member ductility demands and, therefore, damage to structural components. The peak roof displacement limit is then obtained as the product of the system ductility demand limit and the estimated yield displacement of the building.

When limits in peak roof displacement must be enforced simultaneously to control damage to structural and nonstructural components, the smaller of the two peak roof displacement limits must be used in the proposed design methodology.

For simplicity, a limit in peak roof displacement was explicitly considered in the design of the case studies frames in Section 4.6.

4.2.4 Control of Interstory Drift Index as Final Design Objective

The interstory drift index (IDI) perhaps is the best parameter available to estimate the damage a building would suffer after a strong ground motion. The interstory drift index is defined as the displacement of any floor relative to the floor immediately below, normalized by the story height. In this study, the imposition of a limit to the roof displacement is considered to be an indirect way to limit interstory drift and, therefore, damage.

The roof drift index (peak displacement of the roof to the building height) is a weighted average for all the interstory drift indices in a building. Generally, the peak interstory drift index is larger than the roof drift index. Qi and Moehle (1991) report that the interstory drift index can be as much as 30% larger than the roof drift index for reinforced concrete structures. For moment-resistant steel frames, even larger values for the ratio of interstory drift index and roof drift index have been reported; values as high as 1.4 (Collins, 1995) or even 2.0 (Krawinkler, 1997) have been observed in study analysis.

For the case studies developed in Section 4.6, the maximum roof displacement was limited to 1.5% of the building height. The ratio of the peak interstory drift index to the roof drift index was assumed as 1.5. Together, these two values were intended to limit the peak interstory drift index to a value not larger than 2.25%. These values are used for illustration purposes only; appropriate limits for use in design will depend on the design procedure, the type of structural system, and the performance objectives.

4.2.5 Mixed Linear and Nonlinear Procedure

Since it is assumed that YPS account for the nonlinear behavior of the system, linear static analysis can still be used to evaluate the building as designed. Peak roof displacement and interstory drift indices are estimated multiplying results obtained from linear static analysis by an estimated value of the system displacement ductility.

4.3 Limitations

The proposed design methodology applies to cases in which the equivalent SDOF technique is applicable. Buildings should respond predominantly in a single mode and their deformation profiles must reasonably match the deformed shape assumed in design.

Second Order (P-Δ) effects are not explicitly addressed by the methodology, although their influence in the response can be suppressed by limiting peak displacement response and interstory drift to appropriate values.

The methodology is developed to address the strength of the lateral force resisting system only and does not explicitly address design for gravity or wind loads.

4.4 Description of the YPS Design Methodology

In this section, a step by step description of the design methodology is outlined. The procedure is illustrated and validated in Section 4.6, using some numerical examples. The steps are as follow:

a) Based on the geometry of the structure, material properties, and preliminary estimates of members depth, estimate the yield displacement ($\boldsymbol{u_y}$) of the structure for a deformed profile similar to the fundamental mode of vibration. *For many moment resistant steel frames a value between 0.6% to 0.9% of the height of the structure is reasonable*.

b) Identify the desired peak roof displacement limit of the structure ($\boldsymbol{u_u}$). *The value should be selected to limit damage to tolerable amounts and could be associated with a performance objective*.

c) Estimate the allowable system displacement ductility demand of the building as the ratio of the displacements obtained in steps a) and b) ($\boldsymbol{\mu = u_u/u_y}$).

d) Obtain the yield displacement of the equivalent SDOF system ($\boldsymbol{u_y^{sdof}}$) using Equation 3.4. In this equation, the yield displacement for the building obtained in step b) is used in place of the displacement amplitude, *Y(t)*. *Approximate values for the participation factor ($\boldsymbol{L_{eq}/M_{eq}}$), such as those presented in Table 3.1, appear to be adequate for the design of regular buildings*.

e) The yield displacement of the equivalent SDOF system, and the allowable system ductility are used to determine the required yield strength coefficient ($\boldsymbol{C_y}$) from the Yield Point Spectrum associated with the design ground motion.

f) The required strength or design base shear (V_y) of the MDOF system is determined using Equation 3.14. *Approximate values for the effective modal mass coefficient (α), such as those presented in Table 3.1, appear to be adequate for the design of regular buildings*.

g) The design base shear is vertically distributed over the height of the structure to obtain a set of lateral design forces. The base shear can be vertically distributed over the height of the structure using familiar expressions such as the ones in the Uniform Building Code (1997), reproduced here as Equations 4.1, 4.2 and 4.3. The period of the equivalent SDOF can be used as an approximation to the fundamental period of the building in Equation 4.3. This period can be obtained using Equation 2.2. Observe that in the log-log format of the YPS, the parallel lines represent constant period; thus, the approximate SDOF period may be read directly from the YPS.

$$V_y = F_t + \sum_{i=1}^{n} F_i \tag{4.1}$$

$$F_i = \frac{(V_y - F_t)\cdot w_i \cdot h_i}{(\sum_{j=1}^{n} w_j \cdot h_j)} \tag{4.2}$$

$$F_t = 0.07 \cdot T \cdot V_y \tag{4.3}$$

where: F_t is a concentrated force at the top of the building,
F_i is the lateral force applied to each floor of the building,
w_j is the weight of floor j,
h_j is the interstory height of floor j, and
T is the fundamental period of the building.

h) Members sizes and strengths should be selected following modern capacity design methods and ductile detailing provisions recommendations. Strong column-weak beam plastic hinge mechanism are suggested for good ductile behavior, although this is not required. *The following procedure was used to select structural members for all*

the frames of the case study examples. An initial set of members was selected using the forces obtained in step g). Then, the selection was refined using the approximate value of period (Equation 2.2) as a target to be matched by the first mode period of the frame. A difference of ±5% between the actual and the approximate periods was considered acceptable.[1]

i) Finally, linear static analysis is used to calculate the lateral displacements and interstory drift indices for the designed structure. Peak roof displacement and peak interstory drift indices are obtained by amplifying the linear results by the estimated system displacement ductility obtained in step c). For a satisfactory design, the peak linear estimates should be less than the desired limits.

4.5 Nonlinear Analysis for Verification Purposes

Static and dynamic nonlinear analyses were performed on the designed frames for verification purposes. The computer program DRAIN-2DX (Powell et al., 1993) was used for all the nonlinear analyses. A simple inelastic element (Element 02), capable of developing plastic hinges, was located along the centerlines of the frames. Plastic hinge strengths were assumed equal to the yield moments ($F_y S$), with strain hardening equal to 5% of Young's modulus. The yield strength of the steel was assumed as 248.0E+3 kN/m^2 (36 ksi). Contribution of the floor slab, panel zones, action of gravity loads, and P-Δ effects were not modeled.

Nonlinear static analyses (pushover) were used to confirm the actual values of yield strength and yield displacement of the four frames considered. The pushover curves were developed using a displacement control analysis with a displacement pattern proportional to first mode shape.

Nonlinear dynamic analyses were done to compare the peak displacements and interstory drifts developed in the nonlinear dynamic response to the linear estimates obtained with the proposed methodology (step i). Recorded ground motions were used when performing the nonlinear dynamic analysis verifications of each of the designed frames.

---

1 Other ways may be used to obtain the sizes and strengths of the members. In general, the procedure used here to size the members is not a component of the YPS design methodology.

4.6 Design Examples

The MDOF structures considered in this study consist of one set of two 4-story and another set of two 12-story moment-resistant steel frames; all having three bays. The set of 4-story frames are intended to represent low-height buildings while the set of 12-story represents medium-height buildings.

The same performance level was used for the design of all the frames. The desired performance level was to limit the peak roof displacement to 1.5% of the building height. Because the ratio of the maximum expected interstory drift index to the roof drift index was assumed to be 1.5, the peak interstory drift index in any story of the building is expected not to exceed approximately 2.25% under the design ground motions.

The Yield Point Spectra used to design the frames correspond to ground motions that were chosen among the 15 selected for this study (Section 2.7.1). It was desired to have one flexible and one rigid design per set of buildings. For the 4-story buildings set, the ground motions selected were the 250° component (perpendicular to strike) of the 1992 Landers at Lucerne record for the flexible design, and the N-S component of the 1994 Northridge at Newhall L.A. County Fire Station record for the rigid design. For the 12-story building set, the E-W component of the 1985 Michoacan at Secretary of Communication and Transportation (SCT1) and the N-S component of the 1995 Hyogo-Ken Nambu at Takatori-kisu records were selected for the flexible and rigid designs respectively. The frames are named Flexible-4, Rigid-4, Flexible-12 and Rigid-12 for reference.

All the frames were assumed to have an uniform mass distribution. The lower columns were assumed fixed at the base level for all the frames considered. The lowest story height was 5 m. and the remaining stories were 4 m. height; the columns were 8 m. on center.

4.6.1 Case Study 1: Design of Two 4-Story Buildings

4.6.1.1 Description of the 4-Story Moment-Resistant Frames

The general geometry for the 4-story buildings is shown in Figure 4.1. Story heights and weights set are presented in Table 4.1. An uniform story weight of 551 kN was assumed, for a total weight of 2204 kN. The total height of the frame is 17 m. Grade A36 steel was used for all members.

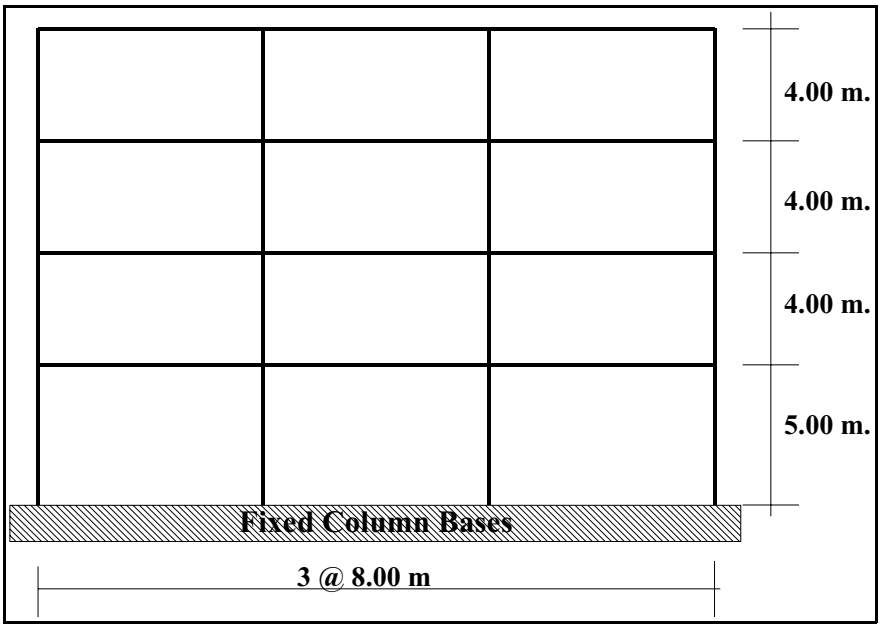

Figure 4.1 Geometry of 4-Story Buildings

Table 4.1 Story Heights and Weights of 4-Story Buildings

Story	Height [m]	Weight [kN]
4	4	551
3	4	551
2	4	551
1	5	551
Total	17	2204

Following the steps presented on Section 4.4 :

step a); limited data suggest that the yield displacement for a steel building, deformed in a pattern similar to the fundamental mode, is often between 0.6 and 0.9% of the building height. For this design, an initial estimate of 0.75% of the building height is assumed for the yield displacement,

$$u_y = (0.75\%)\ (17\ \text{m}) = 12.8\ \text{cm}. \tag{4.5}$$

step b); a peak displacement limit of 1.5% of the building height is assumed, therefore

$$u_u = (1.5\%)\ (17\ \text{m}) = 25.5\ \text{cm}. \tag{4.6}$$

step c); given these values for the ultimate displacement (u_u) and for the yield displacement (u_y), the system displacement ductility limit is

$$\mu = u_u/u_y = 25.5/12.8 = 2 \tag{4.7}$$

step d); the estimated yield displacement of the equivalent SDOF system is obtained using Equation 3.4. For frames with uniformly-distributed masses, a triangular deformed profile was used to apply the equivalent SDOF formulation. The value of the participation factor (L_{eq}/M_{eq}) for the triangular shape, 1.33, is obtained from Table 3.1.

$$u_y^{sdof} = 12.8/1.33 = 9.6\ \text{cm}. \tag{4.8}$$

Steps a) to d) are independent of the ground motion used for design. Now, steps e) to i) are shown for each of the selected design ground motions.

4.6.1.2 Design of Flexible-4 Using the YPS for the Lucerne Ground Motion

step e); entering the YPS for the Lucerne ground motion with a yield displacement equal to 9.6 cm. and a system displacement ductility limit of 2, the minimum acceptable yield strength coefficient (C_y) is approximately to 0.3. This step is illustrated in Figure 4.2.

step f); the minimum required base shear or design yield strength (V_y) for the building may be obtained using Equation 3.14. For the assumed triangular deformed shape, the effective modal mass coefficient (α) is equal 0.86 (Table 3.1) resulting in

$$V_y = (0.86)\ (0.3)\ (2204) = 569\ \text{kN} \tag{4.9}$$

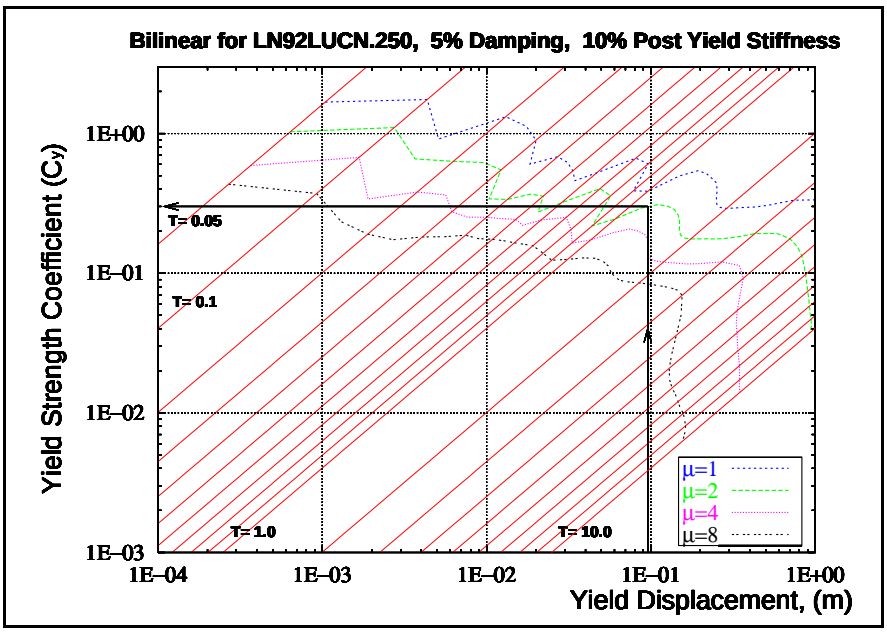

Figure 4.2 Required Yield Strength Coefficient for the Flexible-4 Frame

step g); the base shear obtained in step f), is vertically distributed using Equations 4.1 to 4.3. In order to use these equations, the designer must obtain an approximate value of the fundamental period of the structure. This period may be obtained directly from Figure 4.2, in which the lines of constant period plot as diagonal lines. Noting the logarithmic scale, the period is observed to be between 1.1 and 1.2 sec.

Alternatively, Equation 2.2 may also be used:

$$T = 2 \cdot \pi \cdot \sqrt{\frac{9.6}{0.3 \cdot 980.7}} = 1.13 \, sec. \tag{4.10}$$

Using Equation 4.3 to obtain the additional force applied to the top of the building,

$$F_t = (0.07)\,(1.13)\,(569) = 45 \text{ kN} \tag{4.11}$$

Applying Equation 4.2, the vertical distribution of the yield strength is found. The lateral forces and the story shears are shown in Table 4.2.

Table 4.2 Design Lateral Forces and Story Shears for the Flexible-4 Frame

Story	Force [kN]	Shear [kN]
4	247	247
3	155	402
2	107	509
1	60	569

step h); the remaining design task is to select an appropriate set of members to provide the required strength and stiffness to the frame. Figure 4.3 presents a set of Grade A36 steel members that complies with the imposed strength and stiffness requirements. The only constraint imposed in selecting the structural members was given for the enforcement of a strong column-weak beam plastic mechanism; at each node, the summation of the strength of the columns exceeds those of the beams at least by 20%. This constraint was enforced only as a recommended practice, but is not essential to the proposed YPS design methodology. The fundamental period for the frame shown in Figure 4.3 is 1.16 sec.

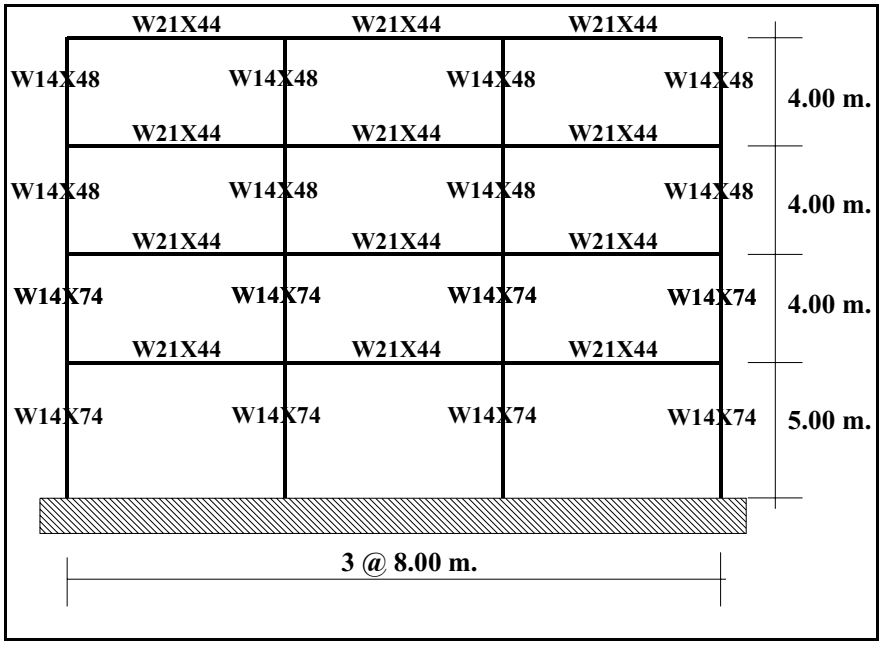

Figure 4.3 Flexible-4 Frame

T_1 = 1.16 sec.

step i); linear static analysis was used to calculate the lateral displacements and interstory drift indices for the designed structure. Table 4.3 shows results of a linear static analysis of the frame presented in Figure 4.3 subjected to the lateral forces of Table 4.2. The third column of Table 4.3 shows the story lateral displacement obtained from the linear analysis, while the fourth column provides an estimate of the peak displacement, obtained by multiplying the elastic displacement by the expected system displacement ductility, 2. Interstory drift indices, calculated using the estimated peak displacements shown in column 4, are in the last column of the table. Table 4.3 shows that the peak roof displacement estimate, 0.261 m, is nearly equal to the limit value of 0.255 m. assumed in **step a)**, and that the maximum linear estimate of the interstory drift index (1.79 %) is less than the nominal limit value (2.25%); therefore the design was considered satisfactory[2].

Table 4.3 Linear Estimates for the Flexible-4 Frame

Story	Height [m]	Displ. [m]	μ * Disp. [m]	IDI [%]
4	**17**	**0.130**	**0.261**	**1.05%**
3	**13**	**0.109**	**0.219**	**1.70%**
2	**9**	**0.075**	**0.150**	**1.79%**
1	**5**	**0.039**	**0.079**	**1.57%**

Results from the nonlinear analyses done for verification are shown in Figures 4.4 and 4.5. Figure 4.4 shows the nonlinear static (pushover) analysis curve of the frame presented on Figure 4.3. A bilinear approximation to the actual pushover curve, as well as estimations for the frame yield displacement u_y and yield strength V_y are shown. The value obtained for the yield displacement, 0.129 m., represents 0.76% of the building height, very close to the initial guess of 0.75%. The strength obtained with this solution, 585 kN, is only 2.8% larger than the required strength.

Figure 4.5 shows the roof displacement history of the building. Notice that the peak displacement, 0.241 m., is nearly equal to the design limit of 0.255 m despite the large residual deformations.

2 Improved techniques for estimating interstory drift indices are discussed in Chapter 5.

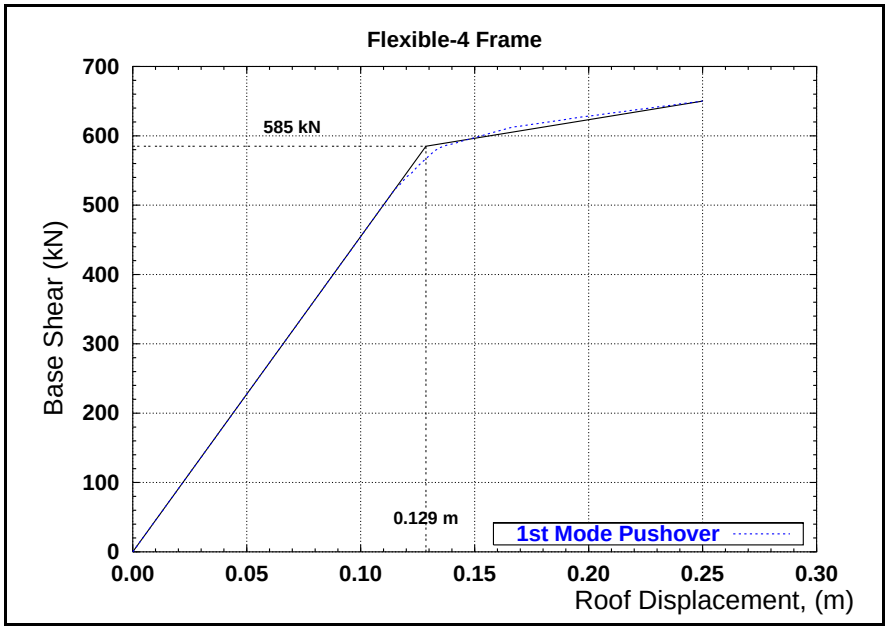

Figure 4.4 Nonlinear Static Analysis of the Flexible-4 Frame

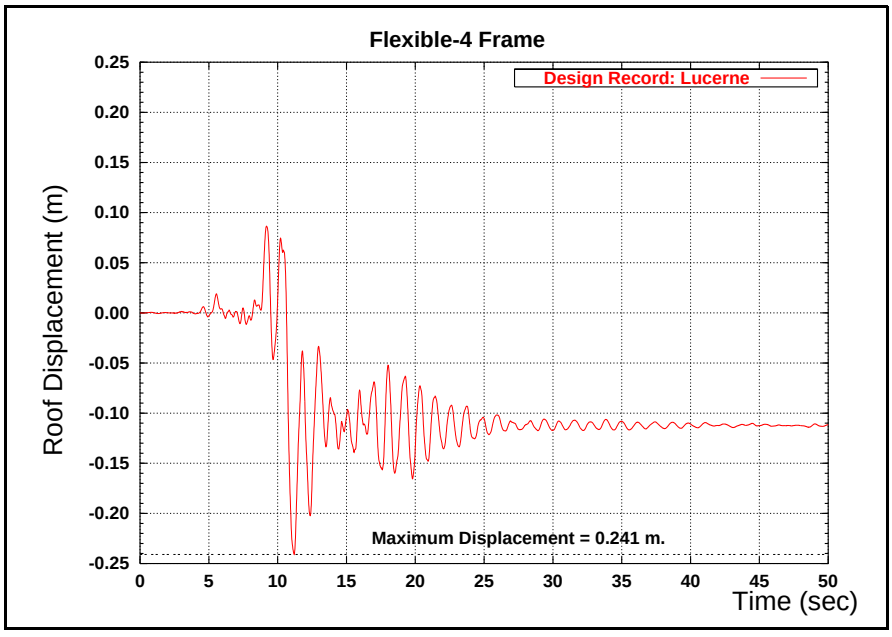

Figure 4.5 Roof Displacement from Nonlinear Dynamic Analysis of the Flexible-4 Frame

Table 4.4 presents values of interstory drift index (IDI) obtained from nonlinear dynamic analysis of this frame subjected to the Landers at Lucerne record. Peak values and their timing are presented for each story. Notice that the nonlinear interstory drift index can be larger than its linear equivalent in some stories. Observe that the nonlinear IDI for the lowest story slightly exceed the nominal limit of 2.25%.

Table 4.4 Interstory Drift Indices from Nonlinear Dynamic Analysis of the Flexible-4

Story	IDI [%]	Time [Sec]
4	**0.60%**	**11.23**
3	**1.04%**	**11.26**
2	**1.85%**	**11.10**
1	**2.28%**	**11.07**

4.6.1.3 Design of Rigid-4 Using the YPS for the Newhall Ground Motion

The design continues from step d) of Section 4.6.1.1.

step e); entering the YPS for the Newhall ground motion, Figure 4.6, with the yield displacement of 9.6 cm. and a system displacement ductility limit of 2, the minimum acceptable yield strength coefficient (C_y) is equal to approximately 0.80. This step is illustrated in Figure 4.6.

step f); the effective modal mass coefficient is the same used in the previous design. The minimum required design yield strength (V_y) for the building is estimated using Equation 3.14 as

$$V_y = (0.86)\ (0.80)\ (2204) = 1516 \text{ kN} \tag{4.12}$$

step g); From Figure 4.6, the period is determined to be about 0.7 sec. Alternatively, using Equation 2.2:

$$T = 2 \cdot \pi \cdot \sqrt{\frac{9.6}{0.80 \cdot 980.7}} = 0.70 \, sec. \tag{4.13}$$

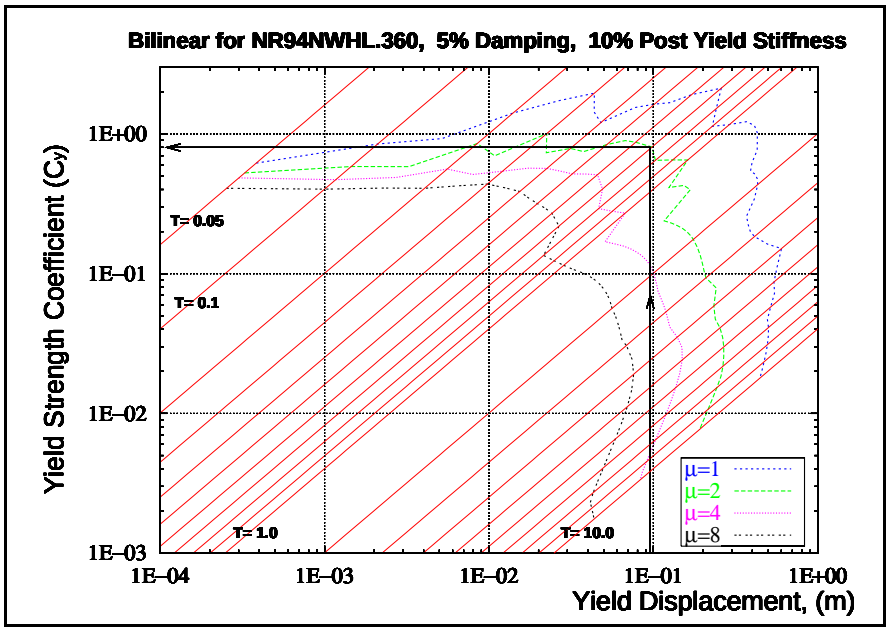

Figure 4.6 Required Yield Strength Coefficient for the Rigid-4 Frame

Applying Equation 4.3, the additional force at the top of the building is

$$F_t = (0.07)\ (0.70)\ (1516) = 74 \text{ kN} \tag{4.14}$$

Using Equation 4.2, the final distribution of the base shear is found. The story forces and shears are shown in Table 4.5.

Table 4.5 Design Lateral Forces and Story Shears for the Rigid-4 Frame

Story	Force [kN]	Shear [kN]
4	631	631
3	426	1057
2	295	1352
1	164	1516

step h); Figure 4.7 presents a set of Grade A36 steel members that complies with the strength and stiffness requirements intended to limit roof drift to 1.5% of the frame height in response to the Northridge at Newhall record. The fundamental period of this design is 0.71 sec.

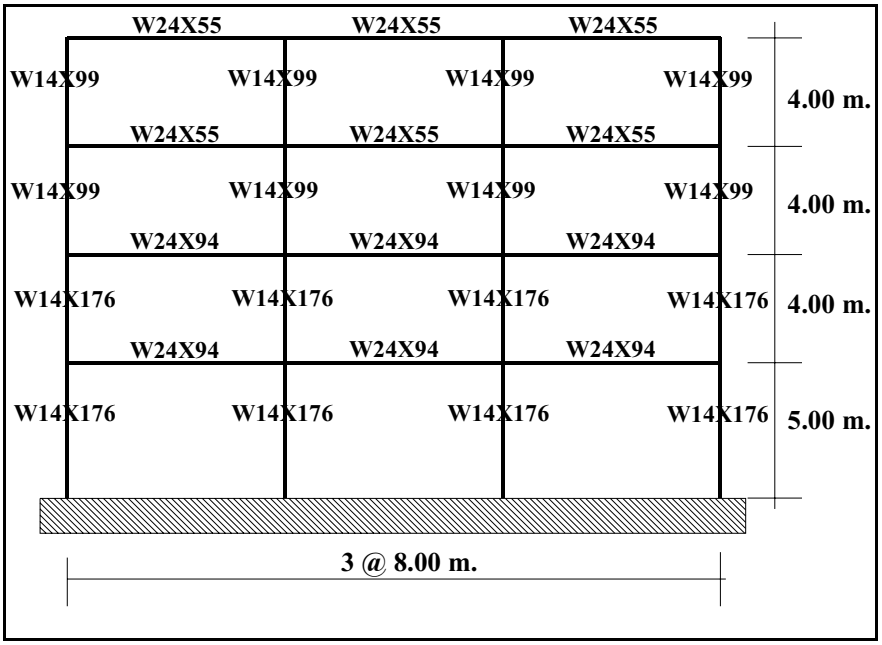

Figure 4.7 Rigid-4 Frame

T_1 = 0.71 Sec.

step i); Table 4.6 presents the results of a linear static analysis of the frame of Figure 4.7 subjected to the lateral forces of Table 4.5. Table 4.6 shows that the peak roof displacement estimate, 0.272 m., is slightly larger than the design limit of 0.255 m. in **step a)**. However, the estimated peak interstory drift index of 1.92 % is less than the limit value 2.25%.

Table 4.6 Linear Estimates for the Rigid-4 Frame

Story	Height [m]	Displ. [m]	μ * Disp. [m]	IDI [%]
4	17	0.136	0.272	1.42%
3	13	0.108	0.215	1.92%
2	9	0.069	0.138	1.62%
1	5	0.037	0.074	1.47%

Results from the nonlinear analyses done for verification are shown in Figures 4.8 and 4.9. Figure 4.8 shows the nonlinear static (pushover) analysis curve of the frame presented on Figure 4.7 A bilinear approximation of the actual pushover curve is also shown, as well as estimates of the frame yield displacement $\boldsymbol{u_y}$ and yield strength $\boldsymbol{V_y}$. Notice that the yield displacement, 0.133 m., represents 0.78% of the building height, close to the initial estimate of 0.75% used in **step b**. The strength obtained with this solution, 1500 kN, is 98.9% of the estimated minimum required strength.

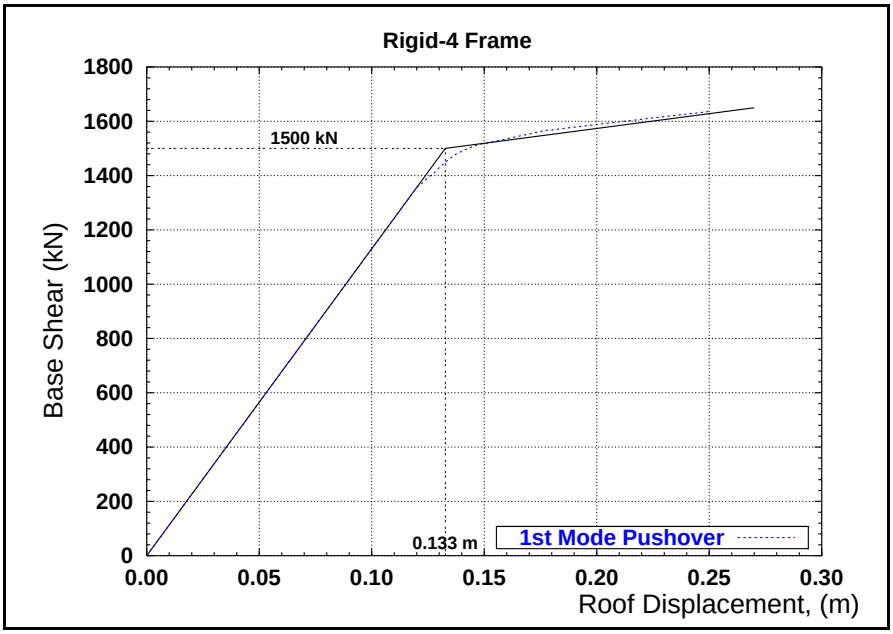

Figure 4.8 Nonlinear Static Analysis of the Rigid-4 Frame

Figure 4.9 shows the roof displacement history of the frame. Observe that the actual peak displacement of the roof, 0.223 m., is slightly less than the design limit for the roof displacement of 0.255 m.

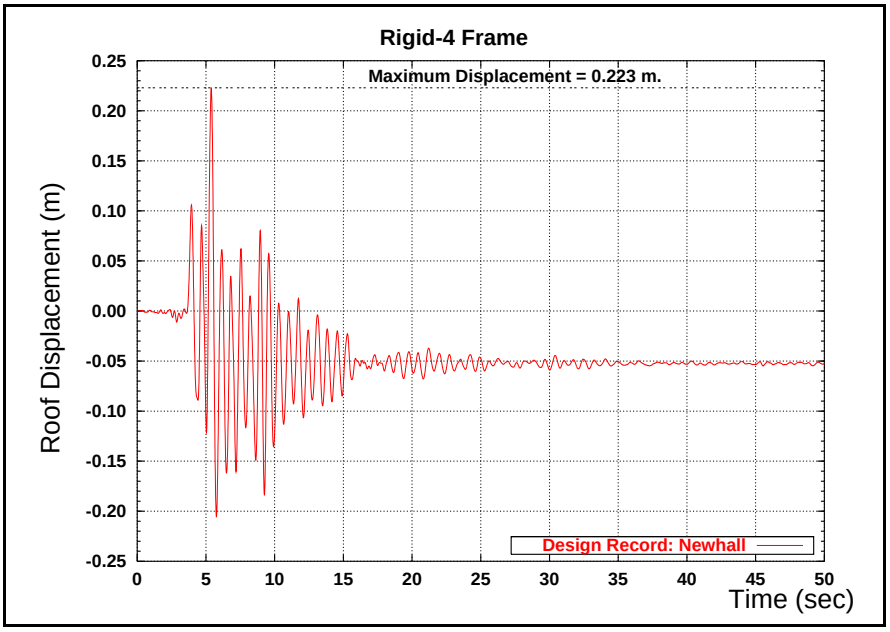

Figure 4.9 Roof Displacement from Nonlinear Dynamic Analysis of the Rigid-4 Frame

Table 4.7 presents values of the interstory drift index (IDI) obtained from nonlinear dynamic analysis of the frame subjected to Newhall record. Peak values and their timing are presented for each story. Although, the maximum interstory drifts shown in Table 4.7 differ from the linear estimates in Table 4.6, for this case the interstory drifts in all stories were less than the nominal limit value of 2.25%.

Table 4.7 Interstory Drift Indices from Nonlinear Dynamic Analysis of the Rigid-4

Story	IDI [%]	Time [Sec]
4	1.05%	5.70
3	1.42%	5.71
2	1.50%	5.40
1	1.64%	5.38

4.6.2 Case Study 2: Design of Two 12-Story Buildings

4.6.2.1 Description of the 12-Story Moment-Resistant Frames

The general geometry for the 12-story buildings is shown in Figure 4.10. Story heights and weights are presented in Table 4.8. An uniform story weight of 551 kN was assumed, for a total weight of 6612 kN. The total height of the frame is 49 m. Grade A36 steel was used for all members.

Table 4.8 Height and Weight of 12-Story Buildings

Story	Height [m]	Weight [kN]
12	4	551
11	4	551
10	4	551
9	4	551
8	4	551
7	4	551
6	4	551
5	4	551
4	4	551
3	4	551
2	4	551
1	5	551
Total	49	6612

Following the steps presented on Section 4.4 :

step a); the yield displacement is estimated to be 0.75% of the building height,

$$u_y = (0.75\%)\ (49)\ \text{m} = 36.8\ \text{cm}. \tag{4.15}$$

step b); a peak displacement limit of 1.5% of the building height is assumed,

$$u_u = (1.5\%)\ (49\ \text{m}) = 73.5\ \text{cm}. \tag{4.16}$$

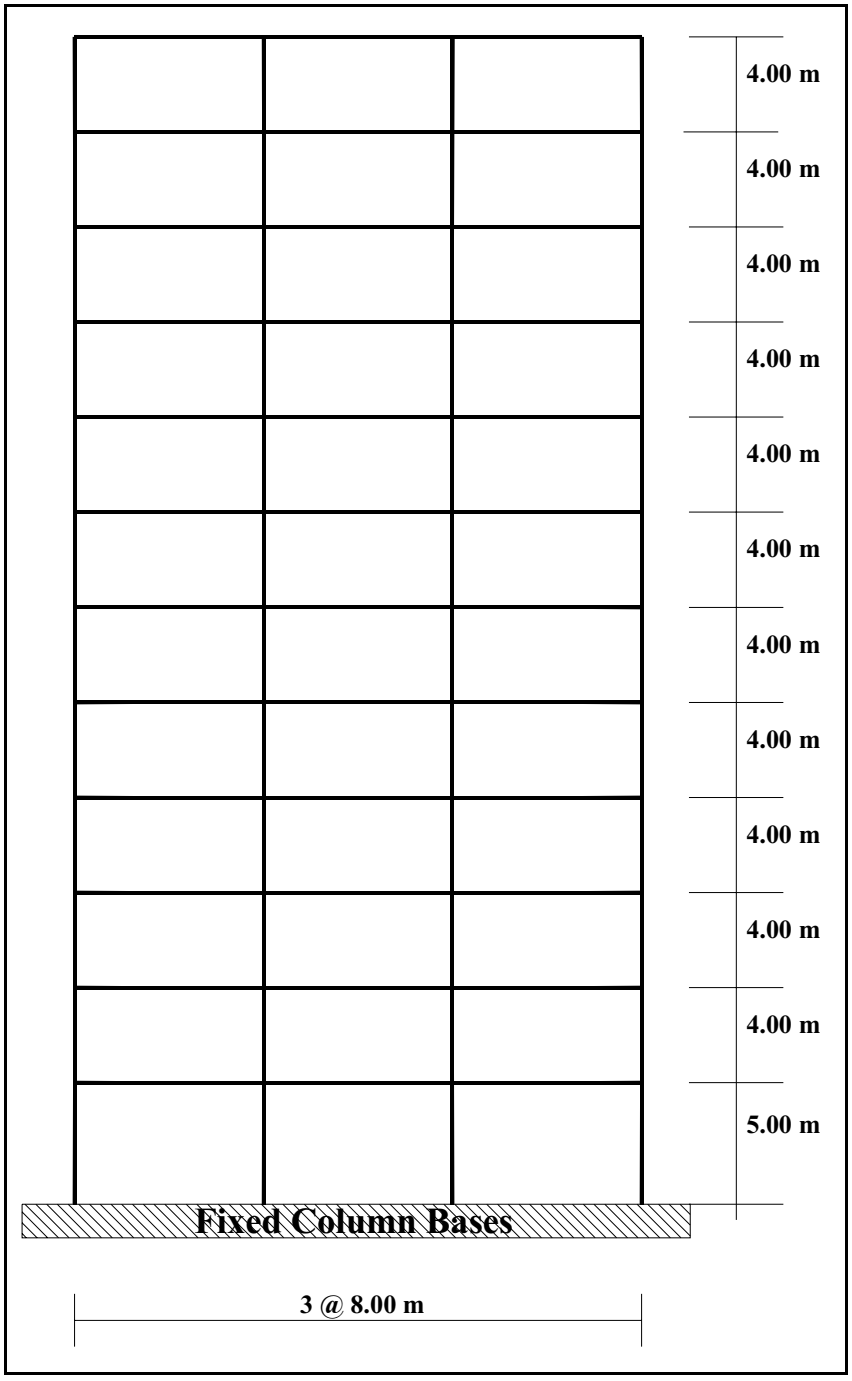

Figure 4.10 Geometry of 12-Story Buildings

step c); given these values for the ultimate displacement (u_u) and for the yield displacement (u_y), the system displacement ductility limit is

$$\mu = u_u/u_y = 73.5/36.8 = 2 \tag{4.17}$$

step d); the yield displacement of the equivalent SDOF system is obtained using Equation 3.4. Assuming a triangular deformed shape, the participation factor, L_{eq}/M_{eq}, for this shape, 1.44, is obtained from Table 3.1.

$$u_y^{sdof} = 36.8/1.44 = 26 \text{ cm.} \tag{4.18}$$

4.6.2.2 Design of Flexible-12 Using the YPS for the SCT1 Ground Motion

step e); entering the YPS for the SCT1 record with a yield displacement equal to 26 cm. and a system displacement ductility limit of 2, an acceptable yield strength coefficient (C_y) is approximately 0.22. This step is illustrated in Figure 4.11.

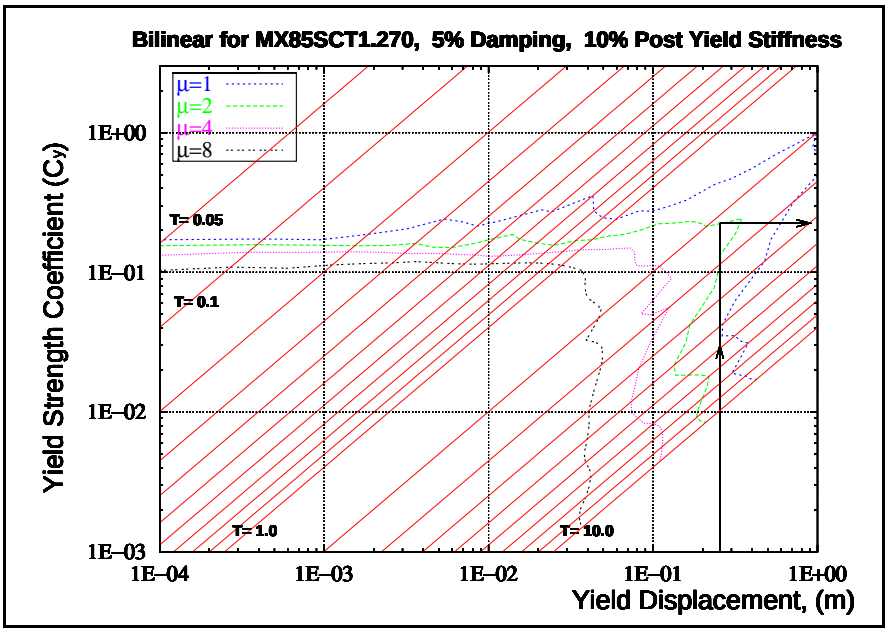

Figure 4.11 Required Yield Strength Coefficient for the Flexible-12 Frame

step f); applying Equation 3.14, the required design base shear or yield strength (V_y) for the building is estimated. For the assumed triangular deformed shape, the effective modal mass coefficient (α) is equal 0.79 (Table 3.1), resulting in

$$V_y = (0.79)\ (0.22)\ (6612) = 1149 \text{ kN} \tag{4.19}$$

step g); the yield strength obtained in step f) is vertically distributed using Equations 4.1 to 4.3. From Figure 4.11, it can be seen that the period is about 2.2 sec. Alternatively, Equation 2.2 may also be used:

$$T = 2 \cdot \pi \sqrt{\frac{26}{0.22 \cdot 980.7}} = 2.18 \text{ sec.} \tag{4.20}$$

Using Equation 4.3 the additional force applied at top of the building is obtained as

$$F_t = (0.07)\ (2.18)\ (1149) = 175 \text{ kN} \tag{4.21}$$

Applying Equation 4.2, the distribution of the yield strength over the height of the frame is found. The lateral forces and the story shears are shown in Table 4.9.

Table 4.9 Design Lateral Forces and Story Shears for the Flexible-12 Frame

Story	Force [kN]	Shear [KN]
12	**322**	**322**
11	**135**	**458**
10	**123**	**581**
9	**111**	**692**
8	**99**	**791**
7	**87**	**878**
6	**75**	**954**
5	**63**	**1017**
4	**51**	**1068**
3	**39**	**1107**
2	**27**	**1134**
1	**15**	**1149**

step h); Figure 4.12 presents a set of Grade A36 steel members that has the intended strength and stiffness to allow the frame to comply with the imposed performance limits when responding to the Michoacan at SCT1 record. The fundamental period for this design is 2.17 sec.

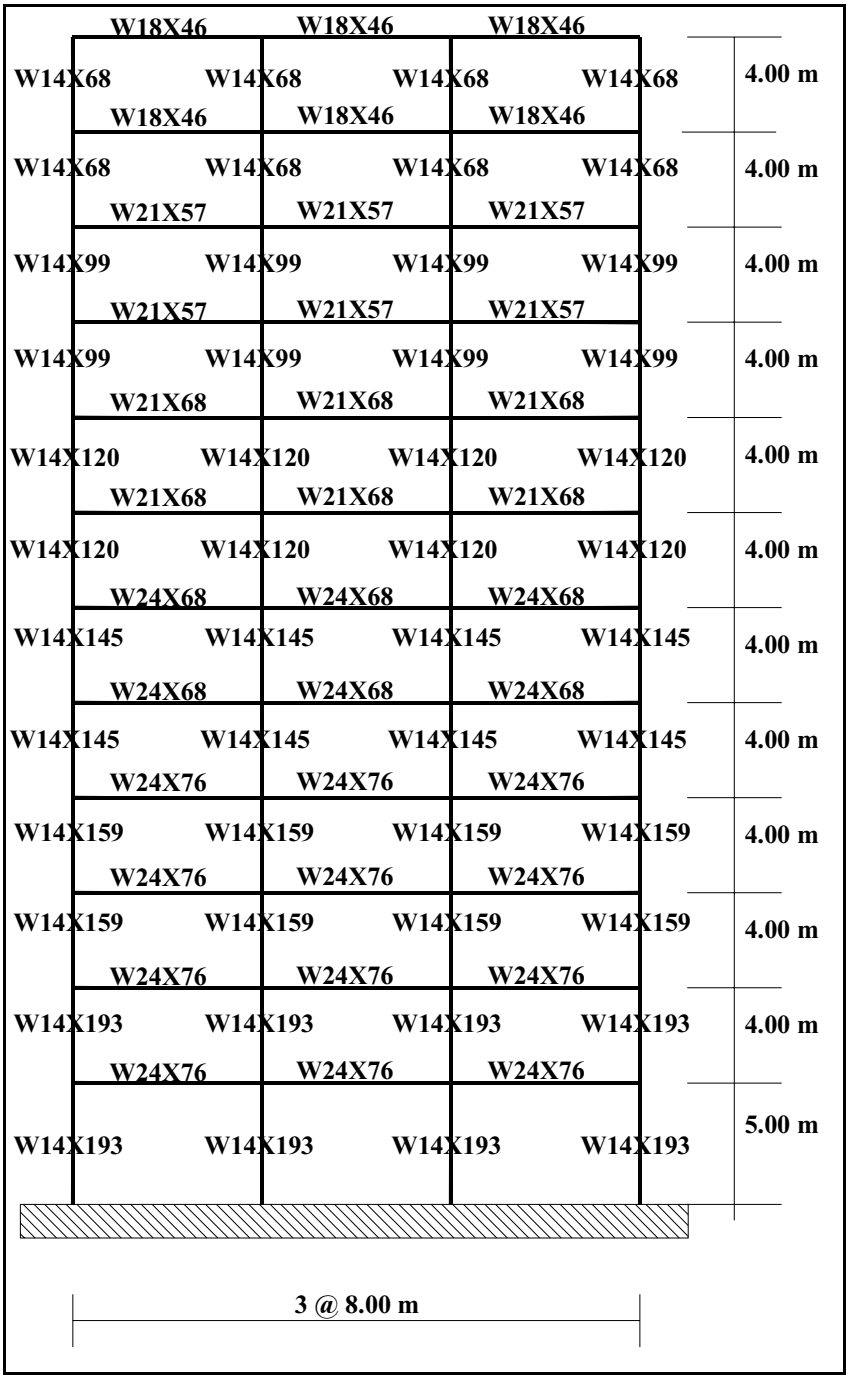

Figure 4.12 Flexible-12 Frame

T_1 = 2.17 Sec.

step i); Table 4.10 shows the results of a linear static analysis of the frame in Figure 4.12 subjected to the lateral forces of Table 4.9. Table 4.10 shows that for this design the peak roof displacement estimate, 0.781 m., is slightly larger than the limit value assumed in **step a**, 0.735 m. The maximum linear estimate of the interstory drift index is 1.77 %, less than the limit value (2.25%).

Table 4.10 Linear Estimates for the Flexible-12 Frame

Story	Height [m]	Displ. [m]	μ * Disp. [m]	IDI [%]
12	49	0.390	0.781	1.32%
11	45	0.364	0.728	1.67%
10	41	0.331	0.661	1.62%
9	37	0.298	0.597	1.75%
8	33	0.263	0.527	1.73%
7	29	0.229	0.458	1.77%
6	25	0.194	0.387	1.67%
5	21	0.160	0.320	1.69%
4	17	0.126	0.253	1.64%
3	13	0.094	0.187	1.66%
2	9	0.060	0.121	1.55%
1	5	0.029	0.059	1.02%

Verification results from static and dynamic nonlinear analyses are presented in the following figures and tables.

Figure 4.13 displays the nonlinear static (pushover) analysis curve of the frame presented on Figure 4.12. A bilinear approximation of the actual pushover curve is shown, as well as estimates for the frame yield displacement $\boldsymbol{u}_y$ and yield strength $\boldsymbol{V}_y$. The value obtained for the yield displacement, 0.353 m., is 0.72% of the building height, close to the initial estimate of 0.75%. The strength obtained with this solution, 1145 kN, is practically equal to the estimated required strength.

Figure 4.14 shows the first 80 seconds of the roof displacement history obtained from nonlinear dynamic analysis. It can be seen that the peak displacement of the roof, 0.666 m., was close to but less than the design displacement limit for this frame, 0.735 m.

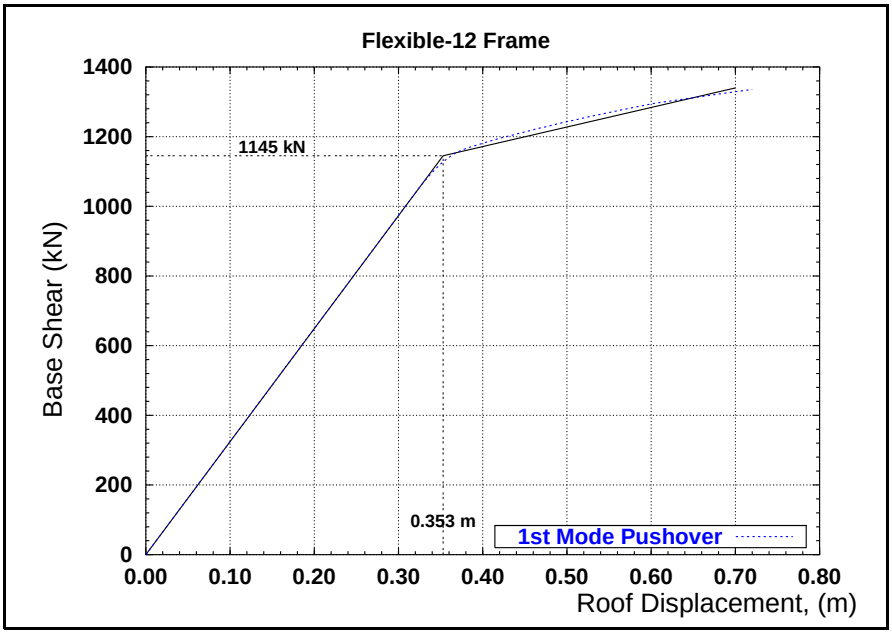

Figure 4.13 Nonlinear Static Analysis of the Flexible-12 Frame

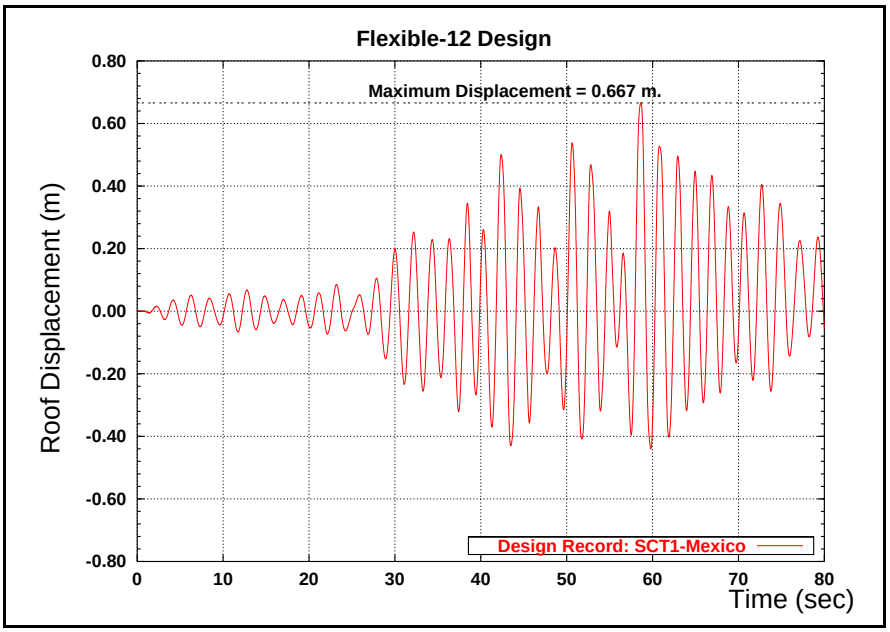

Figure 4.14 Roof Displacement from Nonlinear Dynamic Analysis of the Flexible-12 Frame

Table 4.11 presents interstory drift indices (IDI) for this frame obtained from the nonlinear time history of the frame responding to the Michoacan at Secretary of Communication and Transportation record. Peak values and their timing are presented for each story. The nonlinear dynamic analysis shows that the interstory drift indices are larger than the desired limit, 2.25%, in two stories; but the maximum IDI, 2.37%, is only 5.3% larger than the limit.

Table 4.11 Interstory Drift Indices from Nonlinear Dynamic Analysis of the Flexible-12

Story	IDI [%]	Time [Sec]
12	0.84%	60.59
11	1.14%	60.59
10	1.19%	60.61
9	1.25%	58.30
8	1.33%	58.62
7	1.76%	58.62
6	2.15%	58.61
5	2.37%	58.60
4	2.31%	58.58
3	2.12%	58.57
2	1.76%	58.31
1	1.10%	58.24

4.6.2.3 Design of Rigid-12 Using the YPS for the Takatori-kisu Ground Motion

The design continues from step d) of Section 4.6.2.1.

step e); entering the YPS for the Takatori-kisu record with the equivalent SDOF yield displacement estimate of 26 cm. and a system displacement ductility limit of 2, a yield strength coefficient (C_y) of approximately 0.60 ensures that the ductility demands do not exceed 2. This step is illustrated in Figure 4.15.

step f); the effective modal mass coefficient used here (0.79) is the same used in the previous design. The minimum required yield strength (V_y) for the frame is estimated using Equation 3.14 as

$$V_y = (0.79)\ (0.60)\ (6612) = 3134 \text{ kN} \tag{4.22}$$

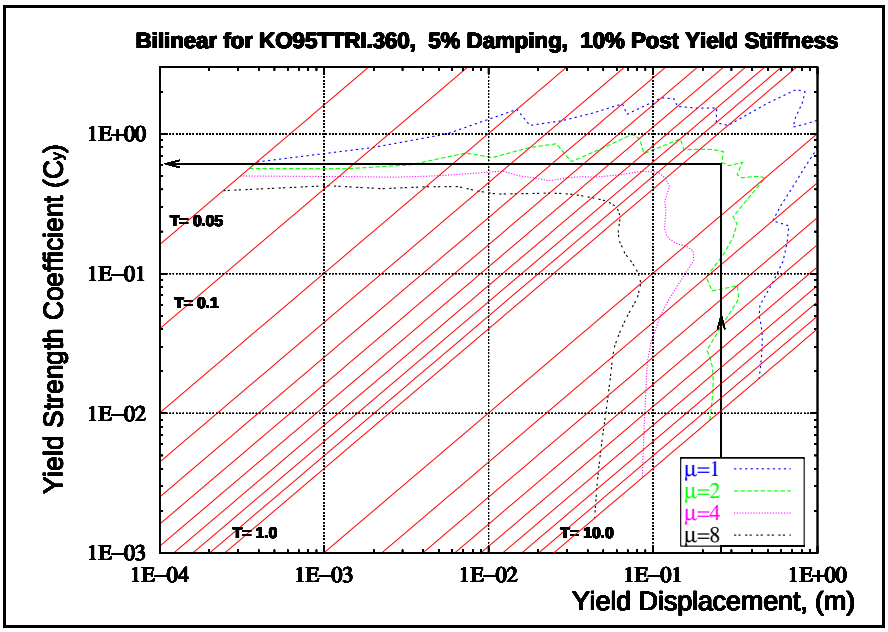

Figure 4.15 Required Yield Strength Coefficient for the Rigid-12 Frame

step g); from Figure 4.15 it can be seen that the period is about 1.3 sec. Alternatively, Equation 2.2 can also be used:

$$T = 2 \cdot \pi \cdot \sqrt{\frac{26}{0.6 \cdot 980.7}} = 1.32 \; sec. \tag{4.23}$$

Using Equation 4.3 the additional force in the top of the building is

$$F_t = (0.07)\,(1.32)\,(3134) = 290 \text{ kN} \tag{4.24}$$

Equation 4.2 gives the distribution of the base shear along the height of the building. The forces and story shears are shown in Table 4.12.

step h); Figure 4.16 presents a set of steel members that satisfy the design requirements imposed for the Hyogo-Ken Nambu at Takatori-kisu record. The fundamental period in this case is 1.25 sec.

Table 4.12 Deign Lateral Forces and Story Shears for the Rigid-12 Frame

Story	Force [kN]	Shear [kN]
12	720	720
11	395	1115
10	360	1475
9	325	1800
8	290	2089
7	255	2344
6	219	2563
5	184	2748
4	149	2897
3	114	3011
2	79	3090
1	44	3134

step i); Table 4.13 shows the results of a linear static analysis of the frame in Figure 4.16 subjected to the lateral forces presented in Table 4.12. For this design, the maximum roof displacement estimate, 0.712 m., is nearly equal to the roof displacement limit of 0.735 m. assumed in **step a**. The maximum interstory drift index, 1.69 %, is less than the nominal limit value of 2.25%.

Table 4.13 Linear Estimates for the Rigid-12 Frame

Story	High [m]	Displ. [m]	μ * Disp. [m]	IDI [%]
12	49	0.356	0.712	1.27%
11	45	0.331	0.661	1.69%
10	41	0.297	0.594	1.60%
9	37	0.265	0.530	1.68%
8	33	0.231	0.463	1.52%
7	29	0.201	0.402	1.58%
6	25	0.169	0.339	1.51%
5	21	0.139	0.278	1.54%
4	17	0.108	0.217	1.50%
3	13	0.078	0.157	1.44%
2	9	0.050	0.099	1.25%
1	5	0.025	0.049	0.99%

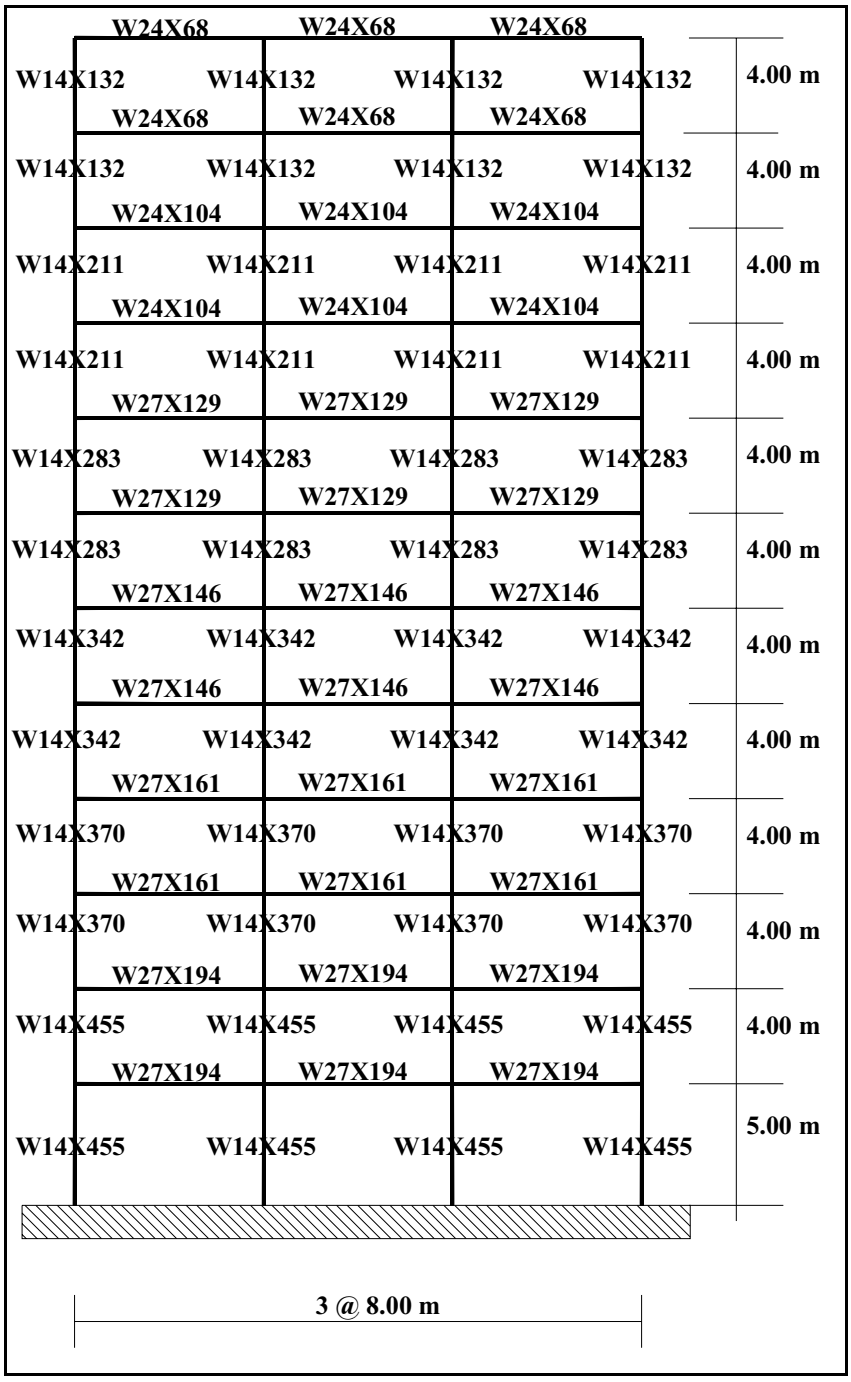

Figure 4.16 Rigid-12 Frame

T_1 = 1.25 Sec.

Results from the nonlinear analyses done to verify the design are shown in Figures 4.17 and 4.18. Figure 4.17 shows the nonlinear static (pushover) analysis curve of the frame. A bilinear approximation of the actual pushover curve is also shown, as well as estimates for the frame yield displacement u_y and yield strength V_y. The value obtained for the yield displacement, 0.335, represents 0.68% of the building height, close to the initial estimate of 0.75%. The strength obtained with this solution, 3100 kN, is 98.9% of required strength.

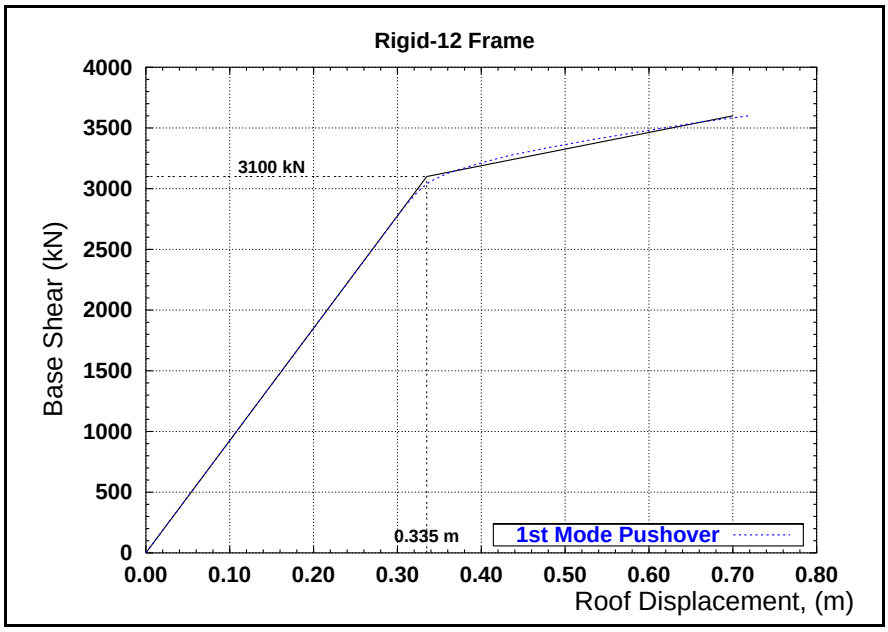

Figure 4.17 Nonlinear Static Analysis of the Rigid-12 Frame

Figure 4.18 shows the roof displacement history obtained from nonlinear analysis of the frame subjected to the Takatori-kisu record. This figure shows that the peak roof displacement estimate, 0.65 m., was less than the design limit of 0.735 m.

Table 4.9 presents values of interstory drift indices (IDI) for the Takatori-kisu record obtained from the nonlinear dynamic analysis. Peak values and their timing are presented for each story. The nonlinear dynamic analysis determined that the interstory drift indices are different than the linear estimates from Table 4.13. Even though only the maximum IDI from the nonlinear dynamic analysis, 2.28%, was larger than the nominal limit of 2.25%. The difference between these two values is only 1.3%.

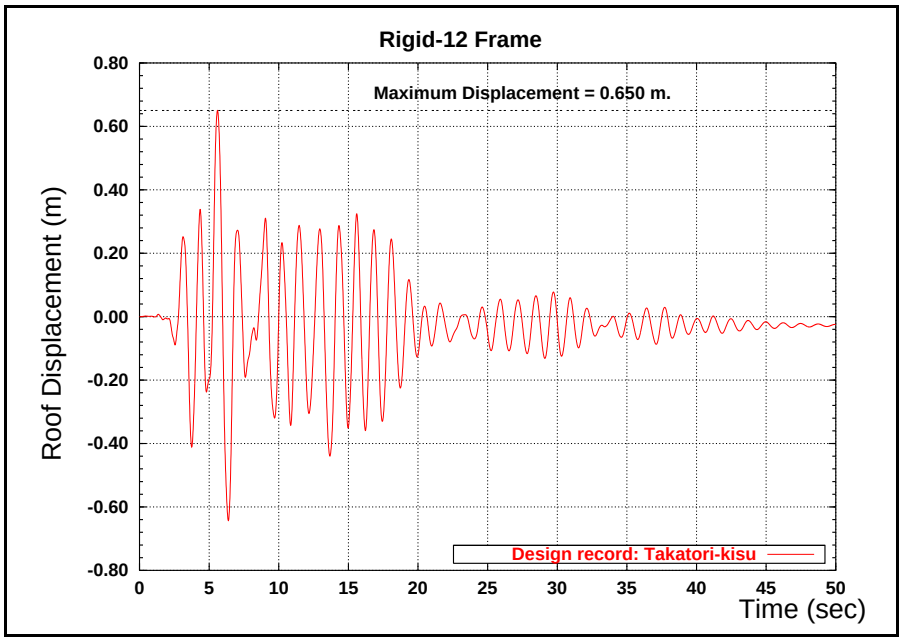

Figure 4.18 Roof Displacement from Nonlinear Dynamic Analysis of the Rigid-12 Frame

Table 4.14 Interstory Drift Indices from Nonlinear Dynamic Analysis of the Rigid-12

Story	IDI [%]	Time [Sec]
12	0.81%	6.84
11	1.33%	5.51
10	1.70%	5.55
9	1.91%	5.57
8	1.87%	5.64
7	1.99%	6.34
6	2.20%	6.35
5	2.28%	6.36
4	2.11%	6.36
3	1.74%	6.34
2	1.23%	6.29
1	0.94%	13.57

4.7 Analysis of Results

This section summarizes some results obtained from the 4 frames designed using the proposed methodology. The discussion is focused in four aspects: roof displacement control, interstory drift index control, stability of yield displacement estimate, and required minimum strength and its relation to the fundamental period of vibration.

4.7.1 Roof Displacement Control

Table 4.15 presents results of peak roof displacement. Linear estimates along with results from nonlinear dynamic analysis are shown. Ratios of peak linear and nonlinear roof displacement to the roof limit imposed for design, and the ratio of the linear estimate to the nonlinear result are included. The table also contains the mean and the standard deviation of this ratios.

Table 4.15 Peak Roof Displacement Comparison

	Roof Limit	Nonlinear Dynamic		Linear Estimate		L/NL
Frame	[m]	Disp. [m]	Ratio	Disp. [m]	Ratio	Ratio
Flexible-4	0.255	0.241	0.94	0.261	1.02	1.08
Rigid-4	0.255	0.223	0.87	0.272	1.07	1.22
Flexible-12	0.735	0.666	0.91	0.781	1.06	1.17
Rigid-12	0.735	0.650	0.88	0.712	0.97	1.10
Mean			0.902		1.030	1.143
Standard Deviation			0.031		0.045	0.065

The ratios of the nonlinear dynamic peak roof displacement to the roof displacement limit are all less than one for all the frames, with a mean of 0.902 and a small dispersion. This indicates that the proposed design methodology was effective in limiting the roof displacement of the frames. The ratios of the linear estimates to nonlinear dynamic results were larger than one for all the frames, with a mean of 1.143, indicating that linear static analyses overestimated the actual response in these frames. Additionally, the ratio of linear static analysis estimates to the intended roof displacement limit was nearly one for all the frames, with a mean of 1.030. Based on these data, results from linear static analysis scaled by the system displacement ductility may possible be an upper bound estimate of peak roof displacement. Furthermore, linear estimates may be directly compared with the intended roof limits.

4.7.2 Interstory Drift Control

Table 4.16 presents results of peak interstory drift indices. Linear IDI estimates along with IDI results from nonlinear dynamic analysis, ratios of calculated IDI to the IDI limit imposed for design, and the ratio of the linear to the nonlinear IDI results are included. The mean and the standard deviation of the ratios are also shown.

Table 4.16 Peak Interstory Drift Index Comparison

Frame	IDI Limit [%]	Nonlinear Dynamic IDI [%]	Nonlinear Dynamic Ratio	Linear Estimate IDI [%]	L/NL Ratio
Flexible-4	2.25%	2.28%	1.01	1.79%	0.79
Rigid-4	2.25%	1.64%	0.73	1.92%	1.17
Flexible-12	2.25%	2.37%	1.05	1.77%	0.75
Rigid-12	2.25%	2.28%	1.01	1.69%	0.74
Mean			0.951		0.862
Standard Deviation			0.150		0.208

The ratio of nonlinear dynamic interstory drift index to interstory drift index limit, although larger then one for three out of the four frames, the excess was very small (1.01, 1.05). The mean for this ratio was 0.951, indicating that proposed design methodology was effective in controlling the peak interstory drift index of the frames.

In general, the ratios of the linear estimates to nonlinear dynamic results were smaller than one, with a mean of 0.862. These results shows that the use of linear analysis to estimate peak interstory drift index consistently underestimated the actual peak interstory drift index.

4.7.3 Yield Displacement Stability

Table 4.17 shows means and standard deviations of the ratio of the yield displacement to the building height for the 4 frames. For all the frames, this ratio was always inside the range of (0.6%-0.9%) suggested in **step b)** of the proposed methodology . The mean, 0.74%, is in the middle of this range, with very small dispersion.

Table 4.17 Ratios of Yield Displacement to Building Height

Frame	Yield Displacement [m]	Height [m]	Ratio [%]
Flexible-4	0.129	17	0.76%
Rigid-4	0.133	17	0.78%
Flexible-12	0.353	49	0.72%
Rigid-12	0.335	49	0.68%
		Mean	0.74%
		Standard Deviation	0.00043

4.7.4 Required Strength

The set of members selected for each frame were effective in providing the frames with the required minimum strength as is shown by the ratio between the required and actual strength presented in Table 4.18.

Table 4.18 also shows the ratio between the actual first mode period and the estimated period. It is important to point out that although the lateral forces obtained in **step g)** of the methodology were used to obtain an initial set of members, the final set was found by stiffening the frame until the actual first mode period matched the estimated period given by the Yield Point Spectra (Equation 2.2).

Table 4.18 Comparison of Required to Actual Strength and First Period of Vibration

	Strength [kN]			Period [sec]		
Frame	Required by YPS	Actual	Ratio	Equation 2.2	Actual 1st	Ratio
Flexible-4	569	585	1.03	1.13	1.16	1.03
Rigid-4	1516	1500	0.99	0.70	0.71	1.01
Flexible-12	1149	1145	1.00	2.18	2.17	1.00
Rigid-12	3134	3100	0.99	1.32	1.25	0.95
Mean			1.00			1.00
Standard Deviation			0.019			0.035

The good correlation between the strength ratio and the period ratio for all the frames suggest that the procedure used to select the set of members for each of the frames, based on the actual period of the frame being designed, was effective in providing the required strength of the multistory system. Although a nonlinear static analysis could be directly used to verify the required strength, techniques to find the periods of the structure are by far much less expensive, easier to use, and more widely accessible than nonlinear static analysis.

4.8 Summary

A methodology for the design of regular multistory buildings is introduced. The methodology is intended to directly limit the roof displacement to a prescribed value. The methodology uses Yield Point Spectra, introduced in Chapter 2, to account for nonlinear behavior in the multistory system. The maximum interstory drift index is limited indirectly using a coefficient that relates the roof drift index to the maximum interstory drift. Static linear analysis can be relied on to apply the methodology.

The methodology was illustrated by designing four frames; a set of two 4-story and a set of two 12-story moment-resistant steel frames. For each set, the design ground motions were selected such that a flexible and a rigid design were obtained per set of buildings. The effectiveness of the methodology was validated using nonlinear static and dynamic analysis.

From the results obtained in Chapter 4, the following was observed:

- Yield Point Spectra can be used to design multistory buildings.
- The proposed design methodology is effective for controlling peak roof displacement and interstory drifts.
- Linear static analysis in conjunction with estimates of system ductilities can be used to obtain estimates of peak roof displacement.
- Results from linear analysis generally underestimate the peak interstory drift index.
- The ratio of yield displacement to building height seems very stable, and may lie in the vicinity of the range (0.6%-0.9%) for many moment-resistant steel frames.

CHAPTER 5

ANALYSIS OF BUILDING PERFORMANCE USING YIELD POINT SPECTRA

5.1 Introduction

The use of nonlinear static procedures (NSPs) to predict seismic force and deformation demands for evaluating the performance of new and existing structures is becoming more common in structural engineering practice. In general, NSPs use nonlinear static analysis (pushover) and the equivalent SDOF formulation to represent the response of a multistory building.

This chapter introduces an analysis method, named the YPSA method, in which Yield Point Spectra are used to estimate peak displacement response, system ductility demands, and interstory drifts. Just as in existing NSPs, the YPSA method uses nonlinear static analysis and the equivalent SDOF formulation to predict the seismic behavior of multistory systems. Therefore, the YPSA method may be classified as a NSP.

In this Chapter, peak displacement response is estimated for the four frames designed in Chapter 4, two 4-story and two 12-story buildings. The frames are analyzed using four methodologies: nonlinear dynamic analysis using DRAIN-2DX (Powell et al., 1993), the Displacement Coefficient Method (FEMA-273/274, 1997), the Capacity Spectrum Method (ATC-40, 1996), and the YPSA method as described in this chapter. For each method, the peak displacement response of the frames is estimated under the action of 15 ground motions (Section 2.7.1). The frames are identified in this Chapter as Flexible-4, Rigid-4, Flexible-12, and Rigid-12.

Additionally, the YPSA method is used to evaluate three procedures to estimate peak interstory drift index (IDI). One procedure uses a single deformed shape for estimating IDI following conventional practice, the other two estimate IDI using the first and second elastic mode shapes.

In each case, results obtained from nonlinear dynamic analysis were used as a basis for evaluating the estimates obtained with the simplified procedures. Results are reported and compared using plots and statistical analysis (means and standard deviations).

5.2 Nonlinear Static Procedures

Nonlinear Static Procedures (NSPs) are simplified techniques used to estimate the maximum expected response of a building during a ground motion. To achieve this objective, NSPs represent the response of a multistory building using an equivalent SDOF system. Two key aspects of these procedures are the nonlinear static analysis (pushover), used to determine the overall capacity of a structure, and the equivalent SDOF modeling technique.

This section reviews the nonlinear static analysis required by NSPs, and briefly summarizes two existing Nonlinear Static Procedures: the Displacement Coefficient Method (DCM) and of the Capacity Spectrum Method (CSM). The equivalent SDOF modeling technique is reviewed in Chapter 3. The NSPs are described in more detail in the FEMA-273 (*Guidelines for the Seismic Rehabilitation of Building*) and the ATC-40 (*Seismic Evaluation and Retrofit of Concrete Buildings*) documents.

Similar to existing NSPs, the YPSA method uses nonlinear static analysis and the equivalent SDOF formulation to predict the seismic behavior of multistory systems. The conceptual development for the YPSA method is presented in Section 5.3

5.2.1 Nonlinear Static Analysis

NSPs require the determination of the structural capacity of the building. The structural capacity is defined as the structure's ability to resist seismic demands, and depends on the strength and deformation capacities of the individual components of the structure.

To determine capacities beyond the elastic limits, some form of nonlinear analysis, such as the pushover procedure is required. In a pushover analysis, the mathematical model of the building, incorporating directly the nonlinear load-deformation characteristic of individual components, is subjected to monotonically increasing lateral forces or displacements until a target displacement is reached. The target displacement is intended to represent the maximum displacement likely to be experienced during the design earthquake.

Pushover analysis permits one to obtain the yield strength and yield displacement (yield point) of a structure. The yield strength and yield displacement are transformed, using Equations 5.1 to 5.3, to represent the yield point of an equivalent SDOF system required by NSP methods.

$$u_y^{SDOF} = \frac{M_{eq}}{L_{eq}} u_y^{MDOF} \tag{5.1}$$

$$C_y = \frac{V_y}{\alpha \cdot W_t} \tag{5.2}$$

$$\alpha = \frac{L_{eq}^2}{M_{eq} \cdot M_t} \tag{5.3}$$

where: u_y^{sdof} is the yield displacement of SDOF,
u_y^{mdof} is the yield displacement of MDOF,
V_y is the yield strength of the MDOF,
C_y is the yield strength coefficient,
W_t is the total weight of the building,
α is the modal mass coefficient,
L_{eq}/M_{eq} is the participation factor,
$\{\varphi\}$ mode shape representing the building lateral deformation,
M_{eq} is defined as $\{\varphi\}^T M \{\varphi\}$,
L_{eq} is defined as $\{\varphi\}^T M \{1\}$, and
M_t is defined as $\{1\}^T M \{1\}$.

The lateral loads (or displacements) used in the pushover analysis are applied in profiles that approximate the likely deformed shape of the building responding to the ground motion induced forces.

In this study, the selected deformed shape ($\{\varphi\}$) used as pattern for the pushover analysis required in the NSP methods is the same deformed shape used to apply the equivalent SDOF formulation (Equation 5.1 to 5.3).

5.2.1.1 Selecting the Appropriate Deformed Shape $\{\varphi\}$

In Chapter 3, values for the participation factor and for the modal mass coefficient were generated using approximate deformed shapes. Those values were used in Chapter 4 to design the four frames that are analyzed in this chapter.

The approximate deformed shapes shown in Chapter 3 may still be used when engineers want to check an existing design. Even though, following recommendation associated with the sophistication Level 3 of the ATC-40 (*Seismic Evaluation and Retrofit of*

Concrete Buildings), in this study the pattern used as a profile to displace or "push" the building was proportional to the fundamental mode shape. This same shape, normalized to one at the top, was used to apply the equivalent SDOF modeling technique.

Beside the ATC-40 recommendation, the reason to assume the fundamental mode as the deformed shape is the idea that the fundamental mode shape would lead to more accurate results compared to other approximate deformed shapes. Additionally, mode shapes are easily obtained using widely available computer programs.

5.2.2 Displacement Coefficient Method

The Displacement Coefficient Method (DCM) uses nonlinear static pushover analysis of the building and a modified version of the equal displacement rule to estimate maximum displacements for MDOF buildings. Similar to other NSPs, the DCM also uses parameters derived from the equivalent SDOF methodology to obtain the displacement estimation.

In the DCM method, peak displacement response is estimated as the product of a series of coefficients and the spectral displacement of an elastic oscillator.

The peak displacement estimate, δ_t is given by

$$\delta_t = C_0 C_1 C_2 C_3 S_a \frac{T_e^2}{4\pi^2} g \tag{5.4}$$

where: $\boldsymbol{C_0}$ is a modification factor to relate spectral displacement to expected roof displacement,
$\boldsymbol{C_1}$ is a modification factor to relate expected maximum displacements to displacement calculated for linear elastic response,
$\boldsymbol{C_2}$ is a modification factor to represent the type of hysteretic response,
$\boldsymbol{C_3}$ is a modification factor to represent dynamic P-Δ effects,
$\boldsymbol{S_a}$ is the response spectrum acceleration,
$\boldsymbol{T_e}$ is the effective fundamental period of the building and
$\boldsymbol{g}$ is the acceleration of gravity.

The coefficient $\boldsymbol{C_0}$ is equivalent to the participation factor. Its value was taken equal to the ratio $\boldsymbol{L_{eq}/M_{eq}}$ defined in this study. The coefficient $\boldsymbol{C_1}$ accounts for the trend that the peak displacement of short period nonlinears system exceeds thatof a linear elastic system having the same period and damping. For short period systems, $\boldsymbol{T_e < T_0}$ ($\boldsymbol{T_0}$ = characteristic period of the ground motion); $\boldsymbol{C_1}$ is given by

$$C_1 = \frac{T_e + (R-1)T_0}{T_e R} \tag{5.5}$$

where $\boldsymbol{R}$ is the ratio of elastic strength demand to calculated yield strength coefficient. For long period systems, $\boldsymbol{T_e > T_0}$, the "equal displacement rule" applies and $\boldsymbol{C_1}$ = 1.0. The values of $\boldsymbol{C_2}$ and $\boldsymbol{C_3}$ were taken as 1.0 for all the cases.

Results for the DCM were obtained using a computer program written for this research. For each case, the response spectrum acceleration, S_a, corresponding to the effective period of the building, was obtained from the actual acceleration records. No smoothed spectrum was used here. Values for the characteristic period of the ground motion T_0 are listed in Table 2.2. The computer program implementing the DCM is included as Appendix B.

5.2.3 Capacity Spectrum Method

The Capacity Spectrum Method is an iterative process in which it is assumed that the peak displacement response of a nonlinear system can be estimated as the response of an elastic system having reduced stiffness and increased damping.

In the Capacity Spectrum Method, a first displacement is estimated using the initial stiffness of the structure assuming elastic response with damping equal to 5% of critical damping. Then, an estimate of the secant stiffness is obtained using the intersection of the displacement estimate and the curve representing the capacity spectrum. Effective viscous damping is revised based on the displacement estimate. Using the current secant stiffness and adjusted damping, a new displacement estimate is obtained. The iterations continue until satisfactory convergence is obtained.

A computer program was written to implement the Capacity Spectrum Method. The program was run using all the parameters corresponding to the Structural Behavior Type A (New Buildings) as defined in ATC-40. The actual ground motion records were used to estimate the elastic response of the 5% damped oscillator, and this response was reduced to account for the increasing damping using equations found in ATC-40. The computer program is included as Appendix C.

5.3 Conceptual Development of the YPSA Method

Similar to others NSPs, the YPSA method requires that the yield strength and yield displacement of the structure be expressed in terms of the yield strength coefficient (C_y) and yield displacement of an equivalent single-degree-of-freedom (u_y^{sdof}). This is done using Equations 5.1 to 5.3

5.3.1 Estimating Peak Displacement Using the YPSA Method

In the YPSA method, the peak displacement estimate of a MDOF system can be obtained using equation 5.6 for any assumed deformed shape $\{\varphi\}$ as

$$u_u^{mdof} = \frac{L_{eq}}{M_{eq}} \mu \; max\left(u_{el}^{sdof}\right) \tag{5.6}$$

where: u_u^{sdof} is the estimated peak displacement of the MDOF system,

L_{eq}/M_{eq} is the participation factor for the assumed deformed shape,

μ is the system displacement ductility, and

$max(u_{el}^{sdof})$ is the maximum elastic displacement of the equivalent SDOF.

The YPS used for the analysis allow to determine the type of response (linear or nonlinear) expected for the structure. Depending on the type of response, the maximum elastic displacement of the equivalent SDOF system, $max(u_{el}^{sdof})$, or the system displacement ductility, μ, are estimated form the YPS for use in Equation 5.6.

For nonlinear response ($\mu > 1$), the system displacement ductility is estimated form the YPS while the maximum elastic displacement of the equivalent SDOF, $max(u_{el}^{sdof})$, must be taken equal to the yield displacement of the equivalent SDOF system.

For elastic response ($\mu \leq 1$), the system displacement ductility must be taken equal to 1 in Equation 5.6 and the maximum elastic displacement of the equivalent SDOF system is estimated form the YPS.

Examples showing the use of Equation 5.6 for elastic and a nonlinear responses are presented in Section 5.4.2.

5.3.2 Estimating Interstory Drift Index Using the YPSA Method

Although the value of maximum roof displacement is a direct way to quantify the overall response of a building, it provides no direct information about localized deformation within a structure. Typically, seismic codes dictate requirements to control the interstory drift in each story rather than the peak roof displacement. The interstory drift index (IDI) is defined as the displacement of any floor relative to the floor immediately below, normalized by the story height.

Investigators have quantified the interstory drift index in recent years (Qi and Moehle, 1991; Collins, Wen and Foutch, 1995; Lepage, 1997). In general, the peak IDI can be expressed as the roof drift index times a coefficient of distortion. The roof drift index is defined as the peak roof displacement normalized by building height. The coefficient of distortion is defined as the ratio of the peak interstory drift index to the average drift index.

In general, the coefficient of distortion, and therefore the IDI, is based on the deformed shape of the building at the moment the peak roof displacement occurs. Since one hypothesis of the equivalent SDOF methodology is that the deformed shape of the structure remains constant during the response, values of the peak IDI depends on the deformed shape assumed in applying the equivalent SDOF methodology. Consistent with this hypothesis, the interstory drift index profile of the structure may be estimated as

$$IDI^{j} = u_{u}^{mdof} \cdot IDI^{j}(\phi) \tag{5.7}$$

where: IDI^{j} is the estimated interstory drift index for story j,

u_{u}^{mdof} is the peak roof displacement of the structure (Equation 5.6), based on the assumed deformed shape $\{\varphi\}$, and

$IDI^{j}(\varphi)$ is the modal interstory drift index for story j, defined as the interstory drift indexed calculated for the assumed deformed shape $\{\varphi\}$.

Results from previous work indicate that use of the average drift ratio combined with the coefficient of distortion to estimate peak IDI is less accurate than the estimates for peak roof displacement. These previous results suggest that the use of only one deformed shape, may be inadequate for accurately estimating interstory drift indices.

Combinations of two deformed shapes may be used to obtain improved interstory drift index estimates. The same procedure used to obtain the peak roof displacement based on

the fundamental mode shape may also be applied to obtain an estimate of the peak roof displacement based on the second mode. For this case the second mode must be assumed as the deformed shape. First and second mode profiles of interstory drift indices are obtained using Equation 5.7 and the the first and second mode shapes respectively.

These two IDI profiles can be combined in various ways to estimate the IDI profile of the building based on two modes. The square root of the sum of the squares and the absolute sum combinations, given in Equation 5.8 and 5.9, are evaluated in this chapter.

$$IDI^{j} = \sqrt{\left(u_{u1}^{mdof} \cdot IDI^{j}(\phi_1)\right)^2 + \left(u_{u2}^{mdof} \cdot IDI^{j}(\phi_2)\right)^2} \tag{5.8}$$

$$IDI^{j} = \left|u_{u1}^{mdof} \cdot IDI^{j}(\phi_1)\right| + \left|u_{u2}^{mdof} \cdot IDI^{j}(\phi_2)\right| \tag{5.9}$$

where IDI^j is the estimated interstory drift index for story j,
$IDI^j(\varphi_i)$ is the modal interstory drift calculated from the assumed mode shape ϕ_i, and
u_u^{mdof} is the peak roof displacement, obtained using Equation 5.6, associated with mode i.

An example showing the use of Equations 5.8 and 5.9 is presented in Section 5.4.3.

5.4 Peak Roof Displacement and IDI Estimates for 4- and 12-Story Frames

Four moment-resistant steel frames, designed in Chapter 4 are analyzed in this section. The frames are identified Flexible-4, Rigid-4, Flexible-12, and Rigid-12. Section 5.4.1 summarizes the main characteristics of the four frames.

According to the ideas expressed in Section 5.2.1.1, the mode shape assumed to estimate peak displacement using the Nonlinear Static Procedures (DCM, CSM, and YPSA method) is the first mode shape. Peak roof displacement estimates for the three NSPs as well as an analysis of results are presented in Section 5.4.2.

First and second mode shape results are combined to calculate interstory drift indices using the YPSA method. Peak IDI estimates obtained using the YPSA method and an analysis of results are presented in Section 5.4.3.

5.4.1 Characteristics of Frames

Table 5.1 shows values corresponding to the first and second mode shapes and modal interstory drift indices for the 4-story frames. Table 5.2 has similar information for the 12-story buildings. All the mode shapes are normalized with respect to the displacement of the top of the frame.

Table 5.1 First and Second Mode Shapes and Modal Interstory Drift Indices of the Flexible-4 and Rigid-4 Frames

Story	Flexible-4				Rigid-4			
Height [m]	1st Mode	IDI(ϕ_1)	2nd mode	IDI(ϕ_2)	1st Mode	IDI(ϕ_1)	2nd mode	IDI(ϕ_2)
4	1.0000	3.66%	1.0000	27.74%	1.0000	5.03%	1.0000	31.14%
4	0.8536	6.45%	-0.1097	23.34%	0.7989	7.08%	-0.2457	21.33%
4	0.5957	7.06%	-1.0432	-3.35%	0.5157	6.04%	-1.0989	-5.88%
5	0.3134	6.27%	-0.9093	-18.19%	0.2743	5.49%	-0.8638	-17.28%

Table 5.2 First and Second Mode Shapes and Modal Interstory Drift Indices of the Flexible-12 and Rigid-12 Frames

Story	Flexible-12				Rigid-12			
Height [m]	1st Mode	IDI(ϕ_1)	2nd mode	IDI(ϕ_2)	1st Mode	IDI(ϕ_1)	2nd mode	IDI(ϕ_2)
4	1.0000	1.13%	1.0000	7.23%	1.0000	1.40%	1.0000	8.24%
4	0.9546	1.70%	0.7109	9.96%	0.9442	2.09%	0.6703	11.23%
4	0.8868	1.87%	0.3124	9.04%	0.8605	2.15%	0.2211	9.15%
4	0.8120	2.17%	-0.0490	8.15%	0.7747	2.35%	-0.1448	7.53%
4	0.7254	2.24%	-0.3751	5.77%	0.6806	2.18%	-0.4460	4.39%
4	0.6356	2.37%	-0.6057	3.45%	0.5932	2.31%	-0.6215	2.25%
4	0.5409	2.29%	-0.7437	0.86%	0.5008	2.23%	-0.7113	0.04%
4	0.4492	2.34%	-0.7780	-1.28%	0.4117	2.28%	-0.7129	-1.78%
4	0.3556	2.29%	-0.7267	-3.08%	0.3205	2.22%	-0.6419	-3.20%
4	0.2640	2.34%	-0.6034	-4.58%	0.2317	2.13%	-0.5138	-4.13%
4	0.1704	2.19%	-0.4203	-5.17%	0.1465	1.84%	-0.3487	-4.21%
5	0.0828	1.66%	-0.2136	-4.27%	0.0728	1.46%	-0.1804	-3.61%

The data contained in Tables 5.1 and 5.2 are plotted in Figures 5.1 and 5.2 respectively. Figure 5.1(a) plots the first and second mode shapes while Figure 5.1(b) plots the modal interstory drift indices for the 4-story frames. Figure 5.2 is similar to Figure 5.1 but for the 12-story buildings.

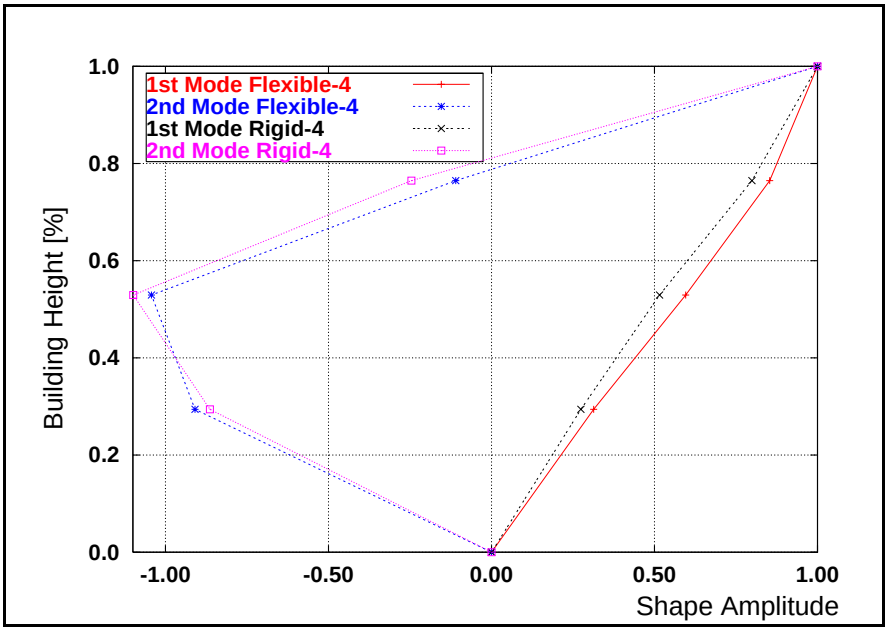

(a)

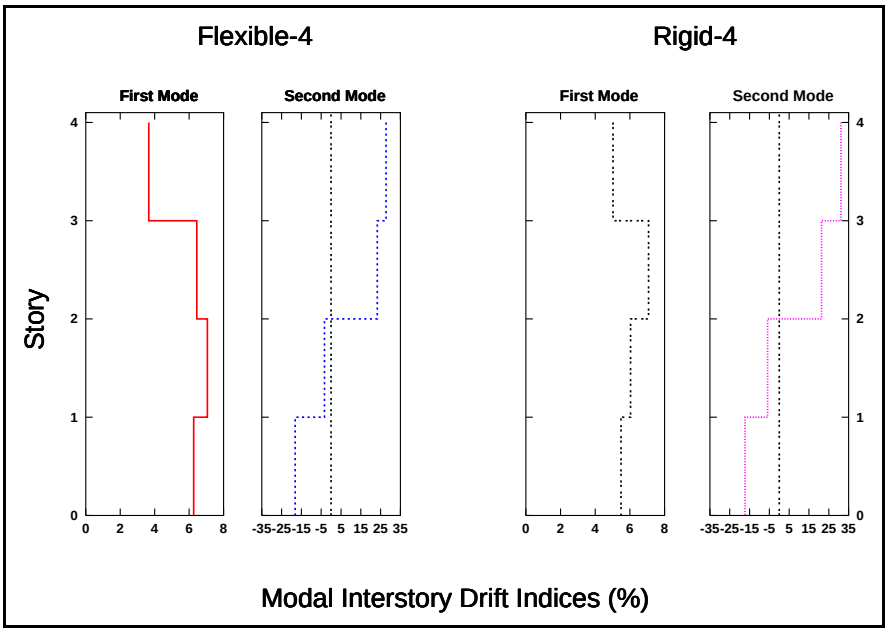

(b)

Figure 5.1 Mode Shapes and Profiles of Modal IDI for the 4-Story Frames

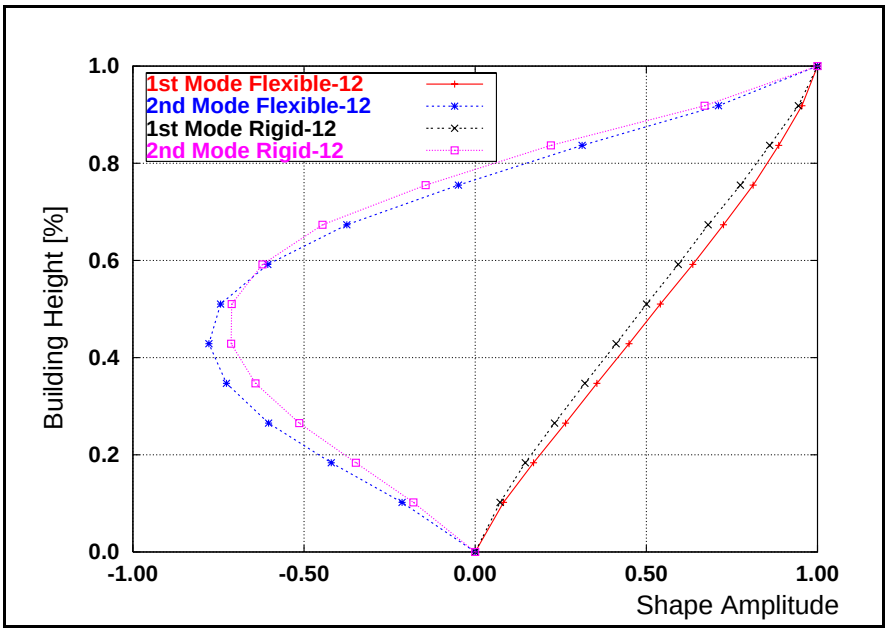

(a)

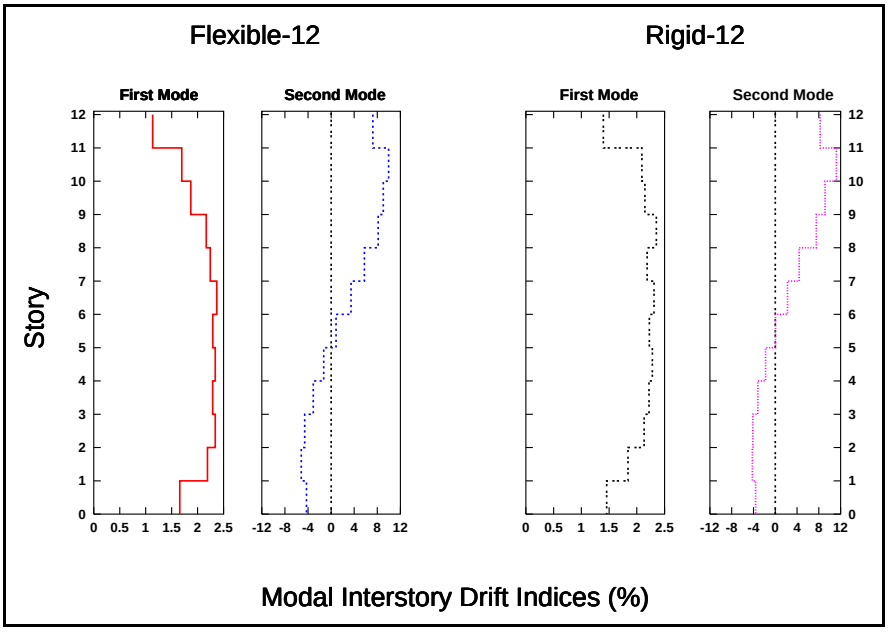

(b)

Figure 5.2 Mode Shapes and Profiles of Modal IDI for the 12-Story Frames

Table 5.3 presents values for the participation factors and the modal mass coefficient for each of the four frames, based on their first and second mode shapes. A uniform story weight of 551 kN was assumed for all frames resulting in a total weight of 2204 kN for the 4-story frames (Flexible-4 and Rigid-4) and 6612 kN for the 12-story frames (Flexible-12 and Rigid-12). Additional information about the frames is presented in Chapter 4. The first mode participation factor and the modal mass coefficient in Table 5.3 are used in the three NSPs for estimating peak roof displacements.

Table 5.3 Participation Factors and Modal Mass Coefficients of the Frames

	1st Mode		2nd Mode	
	L_{eq} / M_{eq}	α_1	L_{eq} / M_{eq}	α_2
Flexible-4	**1.266**	**0.875**	**0.363**	**0.096**
Rigid-4	**1.308**	**0.847**	**0.401**	**0.121**
Flexible-12	**1.372**	**0.786**	**0.568**	**0.118**
Rigid-12	**1.406**	**0.766**	**0.615**	**0.125**

Figure 5.3 to Figure 5.6 show the load-deformation curves obtained from pushover analyses for the Flexible-4, Rigid-4, Flexible-12, and Rigid-12 frames, respectively. The curves were obtained assuming the first and second elastic mode as deformed pattern to displace or "push" the frames. Values of the yield displacement and yield strength for bilinear approximations to the first and second mode load-deformation curves are indicated in the plots.

The pushover curves were obtained by monotonically applying increasing lateral displacements (displacement control nonlinear analysis) in a pattern proportional to the first and second mode shapes of the corresponding frame.

The program DRAIN-2DX (Powell et al., 1993) was used to obtain the pushover curves. A simple inelastic element (Element 02), capable of developing plastic hinges, was used along the centerlines of the frames. Plastic hinge strengths were assumed equal to the yield moments (F_y S) with strain hardening equal to 5% of Young's modulus. The yield strength of the steel was assumed as 248.0E+3 kN/m^2 (36 ksi).

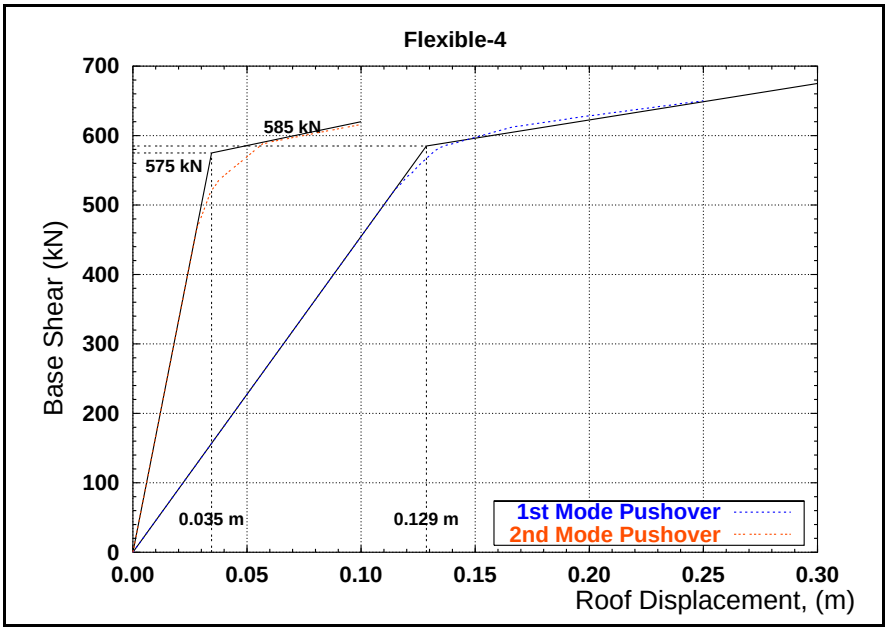

Figure 5.3 First and Second Mode Load-Deformation Curves for the Flexible-4 Frame

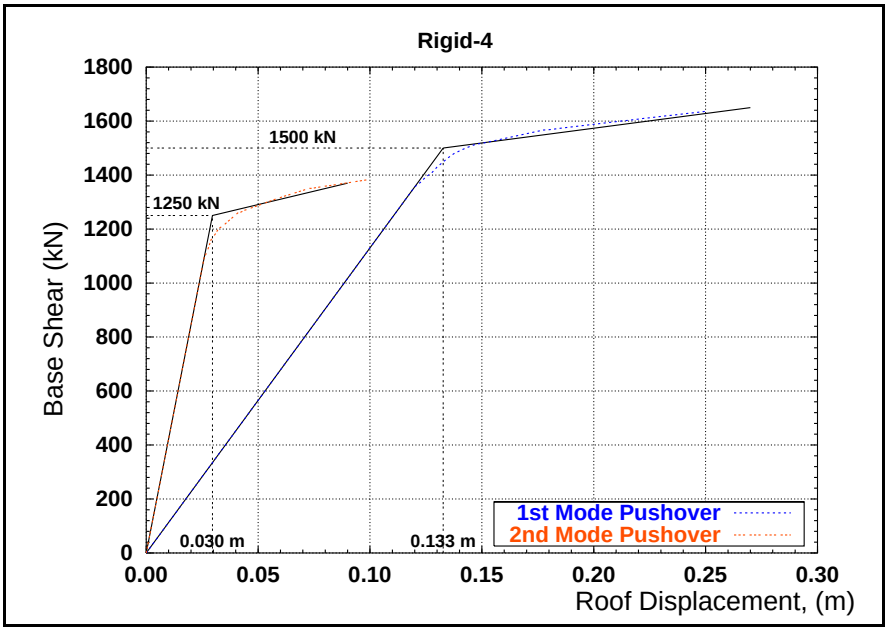

Figure 5.4 First and Second Mode Load-Deformation Curves for the Rigid-4

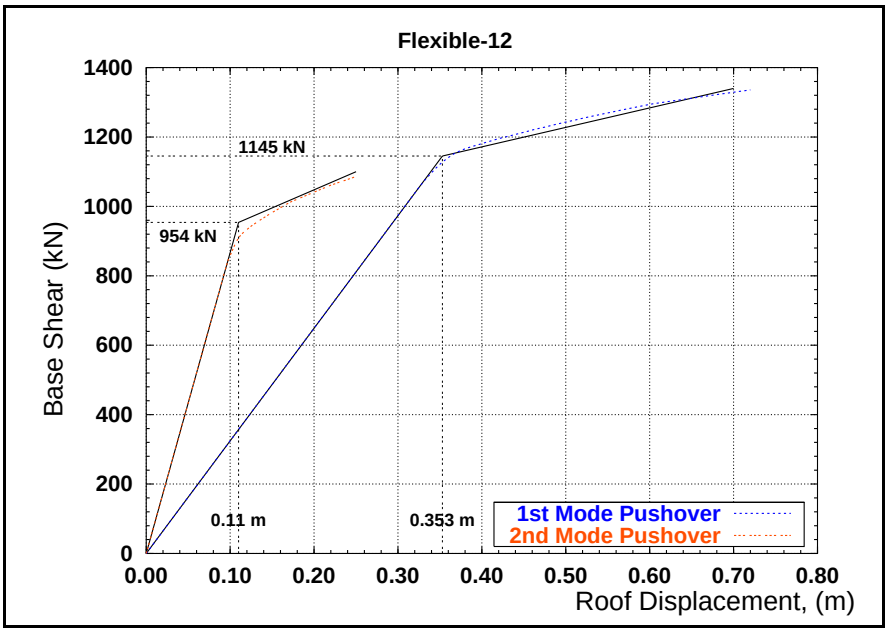

Figure 5.5 First and Second Mode Load-Deformation Curves for the Flexible-12

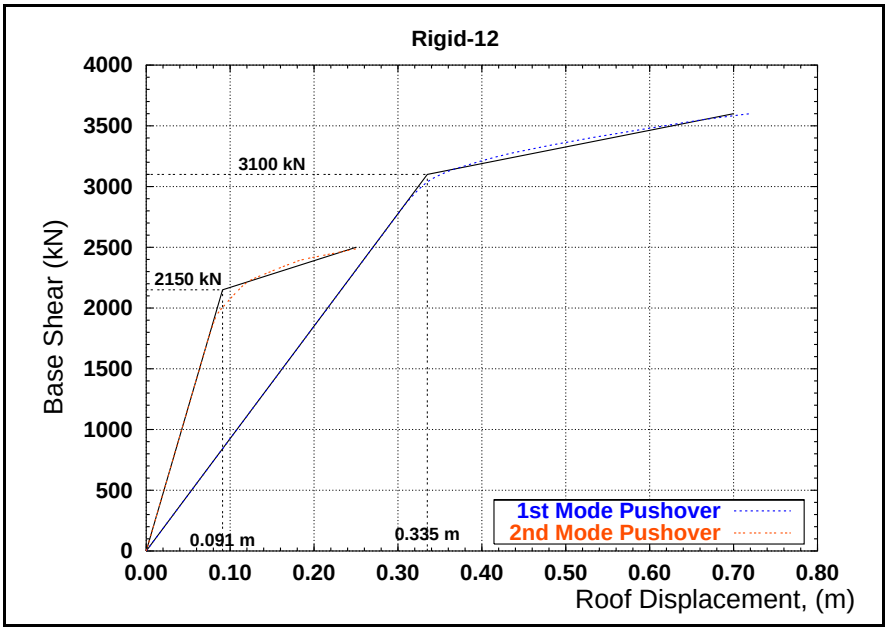

Figure 5.6 First and Second Mode Load-Deformation Curves for the Rigid-12

Table 5.4 shows values of the yield strength and yield displacement for the frames along with corresponding values of the equivalent SDOF systems. The equivalent SDOF yield displacement and strength are obtained using Equation 5.1 and 5.2, and the respective assumed deformed shape (first or second elastic mode shape). All the parameters in part (a) of Table 5.4 relate to the first mode shape while the parameters in part (b) refer to the second mode shape.

Notice that the values of the yield strength coefficients (C_y) in Table 5.4 closely agree with the corresponding original yield strength coefficients used for design (Chapter 4). Those yield strength coefficients were obtained using participation factors corresponding to an approximate triangular deformed shape, indicating that this assumed deformed shape was appropriate for design.

Table 5.4 also lists the periods of vibration corresponding to the first and second mode of the equivalent SDOF obtained using Equation 2.2.

Table 5.4 Yield Strength and Yield Displacement of the Frames

First Mode Parameters

	V_y [kN]	u_y [m]	C_y	u_y^{SDOF} [m]	T_1 [sec]
Flexible-4	**585**	**0.129**	**0.303**	**0.102**	**1.16**
Rigid-4	**1500**	**0.133**	**0.804**	**0.101**	**0.71**
Flexible-12	**1145**	**0.353**	**0.220**	**0.257**	**2.17**
Rigid-12	**3100**	**0.335**	**0.612**	**0.238**	**1.25**

(a)

Second Mode Parameters

	V_y [kN]	u_y [m]	C_y	u_y^{SDOF} [m]	T_2 [sec]
Flexible-4	**575**	**0.035**	**2.708**	**0.095**	**0.38**
Rigid-4	**1250**	**0.030**	**4.682**	**0.074**	**0.25**
Flexible-12	**954**	**0.110**	**1.223**	**0.194**	**0.80**
Rigid-12	**2150**	**0.091**	**2.610**	**0.148**	**0.48**

(b)

5.4.2 Peak Displacement Estimates

Three simplified nonlinear static methods, the Displacement Coefficient Method, the Capacity Spectrum Method and the Yield Point Spectra Analysis method are used to estimate the peak displacement of the roof for the four frames under the action of the 15 ground motions selected for this study.

The results of each simplified procedure are compared with peak displacement obtained from nonlinear dynamic displacement histories analyses of the frames. Results for each procedure are compared using plots and using simple statistical analysis.

A numerical example is provided to illustrate how the YPSA method is used to estimate the peak displacement response of a multistory frame. The Yield Point Spectra corresponding to the 1940 N-S component of the El Centro record (IV40ELCN.180) and Equation 5.6 are used to estimate peak displacements for the Flexible-4 and Rigid-4 frames.

The participation factor for the Flexible-4 frame is 1.266 and for the Rigid-4 frame is 1.308. These factors are in Table 5.3. The equivalent SDOF yield displacements for the Flexible-4 and Rigid-4 frames are 10.2 and 10.1 cm. and the yield strength coefficients are 0.303 and 0.804 respectively (see Table 5.4a).

The equivalent SDOF yield points for these two frames are plotted in Figure 5.7; with 'x' used for the Flexible-4 frame and '**+**' used for the Rigid-4 frame. The periods of vibration of the equivalents SDOF systems are represented by dotted diagonal lines.

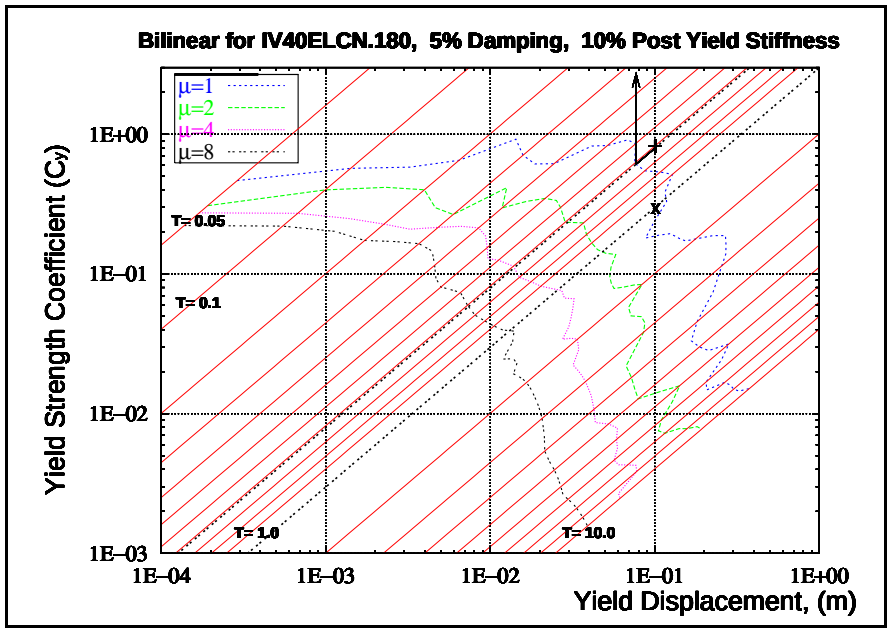

Figure 5.7 Yield Points for the 4-Story Frames

'x' indicates Yield Point for Flexible-4

'+' indicates Yield Point for Rigid-4

In Figure 5.7 it can be seen that the yield point corresponding to the Flexible-4 frame lies between the curves corresponding to ductility of 1 and 2. This yield point is located at about 16% of the distance measured from the curve corresponding to a ductility of 1 to the curve corresponding to a ductility of 2. Therefore, the ductility demand associated with this frame responding to El Centro record is estimated as $2^{0.16} = 1.117$, and its peak displacement is estimated, using Equation 5.6, as:

$$u_u^{mdof} = (1.\ 266)\ (1.117)\ (10.2) = 14.4 \text{ cm.} \tag{5.10}$$

Figure 5.7 also shows that the yield point corresponding to the Rigid-4 frame lies beyond the curve corresponding to ductility of 1; therefore, the response of this frame responding to El Centro record is elastic and the ductility demand to be used in Equation 5.6 must be taken equal to one.

An arrow indicates that the equivalent SDOF system associated with this frame has a maximum elastic displacement of approximately 7.70 cm. Therefore, using Equation 5.6, the estimate of the peak displacement for Rigid-4 frame under El Centro record is equal to:

$$u_u^{mdof} = (1.\ 308)\ (1.0)\ (7.7) = 10.1 \text{ cm.} \tag{5.11}$$

5.4.2.1 Numerical Results

The following figures and tables present results for maximum peak displacement estimated using the YPSA Method, the Displacement Coefficient Method, and the Capacity Spectrum Method. Peak displacements determined by nonlinear dynamic analyses are reported along with displacement estimates obtained using the NSPs.

The participation factors (L_{eq}/M_{eq}) are in Table 5.3, and the equivalent SDOF parameters for the frames are in Table 5.4a.

Peak displacements estimated by the YPSA method are obtained using Equation 5.6 and Yield Point Spectra for the 15 ground motion records considered. For all the frames, the system displacement ductility ( ) or maximum elastic displacement of the equivalent SDOF ($max(u_{el}^{sdof})$) are read from the YPS in the same way as it was illustrated using Figure 5.7. These YPS are presented in Appendix D, Figures D.1(a) to D.30(a), at the end of this report. Tables 5.5 to 5.8 summarize the data used with Equation 5.6.

Results for the Displacement Coefficient Method and the Capacity Spectrum Method were obtained using computer programs specially written for this research. These computer programs are included in Appendix B and C at the end of this work. Tables 5.9 to 5.12 summarize the results for these NSPs.

For all the nonlinear static methods, a post-yield stiffness of 10% of the initial stiffness and damping equal to 5% of critical damping was assumed. For the nonlinear dynamic analysis performed with DRAIN 2DX, the damping parameters for the four frames were set to produce 5% critical damping in the first mode of vibration. The damping parameters were set to also produce 5% critical damping in the 4^{th} and 6^{th} modes for the 4- and 12-story frames, respectively.

Figures 5.8 to 5.11 contain two plots that help to visualize and compare the results obtained with the three simplified NSPs.

In the upper plots of these figures (part a), the peak roof displacement obtained using DRAIN-2DX is plotted on the abscissa while the peak roof displacement estimate obtained with the NSPs are plotted on the ordinate. The diagonal line represents perfect correlation between the peak displacements obtained with the dynamic nonlinear analysis of the frames and the simplified method estimates. Any points below this line represent a displacement underestimation on the part of the simplified method, while points above this line represent displacement overestimation. A dotted vertical line indicates the yield displacement for the frames. This line allows to gauge the accuracy of the NSPs as a function of the degree of nonlinearity in the system.

The lower plot (part b), of Figures 5.8 to 5.11 show the different ground motion records on the abscissa while the ordinate plots the ratio of the NSPs peak displacement estimates and nonlinear dynamic analysis results. The earthquakes are arranged on the abscissa following the order used in Table 5.5. Data supporting theses figures is presented in Tables 5.5 to 5.12.

Part (a) and (b) of Figures 5.8 to 5.11 complement each other; part (a) displays the magnitude of the peak displacement response and the accuracy achieved for each of the NSPs, and part (b) shows the accuracy of the NSPs with respect to each ground motion record.

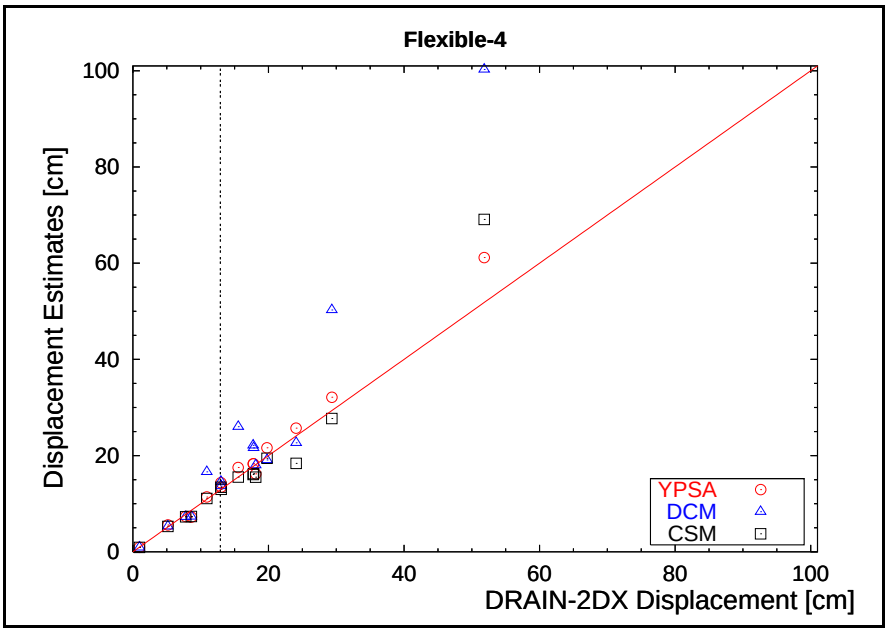

(a)

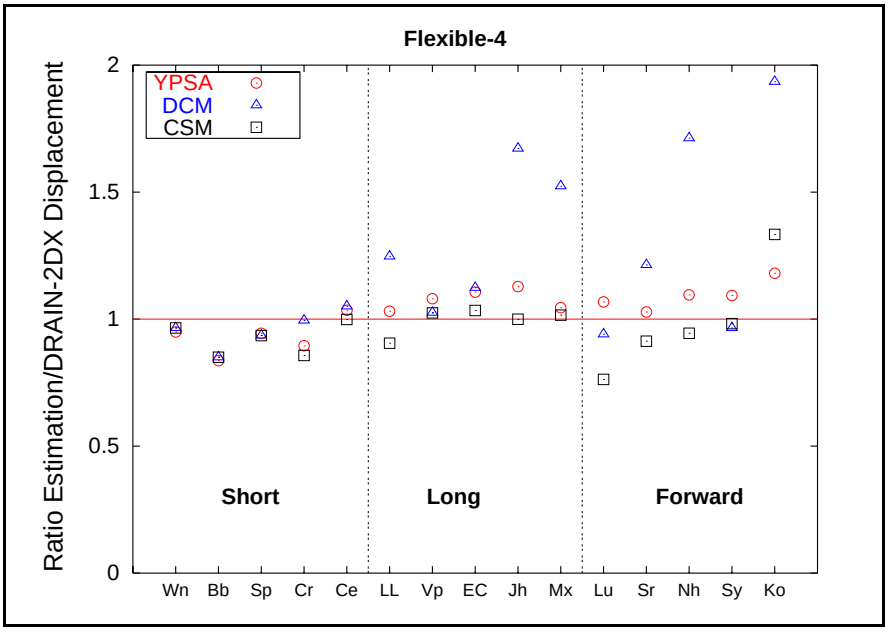

(b)

Figure 5.8 Peak Roof Displacement Comparisons for the Flexible-4 Frame

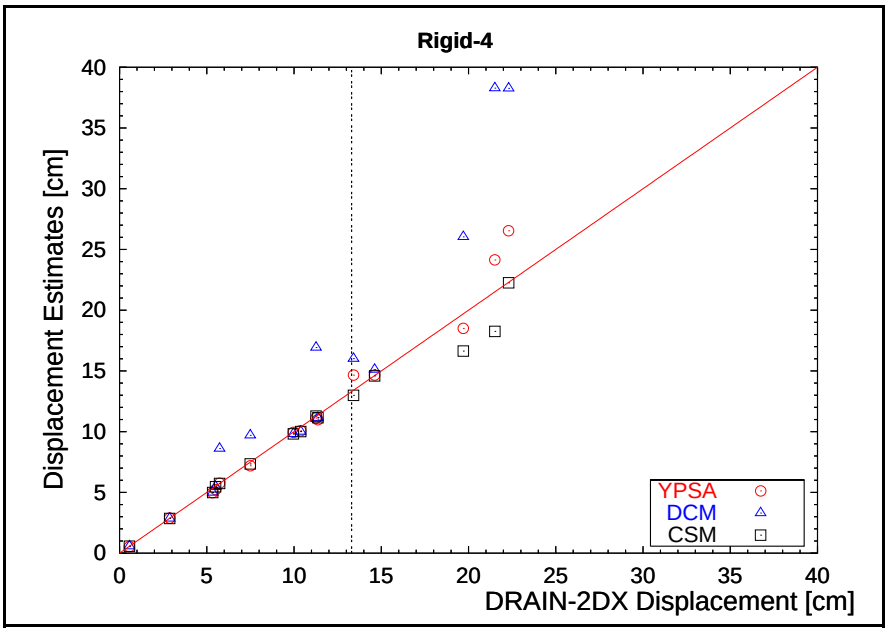

(a)

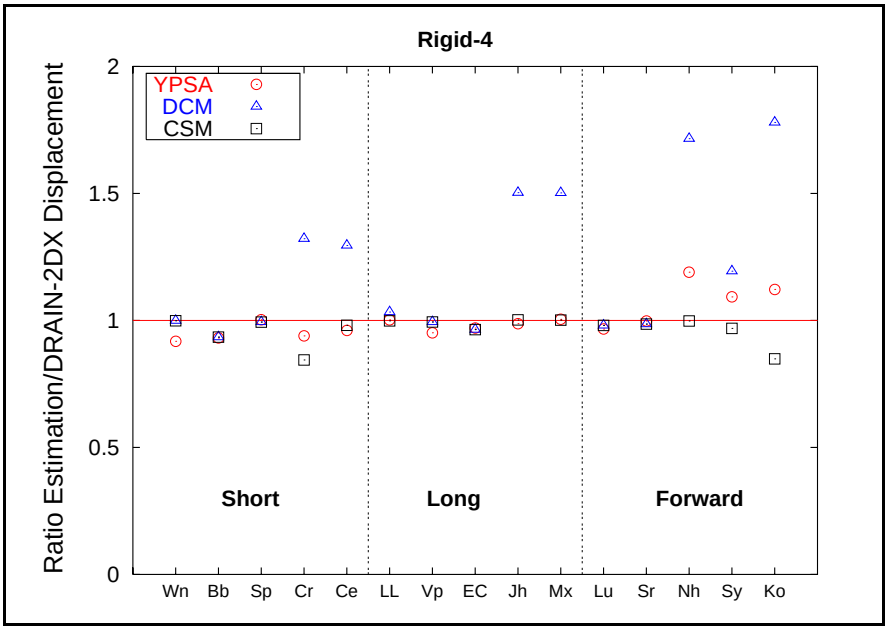

(b)

Figure 5.9 Peak Roof Displacement Comparisons for the Rigid-4 Frame

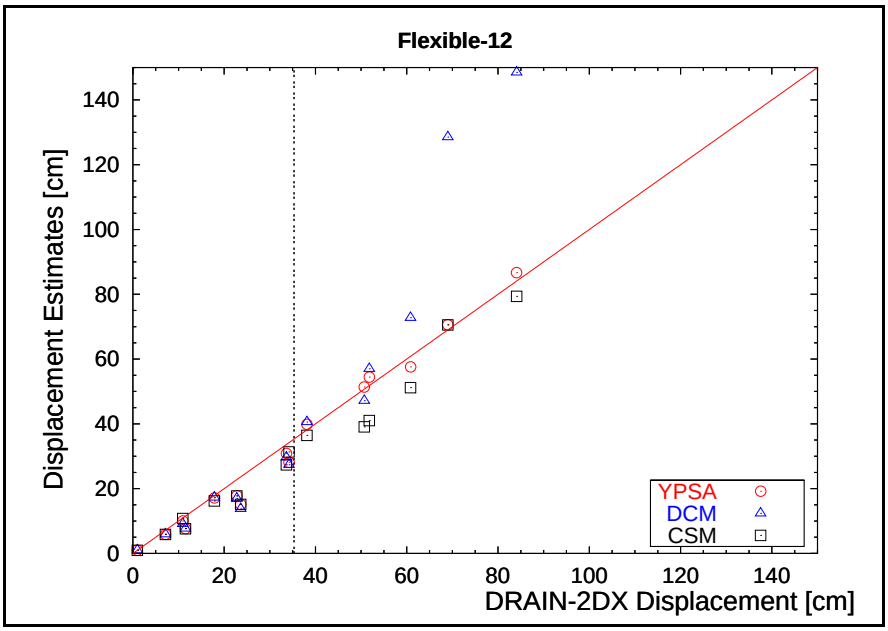

(a)

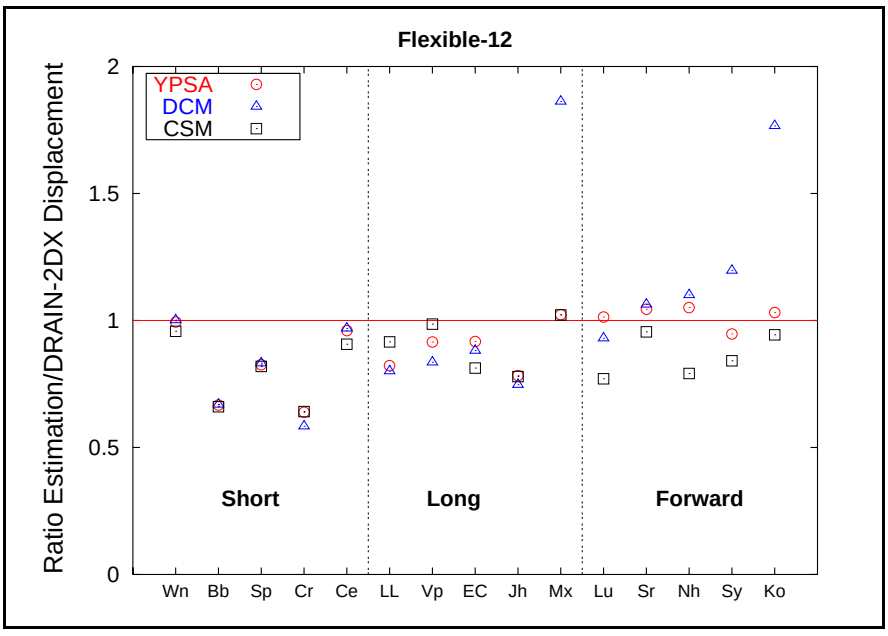

(b)

Figure 5.10 Peak Roof Displacement Comparison for the Flexible-12 Frame

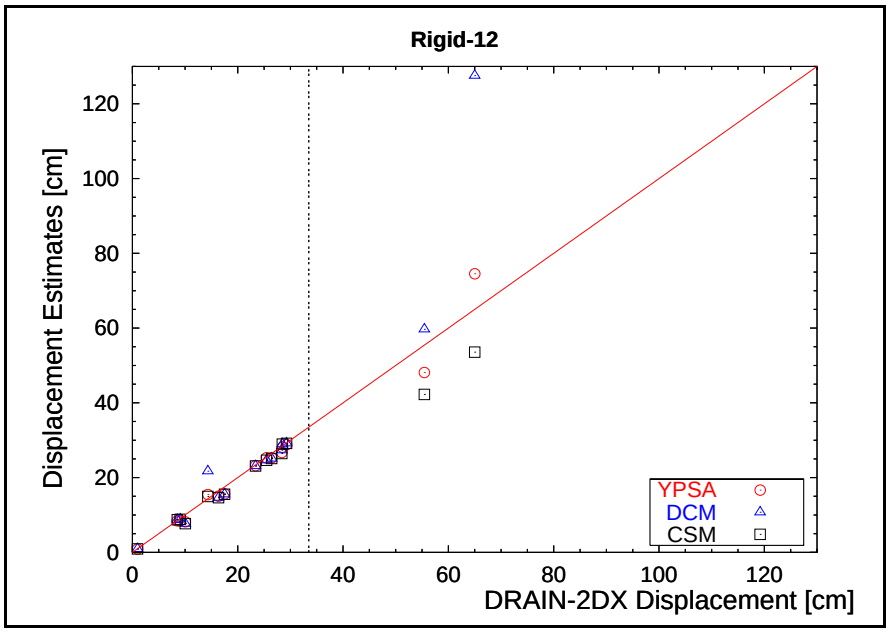

(a)

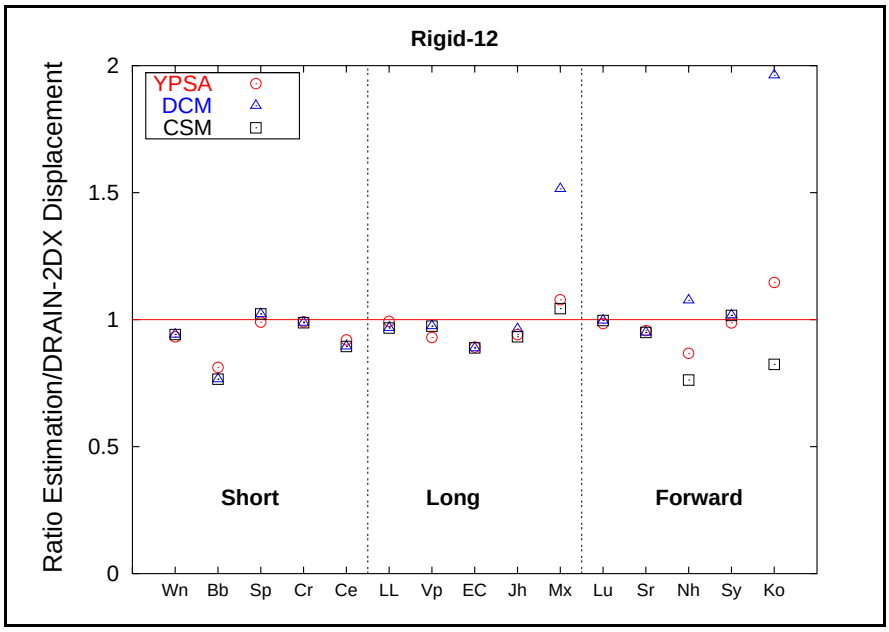

(b)

Figure 5.11 Peak Roof Displacement Comparison for the Rigid-12 Frame

Tables 5.5 to 5.8 compare peak displacement estimates obtained with the YPSA method with corresponding values obtained from nonlinear dynamic analysis response histories of the frames.

The first column on Table 5.5 shows the record identifier[1]. The second column shows the peak displacement obtained using nonlinear dynamic analyses. The data required to apply the YPSA method to estimate peak displacement response are presented in the next three columns. The first of this group of columns shows the maximum elastic displacement of the equivalent SDOF system representing the frame ($\boldsymbol{max(u_{el}^{sdof})}$). For elastic response this value is estimated form the YPS, while for nonlinear response this value is equal to the yield displacement. The next column shows the system displacement ductility for the frame. For elastic response the system ductility demand must be taken as 1, while for nonlinear response this parameter is estimated from the YPS. Figures D.1a to D.30a, included in Appendix D, were used to obtain the values in these two columns. The last column of this group presents the estimated maximum peak displacement for the frame obtained using Equation 5.6. Finally, the last column in Table 5.5 show the ratio between the estimated peak displacement to the corresponded value obtained using nonlinear dynamic histories (DRAIN-2DX). Tables 5.6, 5.7, and 5.8 present similar information for the other frames.

Tables 5.9 to 5.12 compare peak displacement estimates obtained with the Displacement Coefficient Method and the Capacity Spectrum Method with corresponding values obtained from nonlinear dynamic response histories of the frames.

The first column on Table 5.9 shows the record identifier. The second column shows the maximum displacement obtained from nonlinear dynamic analyses of the frames. The next two columns show results obtained with the Displacement Coefficient Method; the first one in this group is the peak displacement estimated for the frame and the second is the ratio between the estimated peak displacement and the corresponding value from nonlinear analyses (DRAIN-2DX). The last two columns show parallel results for the Capacity Spectrum Method. The structure of Tables 5.10, 5.11, and 5.12 present similar information for the other three frames.

1 Record identifiers are described in Section 2.7.1 and contained in Table 2.2

Table 5.5 YPSA Peak Roof Displacement Estimates for Flexible-4

L_{EQ}/M_{EQ} = 1.266

	DRAIN-2DX	YPS Estimation			
Record	u_u^{MDOF} [cm]	u_{elas}^{SDOF} [cm]		u_u^{MDOF} [cm]	Ratio
WN87MWLN.090	0.96	0.7	Elastic	0.9	0.95
BB92CIVC.360	8.63	5.7	Elastic	7.2	0.84
SP88GUKA.360	7.78	5.8	Elastic	7.3	0.94
LP89CORR.090	18.11	10.2	1.260	16.2	0.89
NR94CENT.360	13.02	10.2	1.048	13.5	1.03
CH85LLEO.010	17.74	10.2	1.422	18.3	1.03
CH85VALP.070	5.16	4.4	Elastic	5.6	1.08
IV40ELCN.180	12.99	10.2	1.117	14.4	1.11
LN92JOSH.360	15.55	10.2	1.364	17.5	1.13
MX85SCT1.270	10.91	9.0	Elastic	11.4	1.04
LN92LUCN.250	24.09	10.2	2.000	25.7	1.07
LP89SARA.360	17.80	10.2	1.423	18.3	1.03
NR94NWHL.360	29.35	10.2	2.499	32.1	1.09
NR94SYLH.090	19.79	10.2	1.682	21.6	1.09
KO95TTRI.360	51.82	10.2	4.757	61.2	1.18

Table 5.6 YPSA Peak Roof Displacement Estimates for Rigid-4

L_{EQ}/M_{EQ} = 1.308

	DRAIN-2DX	YPS Estimation			
Record	u_u^{MDOF} [cm]	u_{elas}^{SDOF} [cm]		u_u^{MDOF} [cm]	Ratio
WN87MWLN.090	0.57	0.4	Elastic	0.5	0.92
BB92CIVC.360	5.34	3.8	Elastic	5.0	0.93
SP88GUKA.360	2.87	2.2	Elastic	2.9	1.00
LP89CORR.090	19.70	10.1	1.394	18.5	0.94
NR94CENT.360	7.49	5.5	Elastic	7.2	0.96
CH85LLEO.010	14.62	10.1	1.104	14.7	1.00
CH85VALP.070	5.50	4.0	Elastic	5.2	0.95
IV40ELCN.180	10.38	7.7	Elastic	10.1	0.97
LN92JOSH.360	11.26	8.5	Elastic	11.1	0.99
MX85SCT1.270	5.73	4.4	Elastic	5.8	1.00
LN92LUCN.250	11.37	8.4	Elastic	11.0	0.97
LP89SARA.360	9.96	7.6	Elastic	9.9	1.00
NR94NWHL.360	22.30	10.1	2.000	26.5	1.19
NR94SYLH.090	13.41	10.1	1.104	14.7	1.09
KO95TTRI.360	21.51	10.1	1.819	24.1	1.12

Table 5.7 YPSA Peak Roof Displacement Estimates for Flexible-12

L_{EQ}/M_{EQ} = 1.372

	DRAIN-2DX	YPS Estimation			
Record	u_u^{MDOF} [cm]	u_{elas}^{SDOF} [cm]		u_u^{MDOF} [cm]	Ratio
WN87MWLN.090	0.98	0.7	Elastic	1.0	0.99
BB92CIVC.360	11.51	5.6	Elastic	7.7	0.67
SP88GUKA.360	7.14	4.3	Elastic	5.9	0.83
LP89CORR.090	23.62	11.0	Elastic	15.1	0.64
NR94CENT.360	17.86	12.5	Elastic	17.1	0.96
CH85LLEO.010	34.22	20.5	Elastic	28.1	0.82
CH85VALP.070	10.94	7.3	Elastic	10.0	0.92
IV40ELCN.180	33.64	22.5	Elastic	30.9	0.92
LN92JOSH.360	22.77	13.0	Elastic	17.8	0.78
MX85SCT1.270	69.02	25.7	2.000	70.6	1.02
LN92LUCN.250	50.69	25.7	1.456	51.4	1.01
LP89SARA.360	38.14	25.7	1.129	39.8	1.04
NR94NWHL.360	51.80	25.7	1.542	54.4	1.05
NR94SYLH.090	60.82	25.7	1.631	57.6	0.95
KO95TTRI.360	84.09	25.7	2.456	86.7	1.03

Table 5.8 YPSA Peak Roof Displacement Estimates for Rigid-12

L_{EQ}/M_{EQ} = 1.406

	DRAIN-2DX	YPS Estimation			
Record	u_u^{MDOF} [cm]	u_{elas}^{SDOF} [cm]		u_u^{MDOF} [cm]	Ratio
WN87MWLN.090	0.98	0.7	Elastic	0.9	0.93
BB92CIVC.360	10.04	5.8	Elastic	8.2	0.81
SP88GUKA.360	8.52	6.0	Elastic	8.4	0.99
LP89CORR.090	23.39	16.5	Elastic	23.2	0.99
NR94CENT.360	16.35	10.7	Elastic	15.0	0.92
CH85LLEO.010	25.47	18.0	Elastic	25.3	0.99
CH85VALP.070	9.07	6.0	Elastic	8.4	0.93
IV40ELCN.180	17.50	11.1	Elastic	15.6	0.89
LN92JOSH.360	28.37	19.0	Elastic	26.7	0.94
MX85SCT1.270	14.34	11.0	Elastic	15.5	1.08
LN92LUCN.250	29.27	20.5	Elastic	28.8	0.98
LP89SARA.360	26.45	18.0	Elastic	25.3	0.96
NR94NWHL.360	55.45	23.8	1.436	48.1	0.87
NR94SYLH.090	28.47	20.0	Elastic	28.1	0.99
KO95TTRI.360	65.01	23.8	2.225	74.5	1.15

Table 5.9 DCM and CSM Peak Roof Displacement Estimates for Flexible-4

	DRAIN-2DX	Disp. Coeff. Method		Cap. Spec Method	
Record	u_u^{MDOF} [cm]	u_u^{MDOF} [cm]	Ratio	u_u^{MDOF} [cm]	Ratio
WN87MWLN.090	1.0	0.9	0.97	0.9	0.97
BB92CIVC.360	8.6	7.3	0.85	7.3	0.85
SP88GUKA.360	7.8	7.3	0.94	7.3	0.94
LP89CORR.090	18.1	18.0	0.99	15.5	0.86
NR94CENT.360	13.0	13.7	1.05	13.0	1.00
CH85LLEO.010	17.7	22.1	1.25	16.1	0.91
CH85VALP.070	5.2	5.3	1.03	5.3	1.02
IV40ELCN.180	13.0	14.6	1.12	13.4	1.03
LN92JOSH.360	15.6	26.0	1.67	15.5	1.00
MX85SCT1.270	10.9	16.6	1.52	11.1	1.02
LN92LUCN.250	24.1	22.7	0.94	18.4	0.76
LP89SARA.360	17.8	21.6	1.21	16.3	0.91
NR94NWHL.360	29.4	50.3	1.71	27.7	0.94
NR94SYLH.090	19.8	19.1	0.97	19.4	0.98
KO95TTRI.360	51.8	100.3	1.93	69.1	1.33

Table 5.10 DCM and CSM Peak Roof Displacement Estimates for Rigid-4

	DRAIN-2DX	Disp. Coeff. Method		Cap. Spec Method	
Record	u_u^{MDOF} [cm]	u_u^{MDOF} [cm]	Ratio	u_u^{MDOF} [cm]	Ratio
WN87MWLN.090	0.6	0.6	1.00	0.6	1.00
BB92CIVC.360	5.3	5.0	0.93	5.0	0.93
SP88GUKA.360	2.9	2.9	0.99	2.9	0.99
LP89CORR.090	19.7	26.0	1.32	16.6	0.84
NR94CENT.360	7.5	9.7	1.30	7.3	0.98
CH85LLEO.010	14.6	15.1	1.03	14.6	1.00
CH85VALP.070	5.5	5.5	0.99	5.5	0.99
IV40ELCN.180	10.4	10.0	0.96	10.0	0.96
LN92JOSH.360	11.3	16.9	1.50	11.3	1.00
MX85SCT1.270	5.7	8.6	1.50	5.7	1.00
LN92LUCN.250	11.4	11.1	0.98	11.1	0.98
LP89SARA.360	10.0	9.8	0.99	9.8	0.99
NR94NWHL.360	22.3	38.3	1.72	22.3	1.00
NR94SYLH.090	13.4	16.0	1.19	13.0	0.97
KO95TTRI.360	21.5	38.3	1.78	18.3	0.85

Table 5.11 DCM and CSM Peak Roof Displacement Estimates for Flexible-12

	DRAIN-2DX	Disp. Coeff. Method		Cap. Spec Method	
Record	u_u^{MDOF} [cm]	u_u^{MDOF} [cm]	Ratio	u_u^{MDOF} [cm]	Ratio
WN87MWLN.090	1.0	1.0	1.00	0.9	0.96
BB92CIVC.360	11.5	7.7	0.67	7.6	0.66
SP88GUKA.360	7.1	5.9	0.83	5.8	0.82
LP89CORR.090	23.6	13.8	0.58	15.1	0.64
NR94CENT.360	17.9	17.3	0.97	16.2	0.91
CH85LLEO.010	34.2	27.4	0.80	31.3	0.92
CH85VALP.070	10.9	9.1	0.84	10.8	0.99
IV40ELCN.180	33.6	29.6	0.88	27.3	0.81
LN92JOSH.360	22.8	17.0	0.75	17.7	0.78
MX85SCT1.270	69.0	128.5	1.86	70.5	1.02
LN92LUCN.250	50.7	47.1	0.93	39.1	0.77
LP89SARA.360	38.1	40.6	1.06	36.4	0.96
NR94NWHL.360	51.8	57.0	1.10	41.0	0.79
NR94SYLH.090	60.8	72.8	1.20	51.2	0.84
KO95TTRI.360	84.1	148.5	1.77	79.4	0.94

Table 5.12 DCM and CSM Peak Roof Displacement Estimates for Rigid-12

	DRAIN-2DX	Disp. Coeff. Method		Cap. Spec Method	
Record	u_u^{MDOF} [cm]	u_u^{MDOF} [cm]	Ratio	u_u^{MDOF} [cm]	Ratio
WN87MWLN.090	1.0	0.9	0.94	0.9	0.94
BB92CIVC.360	10.0	7.7	0.77	7.7	0.77
SP88GUKA.360	8.5	8.7	1.02	8.7	1.02
LP89CORR.090	23.4	23.1	0.99	23.1	0.99
NR94CENT.360	16.4	14.6	0.89	14.6	0.89
CH85LLEO.010	25.5	24.6	0.97	24.6	0.97
CH85VALP.070	9.1	8.8	0.97	8.8	0.97
IV40ELCN.180	17.5	15.5	0.89	15.5	0.89
LN92JOSH.360	28.4	27.3	0.96	26.5	0.93
MX85SCT1.270	14.3	21.7	1.51	15.0	1.04
LN92LUCN.250	29.3	29.2	1.00	29.2	1.00
LP89SARA.360	26.5	25.1	0.95	25.1	0.95
NR94NWHL.360	55.5	59.7	1.08	42.3	0.76
NR94SYLH.090	28.5	29.0	1.02	28.9	1.02
KO95TTRI.360	65.0	127.6	1.96	53.6	0.82

5.4.2.2 Analysis of Results

Table 5.13 summarizes the results of Tables 5.5 to 5.12. The mean and the standard deviation of the ratio of the peak displacement estimate and the peak displacement obtained using DRAIN-2DX for each of the NSPs are compared here. These ratios are shown in Tables 5.5 to 5.12. The mean and the standard deviation for each frame responding to the 15 ground motion is presented. Values of the total mean and total standard deviation, over the four frames and the 15 ground motions, are also shown.

Table 5.13 Results for All Cases

	YPSA		DCM		CSM	
	Mean	**Std. Dev.**	**Mean**	**Std. Dev.**	**Mean**	**Std. Dev.**
Flexible-4	**1.034**	**0.092**	**1.210**	**0.338**	**0.968**	**0.126**
Rigid-4	**1.002**	**0.076**	**1.213**	**0.290**	**0.966**	**0.052**
Flexible-12	**0.909**	**0.134**	**1.016**	**0.363**	**0.853**	**0.114**
Rigid-12	**0.962**	**0.081**	**1.062**	**0.296**	**0.931**	**0.089**
All	**0.977**	**0.107**	**1.125**	**0.327**	**0.930**	**0.108**

Values in Table 5.13 confirm tendencies that can be seen in Figures 5.8 to 5.11. In a mean sense, the YPSA method and the CSM estimates of peak displacement response of multistory building are very good. The DCM tends to overestimate response for all the frames. The standard deviation for the YPSA and for the CSM are comparable and, in general can be considered low, while for the DCM the standard deviation is relatively high.

Since these four frames were designed for one particular ground motion and here are being analyzed for a set of records, some of which are weaker than the records used to design the frames, linear elastic response was obtained for many of the analyses. This is particularly true for the stronger frames: Rigid-4 and Rigid-12. (See the displacement ductility column in Tables 5.5 to 5.8.)

In order to have a better idea of the accuracy of each method in nonlinear cases, Table 5.14 shows mean and standard deviation values of the ratio between the displacement estimates for each nonlinear static method and the displacement obtained using DRAIN-2DX, only for those cases having nonlinear behavior.

Values in Table 5.14 indicate that, in a mean sense, results from the Yield Point Spectra analysis method very slightly overestimate the peak displacement of those frames

having nonlinear response, with a small standard deviation for three out of the four frames. For Rigid-12 the standard deviation was quite high compared with the other frames.

For the Capacity Spectrum Method, mean values show that this method tends to underestimate response in the nonlinear cases considered. The standard deviation for the nonlinear cases are similar to corresponding values shown in Table 5.13.

The Displacement Coefficient Method tends to overestimate response even more for the nonlinear cases. The standard deviation for this method becomes larger for the nonlinear cases considered.

Table 5.14 Results for NonLinear Cases

	YPSA		DCM		CSM	
	Mean	**Std. Dev.**	**Mean**	**Std. Dev.**	**Mean**	**Std. Dev.**
Flexible-4	**1.066**	**0.077**	**1.285**	**0.357**	**0.973**	**0.150**
Rigid-4	**1.069**	**0.099**	**1.409**	**0.327**	**0.932**	**0.079**
Flexible-12	**1.018**	**0.038**	**1.320**	**0.394**	**0.887**	**0.101**
Rigid-12	**1.007**	**0.197**	**1.519**	**0.626**	**0.793**	**0.044**

5.4.3 Estimates of Interstory Drift Indices

Interstory drift is traditionally calculated based on the deformed shape of the building under the action of equivalent static design forces. As an alternative, interstory drift can be estimated using the first mode shape, normalized to one on the top, amplified by the the roof peak displacement. This alternate approach is used in Equation 5.7. In both cases interstory drift is estimated using a single deformed shape.

Table 4.16 in Chapter 4 shows that use of only one deformed shape underestimates interstory drift indices for the four frames considered. The YPSA method provides an easy way to obtain interstory drift index estimates based on combinations of two mode shapes.

In this section, interstory drift index estimates calculated using the YPSA method and one mode shape (equation 5.7) and combinations of the first two mode shapes (Equations 5.8 and 5.9) are compared with corresponding peak interstory drift indices obtained from nonlinear dynamic analysis of the frames (DRAIN-2DX).

Yield Point Spectra with damping set to 2.8% of the critical damping were used for the estimations related with the second mode shape to reflect the lower damping assigned to

this mode in the nonlinear dynamic analysis performed using DRAIN-2DX. The mean value of the second mode damping for the four frames analyzed in DRAIN-2DX was approximately 2.8% of the critical damping.

Following is a numerical example to illustrate the use of Yield Point Spectra to estimate interstory drift indices. The interstory drift index for the 4^{th} story of the Flexible-4 frame responding to the 1940 N-S component of the El Centro record (IV40ELCN.180) is estimated using Equation 5.7 (one mode) and Equations 5.8 and 5.9 (combinations of two modes).

Figures 5.1b and 5.2b show profiles of the the first and second modal interstory drift indices for each of the four frames. The data plotted in these figures are contained in Tables 5.1 and 5.2. The modal interstory drift index for the 4^{th} story of the Flexible-4 frame is 3.66% and 27.7% for the first and second modes respectively (See Figure 5.1b or Table 5.1).

In Section 5.4.2, the Yield Point Spectra corresponding to the the 1940 N-S component of the El Centro record (IV40ELCN.180) and first mode parameters were used to estimate a peak displacement response of 14.4E-2 m. for the Flexible-4 frame. A similar calculation, using second mode parameters is done to estimate the peak displacement response of the same frame in the second mode.

For the Flexible-4 frame, the second mode participation factor is 0.363 and can be obtained from Table 5.3. The equivalent SDOF yield displacement and the yield strength coefficient in the second mode are 9.5E-2 m. and 2.708 respectively (see Table 5.4b).

Figure 5.12 shows the Yield Point Spectra corresponding to the El Centro record (IV40ELCN.180) for a damping equal to 2.8% of critical damping. The equivalent SDOF second mode yield point for the Flexible-4 frame is indicated using a 'x' sign, in Figure 5.12. The equivalent second mode period of vibration is shown by a dotted diagonal line.

In Figure 5.12 it can be seen that the yield point lies beyond the curve corresponding to ductility of 1; therefore, the equivalent SDOF associated with second mode of vibration for this building has a maximum elastic displacement of approximately 2.5E-2 m. and a displacement ductility equal to 1.

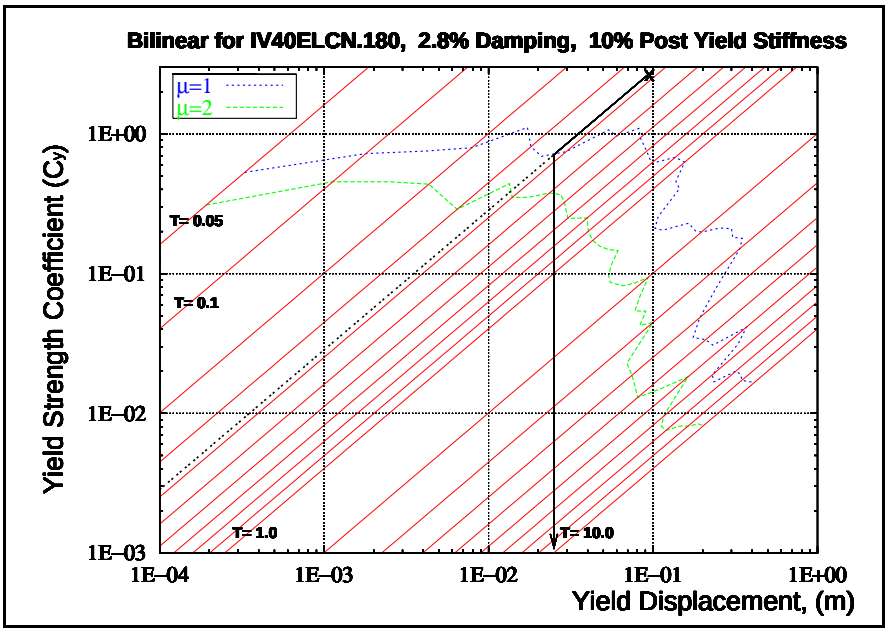

Figure 5.12 Second Mode Yield Point for the Flexible-4 Frame

'x' indicates Second Mode Yield Point for Flexible-4

Using Equation 5.6, the peak displacement estimate for the second mode of the Flexible-4 frame under El Centro record is equal to,

$$(u_u^{mdof})_2 = (0.\ 363)\ (1.0)\ (2.5\text{E-}2) = 9.08\text{E-}3\ \text{m}. \qquad (5.12)$$

Interstory drift indices for the 4th story of Flexible-4 frame can now be obtained using Equations 5.7 to 5.9.

Using Equation 5.7,

$$IDI^4 = (14.4\text{E-}2)\ (3.66\%) = 0.527\% \qquad (5.13)$$

Equation 5.8 leads to

$$IDI^4 = \sqrt{((14.4\text{E-}2 \cdot 3.66\%)^2 + (9.08\text{E-}3 \cdot 27.7\%)^2)} = 0.779\% \qquad (5.14)$$

and Equation 5.9 to

$$IDI^4 = |(14.4E\text{-}2)\ (3.66\%)| + |(9.08E\text{-}3)\ (27.7\%)| = 0.779\% \qquad (5.15)$$

These three IDI estimations are plotted in Figure 5.14(a) for the IV40ELCN.180 record.

5.4.3.1 Numerical Results

Figures 5.13 to 5.24 help to visualize and compare, on a story-by-story basis, the interstory drift indices estimated using Equations 5.7 to 5.9. Similar to the peak roof displacement comparison, results from the nonlinear dynamic analyses are used to evaluate the accuracy of the results obtained with each of the proposed IDI Equations.

Part (a) of Figures 5.13 to 5.24 compares profiles of estimated peak interstory drift indices obtained using Equation 5.7 (a single deformed shape) as well as Equations 5.8 and 5.9 (two deformed shapes combinations). The IDI obtained from nonlinear dynamic analyses are also presented along with results obtained using these three equations.

Part (b) of Figures 5.13 to 5.24 plots, for each story, the ratio of the peak interstory drift index estimates to the peak IDI computed in the nonlinear dynamic analyses.

The nonlinear interstory drift indices used in Figures 5.13 to 5.24 are the peak interstory drift indices in each story regardless of the time they occur. In general, in the dynamic analysis history, peak interstory drifts do not occur simultaneously in all the stories.

Results from the nonlinear dynamic analyses are labeled as 'DRAIN-2DX' in part (a) of Figures 5.13 to 5.24. Results from Equations 5.7 to 5.9 are labeled as IDI Estimate 1, IDI Estimate 2, and IDI Estimate 3, respectively in Figures 5.13 to 5.24.

IDI Profiles Comparison

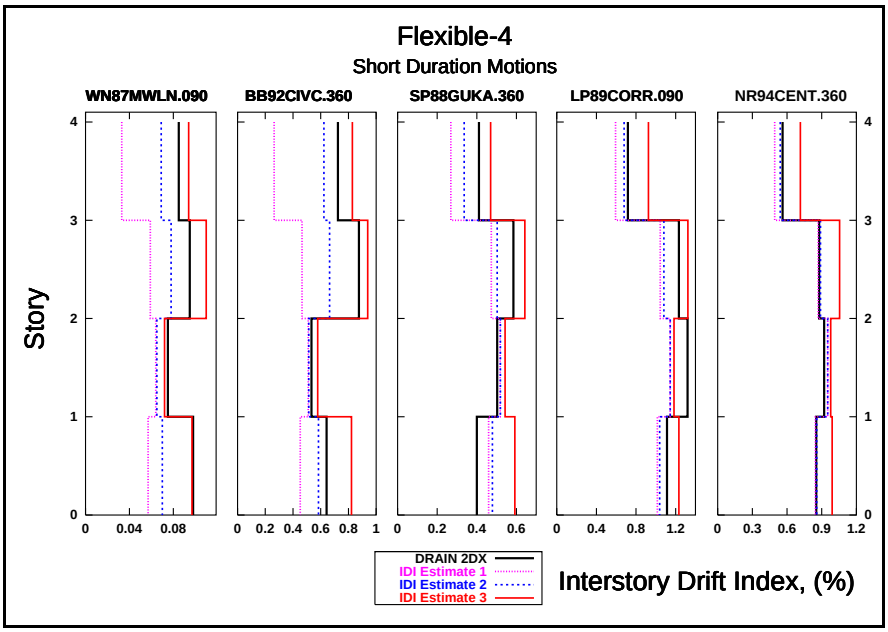

(a)

IDI Ratio Comparison

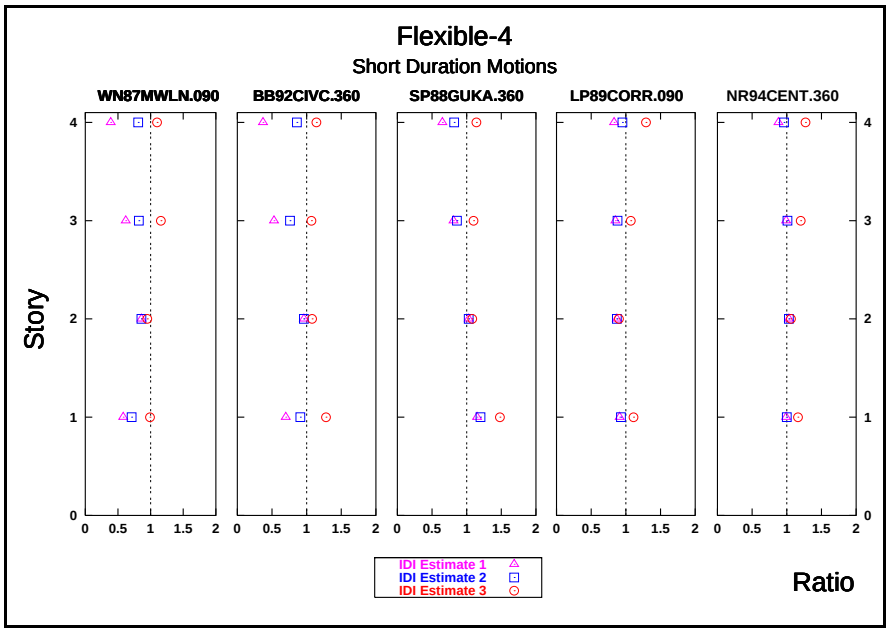

(b)

Figure 5.13 IDI Profile and Ratios Comparison for the Flexible-4 Frame

IDI Profiles Comparison

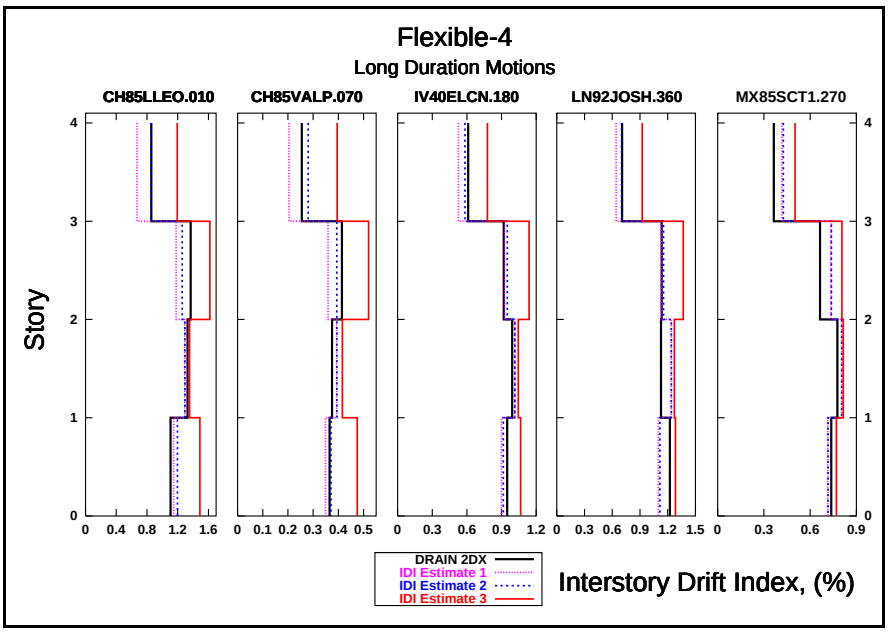

(a)

IDI Ratio Comparison

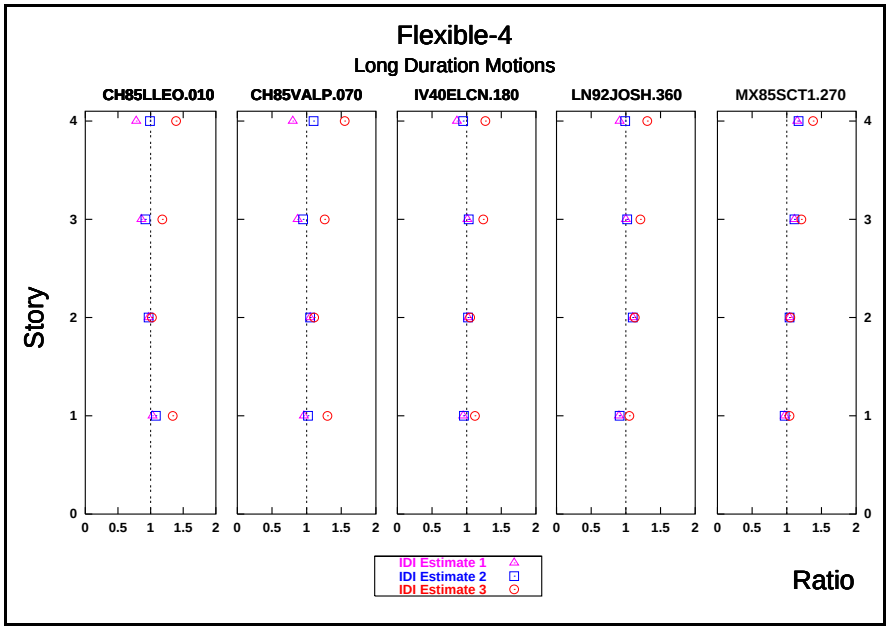

(b)

Figure 5.14 IDI Profile and Ratios Comparison for the Flexible-4 Frame

IDI Profiles Comparison

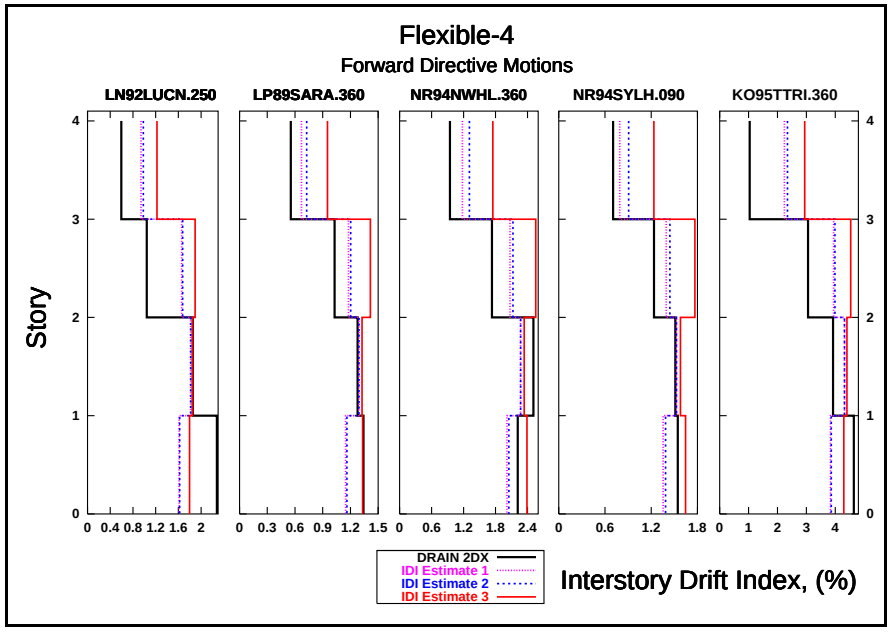

(a)

IDI Ratio Comparison

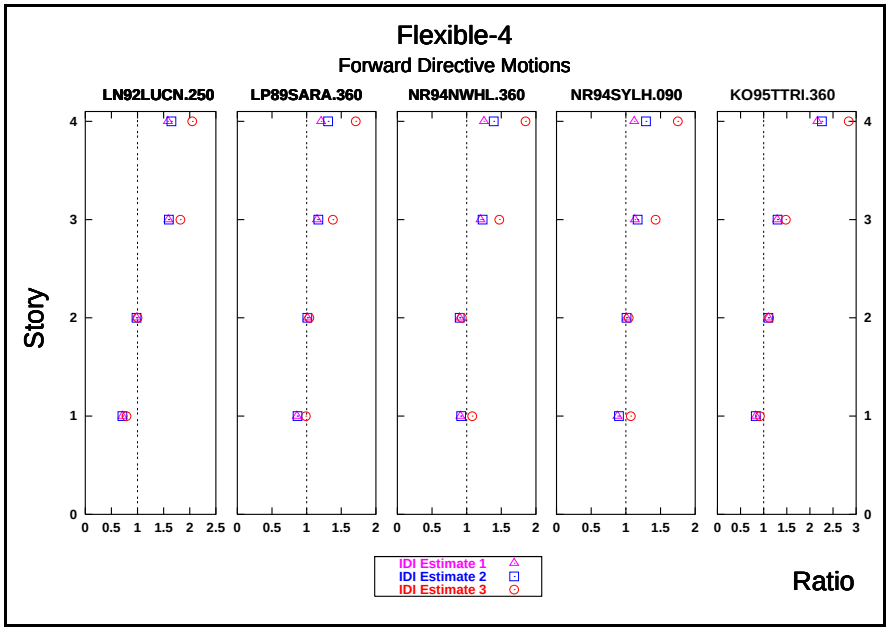

(b)

Figure 5.15 IDI Profile and Ratios Comparison for the Flexible-4 Frame

IDI Profiles Comparison

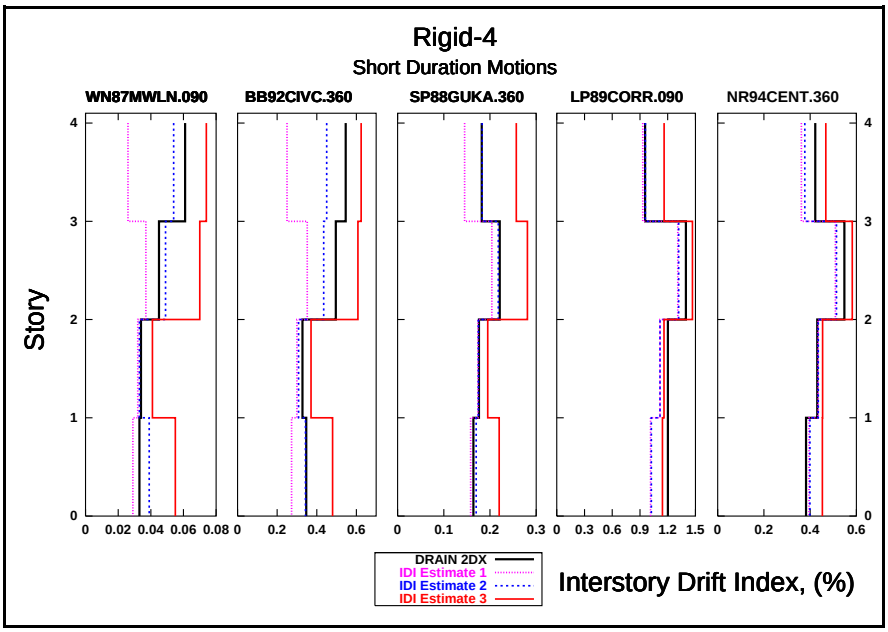

(a)

IDI Ratio Comparison

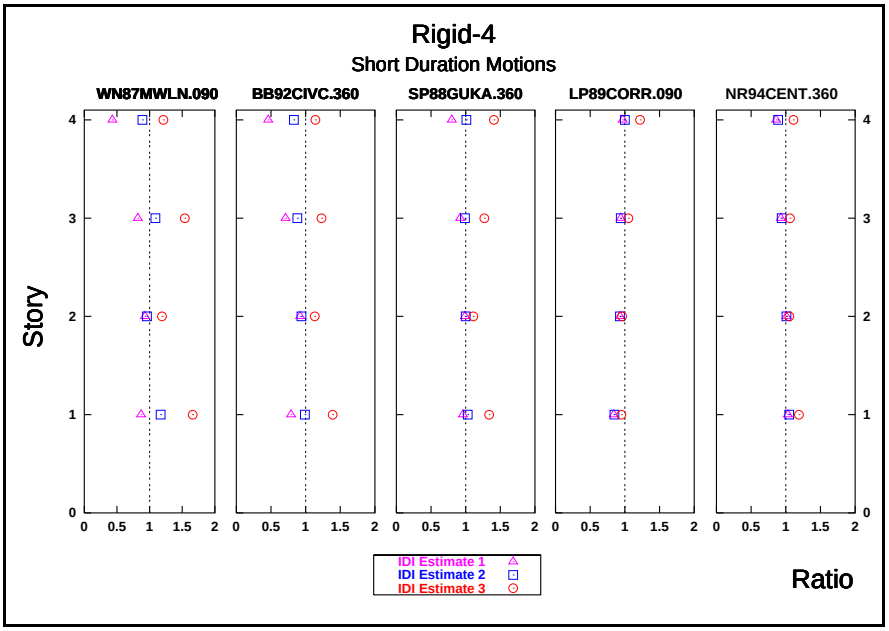

(b)

Figure 5.16 IDI Profile and Ratios Comparison for the Rigid-4 Frame

IDI Profiles Comparison

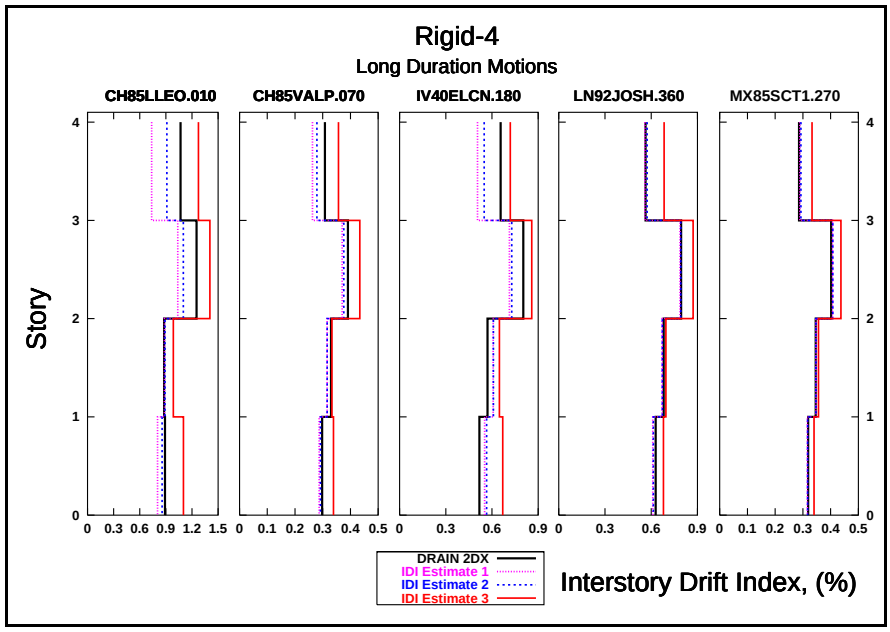

(a)

IDI Ratio Comparison

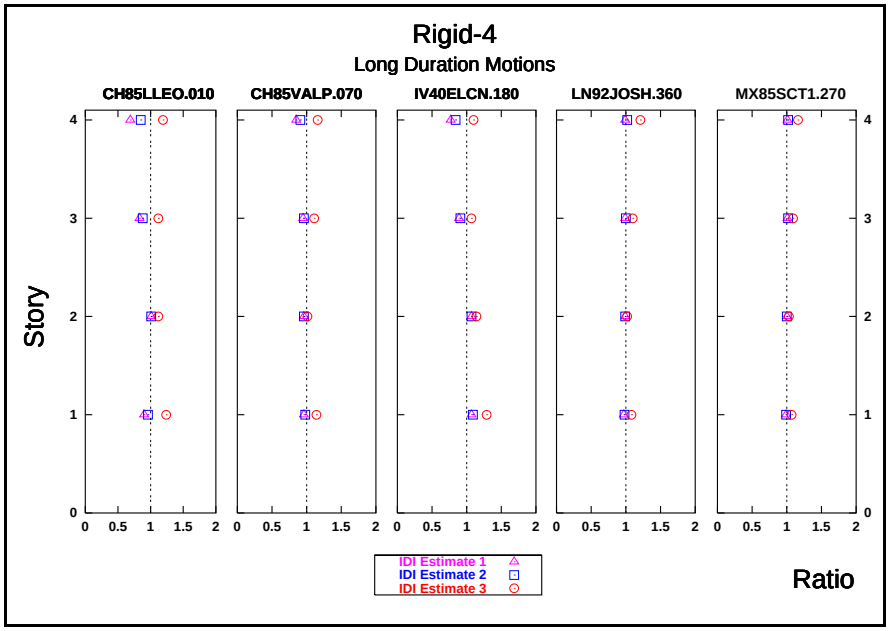

(b)

Figure 5.17 IDI Profile and Ratios Comparison for the Rigid-4 Frame

IDI Profiles Comparison

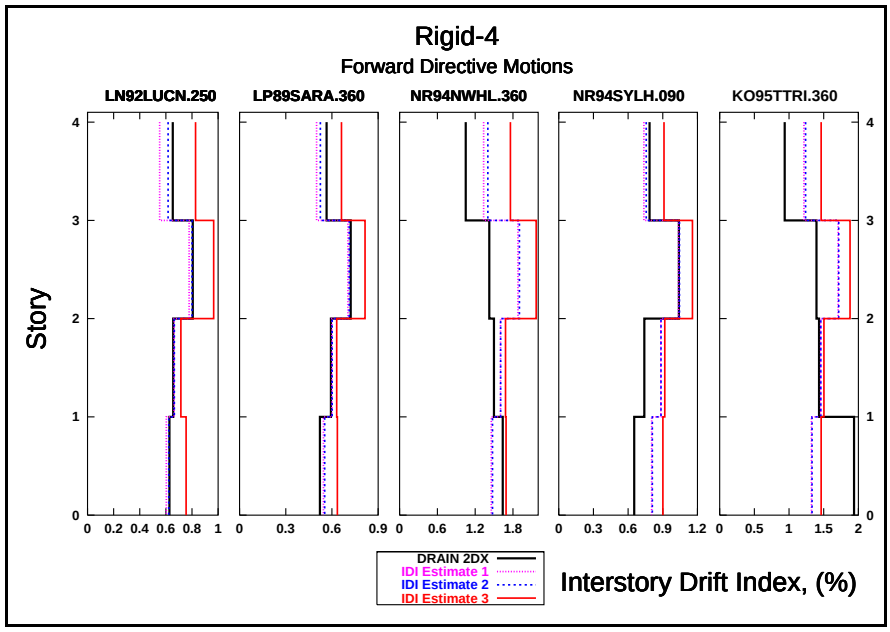

(a)

IDI Ratio Comparison

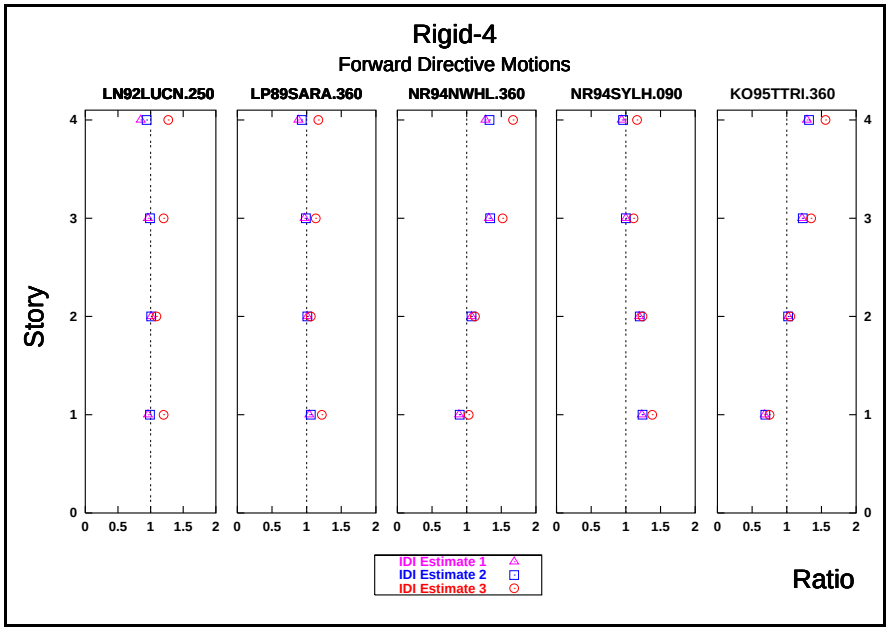

(b)

Figure 5.18 IDI Profile and Ratios Comparison for the Rigid-4 Frame

IDI Profiles Comparison

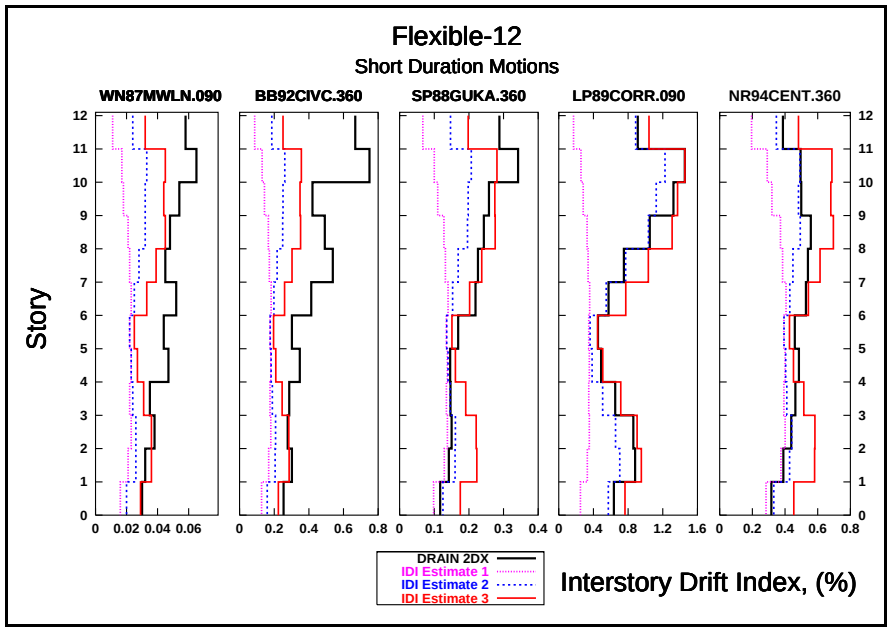

(a)

IDI Ratio Comparison

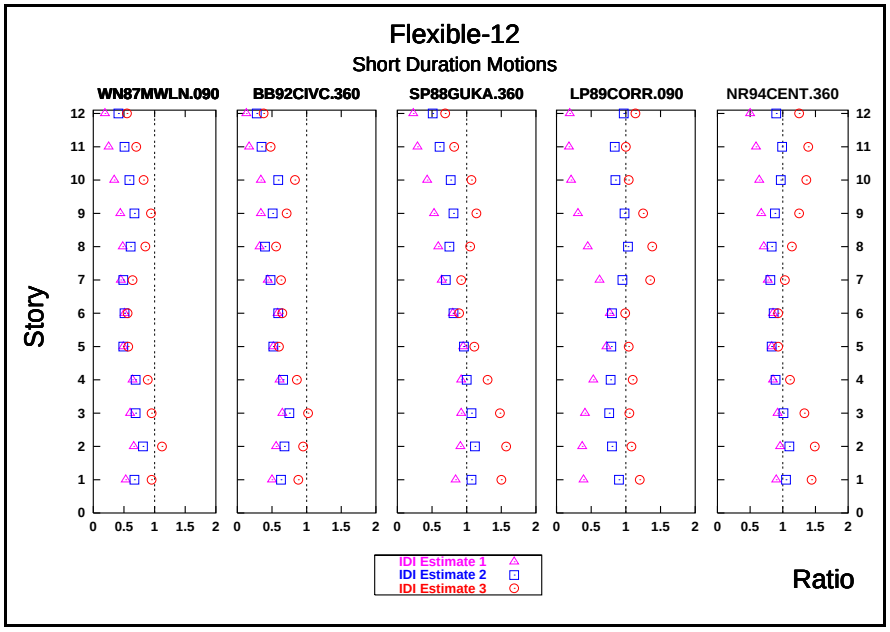

(b)

Figure 5.19 IDI Profile and Ratios Comparison for the Flexible-12 Frame

IDI Profiles Comparison

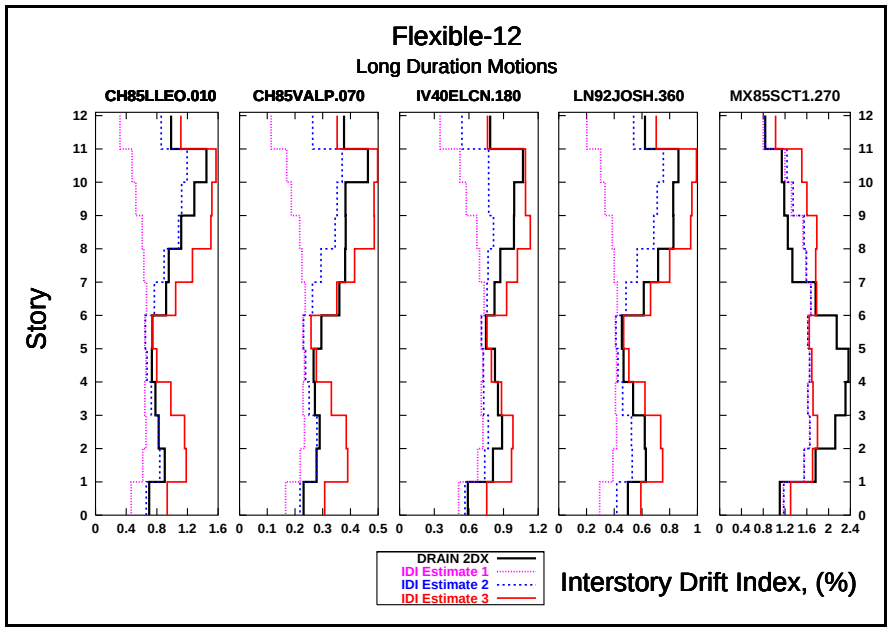

(a)

IDI Ratio Comparison

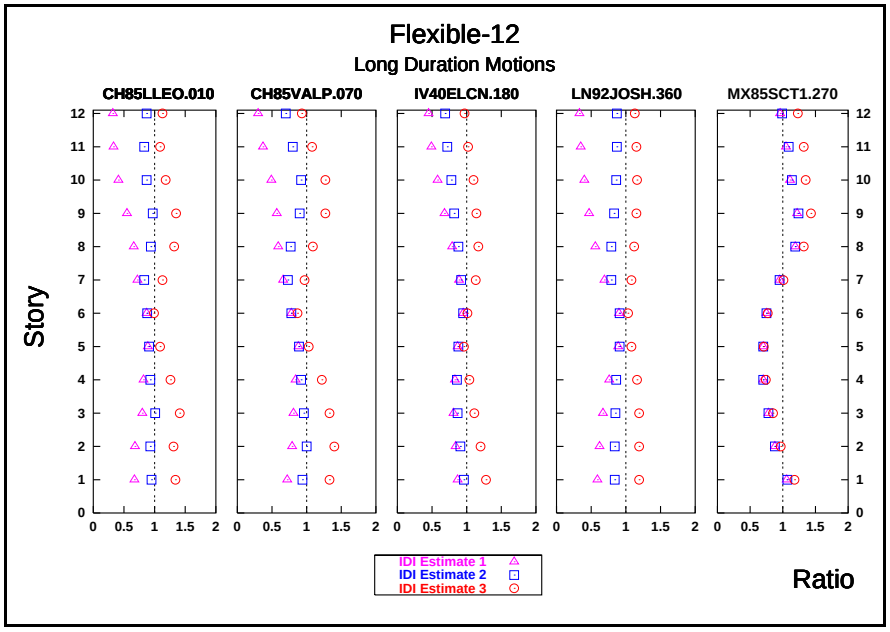

(b)

Figure 5.20 IDI Profile and Ratios Comparison for the Flexible-12 Frame

IDI Profiles Comparison

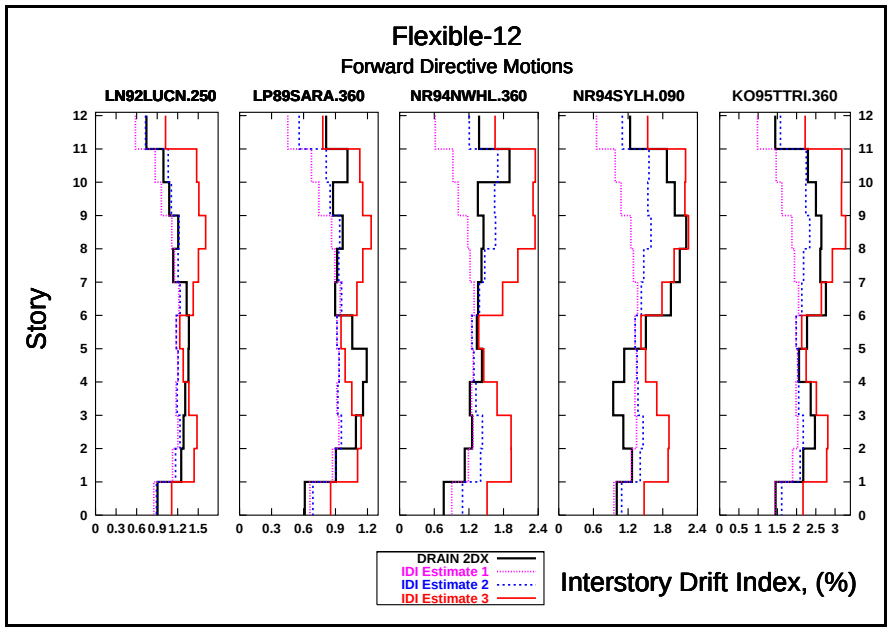

(a)

IDI Ratio Comparison

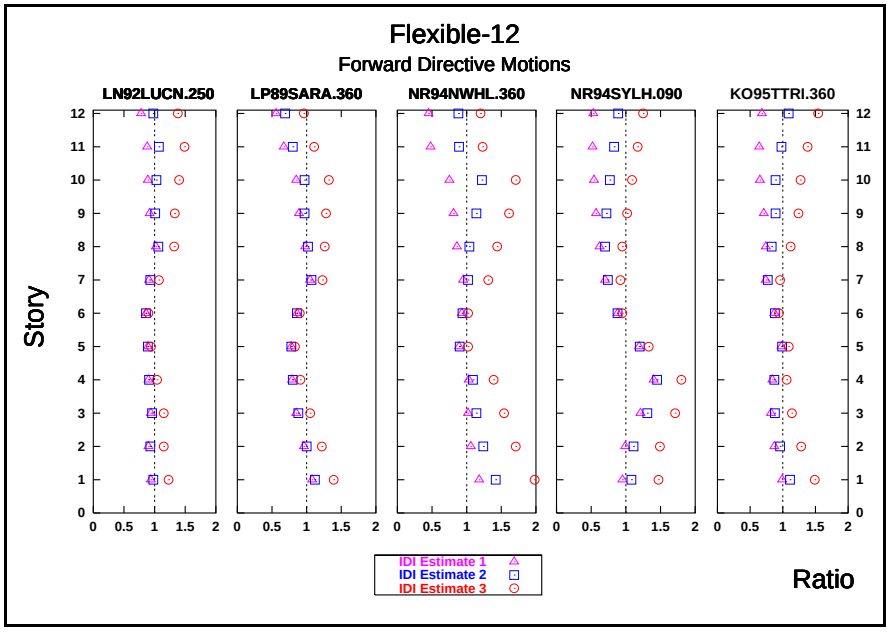

(b)

Figure 5.21 IDI Profile and Ratios Comparison for the Flexible-12 Frame

IDI Profiles Comparison

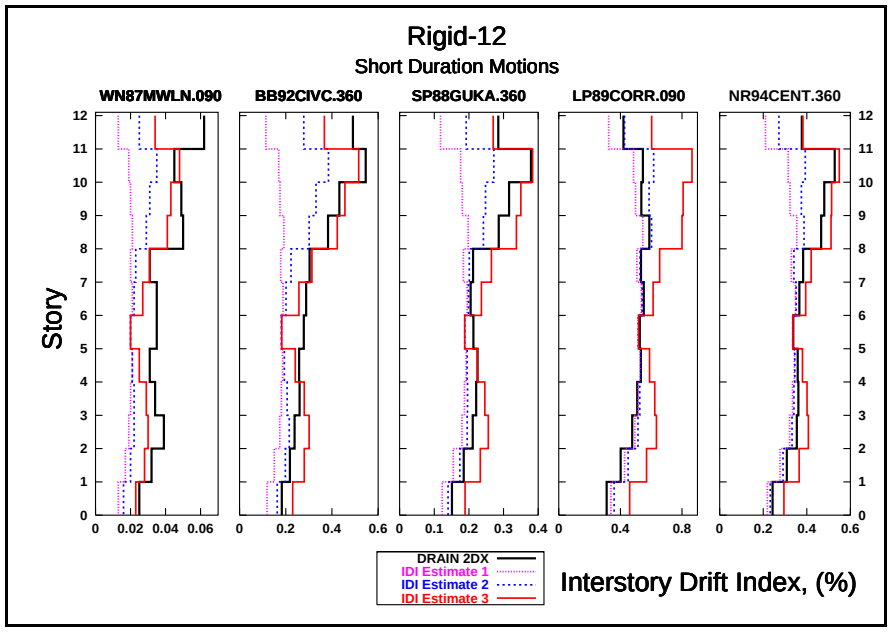

(a)

IDI Ratio Comparison

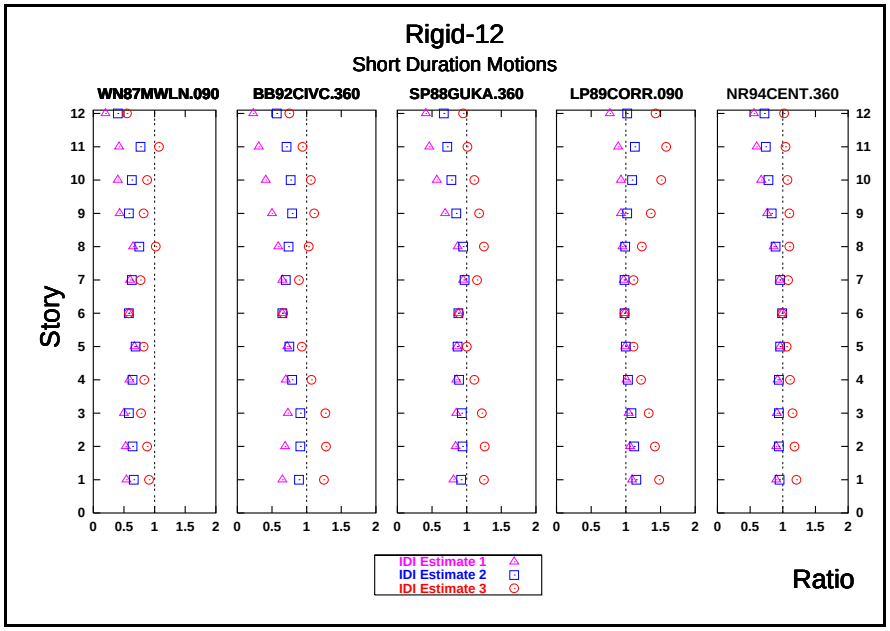

(b)

Figure 5.22 IDI Profile and Ratios Comparison for the Rigid-12 Frame

IDI Profiles Comparison

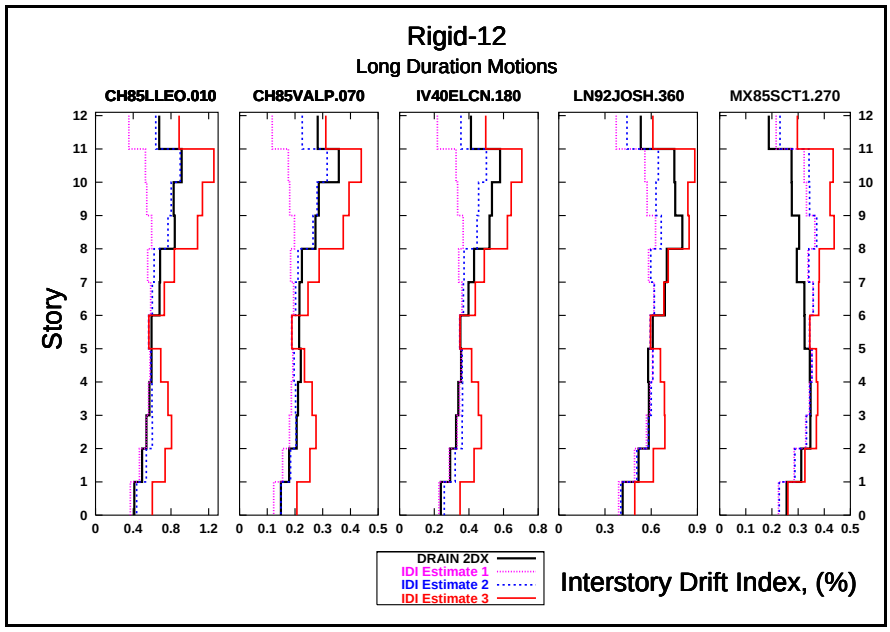

(a)

IDI Ratio Comparison

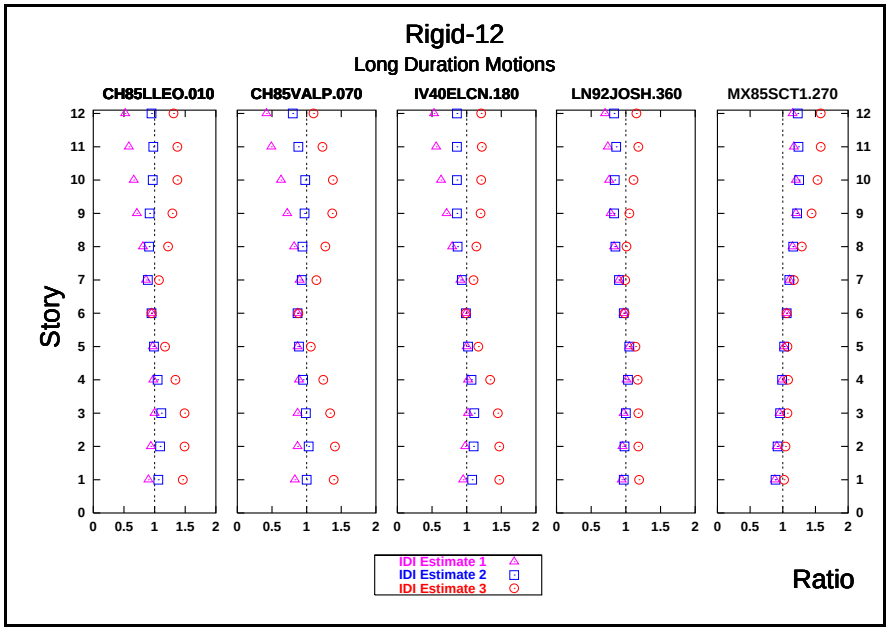

(b)

Figure 5.23 IDI Profile and Ratios Comparison for the Rigid-12 Frame

IDI Profiles Comparison

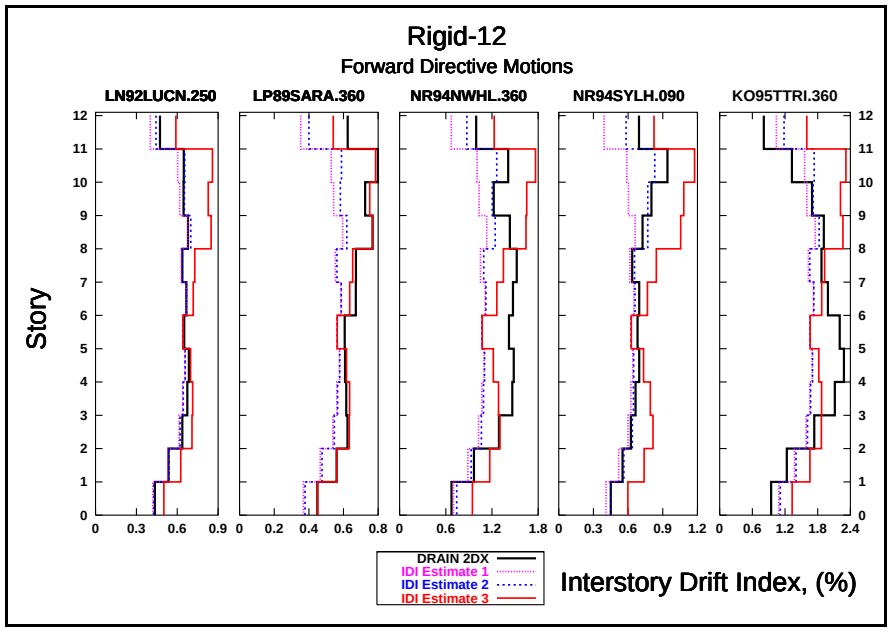

(a)

IDI Ratio Comparison

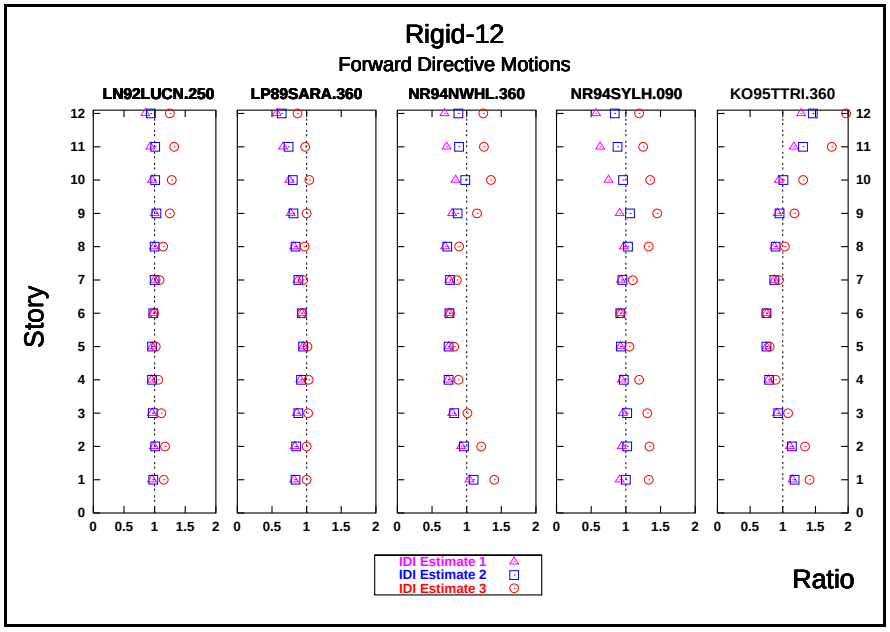

(b)

Figure 5.24 IDI Profile and Ratios Comparison for the Rigid-12 Frame

Parts (a) and (b) of Figures 5.13 to 5.24 complement each other. Part (a) shows the magnitude of the IDI in each story. Profiles along the height of the frames for the three peak IDI estimates and for the peak IDI obtained from nonlinear dynamic analysis are plotted. Part(a) also indicates how well the estimated IDI profile follows the IDI profile obtained from nonlinear dynamic analysis. Part (b) indicates directly the accuracy of each method.

Tables 5.15 to 5.18 present second mode related peak displacement estimates obtained with the YPSA method. The data in these tables is similar to that presented in Tables 5.5 to 5.8 for first mode related peak roof displacement estimates.

The first column on Table 5.15 shows the record identifier. The second column shows the maximum elastic displacement of the equivalent SDOF representing the frame ($\boldsymbol{max(u_{el}^{sdof})}$) obtained assuming the second mode as deformed shape to apply the equivalent SDOF formulation. The next column shows the second mode system displacement ductility estimate for the frame. Values in the second and third columns are obtained directly from YPS in the way illustrated using Figure 5.12. Part (b) of Figures D.1 to D.30 (Appendix D), was used to obtain the values in these columns. The last column presents the estimated second mode peak displacement for the frame obtained using Equation 5.6. Tables 5.16, 5.17, and 5.18 present the same information for the other three frames.

Table 5.15 Second Mode Peak Roof Displacement Estimates for Flexible-4

	YPS 2nd Mode Estimation		
Record	u_{elas}^{SDOF} [cm]		u_u^{MDOF} [cm]
WN87MWLN.090	0.60	Elastic	0.22
BB92CIVC.360	5.60	Elastic	2.03
SP88GUKA.360	2.00	Elastic	0.73
LP89CORR.090	3.30	Elastic	1.20
NR94CENT.360	2.20	Elastic	0.80
CH85LLEO.010	5.20	Elastic	1.89
CH85VALP.070	1.90	Elastic	0.69
IV40ELCN.180	2.50	Elastic	0.91
LN92JOSH.360	2.80	Elastic	1.02
MX85SCT1.270	0.84	Elastic	0.30
LN92LUCN.250	2.80	Elastic	1.02
LP89SARA.360	2.80	Elastic	1.02
NR94NWHL.360	5.70	Elastic	2.07
NR94SYLH.090	4.40	Elastic	1.60
KO95TTRI.360	7.00	Elastic	2.54

Table 5.16 Second Mode Peak Roof Displacement Estimates for Rigid-4

	YPS 2nd Mode Estimation		
Record	u_{elas}^{SDOF} [cm]		u_u^{MDOF} [cm]
WN87MWLN.090	0.38	Elastic	0.15
BB92CIVC.360	3.00	Elastic	1.20
SP88GUKA.360	0.90	Elastic	0.36
LP89CORR.090	1.85	Elastic	0.74
NR94CENT.360	0.85	Elastic	0.34
CH85LLEO.010	4.30	Elastic	1.72
CH85VALP.070	0.75	Elastic	0.30
IV40ELCN.180	1.70	Elastic	0.68
LN92JOSH.360	1.00	Elastic	0.40
MX85SCT1.270	0.35	Elastic	0.14
LN92LUCN.250	2.20	Elastic	0.88
LP89SARA.360	1.30	Elastic	0.52
NR94NWHL.360	3.40	Elastic	1.36
NR94SYLH.090	1.40	Elastic	0.56
KO95TTRI.360	2.00	Elastic	0.80

Table 5.17 Second Mode Peak Roof Displacement Estimates for Flexible-12

	YPS 2nd Mode Estimation		
Record	u_{elas}^{SDOF} [cm]		u_u^{MDOF} [cm]
WN87MWLN.090	0.51	Elastic	0.29
BB92CIVC.360	4.00	Elastic	2.27
SP88GUKA.360	3.20	Elastic	1.82
LP89CORR.090	19.36	1.09	12.04
NR94CENT.360	7.00	Elastic	3.98
CH85LLEO.010	19.36	Elastic	11.00
CH85VALP.070	5.80	Elastic	3.30
IV40ELCN.180	10.00	Elastic	5.68
LN92JOSH.360	12.20	Elastic	6.93
MX85SCT1.270	5.50	Elastic	3.13
LN92LUCN.250	10.70	Elastic	6.08
LP89SARA.360	8.00	Elastic	4.55
NR94NWHL.360	19.36	1.30	14.32
NR94SYLH.090	19.36	1.11	12.24
KO95TTRI.360	19.36	1.56	17.14

Table 5.18 Second Mode Peak Roof Displacement Estimates for Rigid-12

	YPS 2nd Mode Estimation		
Record	u_{elas}^{SDOF} [cm]		u_{u}^{MDOF} [cm]
WN87MWLN.090	0.42	Elastic	0.258
BB92CIVC.360	5.00	Elastic	3.077
SP88GUKA.360	3.00	Elastic	1.846
LP89CORR.090	5.50	Elastic	3.385
NR94CENT.360	3.40	Elastic	2.092
CH85LLEO.010	10.50	Elastic	6.461
CH85VALP.070	3.80	Elastic	2.338
IV40ELCN.180	5.50	Elastic	3.385
LN92JOSH.360	4.70	Elastic	2.892
MX85SCT1.270	1.60	Elastic	0.985
LN92LUCN.250	3.70	Elastic	2.277
LP89SARA.360	3.70	Elastic	2.277
NR94NWHL.360	11.00	Elastic	6.769
NR94SYLH.090	8.50	Elastic	5.231
KO95TTRI.360	11.00	Elastic	6.769

5.4.3.2 Analysis of Results

Some observations with respect to the accuracy of simplified equations used to estimate interstory drift index can be pointed out with help from Figures 5.13 to 5.24 and statistical analysis of the results. Tables 5.19 and 5.20 present statistics, for all the ground motions, of the ratios between the peak interstory drift index estimates and the corresponding value obtained from nonlinear dynamic analyses. Mean and standard deviations are shown for the three IDI estimates.

For each frame, Table 5.19 shows the mean and standard deviation of the ratio of the absolute peak IDI estimation to the absolute maximum IDI from the nonlinear dynamic analyses, regardless of the story in which these two values occurred.

Table 5.19 Ratio of Absolute Peak IDI Estimates to Peak IDI Computed in Nonlinear Dynamic Analysis

	IDI Estimate 1		IDI Estimate 2		IDI Estimate 3	
	Mean	Std. Dev.	Mean	Std. Dev.	Mean	Std. Dev.
Flexible-4	0.905	0.134	0.926	0.090	1.081	0.101
Rigid-4	0.912	0.137	0.958	0.080	1.131	0.090
Flexible-12	0.570	0.200	0.755	0.158	1.002	0.220
Rigid-12	0.695	0.203	0.847	0.141	1.139	0.181

For the 4-story frames, Table 5.19 shows that the mean results obtained using IDI Estimate 1 (first mode shape and Equation 5.7) are good, although a little low compared to results obtained from nonlinear dynamic analyses. Use of IDI Estimate 2 (two mode shapes and Equation 5.8; SRSS) produces better mean estimates with significant reduction in the dispersion of the results compared with IDI Estimate 1. Mean results from IDI Estimate 3 (two mode shapes and Equation 5.9; ABS Max) are also good for the 4-story building; although, this equation overestimates mean results and has a larger standard deviation.

For the 12-story frames, Table 5.19 shows that the mean results obtained using IDI Estimate 1 are significantly below the results obtained from nonlinear dynamic analyses with a dispersion larger than the one obtained for the 4-story frames using the same equation. Use of IDI Estimate 2 produces better mean estimates compared with IDI Estimate 1 but not as good as the mean results obtained for the 4-story frames using the same equation. There was a reduction in the dispersion of the results compared with IDI Estimate 1. Mean results from IDI Estimate 3 are good for the 12-story building. This equation slightly overestimates mean results and has larger dispersion compared with IDI Estimate 2.

Tables 5.20 and 5.21 show statistics, including results from all the ground motions, for each individual story and all the stories collectively for the frames considered.

Table 5.20 Statistics of Story Ratios of Estimated IDI to Computed IDI for 4-Story Frames

Flexible-4

	IDI Estimate 1		IDI Estimate 2		IDI Estimate 3	
Story	**Mean**	**Std. Dev.**	**Mean**	**Std. Dev.**	**Mean**	**Std. Dev.**
4	**0.995**	**0.453**	**1.166**	**0.384**	**1.538**	**0.458**
3	**0.999**	**0.264**	**1.056**	**0.219**	**1.285**	**0.200**
2	**0.995**	**0.074**	**0.996**	**0.073**	**1.038**	**0.069**
1	**0.888**	**0.142**	**0.929**	**0.126**	**1.115**	**0.177**
Total	**0.970**	**0.272**	**1.036**	**0.243**	**1.243**	**0.324**

Rigid-4

	IDI Estimate 1		IDI Estimate 2		IDI Estimate 3	
Story	**Mean**	**Std. Dev.**	**Mean**	**Std. Dev.**	**Mean**	**Std. Dev.**
4	**0.871**	**0.239**	**0.983**	**0.154**	**1.250**	**0.169**
3	**0.964**	**0.150**	**1.010**	**0.125**	**1.196**	**0.159**
2	**1.006**	**0.069**	**1.012**	**0.064**	**1.089**	**0.072**
1	**0.946**	**0.129**	**0.998**	**0.130**	**1.195**	**0.212**
Total	**0.947**	**0.162**	**1.001**	**0.120**	**1.182**	**0.168**

Table 5.21 Statistics of Story Ratios of Estimated IDI to Computed IDI for 12-Story Frames

Flexible-12

	IDI Estimate 1		IDI Estimate 2		IDI Estimate 3	
Story	Mean	Std. Dev.	Mean	Std. Dev.	Mean	Std. Dev.
12	0.440	0.236	0.781	0.233	1.048	0.311
11	0.484	0.251	0.813	0.202	1.096	0.272
10	0.575	0.244	0.881	0.173	1.197	0.227
9	0.644	0.242	0.889	0.182	1.206	0.211
8	0.704	0.233	0.856	0.202	1.140	0.228
7	0.746	0.179	0.812	0.173	1.025	0.205
6	0.811	0.123	0.817	0.123	0.894	0.137
5	0.831	0.176	0.844	0.176	0.956	0.204
4	0.831	0.202	0.893	0.194	1.125	0.256
3	0.813	0.187	0.927	0.165	1.219	0.240
2	0.804	0.188	0.955	0.147	1.276	0.221
1	0.814	0.235	0.987	0.191	1.323	0.258
Total	0.708	0.245	0.871	0.186	1.126	0.259

Rigid-12

	IDI Estimate 1		IDI Estimate 2		IDI Estimate 3	
Story	Mean	Std. Dev.	Mean	Std. Dev.	Mean	Std. Dev.
12	0.629	0.298	0.853	0.259	1.170	0.344
11	0.690	0.256	0.915	0.188	1.252	0.238
10	0.740	0.214	0.914	0.155	1.236	0.187
9	0.788	0.189	0.906	0.149	1.196	0.173
8	0.843	0.139	0.900	0.118	1.129	0.133
7	0.881	0.128	0.896	0.122	1.027	0.120
6	0.885	0.139	0.885	0.139	0.887	0.138
5	0.895	0.122	0.905	0.119	1.015	0.122
4	0.885	0.131	0.918	0.125	1.105	0.157
3	0.890	0.135	0.947	0.131	1.186	0.186
2	0.898	0.142	0.976	0.126	1.246	0.177
1	0.891	0.155	0.979	0.133	1.263	0.181
Total	0.826	0.195	0.916	0.151	1.143	0.214

For the 4-story frames, Table 5.20 shows that the use of one mode to estimate interstory drift indices (IDI Estimate 1) produces good mean results for all the stories of the frames. While results for the second and third floor are very good in general, estimates for the other stories are a little low. Mean results from IDI Estimate 2 may be considered to be better than those of IDI Estimate 1. Additionally, there is reduction in the dispersion of the results. In general, IDI Estimate 3 overestimates mean results for interstory drift indices, with dispersions comparable to those obtained using IDI Estimate 1. Looking at the stories collectively, IDI Estimate 1 underestimates mean results of interstory drift indices while IDI Estimate 2 slightly overestimates them. The results of dispersion for IDI Estimate 2 was lower than that for IDI Estimate 1. IDI Estimate 3 overestimates mean results of interstory drift indices, and has larger dispersion compared with the other two estimates.

For the 12-story frames, Table 5.21 shows that mean results obtained using IDI Estimate 1 and IDI Estimate 2 underestimate interstory drift indices for any individual story of the frames. Although both underestimate interstory drift indices, estimates obtained using IDI Estimate 2 are more accurate than those of IDI Estimate 1. The dispersion in the results for IDI Estimate 2 was lower than that for IDI Estimate 1. In general, IDI Estimate 3 overestimates mean interstory drift indices, with larger dispersion compared with IDI Estimate 1 and IDI Estimate 2.

IDI Estimate 2 is definitely better at the upper and lower stories of the frames compared with IDI Estimate 1 and IDI Estimate 3, although the accuracy of the peak interstory drift indices estimates was reduced towards the top of the frames for IDI Estimate 1 and IDI Estimate 2. On the other hand, IDI Estimate 3 produces better results toward the center of the frame, and is less accurate at the lower stories.

For all the frames, Equation 5.8 (IDI Estimate 2) results in the lowest dispersion of all the equations considered. In general, the dispersion associated with this estimate increases towards the top and bottom stories of the frames, with greatest dispersion toward the top.

5.5 The Flexible-12 Frame and the LP89CORR.090 Record

There were some cases, particularly with the Flexible-12 frame, in which the three nonlinear procedures gave poor estimates of the peak roof displacement, even for responses in the linear range. Examples of these poor results are the peak displacement estimates for the BB92CICV.360, the LP89CORR.090 and the LN92JOSH.360 records (See Figure 5.10-b). For these three cases, the response was presumed to be elastic because peak displacements estimated using simplified nonlinear static procedures and even the peak displacement calculated using nonlinear dynamic analysis (DRAIN-2DX) were smaller, as summarized in Table 5.22, than the yield displacement of this frame in a first mode pushover analysis, 35.3 cm. (See Figure 5.5).

Table 5.22 Peak Roof Displacement for Flexible-12

Record	Drain-2DX u_u^{MDOF} [cm]	YPSA u_u^{MDOF} [cm]	DCM u_u^{MDOF} [cm]	CSM u_u^{MDOF} [cm]
bb92civc.360	11.51	7.68	7.70	7.60
lp89corr.090	23.62	15.09	13.78	15.15
ln92josh.360	22.77	17.84	17.01	17.74

Although a general explanation for the poor performance of the NSPs in these three cases could not be identified, an explanation was found for the Loma Prieta at Corralitos record. The Yield Point Spectra for the LP89CORR.090 record, shown in Figure 5.25, helps to understand the response of Flexible-12 frame under this record. The equivalent SDOF first mode yield point for the Flexible-12 frame (C_y = 0.22 and u_y^{sdof} =0.257 m.; see Table 5.4a) is indicated in the figure using a 'x' sign. The equivalent period of vibration, 2.17 sec., is represented by a dotted diagonal line.

Figure 5.25 shows that the equivalent SDOF yield point for this frame lies well beyond the constant ductility curve representing a displacement ductility of one; therefore, elastic response was assumed. Notice that the equivalent first mode period, 2.17 sec., coincides with a depression in the elastic spectrum, reducing the peak displacement demand, indicated with an arrow in Figure 5.25, for this frame

On the other hand, Figure 5.25 also shows that elastic demands are particularly high for oscillators having periods in the 0.6 to 0.9 sec. range. Since the second mode of vibration

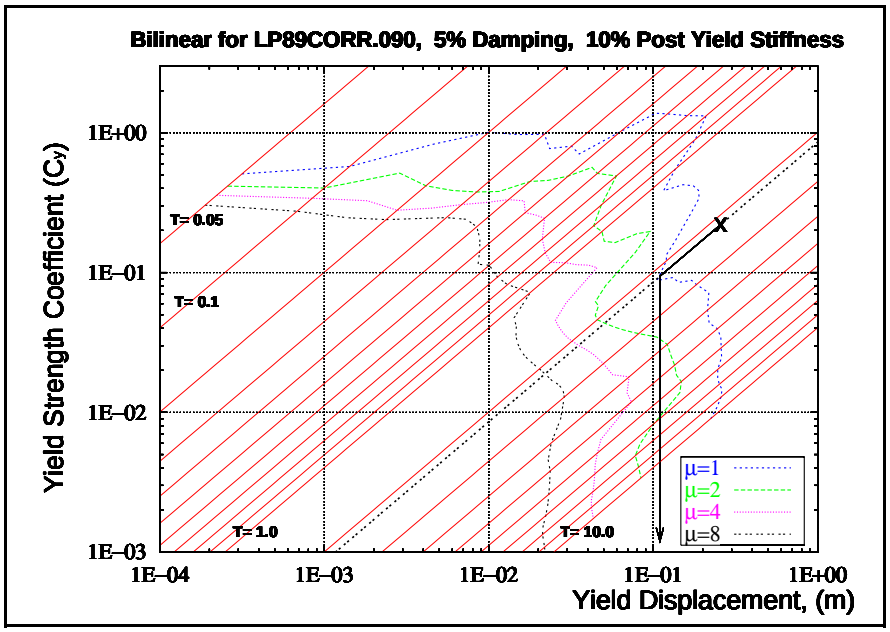

Figure 5.25 5% Damped Yield Point Spectra for Loma Prieta at Corralitos
The 'x' Sign Indicates the First Mode Yield Point of the Flexible-12 Frame

of the Flexible-12 frame has a period of 0.80 sec. (Table 5.4b), it was considered that the response of Flexible-12 frame to this record may have been significantly influenced by the second mode of vibration.

Figure 5.26 shows the Yield Point Spectra for the LP89CORR.090 record generated using damping equal to 2.8%. In this figure, the equivalent SDOF second mode yield point for the Flexible-12 frame (C_y = 1.2 and u_y^{sdof} = 0.19 m.; see Table 5.4b) is indicated with a 'x' sign. This figure shows that the second mode period of the Flexible-12 frame was very excited. Even more, the figure suggests that some nonlinear behavior occurs in the frame because the yield point for the second mode lies between the curves of displacement ductilities 1 and 2.

The YPS estimate for the peak roof displacement using the first mode of vibration for this record is 15.1 cm. (see Table 5.7) while a similar estimate for the second mode is 12.04 cm. (see Table 5.17). The peak roof displacement estimate for second mode represents a 80% of that due to the first mode. The mean for this ratio considering the 15 ground motion was 28% for this frame, confirming the high influence of the second mode in the response of this frame to the Loma Prieta at Corralitos record.

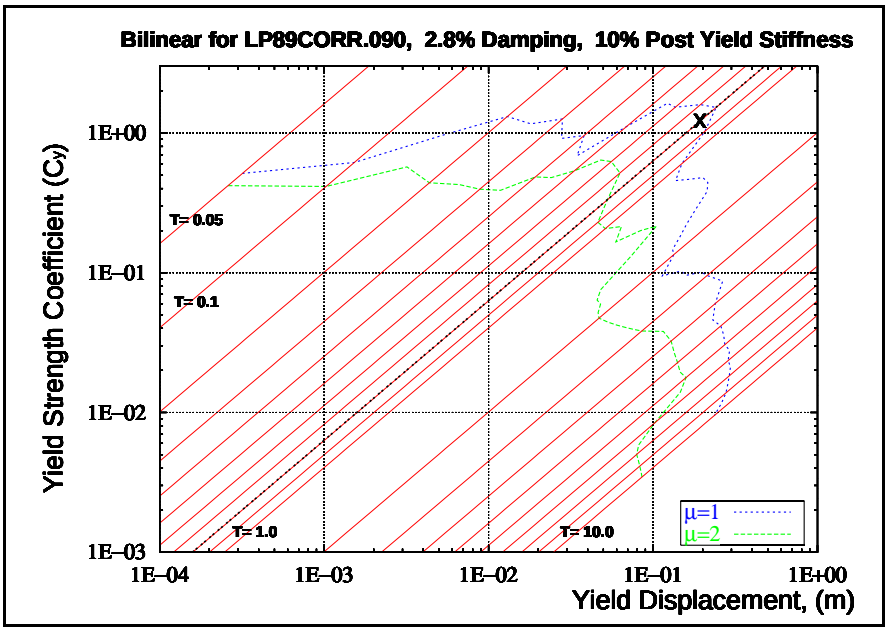

Figure 5.26 2.8% Damped Yield Point Spectra for Loma Prieta at Corralitos
The 'x' Sign Indicates the Second Mode Yield Point of the Flexible-12 Frame

Analysis using DRAIN-2DX confirmed that nonlinear behavior occurs in this frame during its response to the LP89CORR.090 record.

Figure 5.27 shows plastic hinges formed in Flexible-12 frame after being subjected to the Loma Prieta at Corralitos record. A total of 36 plastic hinges were produced by this record, 32 beam hinges and 4 column hinges. Plastic hinges are shown as dark circles. This figure confirms that the Flexible-12 frame experienced nonlinear deformations responding to the LP89CORR.090 record.

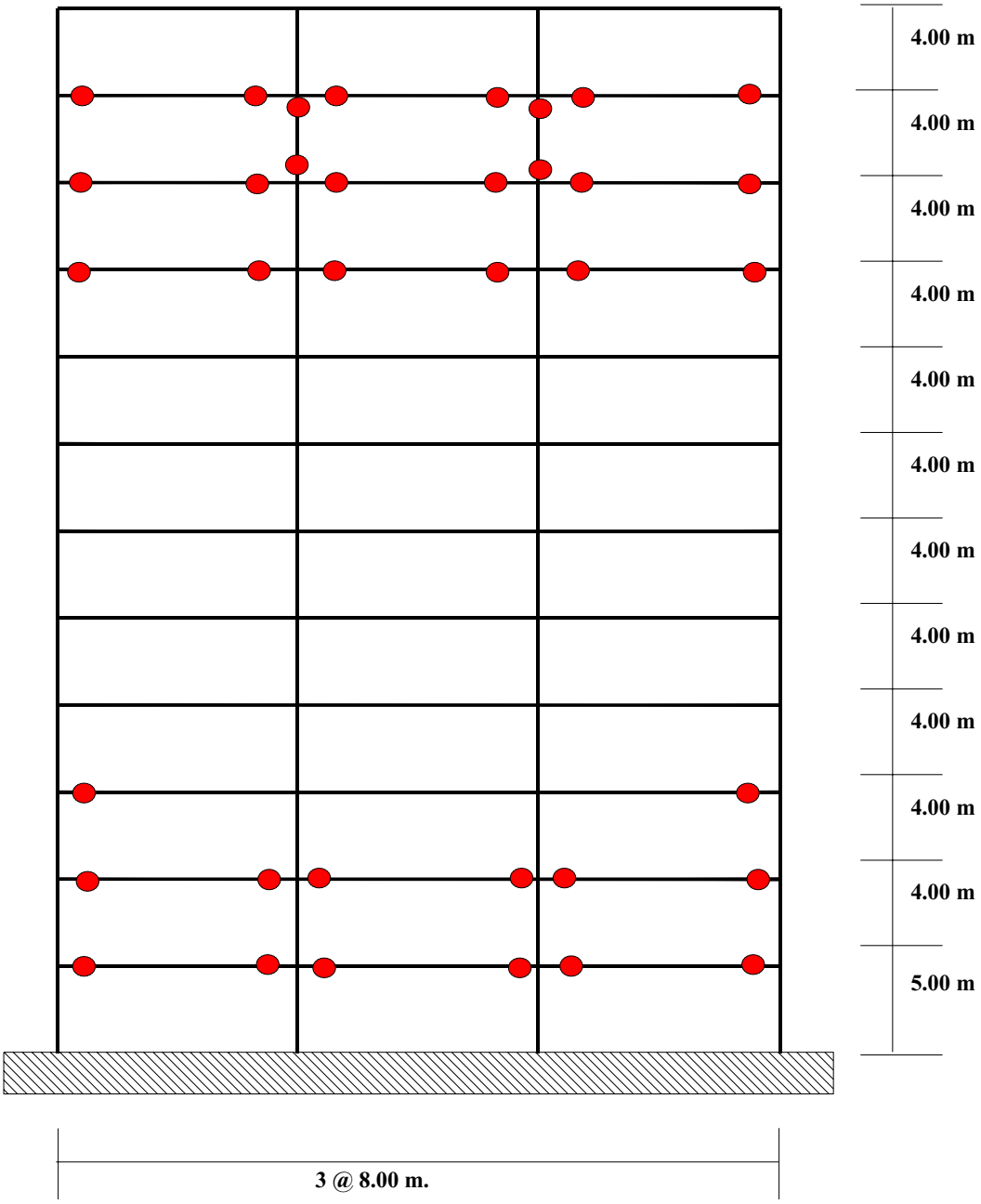

Figure 5.27 Plastic Hinges Formed During Response to the Corralitos Record

5.6 Summary

A method to estimate peak displacement of multistory buildings was introduced, and was identified as the YPSA method to differentiate it from the YPS design methodology presented in Chapter 4. The YPSA method was classified as a nonlinear static procedure (NSP).

Peak displacement estimates were obtained with three NSPs (the Displacement Coefficient Method, the Capacity Spectrum Method and the YPSA method) and compared using plots and tables. Mean and standard deviation statistics for the three NSPs were shown and discussed.

Peak displacements corresponding to the second mode of vibration were obtained using the YPSA method. These second mode related peak displacements and corresponding values obtained for the first mode were combined to estimate interstory drift indices (IDI). Results of the three IDI estimates are compared using plots, tables and simple statistics.

A special case in which the second mode causes significant yielding in one of the frames analyzed was detected. For this particular case, the YPSA method was able to predict the second mode related nonlinear behavior of the frame.

CHAPTER 6

SUMMARY AND CONCLUSIONS

6.1 Summary and Conclusions

This chapter summarizes the results obtained during the course of this study in relation to three main objectives.

The first objective was to explore the utility of a new representation of constant ductility response spectra named Yield Point Spectra (YPS). These spectra were used directly for the design and analysis of SDOF structures. For design, graphical procedures were used to determine combinations of strength and stiffness to limit drift and displacement ductility demands to prescribed values. For analysis, accurate estimates of the the peak displacement and displacement ductility demands of the SDOF structures were obtained using the logarithmic form of YPS. An application of YPS to the performance-based design of a SDOF structure was illustrated with an example. Yield Point Spectra for 15 ground motion records and two load-deformation models were presented.

The second objective was to outline a design methodology for the seismic design of regular multistory buildings using Yield Point Spectra. The methodology was formulated to be as similar to current code approaches as possible. A minimum base shear strength for design was determined based on user specified limits on peak roof displacement and interstory drift. In contrast to current code approaches, which rely on an estimated period of vibration, the proposed methodology uses an estimated yield displacement of the frame as the initial parameter for seismic design. The methodology was illustrated by designing four moment-resistant steel frames. The effectiveness of the methodology to limit peak roof displacement and interstory drift was validated using nonlinear static and dynamic analyses.

The third objective was to develop a method in which YPS are used to estimate peak displacement response and interstory drift of multistory frames. The method was identified as the YPSA method, and classified as a Nonlinear Static Procedure (NSP). The YPSA method was compared with others NSPs and with results from nonlinear dynamic analyses. The YPSA method was also used to estimate interstory drift indices (IDI) using deformed shapes of the frames based on the first mode and combinations of the first and second mode shapes.

The second and third objectives relate to the analysis and design of multistory buildings. To achieve these objectives it was necessary to transform the multistory building response to an equivalent SDOF system using established techniques. For the transformation, the equivalent SDOF methodology requires the assumption of a deformed shape. For design of the four case study frames, the deformed shape assumed had a triangular distribution of lateral deflections. For the analysis of the frames, the assumed deformed shape was the first elastic mode shape.

Finally, a peculiar case was identified in which the YPSA method detected the nonlinear response in the second mode of vibration of one of the case study frames.

Based on the observations and analyses of results obtained from the set of four frames and the fifteen ground motions considered in this study, the following conclusions and trends were identified:

(1) Yield Point Spectra are useful for the analysis and design of SDOF systems. Yield Point Spectra allow one to estimate the peak displacement and the displacement ductility demands of SDOF structures. These spectra are also useful for establishing combinations of strength and stiffness required to limit drift and displacement ductility demands to arbitrary values.

(2) Yield Point Spectra provide a graphical approach to consider multiple performance levels in performance-base seismic design. Individual YPS, representing a given intensity of ground shaking and recurrence interval, may be used to define an admissible design region conforming to specific performance levels. Two or more of these admissible design regions may be superimposed to define a final design region according to the performance objective.

(3) The equivalent SDOF methodology is useful for modeling the response of multistory framed structures. The methodology permits analysis and design of multistory systems using the Yield Point Spectra developed for SDOF oscillators.

(4) The proposed YPS design methodology was shown to be effective for limiting the peak displacement response and interstory drift of the four example frames to the intended values

(5) The use of yield displacement as an alternative to period as fundamental parameter for seismic design seems feasible. For the four frames designed using this assumption, the ratio of yield displacement to building height was within the suggested range (0.6%-0.9%). Values of the yield displacement varied from 0.68% to 0.79% of the building height for the four frames, while the fundamental period of vibration varied from 0.71 to 1.16 sec. for the 4-story frames and from 1.25 to 2.17 sec. for the 12-story frames.

(6) In general, buildings require a minimum lateral strength to control inelastic response demands. The procedure used to provide the four example frames with the required minimum strength was very effective. The procedure consists in obtaining preliminary sizes for the structural members based on the design forces prescribed by the proposed design methodology. After that, the design is refined using the approximate value of the equivalent period (Equation 2.2) as a target to be matched by the actual first mode period of the frame. If this observation, which is a consequence of the stability of the yield displacement, is confirmed by future studies, then to provide a moment-resistant steel frame with the required strength it would be sufficient to give it a fundamental period equal or less than the equivalent period obtained from Yield Point Spectra. Furthermore, the nonlinear static analysis (pushover) would be dispensable as a tool to verify the strength of moment resistant steel frames. This observation also would be very useful for all Nonlinear Static Procedures (NSPs).

(7) Approximate deformed shapes, in particular the triangular shape assumed to apply the equivalent SDOF formulation to design the case study frames, appear to be adequate for framed buildings. Although the other two parabolic deformed shapes were not used, they may be appropriate for different building systems.

(8) Peak displacement estimates given by the YPSA method, the Displacement Coefficient Method (DCM) and the Capacity Spectrum Method (CSM) were compared for the four case-study frames. In a mean sense, results from the YPSA method and from the CSM are similar although the YPSA method gave slightly more accurate mean estimates for the four frames and 15 ground motions. The dispersion of the peak displacement estimates using the YPSA method was smaller than the dispersion obtained using the CSM for the four frames and 15 ground motions. The DCM overestimated mean results of the peak displacements and had greater results in dispersion than the other two methods.

(9) Even though the CSM and the YPSA methods provide similar accuracy for estimating peak displacement response, the simplicity of the YPSA method makes it more attractive. In the YPSA method, peak displacement estimates are obtained by simply "reading" system displacement ductility and maximum elastic displacement from the Yield Point Spectra. In the CSM, peak displacement estimates are obtained using a more elaborate iterative process.

(10) In general, interstory drift index estimates were less accurate then peak roof displacement estimates.

(11) Peak roof displacements can be estimated using linear static analysis and the design lateral forces obtained by distributing the base shear strength along the height of the building. Ultimate roof displacement is obtained by multiplying displacements computed under the design lateral forces by the system ductility demand read from YPS. However, a similar procedure underestimates values for interstory drift indices.

(12) Profiles of interstory drift obtained using one deformed shape (fundamental mode shape) amplified by the peak roof displacement, in a mean sense, provided good interstory drift estimates for the 4-story frames; although, the dispersion of these estimates was a little high. For the 12-story frames, the use of a single deformed shape was inadequate for good interstory drift estimates. The inclusion of a second mode shape, combined with the

fundamental mode shape using the SRSS rule, to obtain interstory drift indices improves the estimates and reduces their dispersion.

(13) The accuracy of peak roof displacements and interstory drift indices estimated using the YPSA method show no particular tendency with respect to the three ground motion categories: short duration, long duration and forward directivity.

6.2 Suggestions for Future Research

This research provides a basic framework for a methodology for the seismic design of regular framed buildings. However, some issues remain unresolved and should be addressed before the proposed methods may be generally recommended. Some of these are:

1) Yield Displacement Stability. It was shown that the ratio of the yield displacement to the building height for moment resistant frames is very stable. This ratio and its stability should be addressed for other structural systems such as reinforced concrete moment frames and shear walls.
2) Smoothed Yield Point Spectra. Current code provisions prescribe smoothed design spectra for design of building structures. The effectiveness of smoothed YPS constructed from elastic spectra reduced using period-dependent strength reduction factors should be verified.
3) Irregular Buildings. The proposed methodologies were effective controlling the peak roof displacement and interstory drift of regular frame structures. The accuracy of the methodologies addressing the same parameters in irregular buildings should be addressed. Irregularities in mass distribution and soft stories should be studied.

APPENDIX A

SELECTED GROUND MOTIONS

Figures A.1 to A.15 presents detailed plots of the ground motion selected for this study. These ground motion are listed in Table 2.2.

Each figure contain plots presenting time series data corresponding to the acceleration, velocity and displacement for the record. Additionally, equivalent velocity spectra and pseudo-acceleration spectra are also shown. These spectra were used to establish the characteristic periods of the ground motions.

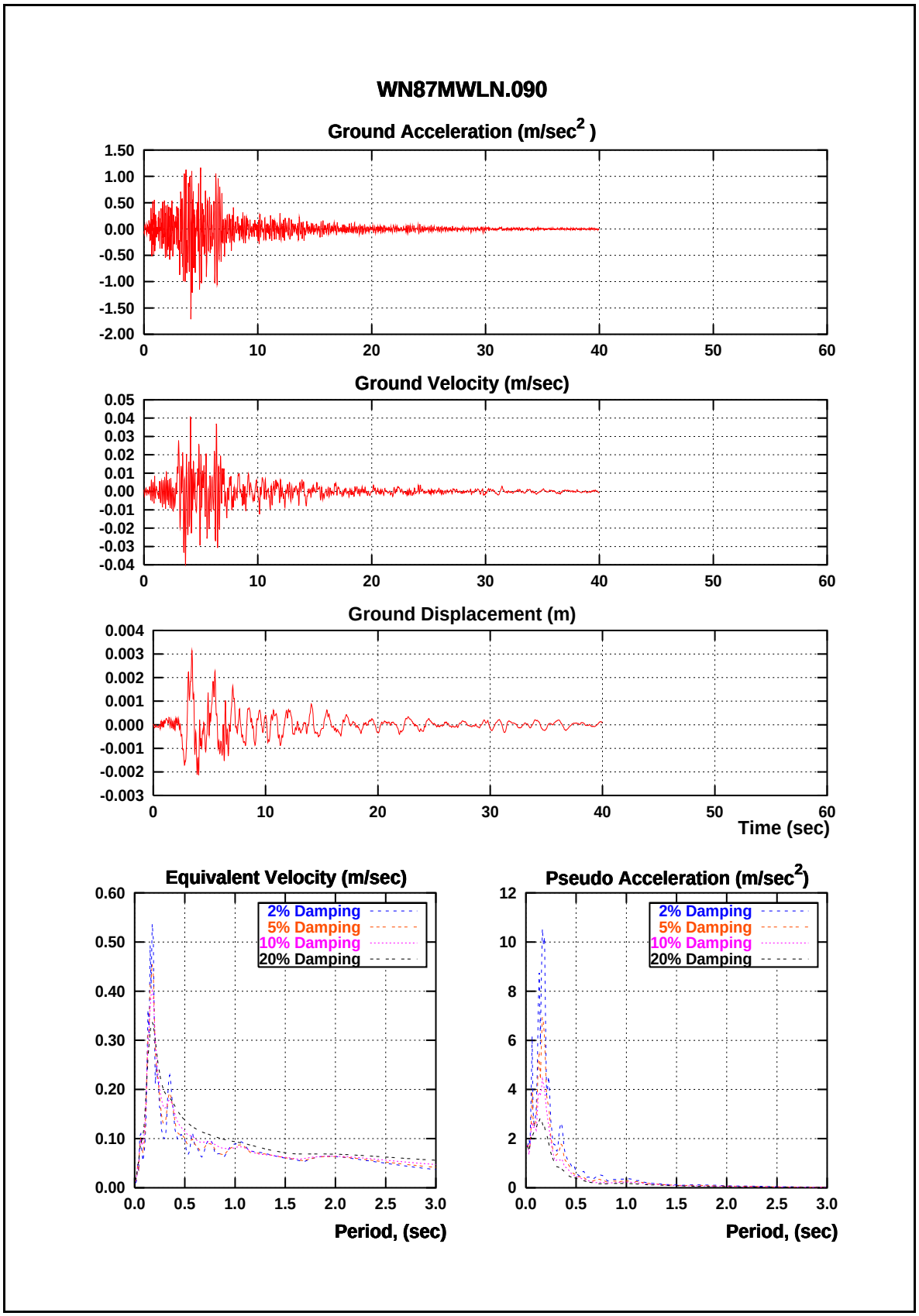

Figure A.1 Characteristics of the WN87MWLN.090 Ground Motion

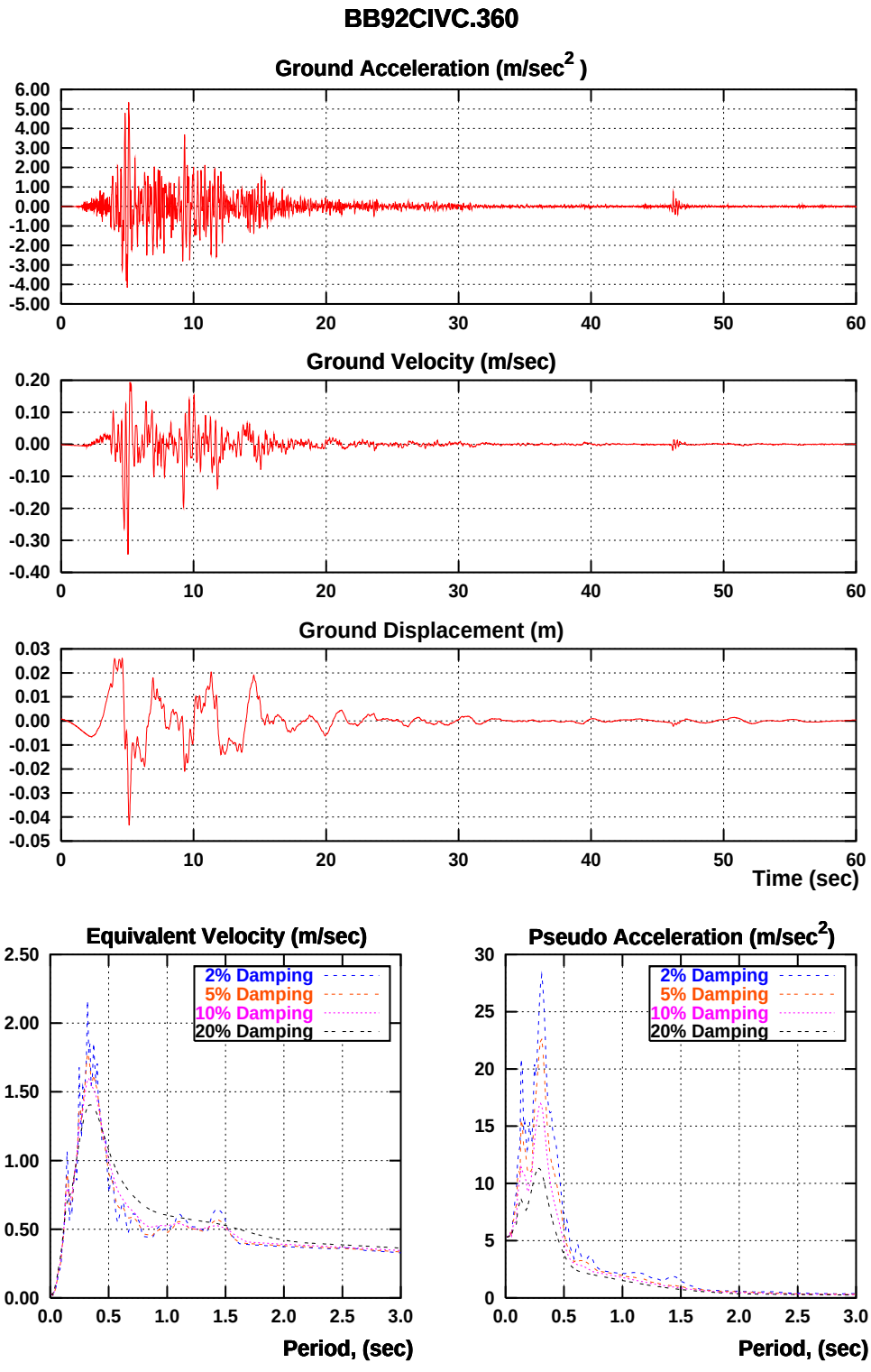

Figure A.2 Characteristics of the BB92CIVC.360 Ground Motion

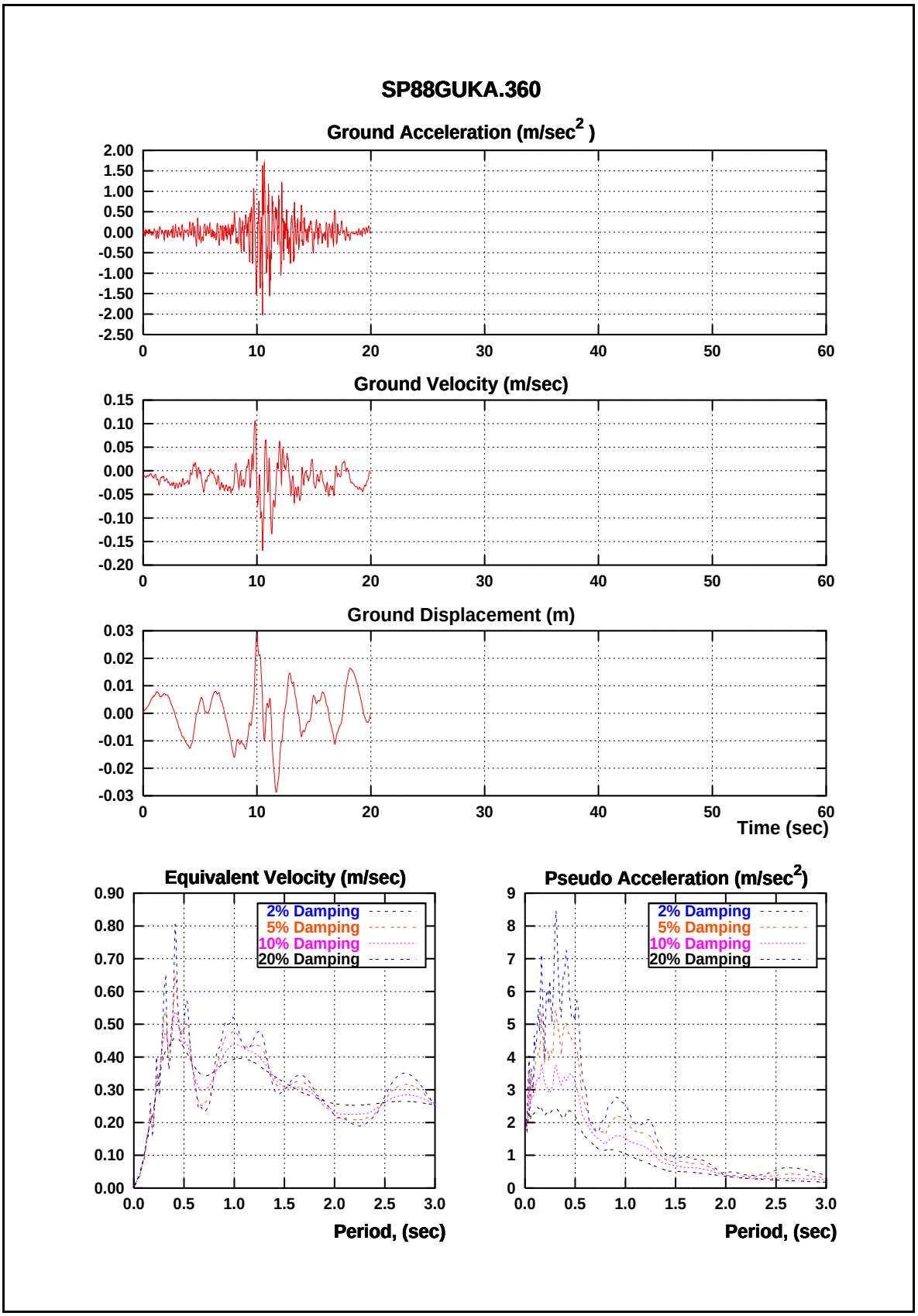

Figure A.3 Characteristics of the SP88GUKA.360 Ground Motion

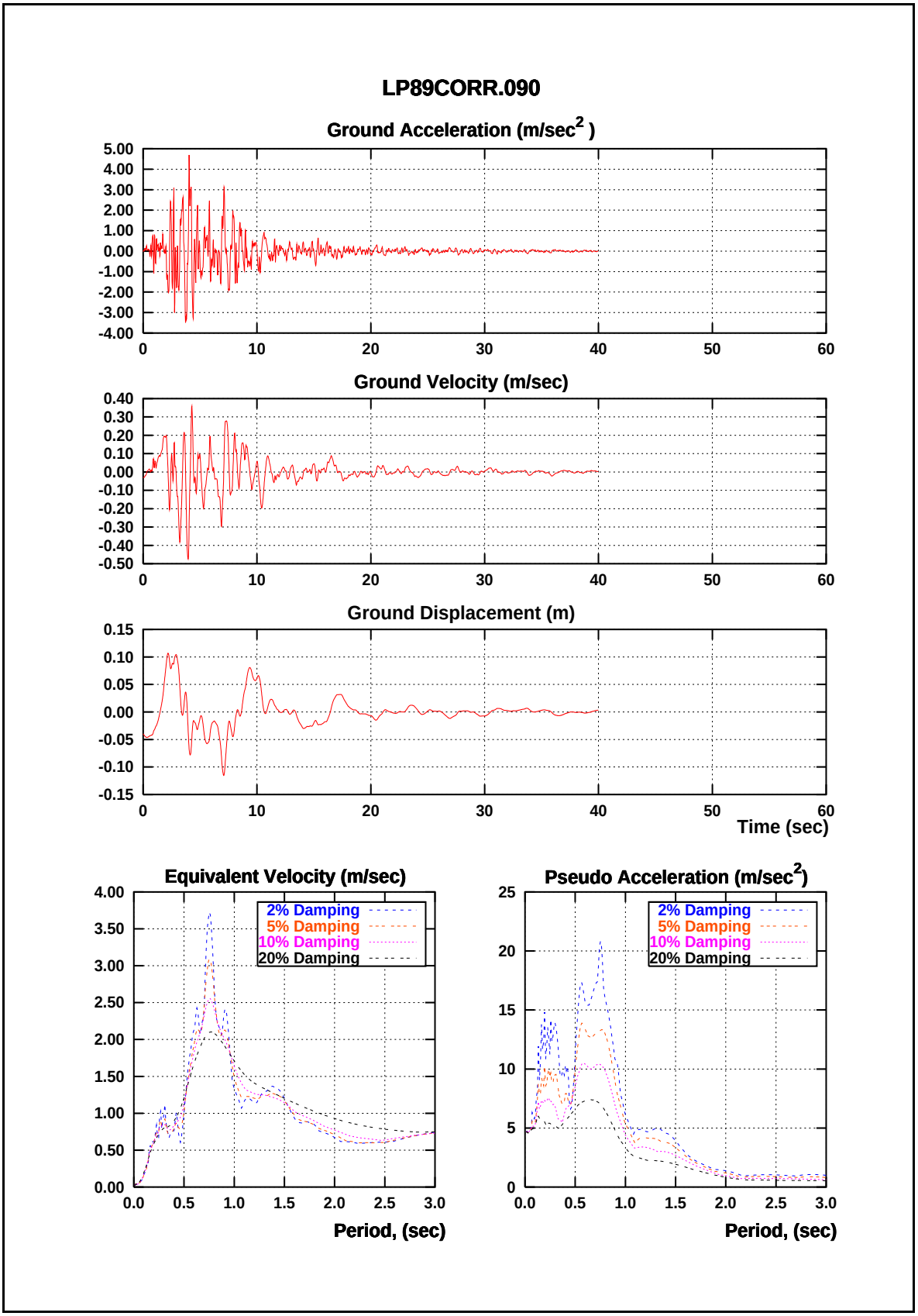

Figure A.4 Characteristics of the LP89CORR.090 Ground Motion

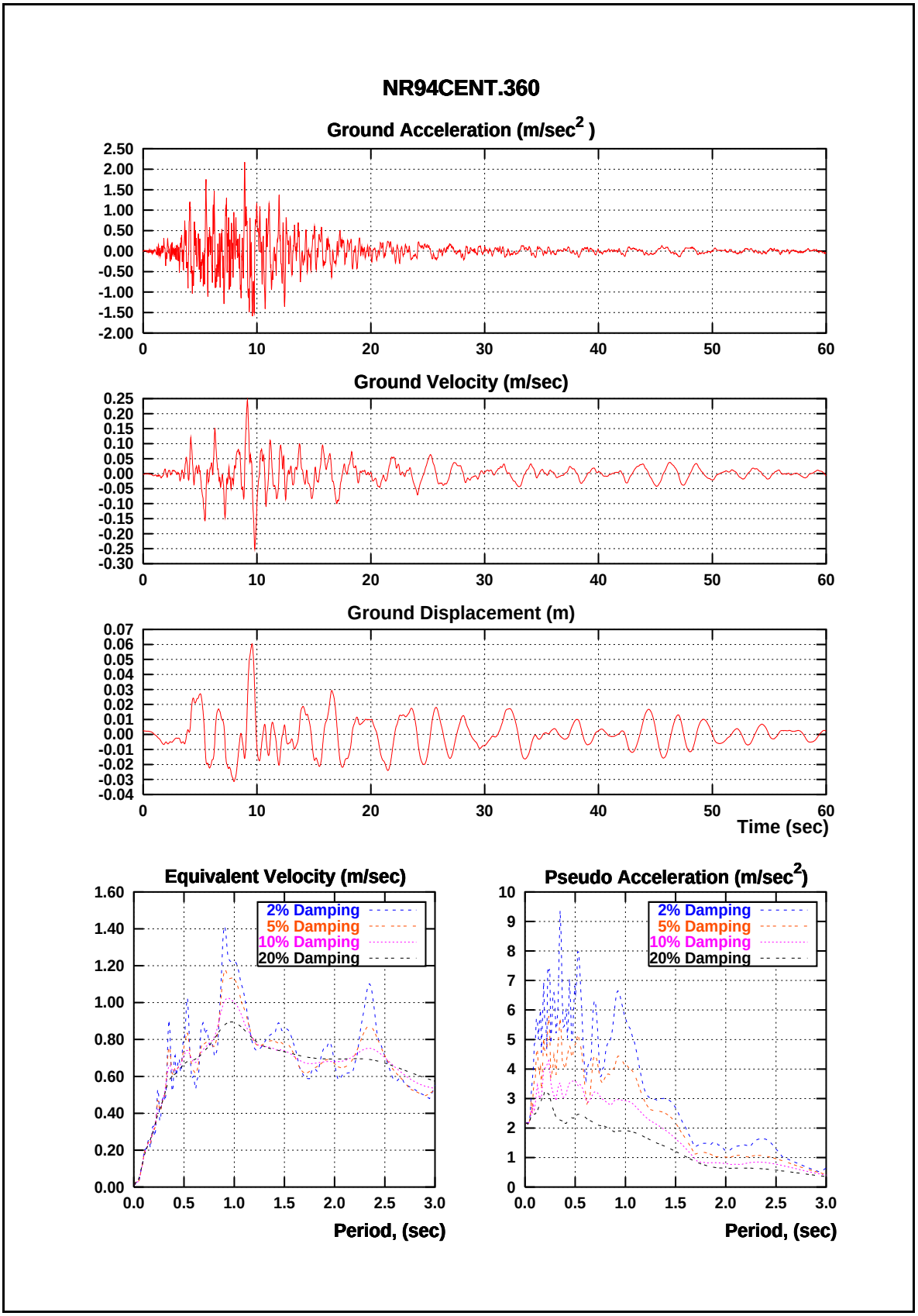

Figure A.5 Characteristics of the NR94CENT.360 Ground Motion

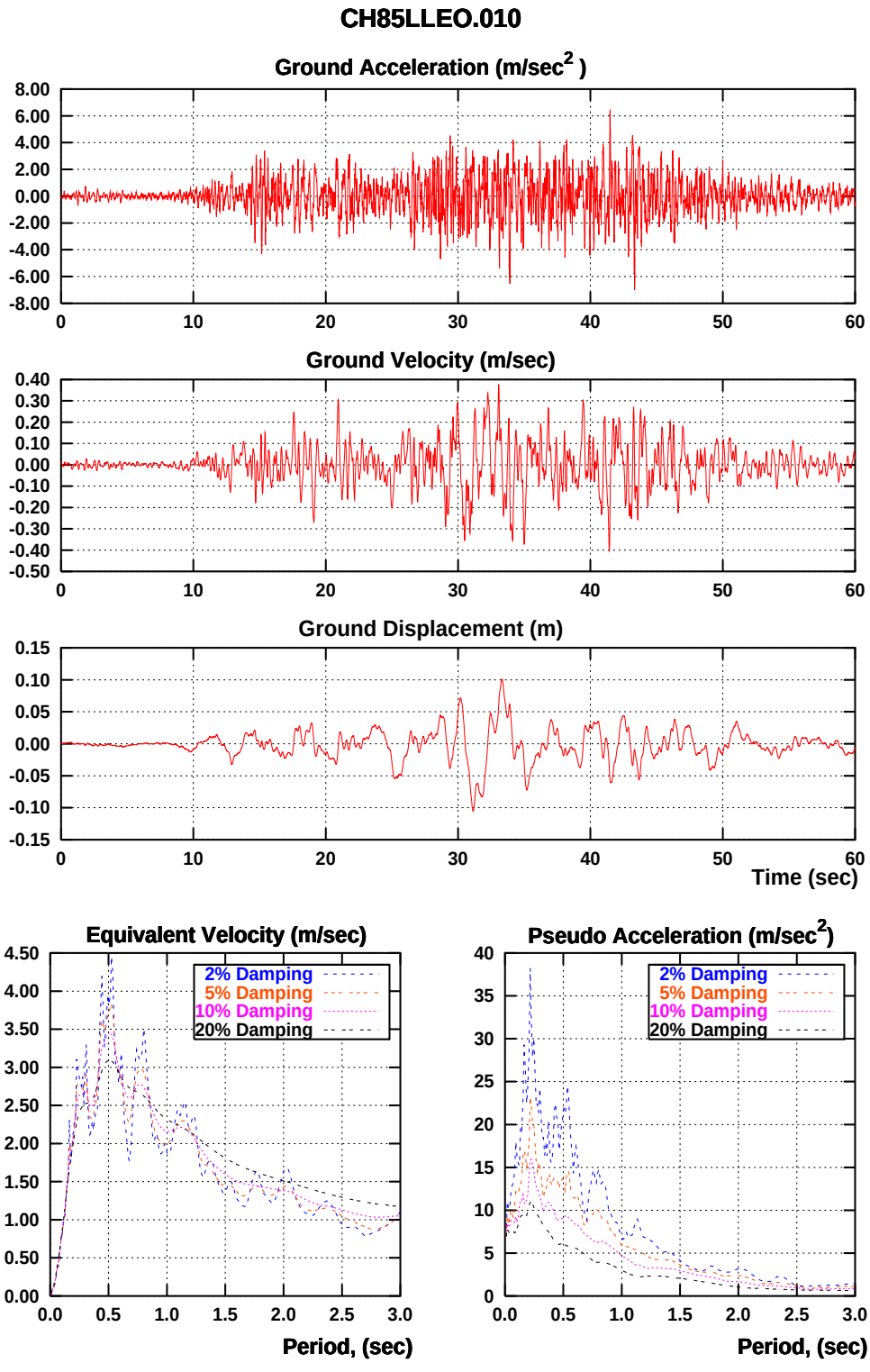

Figure A.6 Characteristics of the CH85LLEO.010 Ground Motion

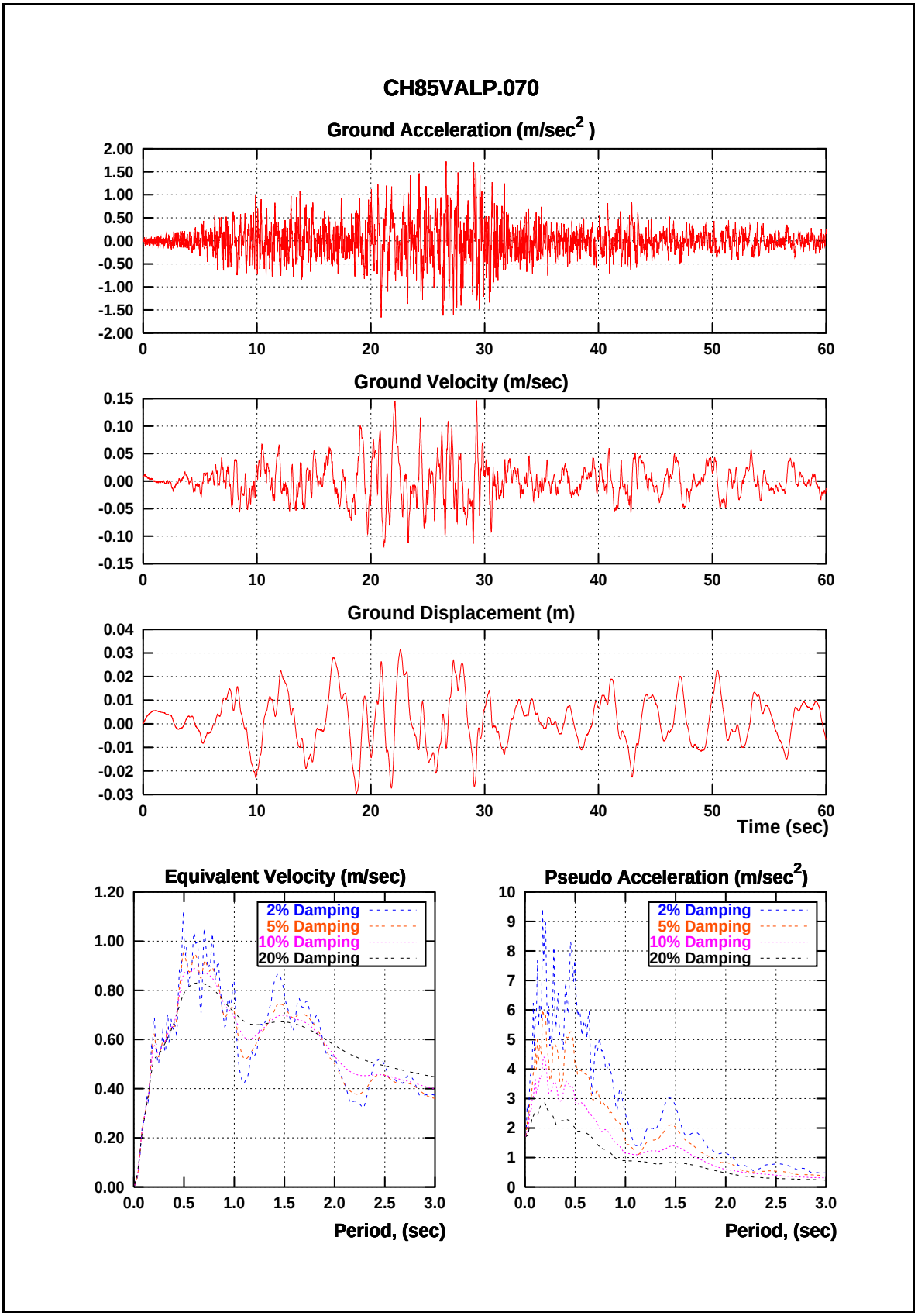

Figure A.7 Characteristics of the CH85VALP.070 Ground Motion

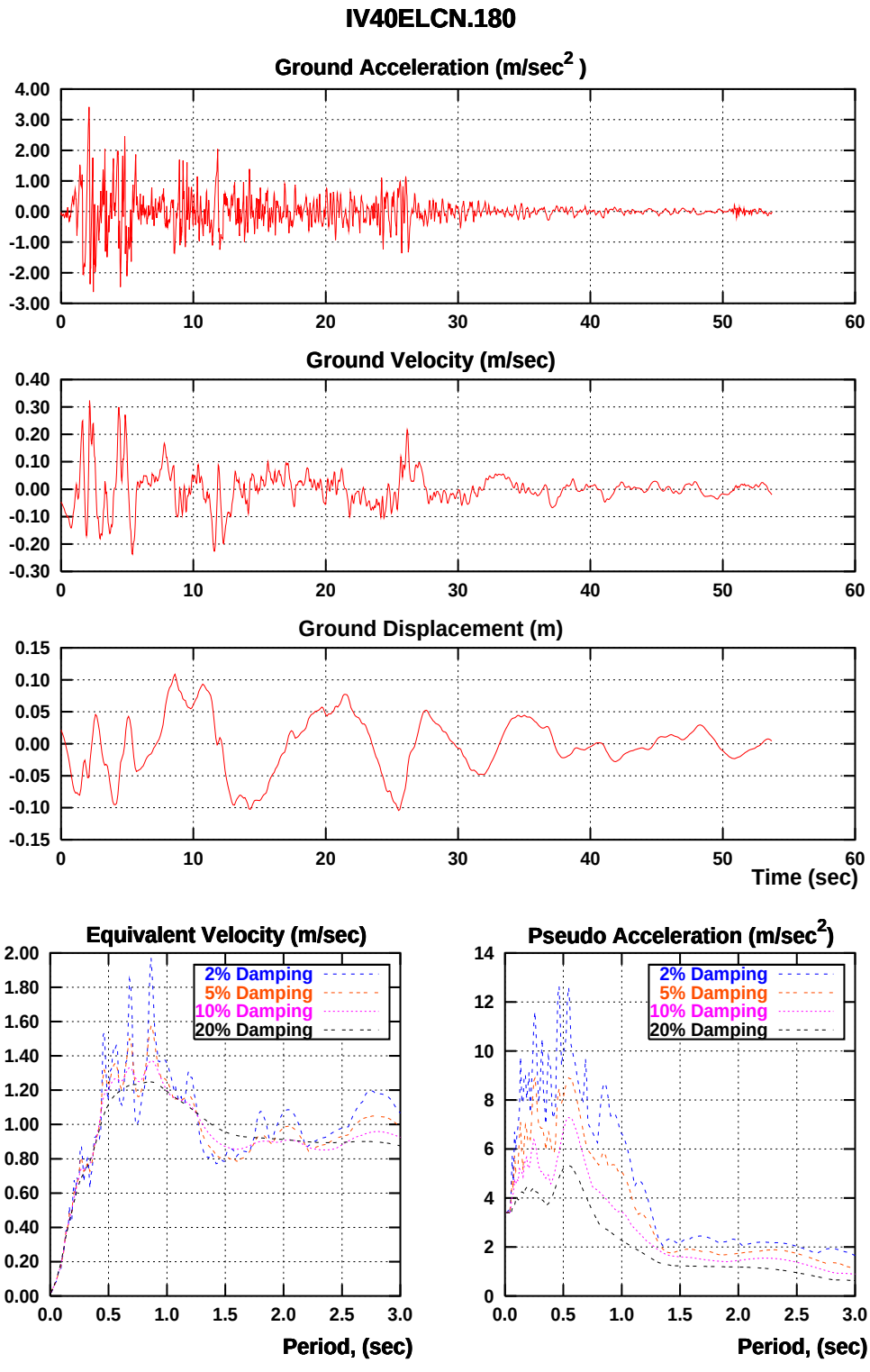

Figure A.8 Characteristics of the IV40ELCN.180 Ground Motion

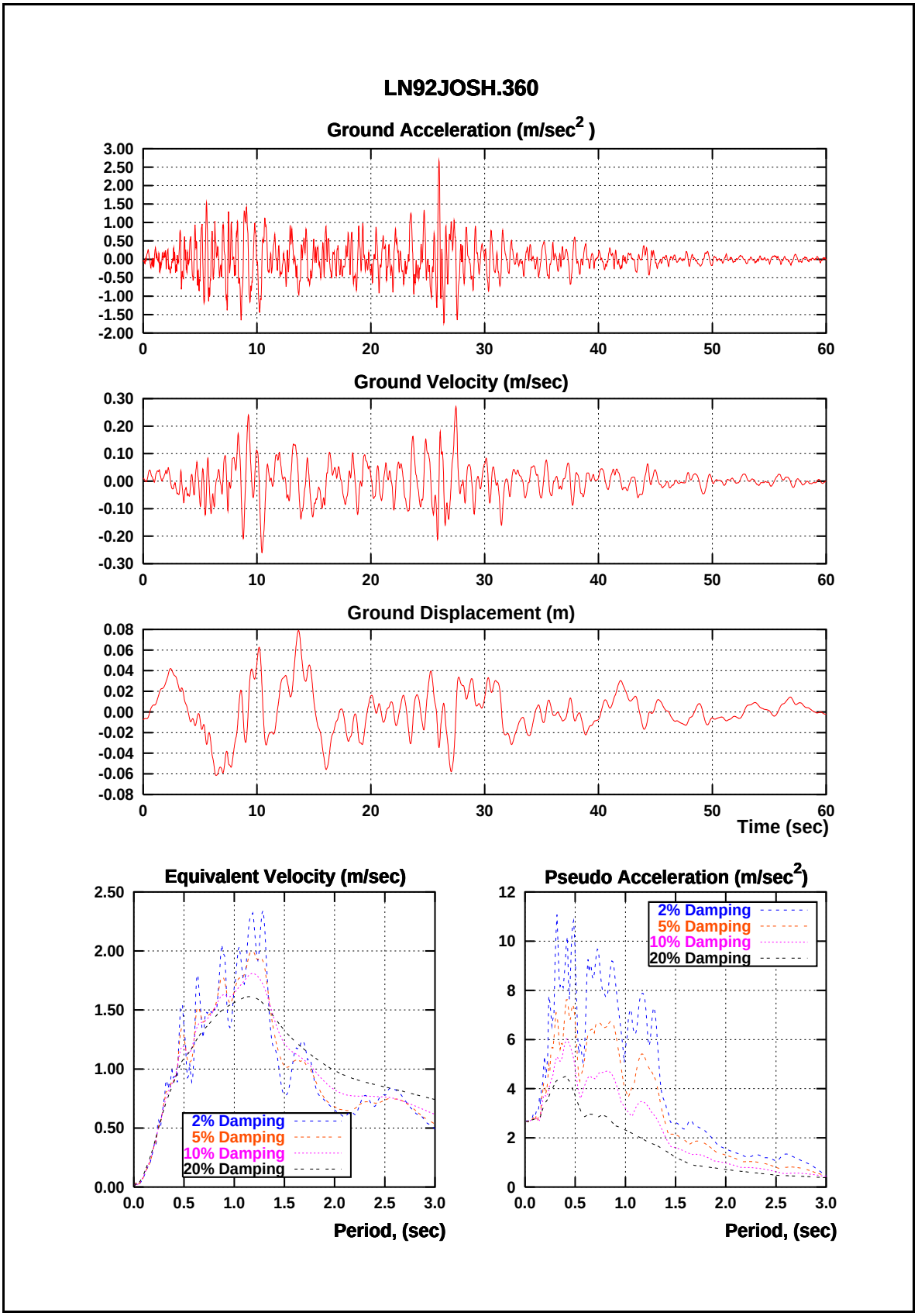

Figure A.9 Characteristics of the LN92JOSH.360 Ground Motion

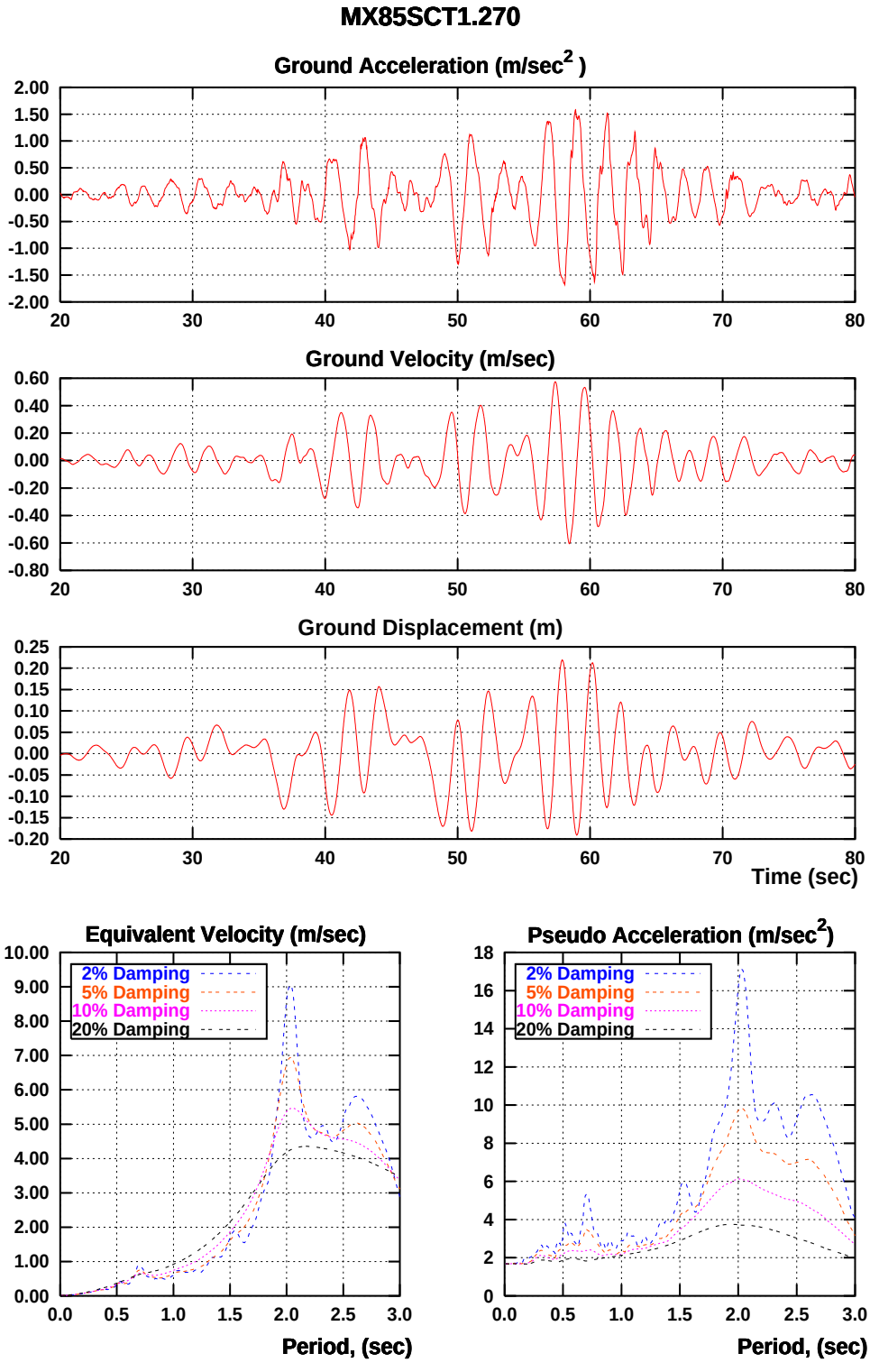

Figure A.10 Characteristics of the MX85SCT1.270 Ground Motion

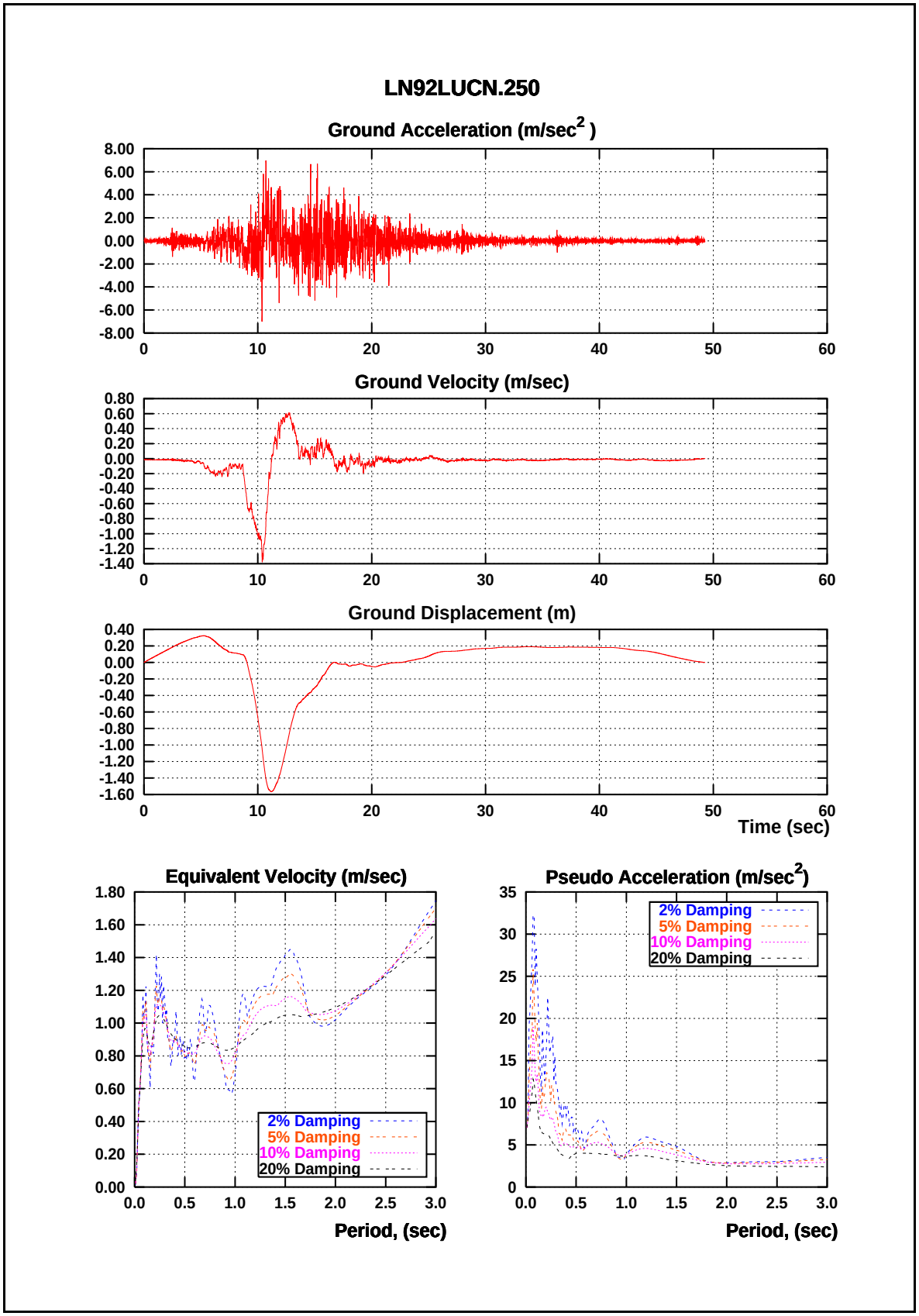

Figure A.11 Characteristics of the LN92LUCN.250 Ground Motion

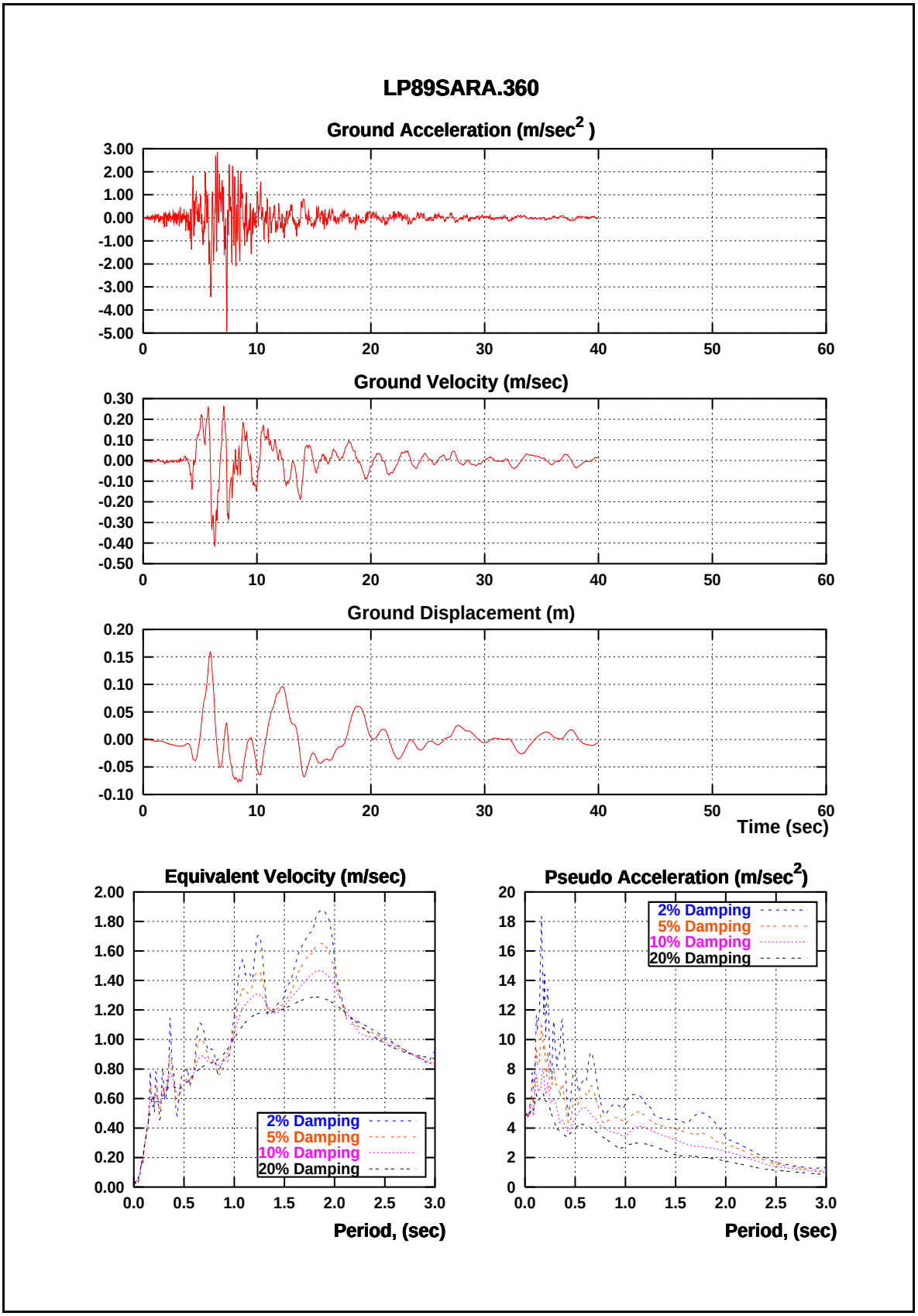

Figure A.12 Characteristics of the LP89SARA.360 Ground Motion

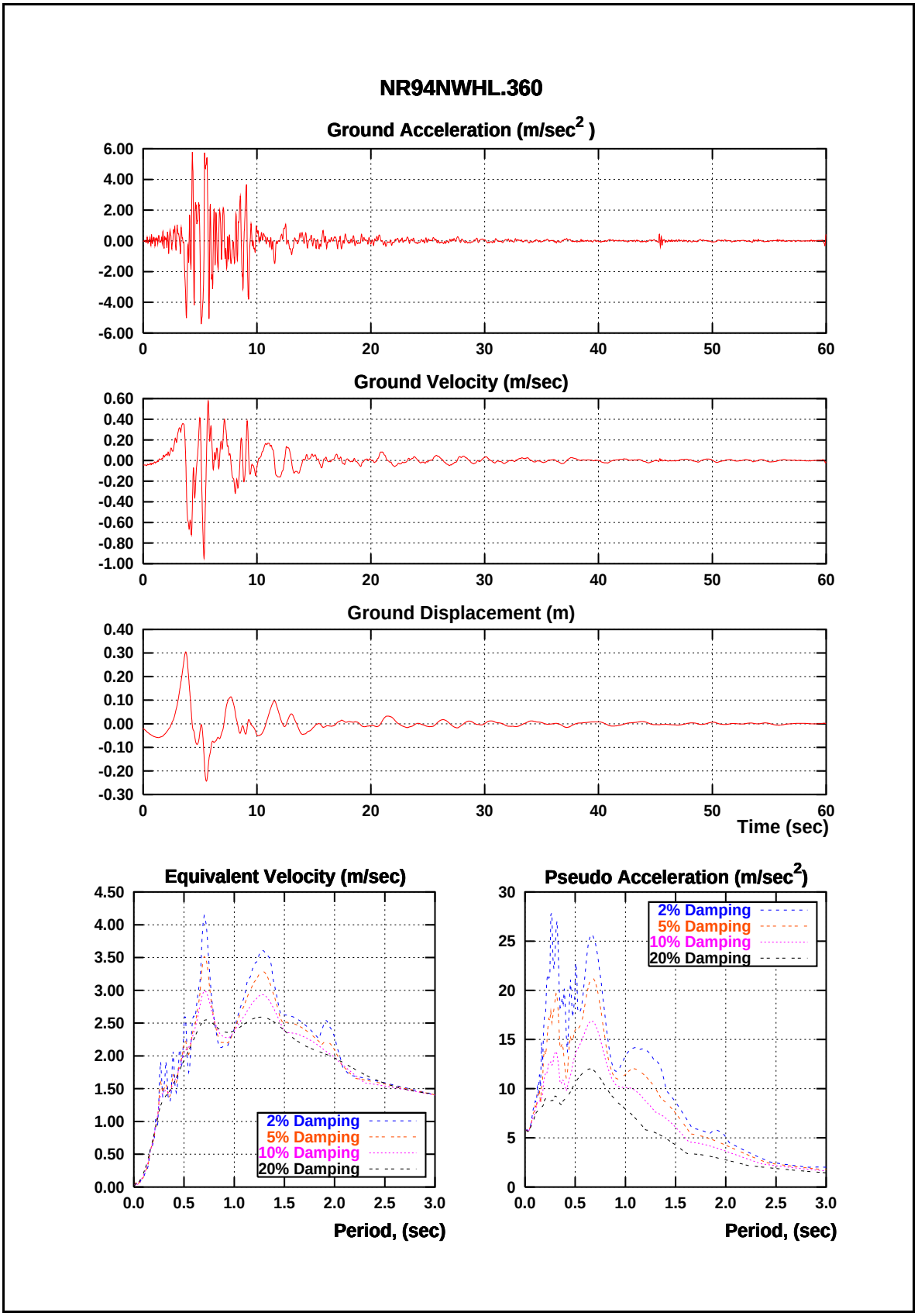

Figure A.13 Characteristics of the NR94NWHL.360 Ground Motion

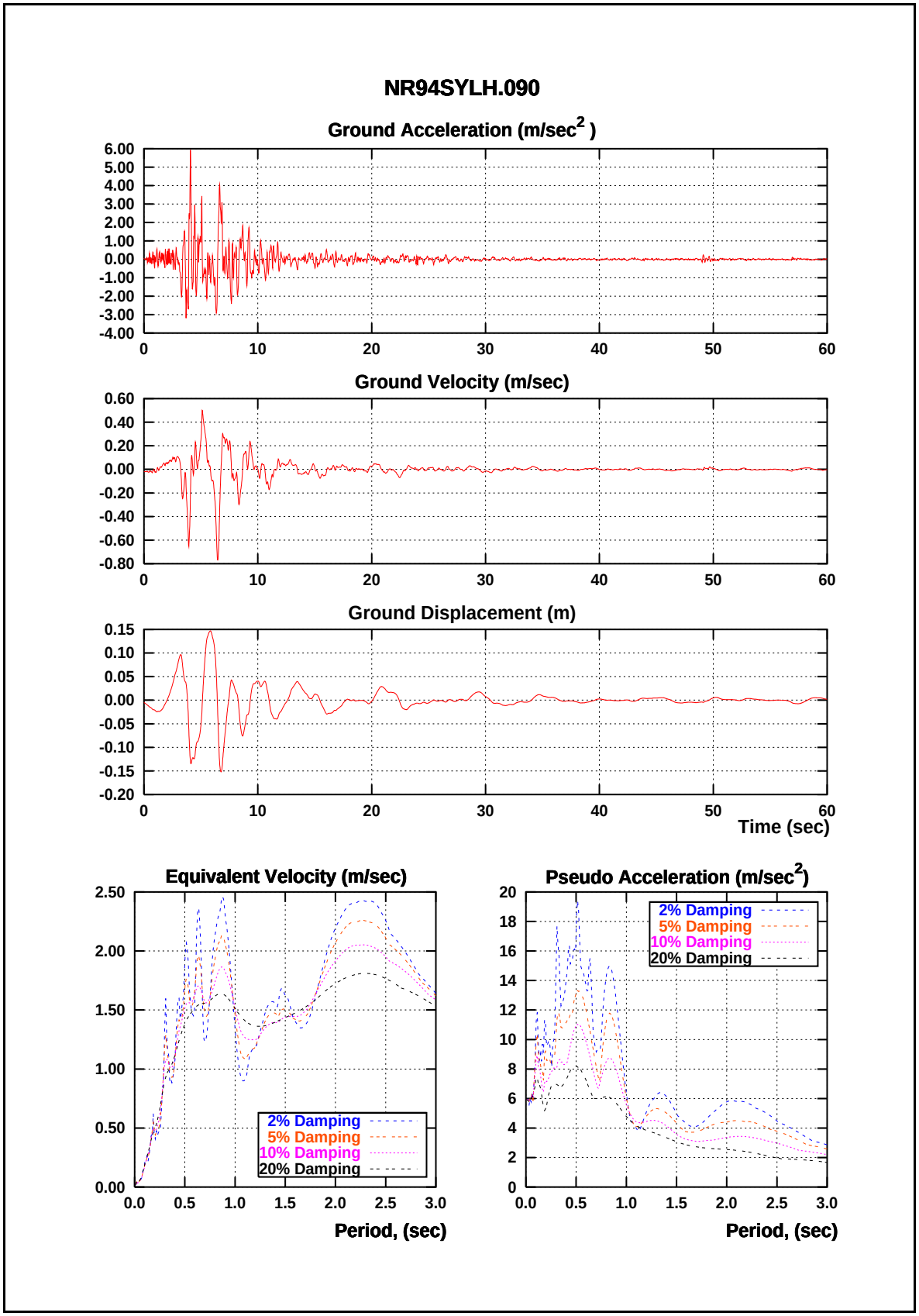

Figure A.14 Characteristics of the NR94SYLH.090 Ground Motion

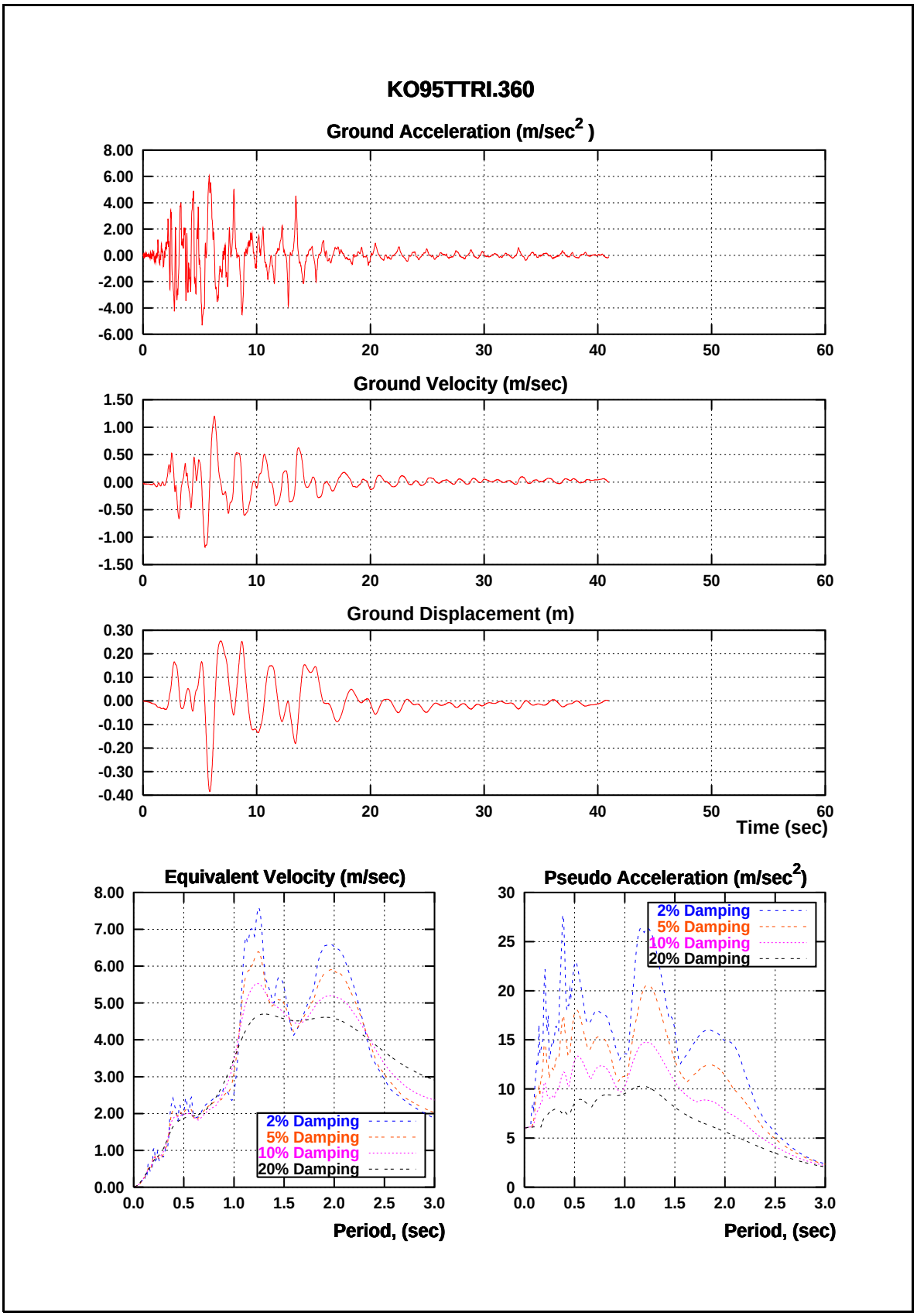

Figure A.15 Characteristics of the KO95TTRI.360 Ground Motion

APPENDIX B

C++ PROGRAM FOR DISPLACEMENT COEFFICIENT METHOD ESTIMATES

This appendix presents the listing of a computer program implementing the Displacement Coefficient Method. The program is written using the programing language C++ and is called DCM. No units are implicit in the program, therefore the input data must be provided in consistent units.

The syntax to use the program is as follows:

DCM ***record_file_name*** T_o ***effective_period damping*** W V_y^{MDOF} C_0 C_2 C_3

where:

record_file_name	is the name of a file containing the acceleration ground motion,
T_o	is the characteristic period of the ground motion,
effective_period	is the period assumed for the equivalent SDOF system,
W	is the total weight of the multistory system,
V_y^{MDOF}	is the strength of the multistory system, and
C_0, C_2, C_3	are as defined in the Displacement Coefficient Method.

The value of C_1, the modification factor to relate expected maximum inelastic displacement to displacement calculated for linear elastic response, is calculated by the program.

For all the results of the Displacement Coefficient Method shown along this work, the valued of C_2 and C_3 were assumed as one (1).

All the numerical parameters used to run the DCM program are floating points numbers.

The structure of the record containing the acceleration ground motion is as follows:

1st line; void line. May be used to identify the ground motion.

2nd line; one floating point number. Used to scale the ground motion accelerations.

3rd line; integer number. Number of data points in the acceleration record.

The rest of the file consists of two floating point numbers per line. The first number is the time and the second number is the acceleration.

Following is the list of the DCM program.

```
#include <stdio.h>
#include <iostream.h>
#include <fstream.h>
#include <iomanip.h>
#include <stdlib.h>
#include <math.h>
#include <float.h>
#include <dimen.h>

typedef double real;

// Input and output streams
   ifstream infile;
   ofstream outfile;
// end of Input and output streams

real response(const real &k,
              const  real &m,
              const  real &w,
              const  real &wd,
              const  real &dammp,
              real *time,
              real *accel,
              const unsigned short &n);


main(int argc, char *argv[])
{

//  Local Variables
    int i,n;
    real period, damping,tg,totalWeigth,c0,c1,c2,c3;
    real *accel, *time, deltat, ctte;
    real k,m,w,wd,vy;
    real sa,disp;
    const real PI=3.14159265358979323846;
    char buffer[256];
//  End of local variables

//   _control87(EM_UNDERFLOW, EM_UNDERFLOW);
   if (argc < 10) {
      cout << "Use: dcm record_file_name Tg period damping W MDOFVy C0 C2 C3 (C1 
      exit(0);
   } /* endif */

   infile.open(argv[1]);
   if (!infile) {
      cerr << "Earthquake record file not found\n";
      exit(1);
   } /* endif */
   tg=atof(argv[2]);
   period=atof(argv[3]);
   damping=atof(argv[4]);
   totalWeigth=atof(argv[5]);
   vy=atof(argv[6]);
   c0=atof(argv[7]);
   c2=atof(argv[8]);
   c3=atof(argv[9]);

   infile.getline(buffer,80);            // reading one useless dataline
   infile >> ctte;
//   infile.getline(buffer,80);
   infile >> n;                          // Reading Matrix Order

   dimVec(accel,1,n);                      // dimensioning arrray
   dimVec(time,1,n);                       // and matrices
   m=1.0;
   for (i=1;i<=n;i++) {
      infile >> time[i] >> accel[i];     // Reading the time and acceleration
      accel[i]*=ctte;
   } // endfor

   deltat=time[2]-time[1];            // deltat constant



   k = 4*PI*PI*m/(period*period);
   w = 2*PI/period; // sqrt(k/m);
   wd = w*sqrt(1-damping*damping);

   disp=response(k,m,w,wd,damping,time,accel,n);
   sa=disp*w*w;

   if (period >= tg) {
      c1=1.0;
   } else {
      real R;
      R=sa*totalWeigth/(vy*c0);
      c1=(1+(R-1)*tg/period)/R;
      if (c1 < 1) {
         c1 = 1.0;
      } /* endif */
      if (c1 > 1.5) {
         c1 = 1.5;
      } /* endif */
   } /* endif */

   cout << "displacement for "
        << argv[1] << " = "
        << disp*c0*c1*c2*c3 << endl;
//        << " units.\n";



   freeVec(accel,1);
   freeVec(time,1);


   return 0;
}


real response(const real &k,
              const  real &m,
              const  real &w,
              const  real &wd,
              const  real &dammp,
              real *time,
              real *p,
              const unsigned short &n)
{
   real a0, a1,a2,a3, d0;
   real EXP, COS, SIN,CUB_W, C, D;
   real alpha;
   real tau;
   real vim1=0.0;
   real accel,max_disp;
   unsigned short i,im1;

   d0 = 0;                 // initial  displacement
```

```
   max_disp = 0.0;
   tau = time[2] - time[1];
   EXP = exp(-dammp*w*tau);
   COS = cos(wd*tau);
   SIN = sin(wd*tau);
   CUB_W = w*w*w;

   for (i=2,im1=1;i<=n+1;i++,im1++) {
      alpha = (p[i]-p[im1])/tau;
      a0 = p[im1]/k -2*dammp*alpha/(m*CUB_W);
      a1 = alpha/k;
      a2 = d0 - a0;
      a3 = (vim1 + dammp*w*a2 - a1)/wd;
      C = (wd*a3-dammp*w*a2);
      D = (a2*wd+dammp*w*a3);


      d0 = a0 + a1*tau + a2*EXP*COS + a3*EXP*SIN;
      vim1 = a1 + C*EXP*COS - D*EXP*SIN;


      if (fabs(d0) > max_disp) {
         max_disp = fabs(d0);
      } /* endif */
   }  /* endfor */
   return (max_disp);
}


++++++++++++++++++++++++++ dimen.h ++++++++++++++++++++++++

#ifndef DIMEN_H
#define DIMEN_H
#include<iostream.h>
#include<stdlib.h>

template <class T, class entero>
void dimVec(T *(&v),
            const int offset,
            const entero size)
{
   v = new T [size];
   if (!v) {
     cout << "(V)No hay suficiente memoria para analizar este problema" << endl ;
     exit (1);
   }
   v -= offset;
}



template <class T, class entero>
void dimMat(T **(&m),
            const int nrl,
            const entero nrow,
            const int ncl,
            const entero ncol)
{
   unsigned long i, nrh;

   nrh=nrow+nrl-1;


   m = (T **) new T* [nrow];
   if (!m) {
     cout << "(M1)No hay suficiente memoria  para analizar este problema" << endl
     exit (1);
   }
   m -= nrl;
   m[nrl]= new T [nrow*ncol];
   if (!m[nrl]) {
     cout << "(M2)No hay suficiente memoria  para analizar este problema" << endl
     exit (1);
   }
   m[nrl]-= ncl;
   for (i=nrl+1;i<=nrh;i++)
      m[i] = m[i-1]+ncol;
   /* endfor */
}


template <class T>
void freeVec(T *(&v),
             const int offsets)
{
   delete  (v+offsets);
}


template <class T>
void freeMat(T **(&m),
             const int nrl,
             const int ncl)
{
   m[nrl] += ncl;
   delete m[nrl];
   m += nrl;
   delete[] m;
}
#endif // End of dinen.h

++++++++++++++++++++++++++ dimen.h ++++++++++++++++++++++++
```

APPENDIX C

C++ PROGRAM FOR CAPACITY SPECTRUM METHOD ESTIMATES

This appendix presents the listing of a computer program implementing the Capacity Spectrum. The program is written using the programing language C++ and is referenced as CSM. No units are implicit in the program, therefore the input data must be provided in consistent units.

The syntax to use the program is as follows:

CSM ***record_file_name*** V_y^{SDOF} u_y^{SDOF} post-yield_stiffness(%) ***PF1*** T_o

where:

record_file_name	is the name of a file containing the acceleration ground motion,
V_y^{SDOF}	is the strength of the equivalent SDOF,
u_y^{SDOF}	is the yield displacement of the equivalent SDOF,
post-yield_stiffness(%):	is the post-yield stiffness expressed as a percentage of initial stiffness,
PF1	is the participation factor, and
T_o	is the characteristic period of the ground motion.

All the numerical parameters used to run the CSM program are floating point numbers.

The structure of the record containing the acceleration ground motion is as follows:

1st line; void line. May be used to identify the ground motion.

2nd line; one floating point number. Used to scale the ground motion accelerations.

3rd line; integer number. Number of data points in the acceleration record.

The rest of the file consists of two floating point numbers per line. The first number is the time and the second number is the acceleration.

Following is the list of the CSM program.

```
#include <stdio.h>
#include <iostream.h>
#include <fstream.h>
#include <iomanip.h>
#include <stdlib.h>
#include <math.h>
#include <float.h>
#include <dimen.h>

typedef double real;

// Input and output streams
   ifstream infile;
   ofstream outfile;
// end of Input and output streams

real response(const real &k,
              const  real &m,
              const  real &w,
              const  real &wd,
              const  real &dammp,
              real *time,
              real *accel,
              const unsigned short &n);


main(int argc, char *argv[])
{

//  Local Variables
    const int nmax = 100;
    const real PI=3.14159265358979323846;
    char buffer[256];
    int i, n, count=0 ;
    real dy,fy,pys,pf1, tg;
    real ca, cv;
    real k, m, period, w, wd;
    real dpi,fpi,deltat,ctte,damping,b0,beff,k_factor;
    real sra, srv,Ts;
    real olddpi, temp;
    real *time, *accel;
//  End of local variables

//   _control87(EM_UNDERFLOW, EM_UNDERFLOW);
   if (argc < 6) {
      cout << "Use: csmv2 record_file_name  SDOFVy   SDOFdy   post-yield_stiffnes
      exit(0);
   } /* endif */

   infile.open(argv[1]);
   if (!infile) {
      cerr << "Earthquake record file not found\n";
      exit(1);
   } /* endif */
   fy=atof(argv[2]);
   dy=atof(argv[3]);
   k = fy/dy;
   pys=atof(argv[4])*.01*k;
   pf1=atof(argv[5]);
   tg=atof(argv[6]);

   infile.getline(buffer,80);            // reading one useless dataline
   infile >> ctte;
//   infile.getline(buffer,80);
   infile >> n;                          // Reading Matrix Order
   dimVec(accel,1,n);                      // dimensioning arrray
   dimVec(time,1,n);                       // and matrices

   for (i=1;i<=n;i++) {
      infile >> time[i] >> accel[i];     // Reading the time and acceleration
      accel[i]*=ctte;
      if (fabs(accel[i]) > ca) {
         ca=fabs(accel[i]);
      } /* endif */
   } // endfor
   cv= 2.5*ca*tg;

   deltat=time[2]-time[1];            // deltat constant
   m=1.0;
   damping=beff=.05; // to start with
   period=2*PI*sqrt(m/k);
   w = 2*PI/period; // sqrt(k/m);
   wd = w*sqrt(1-damping*damping);
   dpi=response(k,m,w,wd,damping,time,accel,n);

   if (dpi > dy) {
//      fpi=fy+pys*(dpi-dy);
      do {
         count ++;
         fpi=fy+pys*(dpi-dy);

         b0=2*(fy*dpi-dy*fpi)/(PI*fpi*dpi);

         if (b0 <= .1625) {                      //
            k_factor=1.0;                        //
         } else if (b0 >= .45) {                 // This is consistent with
            k_factor=7/9;                        // Fig. 8.15 ATC-40
         } else {                                // type A structures
            k_factor=1.0 - 8/10.35*(b0 -.1625);  //
         } /* endif */                           //

         beff=b0*k_factor+0.05;                                  //
         if (beff > 0.40) {                                      //
            beff = 0.4;                                          // This is consistent wi
         } else if (beff < 0.05){                                // Fig. 8.16 ATC-40
            beff = 0.05;                                         // type A structures
         } /* endif */                                           //
                                                                 //

         sra=(3.21-0.68*log(beff*100))/2.12;     // Eq. 8.9
         srv=(2.31-0.41*log(beff*100))/1.65;     // Eq. 8.10

         if (sra < 0.33) {
            sra = 0.33;
         } /* endif */
         if (srv < 0.50) {
            srv = 0.50;
         } /* endif */

         Ts=srv*cv/(2.5*sra*ca);


         k=fpi/dpi;
         period=2*PI*sqrt(m/k);
         w = sqrt(k/m); // sqrt(k/m);
         wd = w*sqrt(1-damping*damping);
         olddpi=dpi;
         dpi=response(k,m,w,wd,damping,time,accel,n);
         if (period > Ts) {
            dpi=dpi*srv;
         } else {
```

```
            dpi=dpi*sra;
         } /* endif */

         if (dpi < dy) {
            dpi = (olddpi+dy)*0.5;
         } /* endif */
         temp = dpi/olddpi;

//         cout.setf(ios::fixed);
//         cout.precision(6);
//         cout << "olddpi: " << olddpi*pf1
//              << "   dpi: "<< dpi*pf1
//              << "    ratio : " << temp << endl;

      } while ( (temp > 1.01 || temp < 0.99) &&  count < nmax ); /* enddo */

   } /* endif */
   cout.setf(ios::fixed);
   cout.precision(6);
   if (count >= nmax) {
      dpi = 0.5*(dpi+olddpi);
   } /* endif */

   cout << "disp. for "
        << argv[1] << " = "
        << dpi*pf1 << " , # of itarations: " << count <<" final damping: "<< beff

   freeVec(accel,1);
   freeVec(time,1);

   return 0;
}


real response(const real &k,
              const  real &m,
              const  real &w,
              const  real &wd,
              const  real &dammp,
              real *time,
              real *p,
              const unsigned short &n)
{
   real a0, a1,a2,a3, d0;
   real EXP, COS, SIN,CUB_W, C, D;
   real alpha;
   real tau;
   real vim1=0.0;
   real accel,max_disp;
   unsigned short i,im1;

   d0 = 0;                  // initial  displacement
   max_disp = 0.0;
   tau = time[2] - time[1];
   EXP = exp(-dammp*w*tau);
   COS = cos(wd*tau);
   SIN = sin(wd*tau);
   CUB_W = w*w*w;

   for (i=2,im1=1;i<=n+1;i++,im1++) {
      alpha = (p[i]-p[im1])/tau;
      a0 = p[im1]/k -2*dammp*alpha/(m*CUB_W);
      a1 = alpha/k;
      a2 = d0 - a0;
      a3 = (vim1 + dammp*w*a2 - a1)/wd;
      C = (wd*a3-dammp*w*a2);
      D = (a2*wd+dammp*w*a3);


      d0 = a0 + a1*tau + a2*EXP*COS + a3*EXP*SIN;
      vim1 = a1 + C*EXP*COS - D*EXP*SIN;


      if (fabs(d0) > max_disp) {
         max_disp = fabs(d0);
      } /* endif */
   }  /* endfor */
   return (max_disp);
}



++++++++++++++++++++++++++++ dimen.h ++++++++++++++++++++++++++

#ifndef DIMEN_H
#define DIMEN_H
#include<iostream.h>
#include<stdlib.h>

template <class T, class entero>
void dimVec(T *(&v),
            const int offset,
            const entero size)
{
   v = new T [size];
   if (!v) {
     cout << "(V)No hay suficiente memoria para analizar este problema" << endl ;
     exit (1);
   }
   v -= offset;
}


template <class T, class entero>
void dimMat(T **(&m),
            const int nrl,
            const entero nrow,
            const int ncl,
            const entero ncol)
{
   unsigned long i, nrh;

   nrh=nrow+nrl-1;


   m = (T **) new T* [nrow];
   if (!m) {
     cout << "(M1)No hay suficiente memoria  para analizar este problema" << endl
     exit (1);
   }
   m -= nrl;
   m[nrl]= new T [nrow*ncol];
   if (!m[nrl]) {
     cout << "(M2)No hay suficiente memoria  para analizar este problema" << endl
     exit (1);
   }
   m[nrl]-= ncl;
   for (i=nrl+1;i<=nrh;i++)
      m[i] = m[i-1]+ncol;
   /* endfor */
}
```

```
template <class T>
void freeVec(T *(&v),
             const int offsets)
{
   delete  (v+offsets);
}


template <class T>
void freeMat(T **(&m),
             const int nrl,
             const int ncl)
{
   m[nrl] += ncl;
   delete m[nrl];
   m += nrl;
   delete[] m;
}
#endif // End of dinen.h

++++++++++++++++++++++++++++ dimen.h ++++++++++++++++++++++++++
```

APPENDIX D

YIELD POINT SPECTRA USED FOR PEAK DISPLACEMENT AND IDI ESTIMATES

Peak displacements estimates made in Chapter 5 using the YPSA method were obtained using Equation 5.6 and Yield Point Spectra for the 15 ground motion records considered. For all the frames, the system displacement ductility (μ) and maximum elastic displacement of the equivalent SDOF system (***max(u_{el}^{sdof})***) are obtained directly from the YPS shown in Figures D.1 to D.30.

Figures D.1 to D.15 are used for estimates related to the 4-story frames and Figures D.16 to D.30 for those related with the 12-story frames. Part (a) of Figures D.1 to D.30 plot the YPS used to estimate peak roof displacement assuming the first mode as deformed shape. Data obtained from the YPS in part (a) are presented in Tables 5.5 to 5.8. Part (b) of Figures D.1 to D.30 contains the YPS used for the peak roof displacement estimates assuming the second mode as deformed shape. Data obtained from these YPS are presented in Tables 5.15 to 5.18. The first mode and second mode periods of vibration of the equivalent SDOF systems representing the four frames are represented in the figures by dotted diagonal lines.

Table D.1 summarize the data corresponding to the first and second mode yield points and the periods for the four frames considered.

Table D.1 Equivalent SDOF Yield Strength Coefficients, Yield Displacements, and Periods of the Frames

First Mode Yield Point and Period Frames

	C_y	u_y^{SDOF} [m]	T_1 [sec]
Flexible-4	**0.303**	**0.102**	**1.16**
Rigid-4	**0.804**	**0.101**	**0.71**
Flexible-12	**0.220**	**0.257**	**2.17**
Rigid-12	**0.612**	**0.238**	**1.25**

(a)

Second Mode Yield Point and Periods For Frames

	C_y	u_y^{SDOF} [m]	T_2 [sec]
Flexible-4	**2.708**	**0.095**	**0.38**
Rigid-4	**4.682**	**0.074**	**0.25**
Flexible-12	**1.223**	**0.194**	**0.80**
Rigid-12	**2.610**	**0.148**	**0.48**

(b)

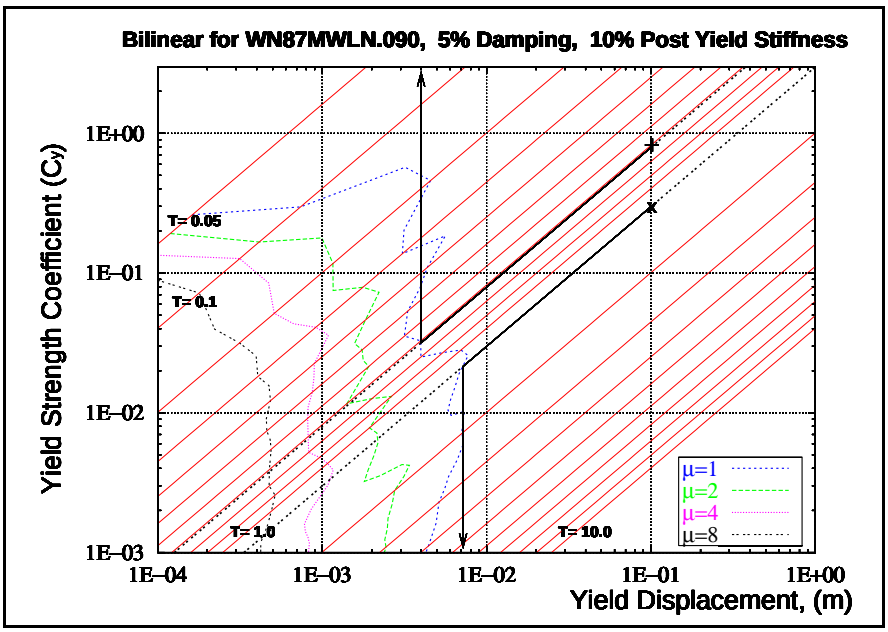

(a)

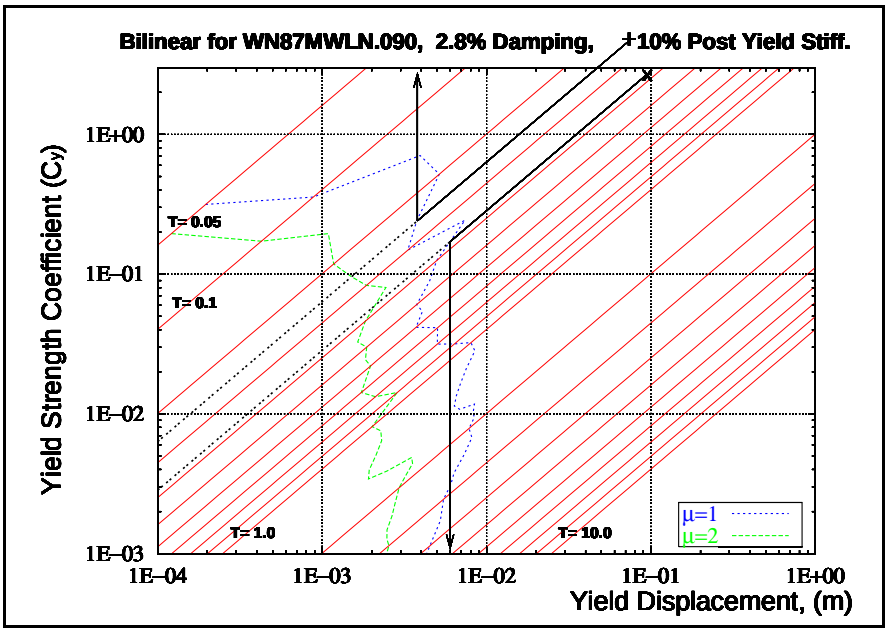

(b)

Figure D.1 YPS For WN87MWLN.090 and Yield Points for the 4-Story Frames

'x' indicates Yield Point for the Flexible-4

'+' indicates Yield Point for the Rigid-4

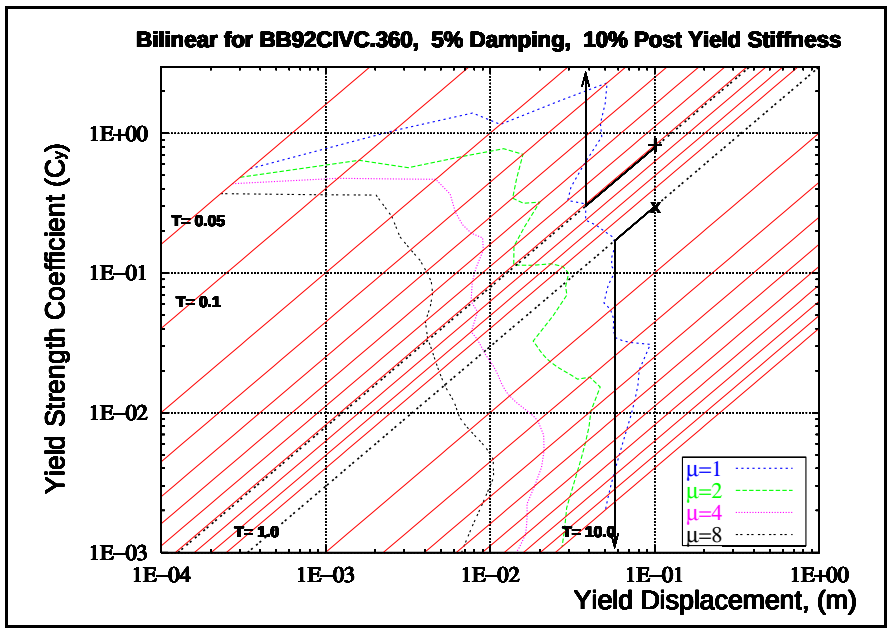

(a)

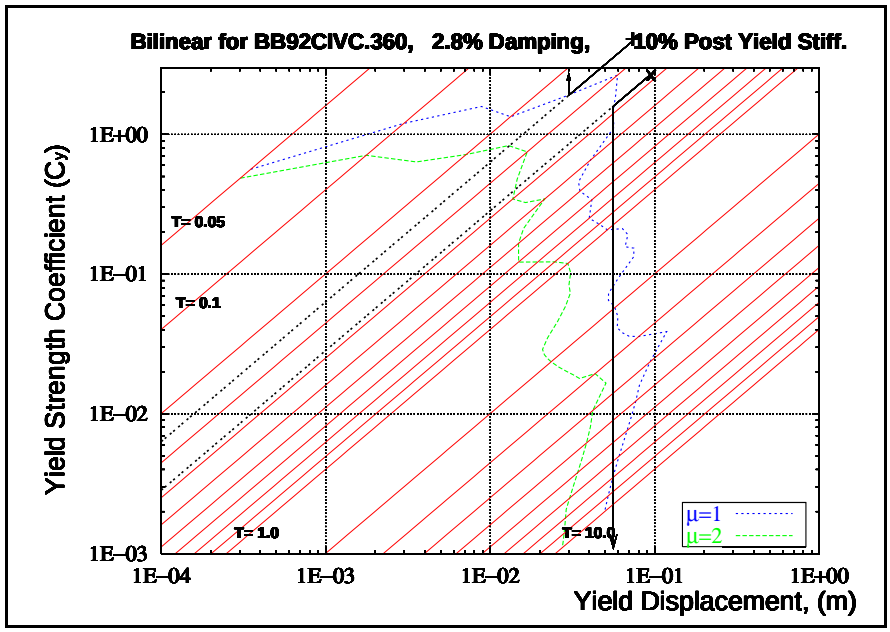

(b)

Figure D.2 YPS For BB92CIVC.360 and Yield Points for the 4-Story Frames

'x' indicates Yield Point for the Flexible-4

'+' indicates Yield Point for the Rigid-4

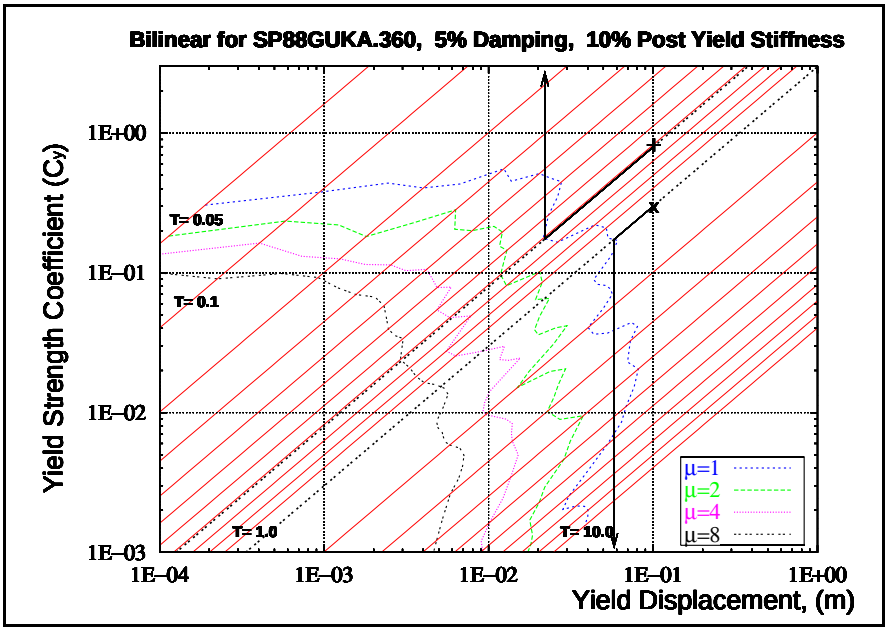

(a)

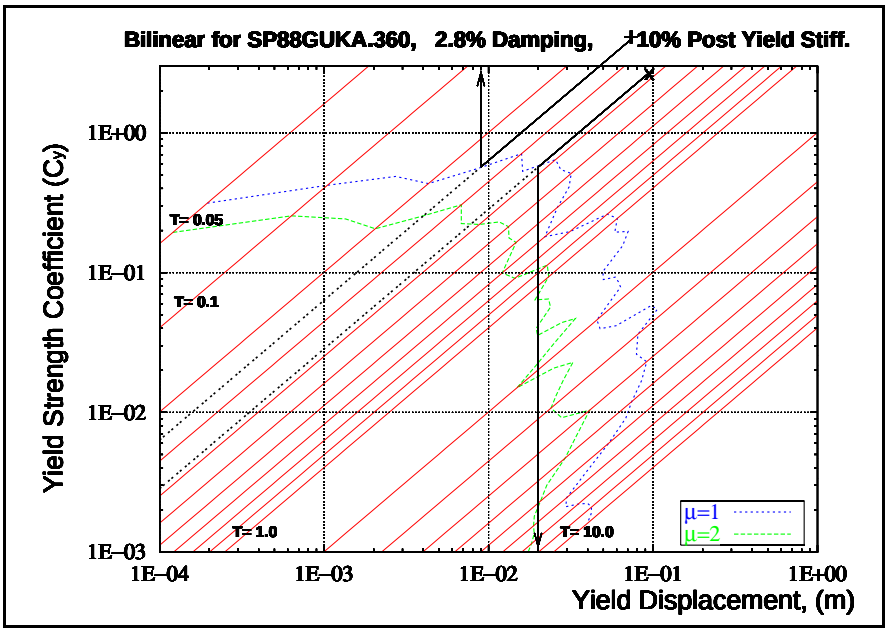

(b)

Figure D.3 YPS For SP88GUKA.360 and Yield Points for the 4-Story Frames

'x' indicates Yield Point for the Flexible-4

'+' indicates Yield Point for the Rigid-4

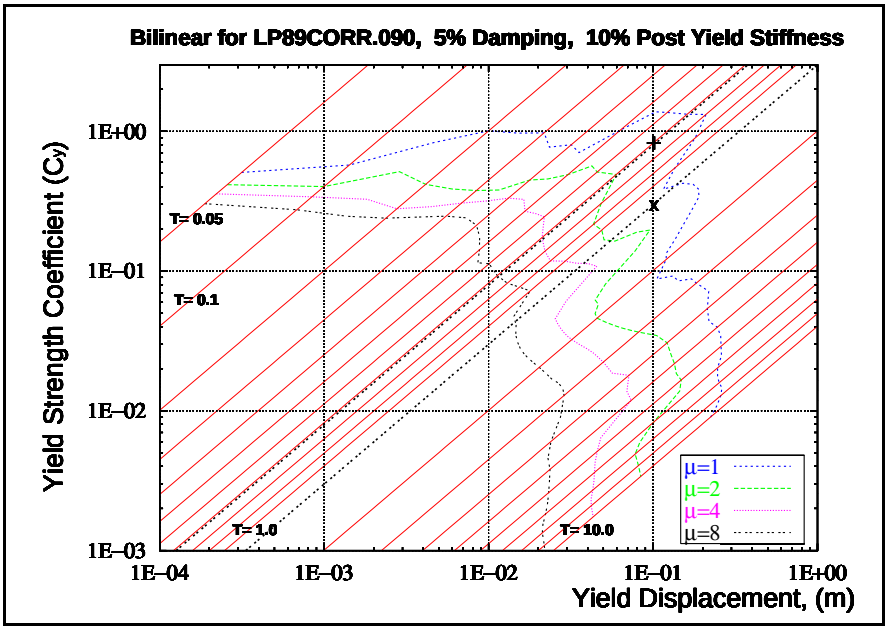

(a)

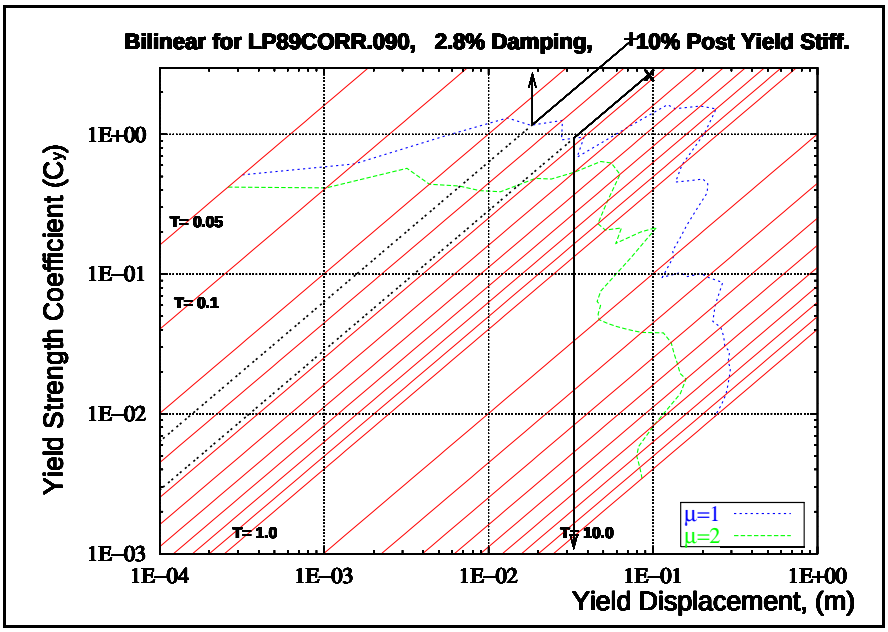

(b)

Figure D.4 YPS For LP89CORR.090 and Yield Points for the 4-Story Frames

'x' indicates Yield Point for the Flexible-4

'+' indicates Yield Point for the Rigid-4

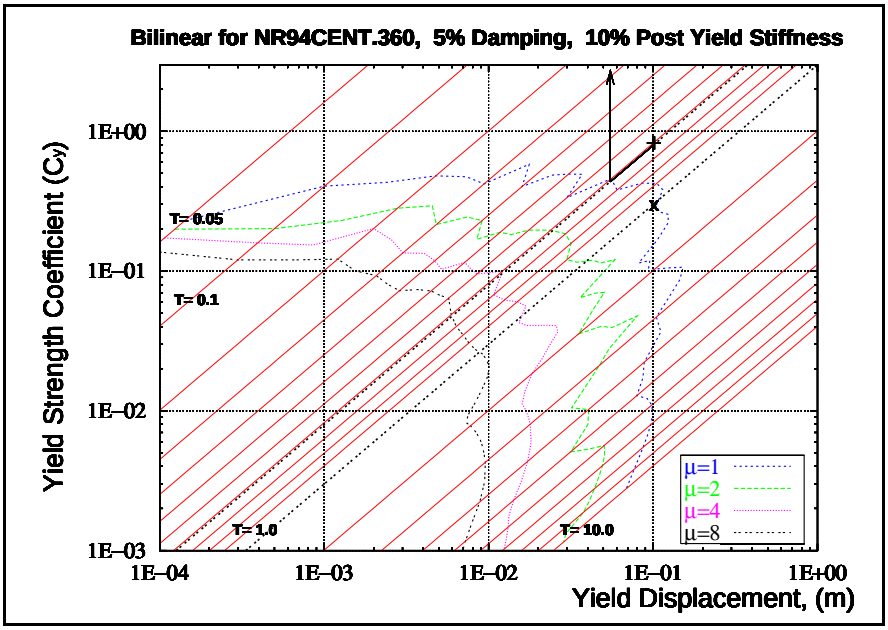

(a)

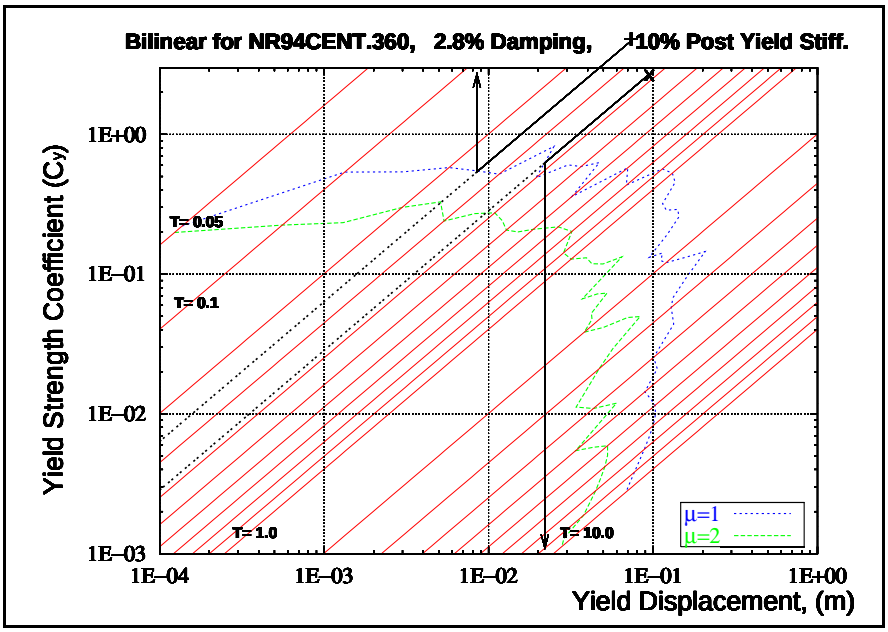

(b)

Figure D.5 YPS For NR94CENT.360 and Yield Points for the 4-Story Frames

'x' indicates Yield Point for the Flexible-4

'+' indicates Yield Point for the Rigid-4

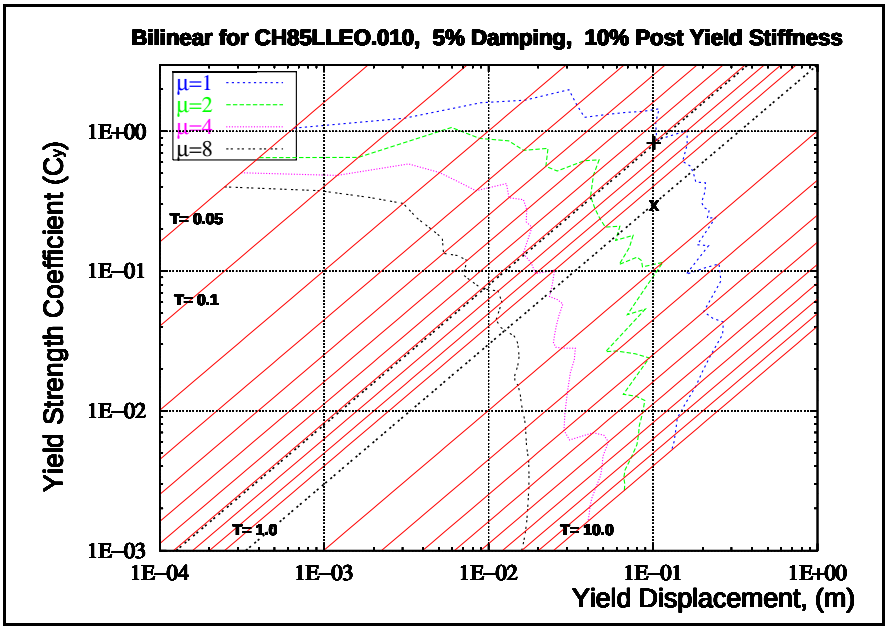

(a)

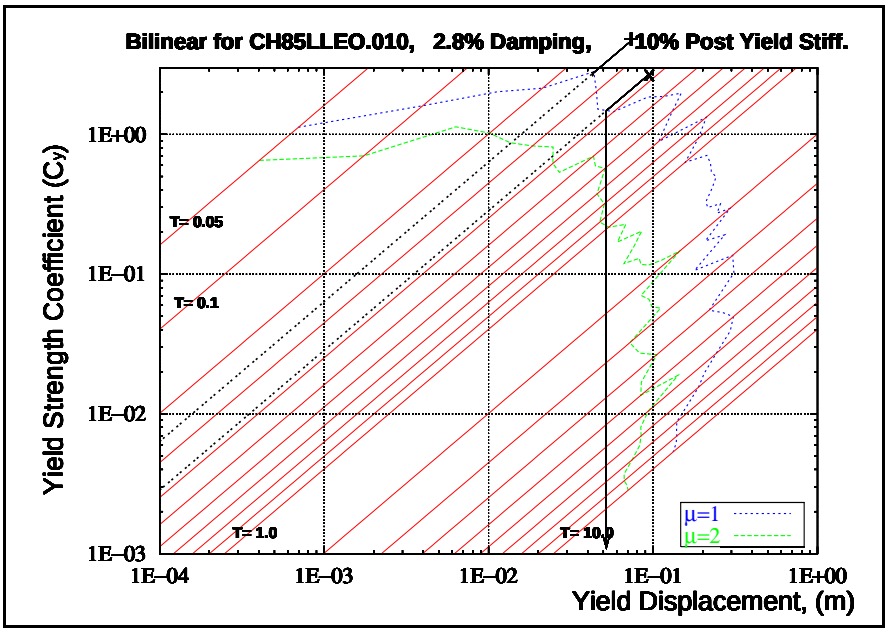

(b)

Figure D.6 YPS For CH85LLEO.010 and Yield Points for the 4-Story Frames

'x' indicates Yield Point for the Flexible-4

'+' indicates Yield Point for the Rigid-4

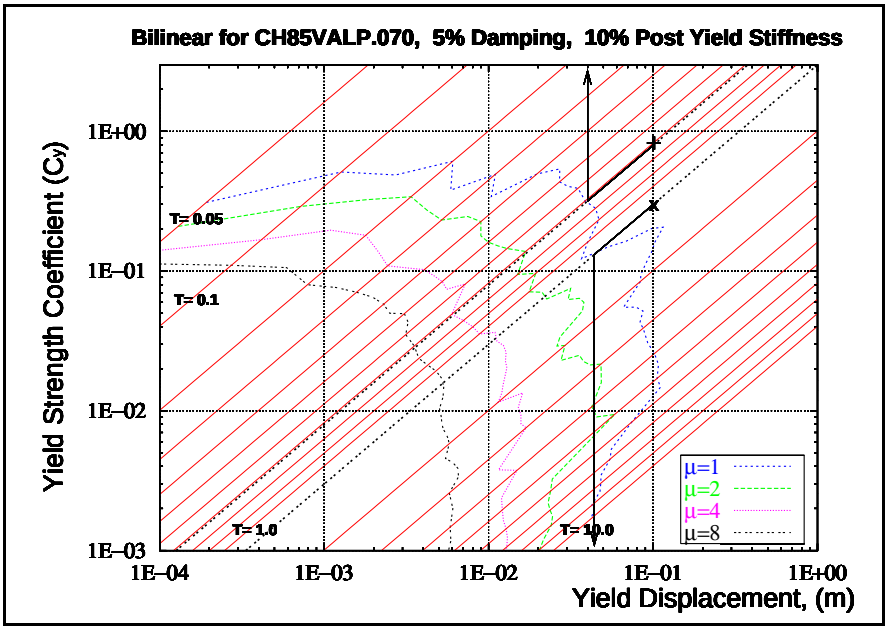

(a)

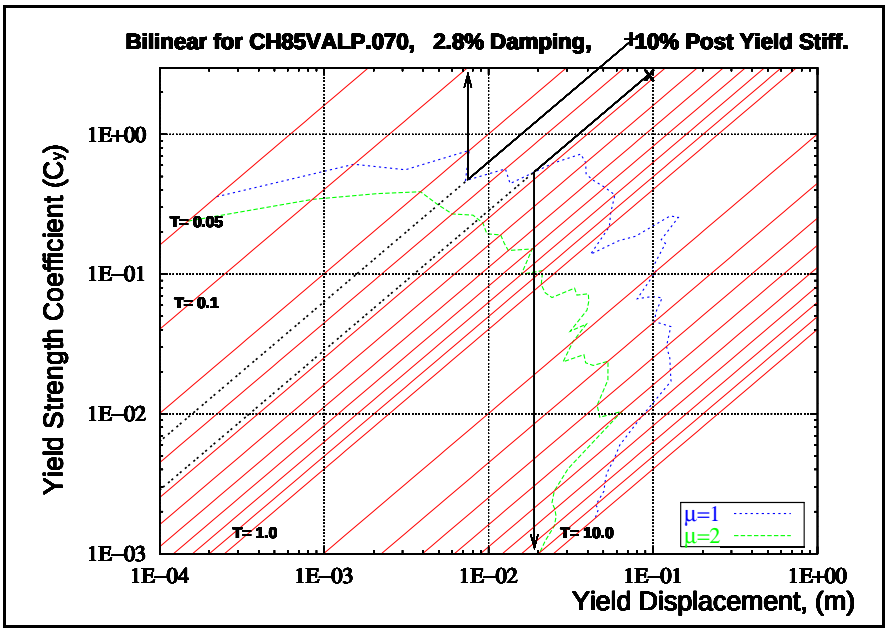

(b)

Figure D.7 YPS For CH85VALP.070 and Yield Points for the 4-Story Frames

'x' indicates Yield Point for the Flexible-4

'+' indicates Yield Point for the Rigid-4

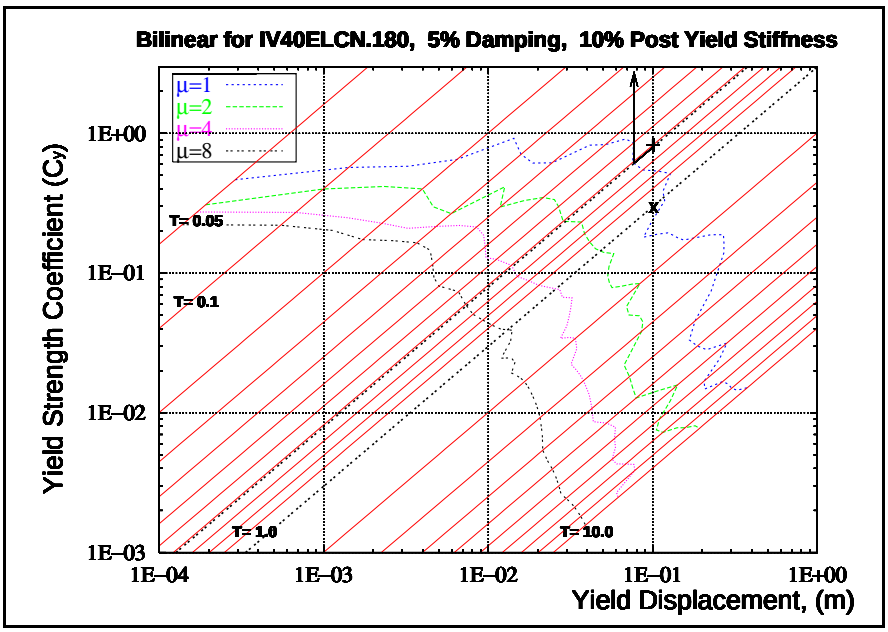

(a)

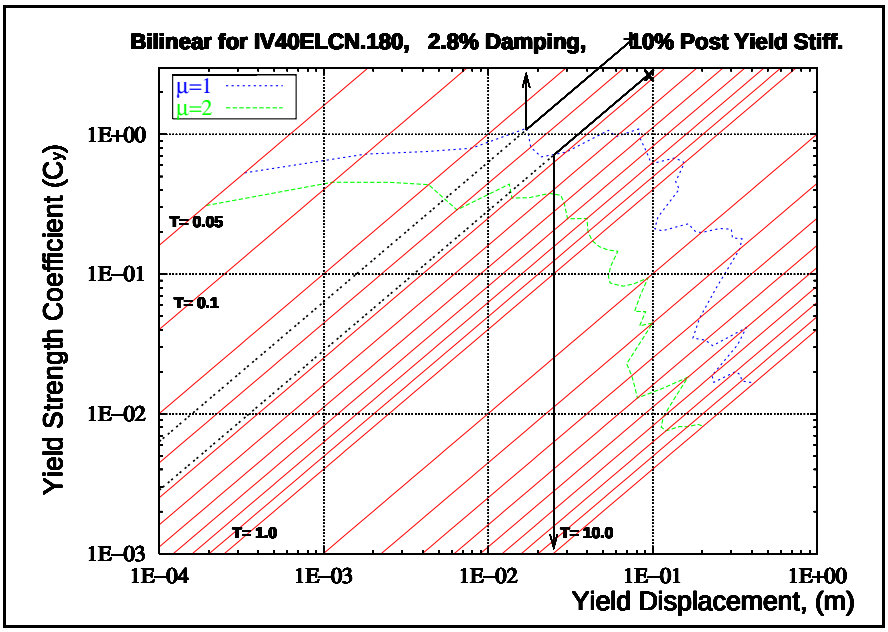

(b)

Figure D.8 YPS For IV40ELCN.180 and Yield Points for the 4-Story Frames

'x' indicates Yield Point for the Flexible-4

'+' indicates Yield Point for the Rigid-4

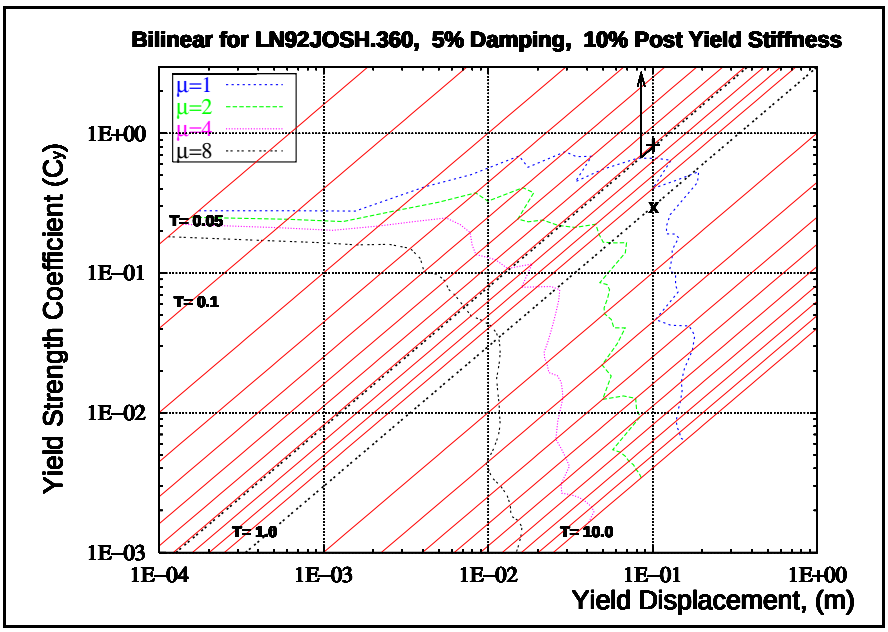

(a)

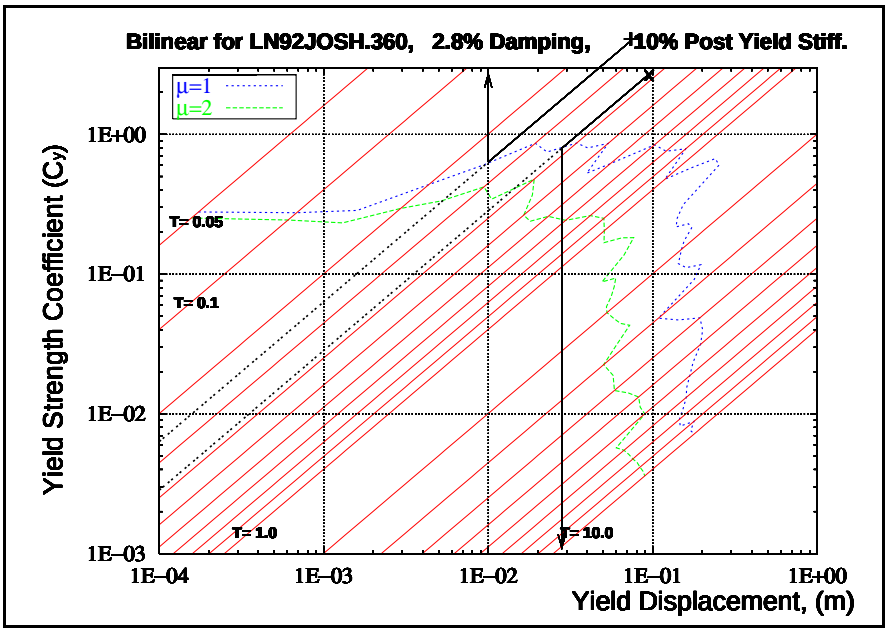

(b)

Figure D.9 YPS For LN92JOSH.360 and Yield Points for the 4-Story Frames

'x' indicates Yield Point for the Flexible-4

'+' indicates Yield Point for the Rigid-4

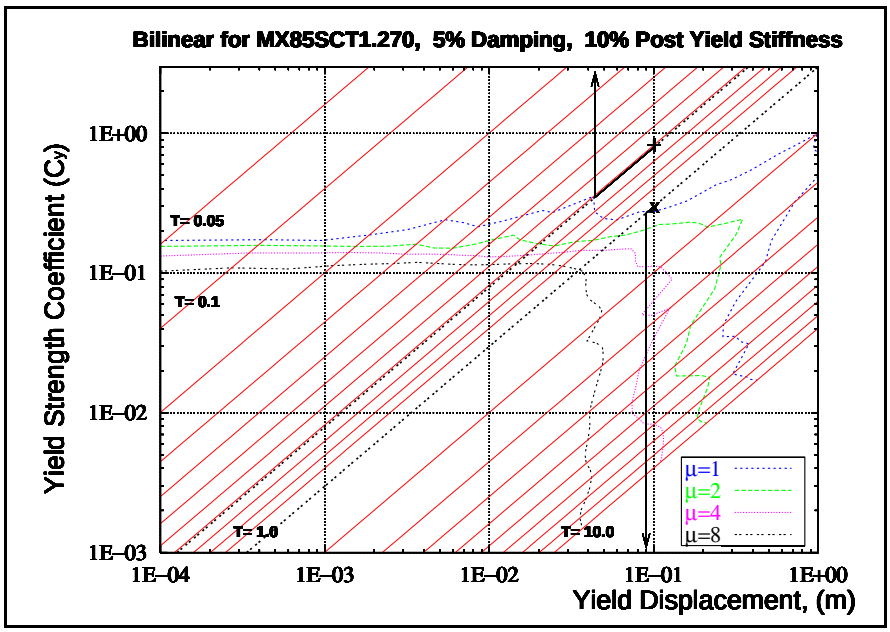

(a)

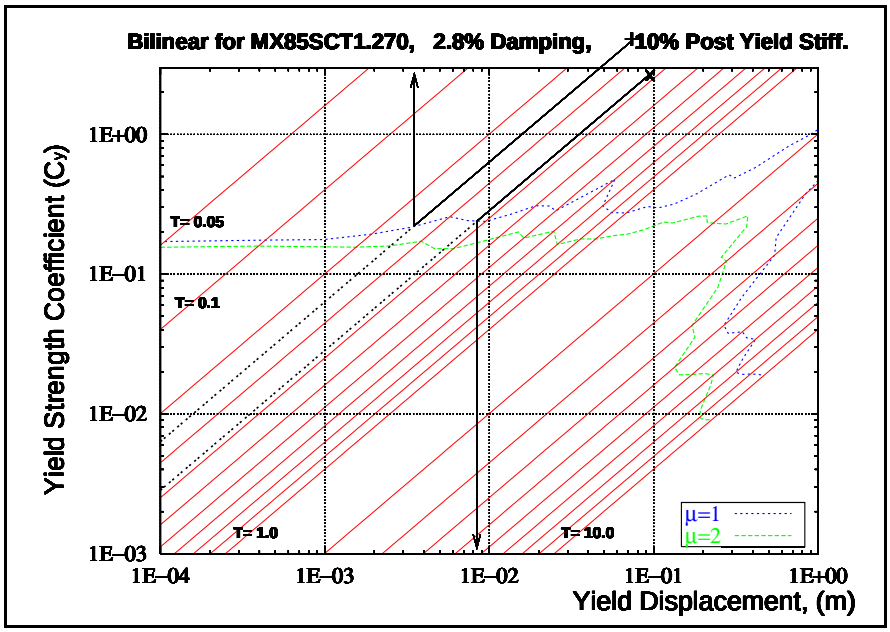

(b)

Figure D.10 YPS For MX85SCT1.270 and Yield Points for the 4-Story Frames

'x' indicates Yield Point for the Flexible-4

'+' indicates Yield Point for the Rigid-4

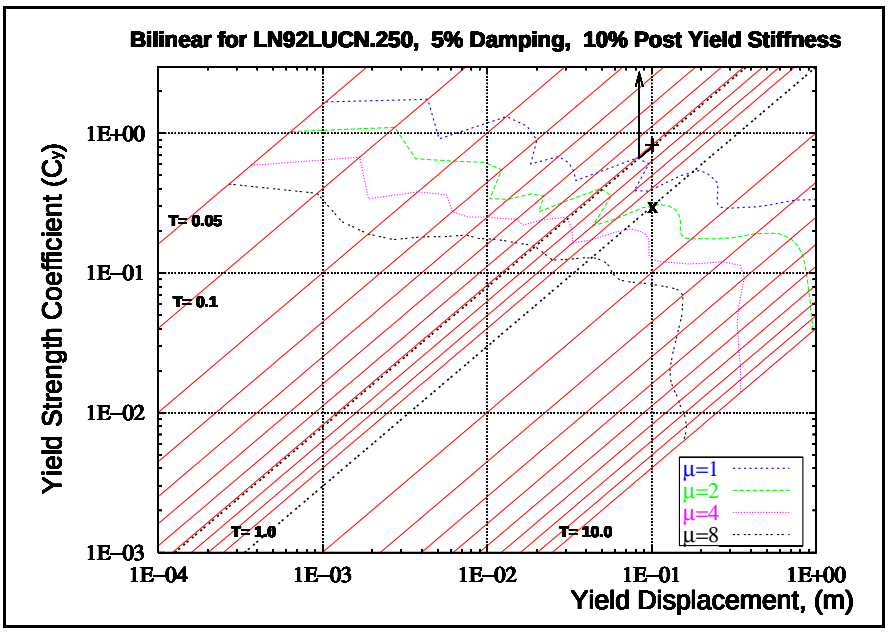

(a)

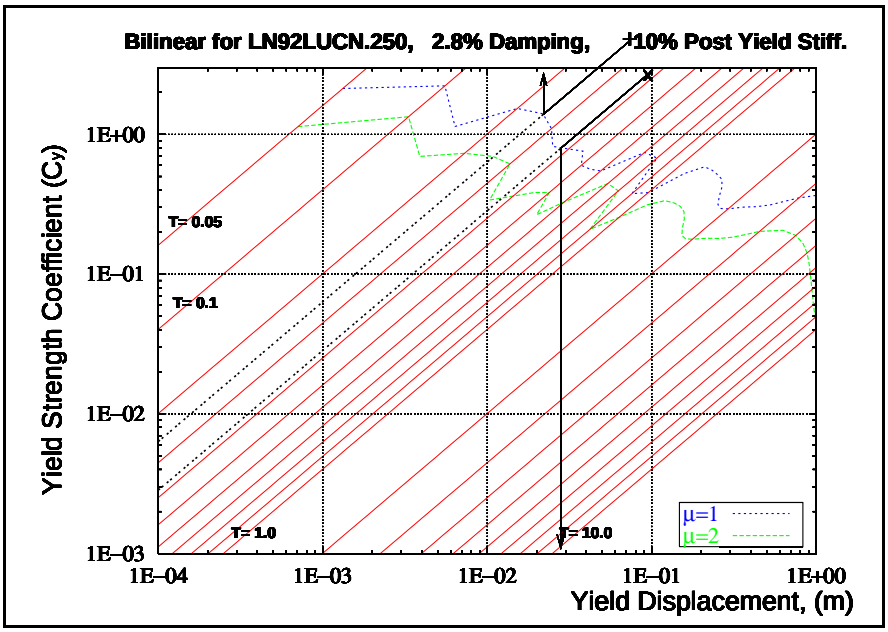

(b)

Figure D.11 YPS For LN92LUCN.250 and Yield Points for the 4-Story Frames

'x' indicates Yield Point for the Flexible-4

'+' indicates Yield Point for the Rigid-4

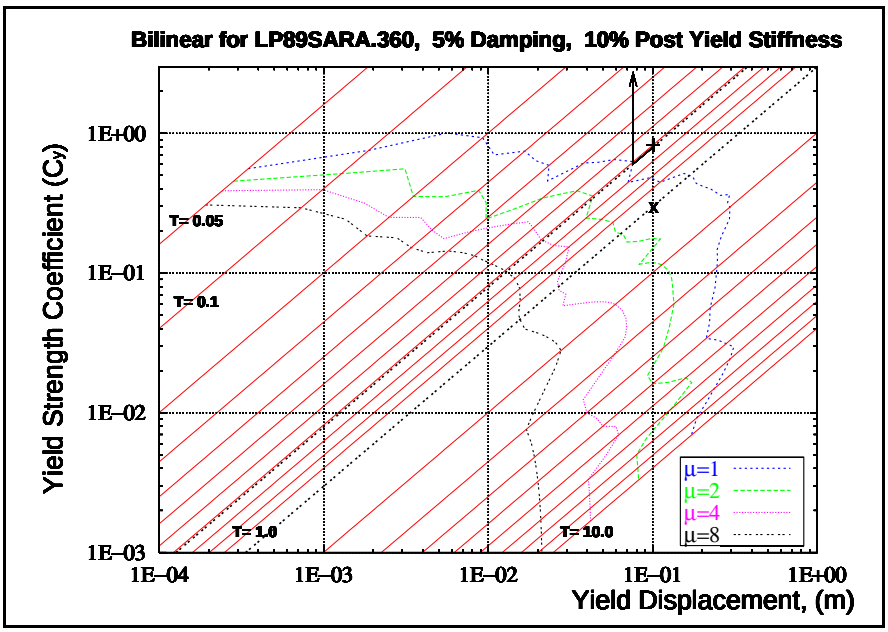

(a)

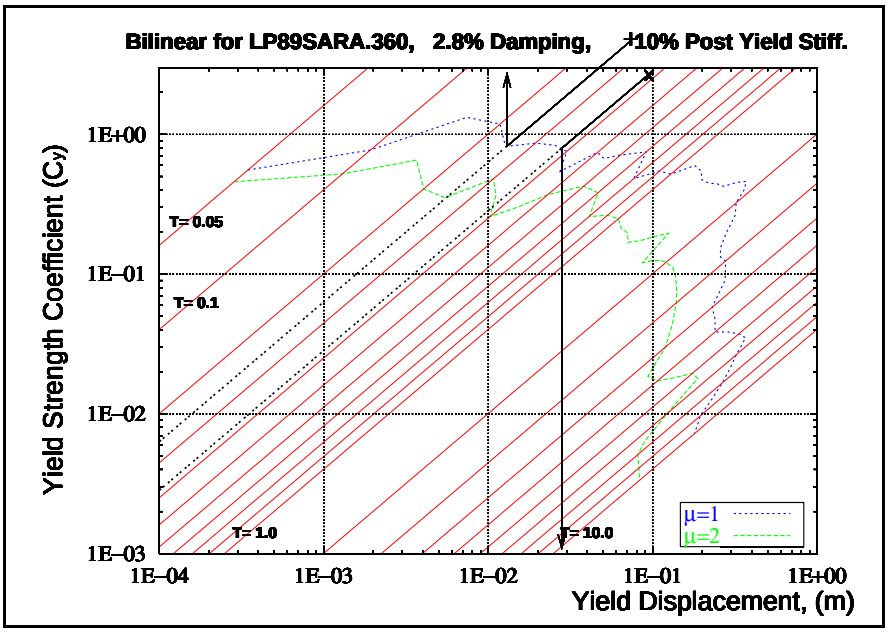

(b)

Figure D.12 YPS For LP89SARA.360 and Yield Points for the 4-Story Frames

'x' indicates Yield Point for the Flexible-4

'+' indicates Yield Point for the Rigid-4

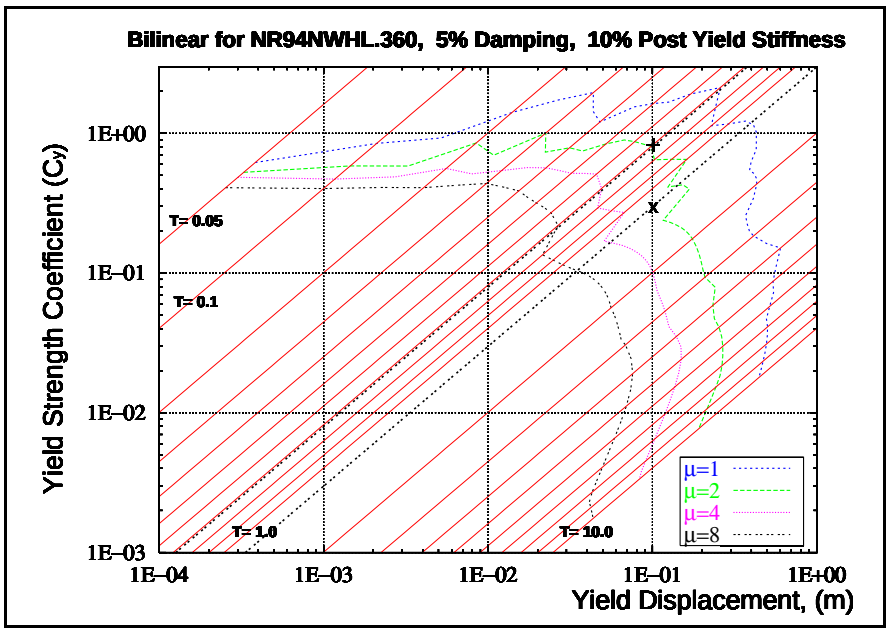

(a)

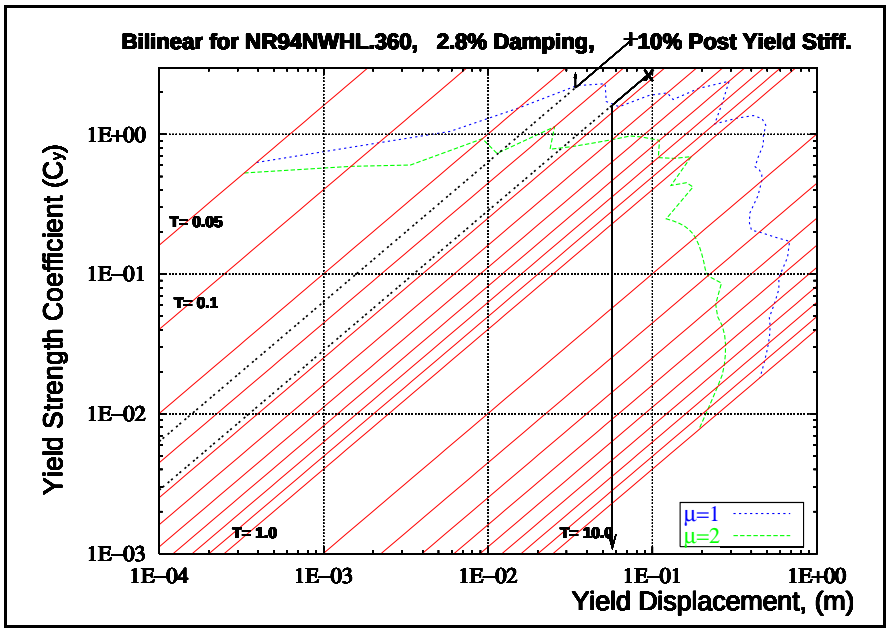

(b)

Figure D.13 YPS For NR94NWHL.360 and Yield Points for the 4-Story Frames

'x' indicates Yield Point for the Flexible-4

'+' indicates Yield Point for the Rigid-4

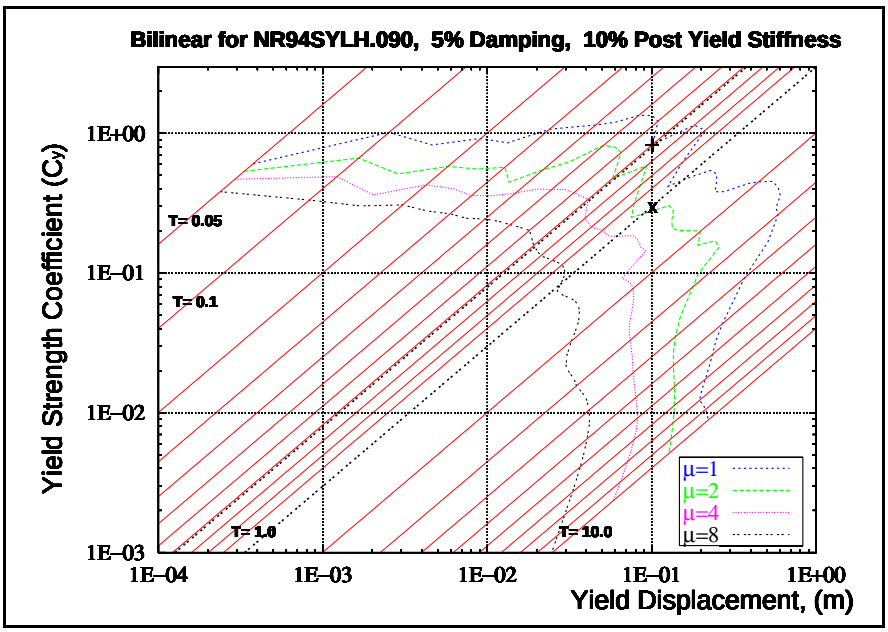

(a)

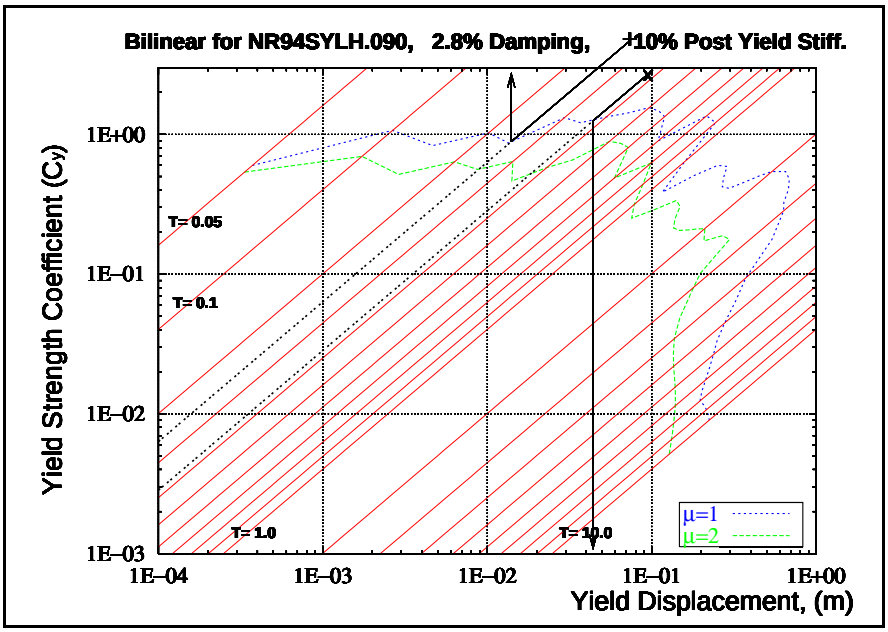

(b)

Figure D.14 YPS For NR94SYLH.090 and Yield Points for the 4-Story Frames

'x' indicates Yield Point for the Flexible-4

'+' indicates Yield Point for the Rigid-4

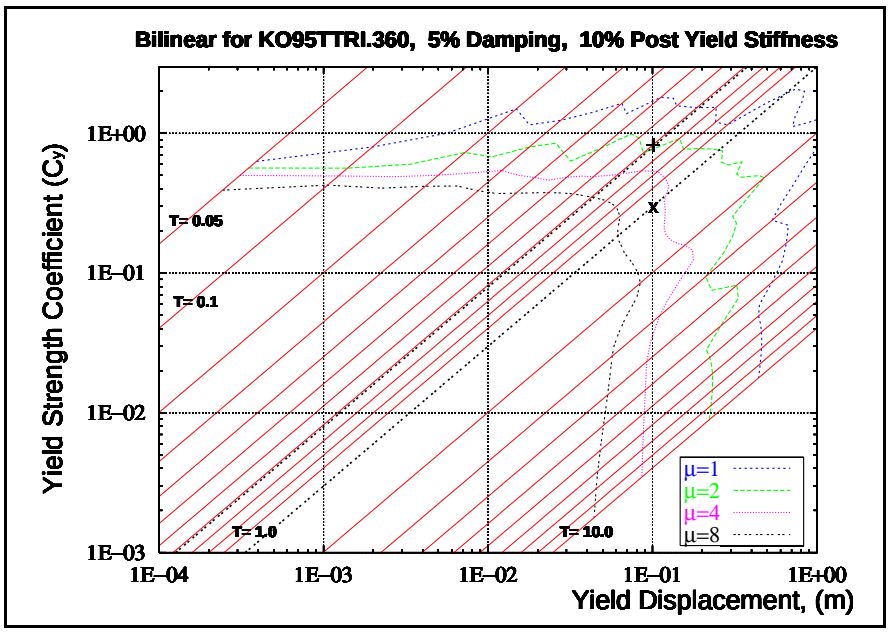

(a)

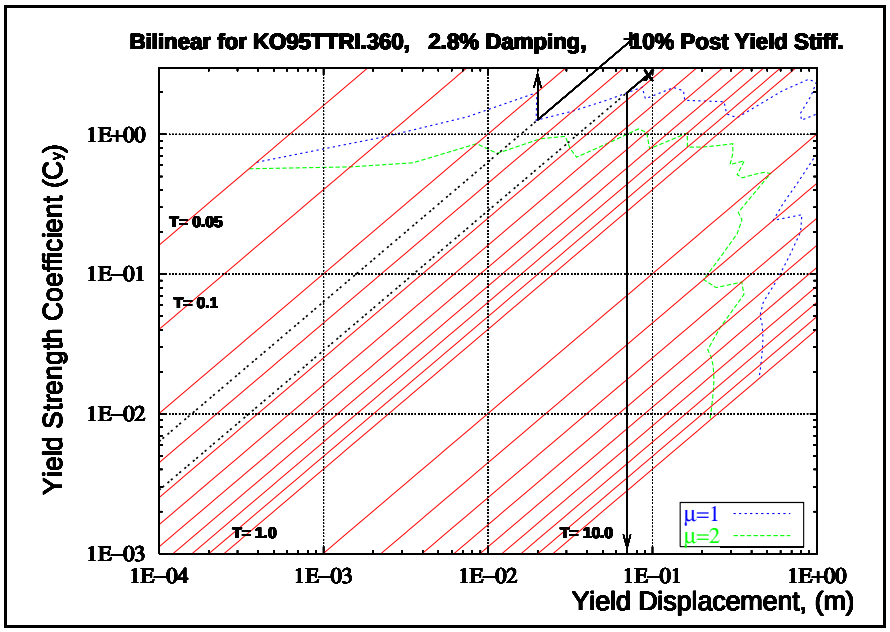

(b)

Figure D.15 YPS For KO95TTRI.360 and Yield Points for the 4-Story Frames

'x' indicates Yield Point for the Flexible-4

'+' indicates Yield Point for the Rigid-4

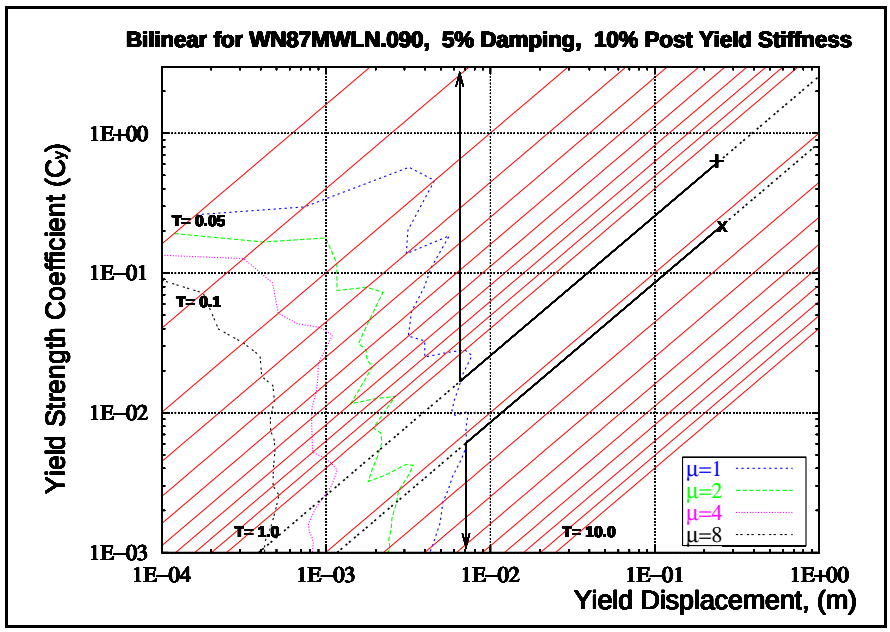

(a)

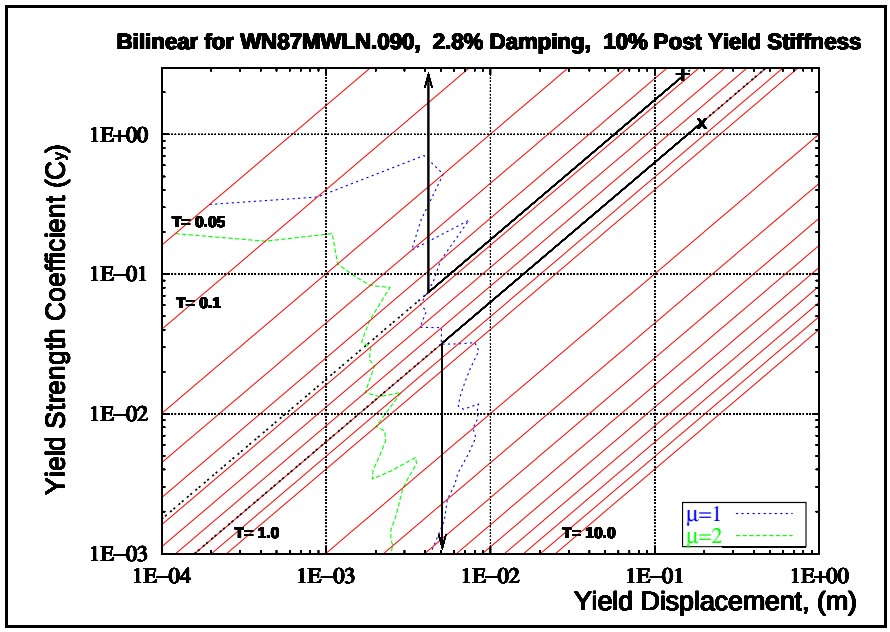

(b)

Figure D.16 YPS For WN87MWLN.090 and Yield Points for the 12-Story Frames

'x' indicates Yield Point for the Flexible-12

'+' indicates Yield Point for the Rigid-12

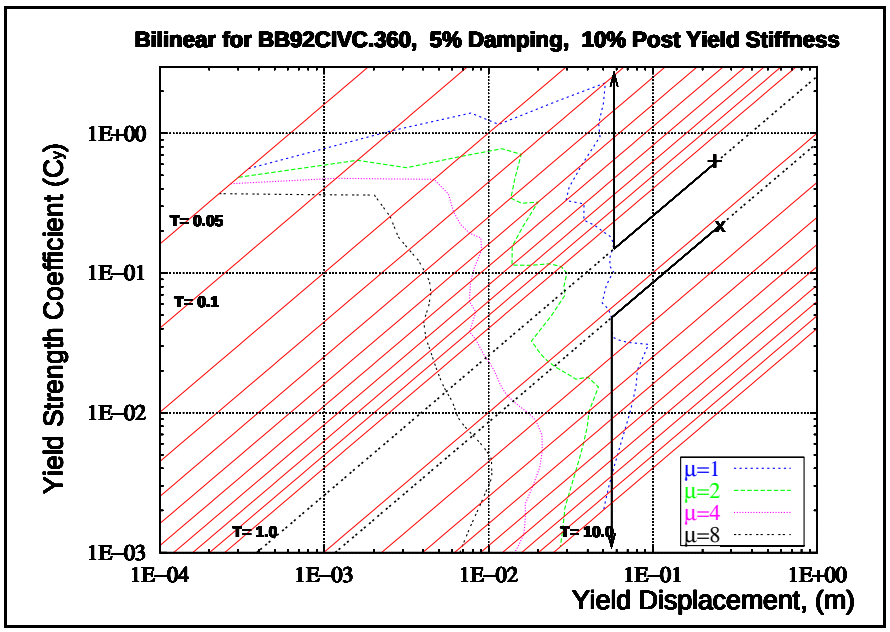

(a)

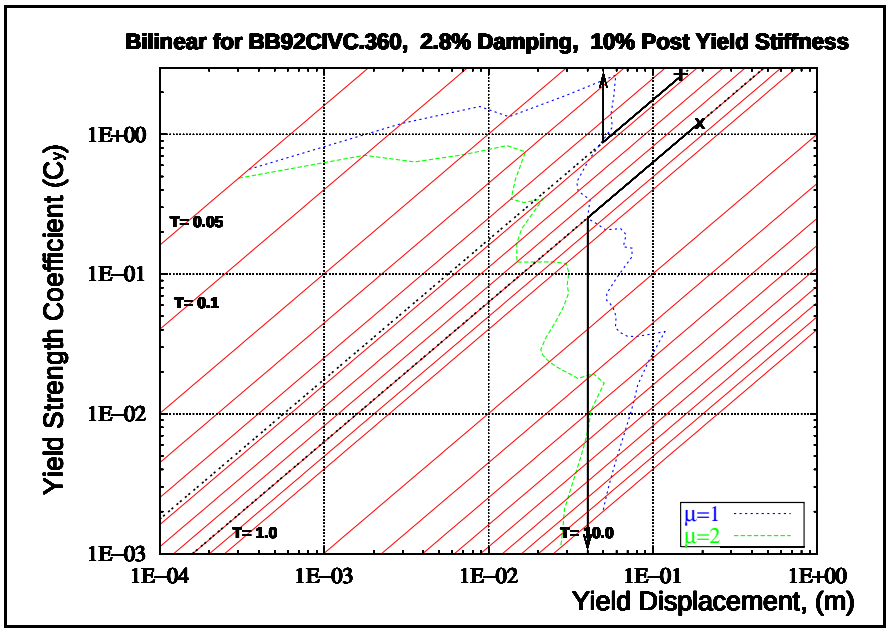

(b)

Figure D.17 YPS For BB92CIVC.360 and Yield Points for the 12-Story Frames

'x' indicates Yield Point for the Flexible-12

'+' indicates Yield Point for the Rigid-12

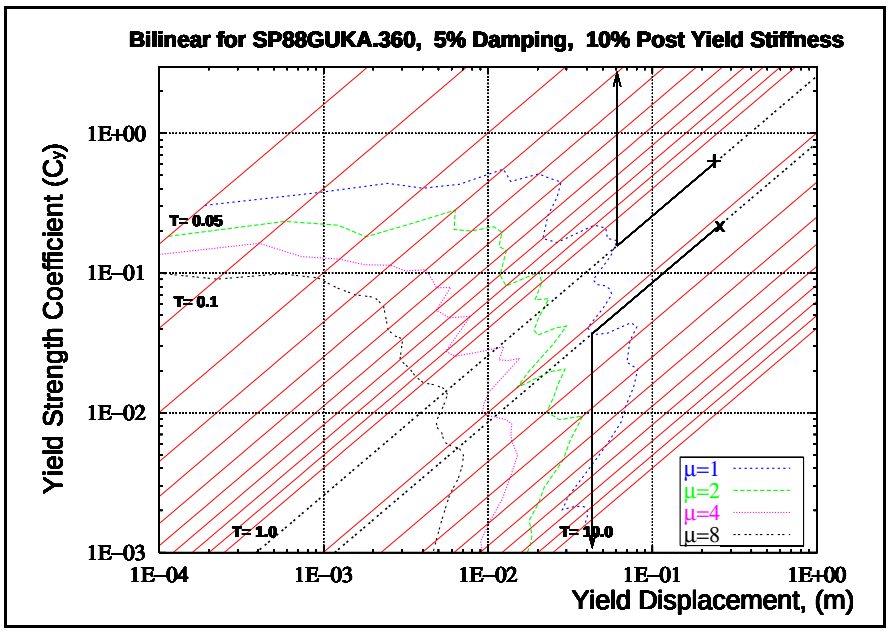

(a)

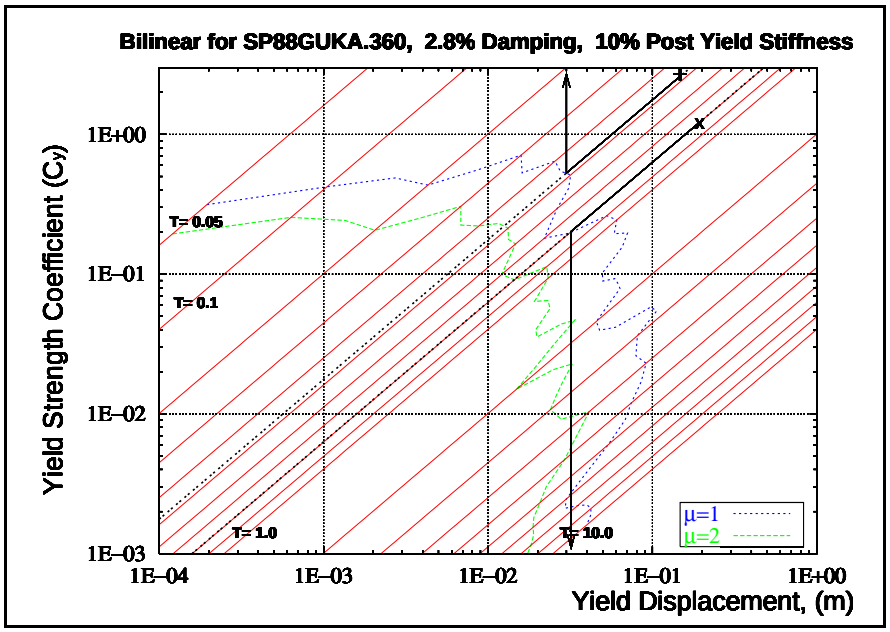

(b)

Figure D.18 YPS For SP88GUKA.360 and Yield Points for the 12-Story Frames

'x' indicates Yield Point for the Flexible-12

'+' indicates Yield Point for the Rigid-12

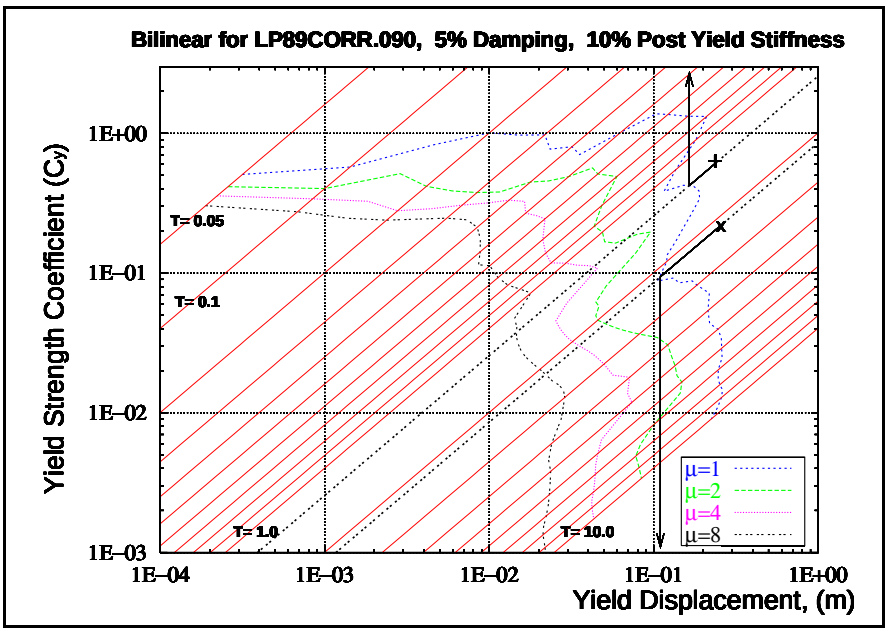

(a)

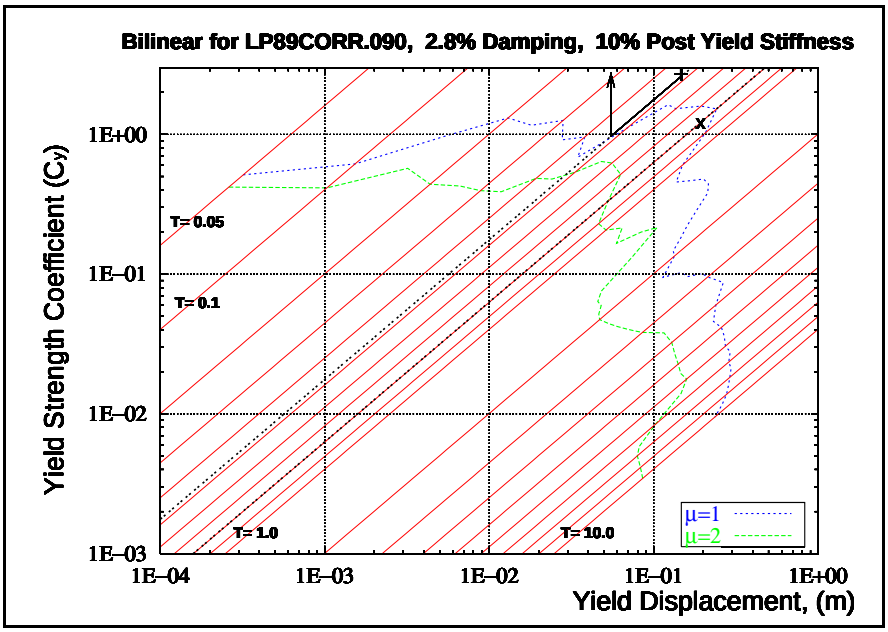

(b)

Figure D.19 YPS For LP89CORR.090 and Yield Points for the 12-Story Frames

'x' indicates Yield Point for the Flexible-12

'+' indicates Yield Point for the Rigid-12

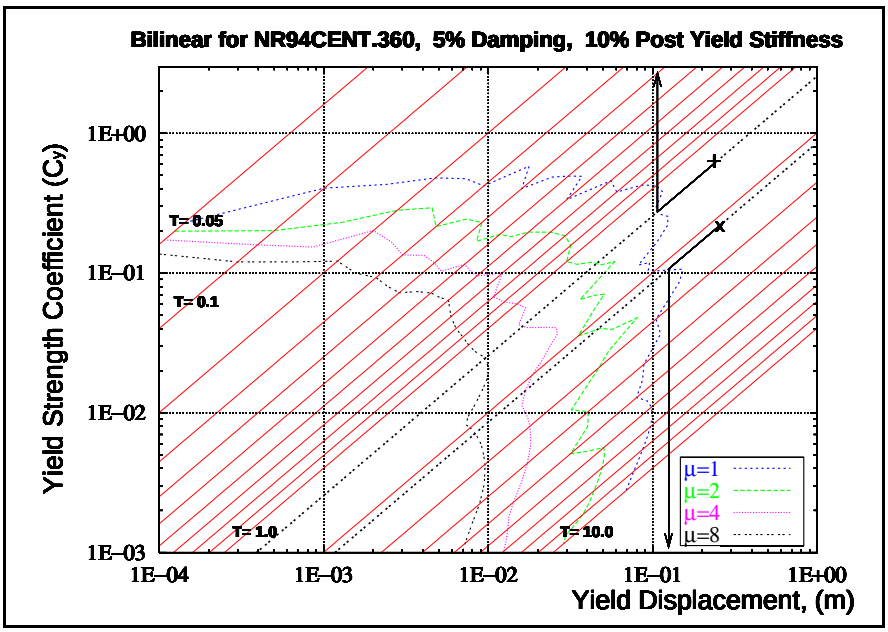

(a)

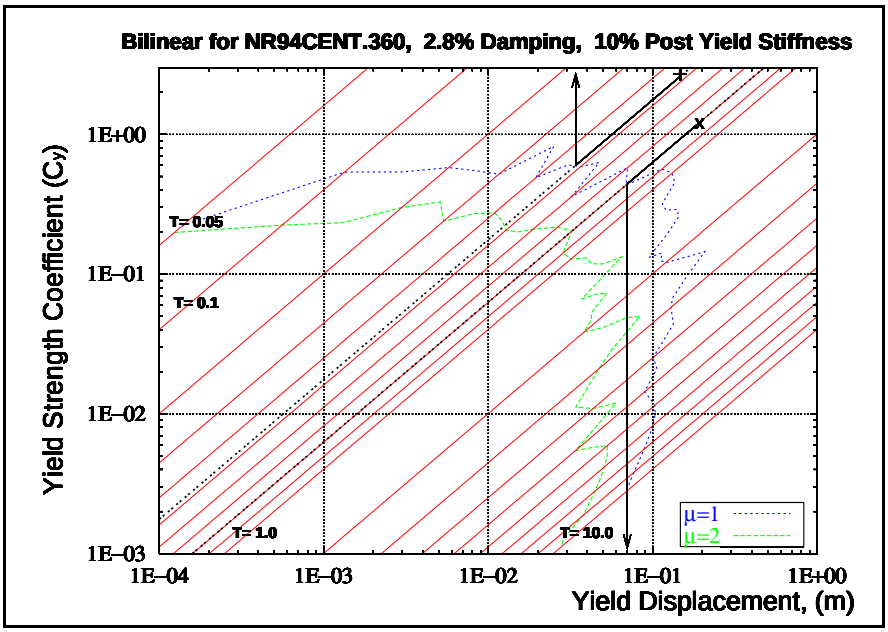

(b)

Figure D.20 YPS For NR94CENT.360 and Yield Points for the 12-Story Frames

'x' indicates Yield Point for the Flexible-12

'+' indicates Yield Point for the Rigid-12

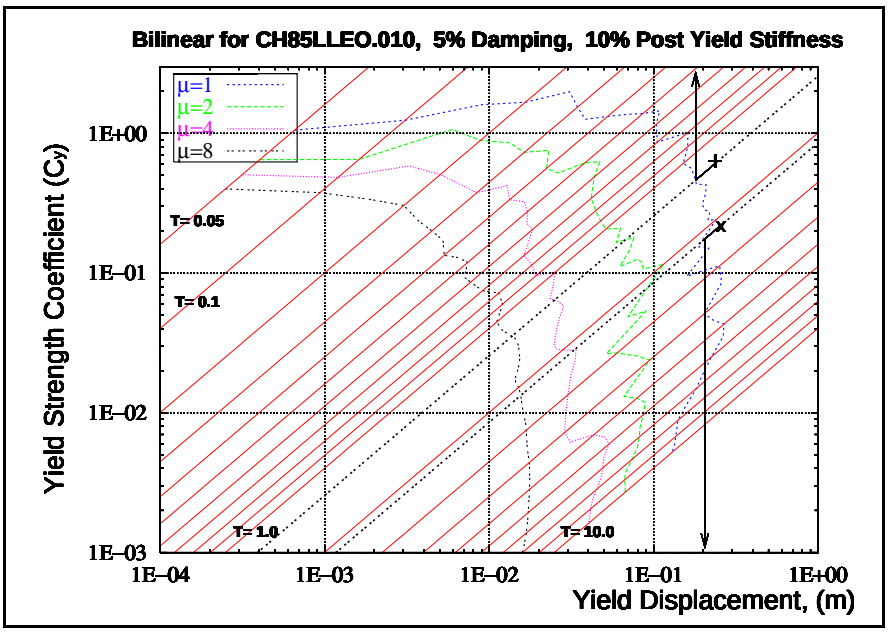

(a)

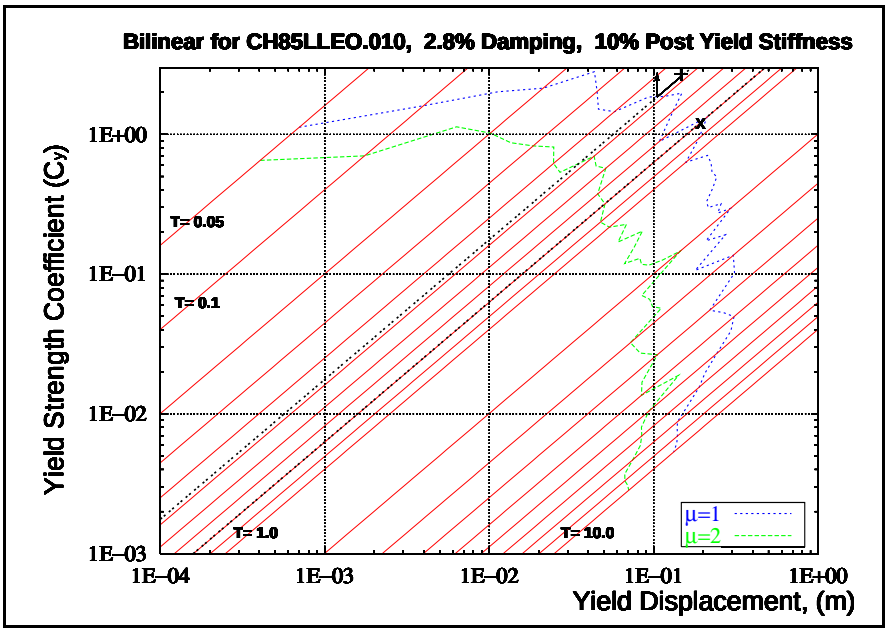

(b)

Figure D.21 YPS For CH85LLEO.010 and Yield Points for the 12-Story Frames

'x' indicates Yield Point for the Flexible-12

'+' indicates Yield Point for the Rigid-12

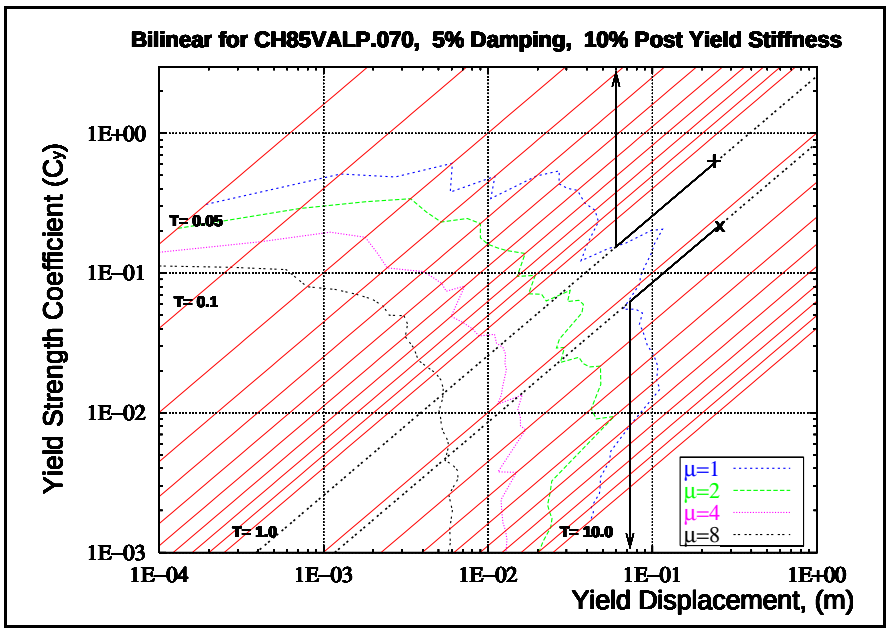

(a)

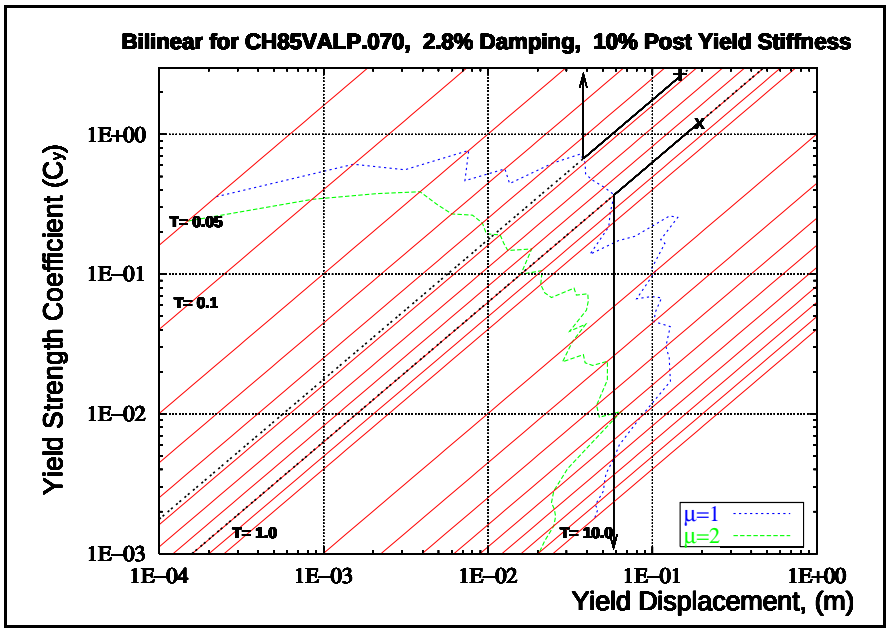

(b)

Figure D.22 YPS For CH85VALP.070 and Yield Points for the 12-Story Frames

'x' indicates Yield Point for the Flexible-12

'+' indicates Yield Point for the Rigid-12

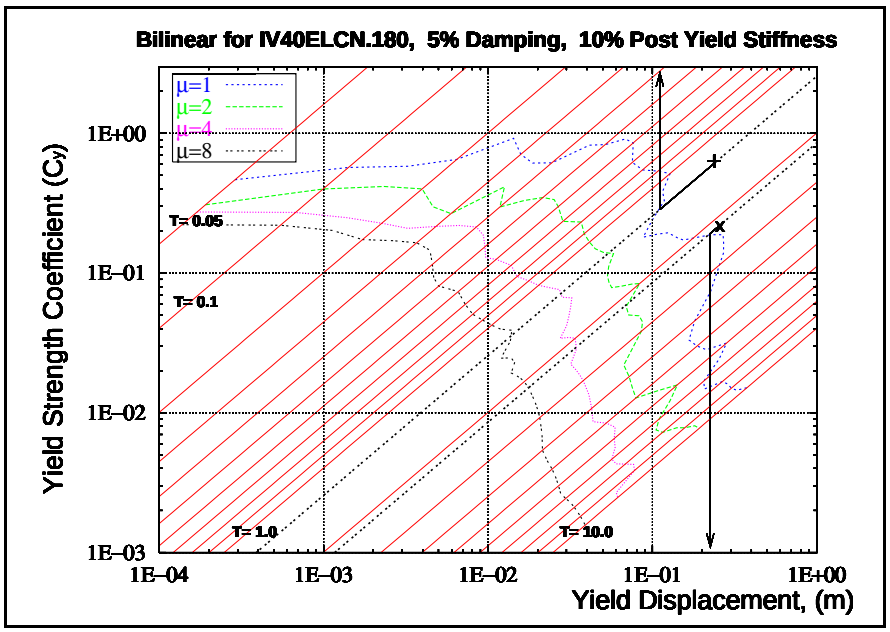

(a)

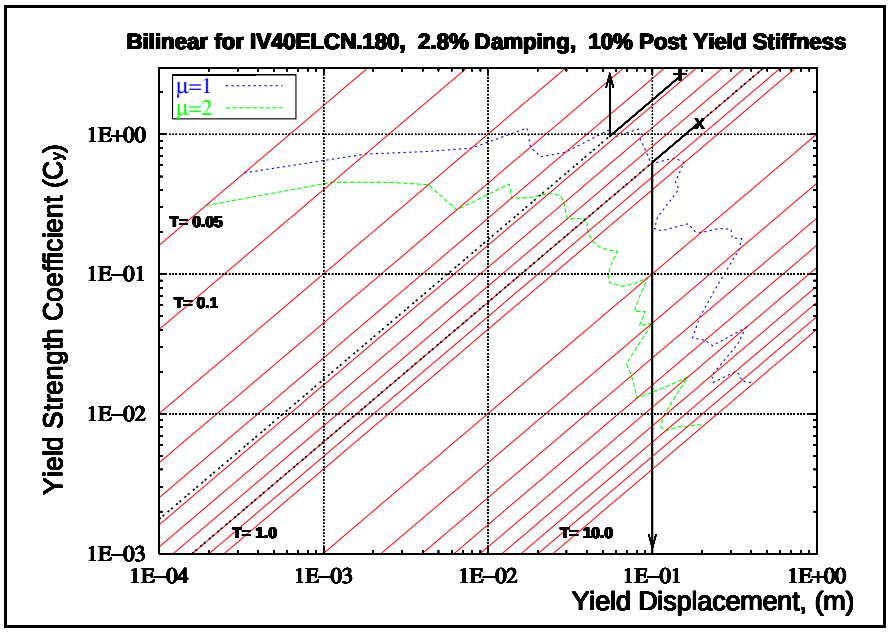

(b)

Figure D.23 YPS For IV40ELCN.180 and Yield Points for the 12-Story Frames

'x' indicates Yield Point for the Flexible-12

'+' indicates Yield Point for the Rigid-12

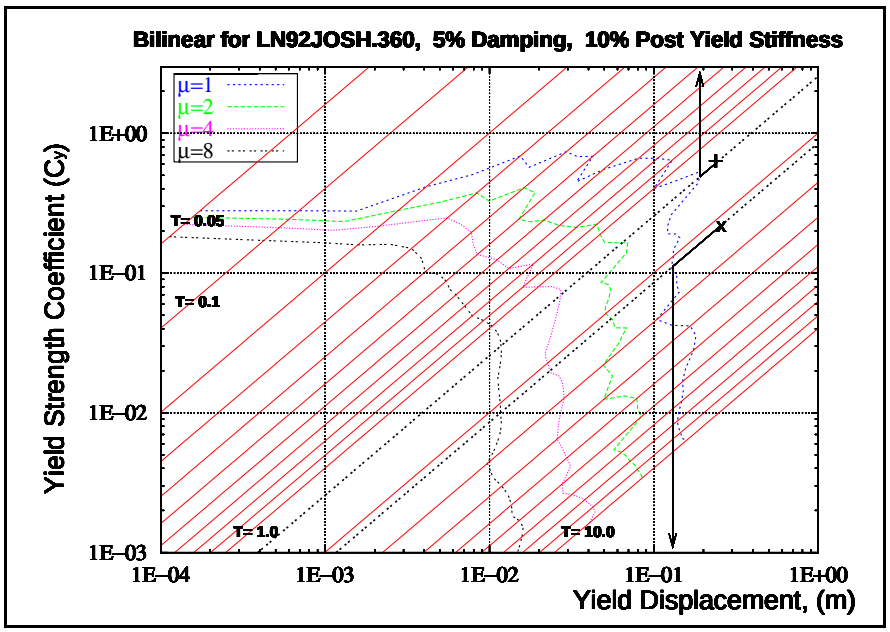

(a)

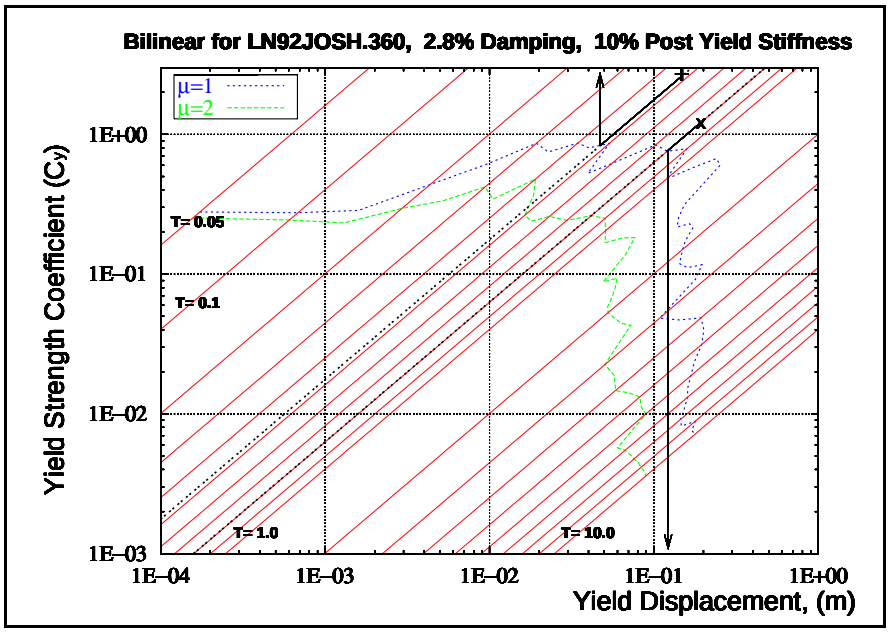

(b)

Figure D.24 YPS For LN92JOSH.360 and Yield Points for the 12-Story Frames

'x' indicates Yield Point for the Flexible-12

'+' indicates Yield Point for the Rigid-12

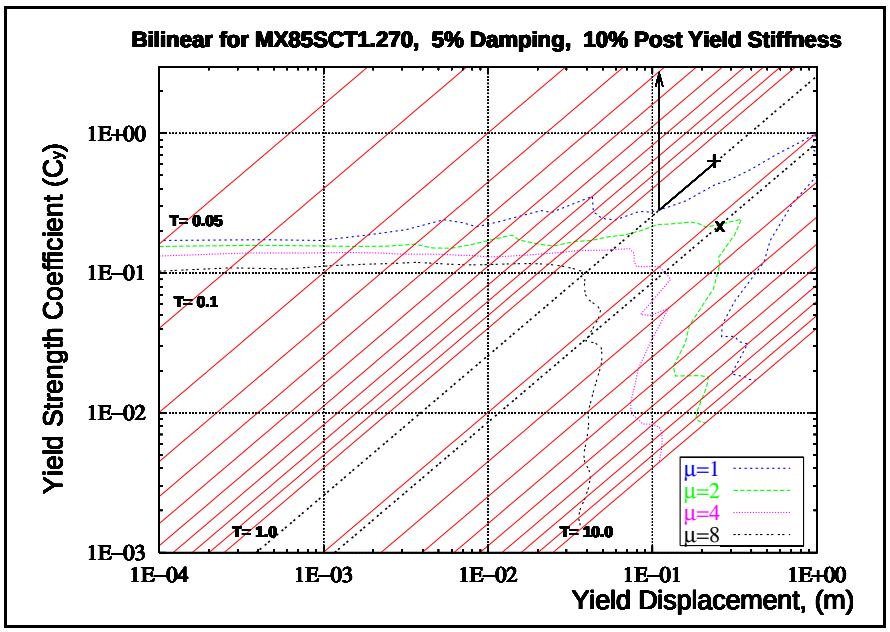

(a)

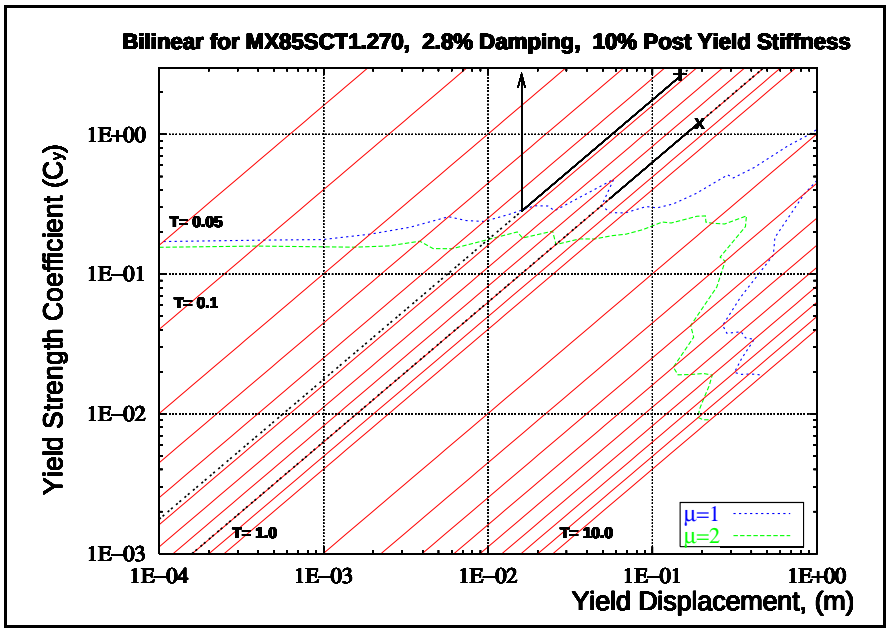

(b)

Figure D.25 YPS For MX85SCT1.270 and Yield Points for the 12-Story Frames

'x' indicates Yield Point for the Flexible-12

'+' indicates Yield Point for the Rigid-12

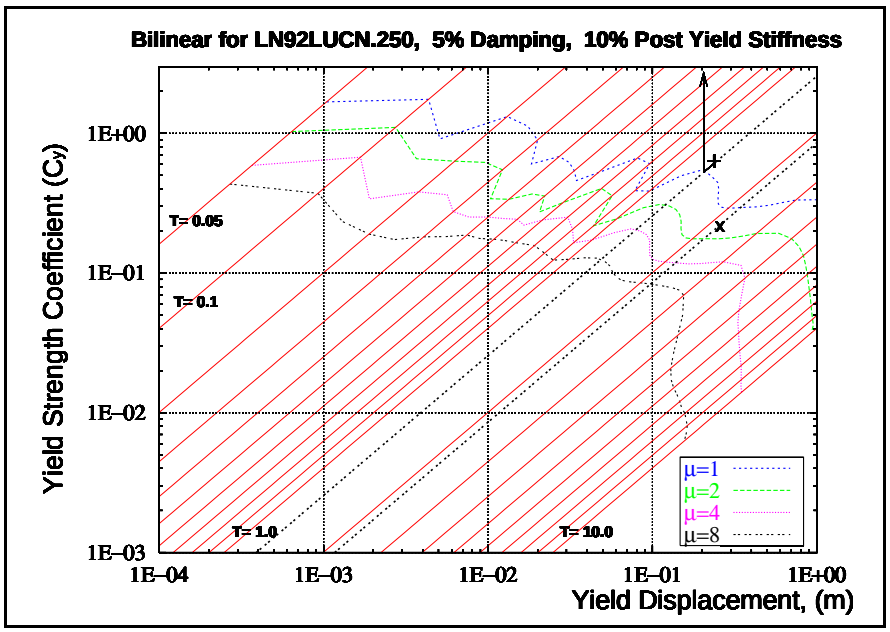

(a)

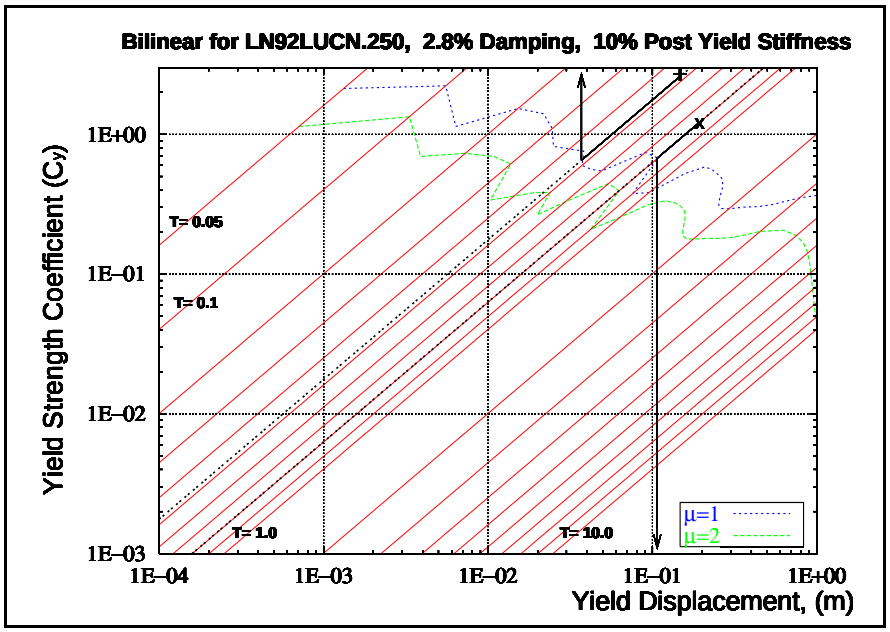

(b)

Figure D.26 YPS For LN92LUCN.250 and Yield Points for the 12-Story Frames

'x' indicates Yield Point for the Flexible-12

'+' indicates Yield Point for the Rigid-12

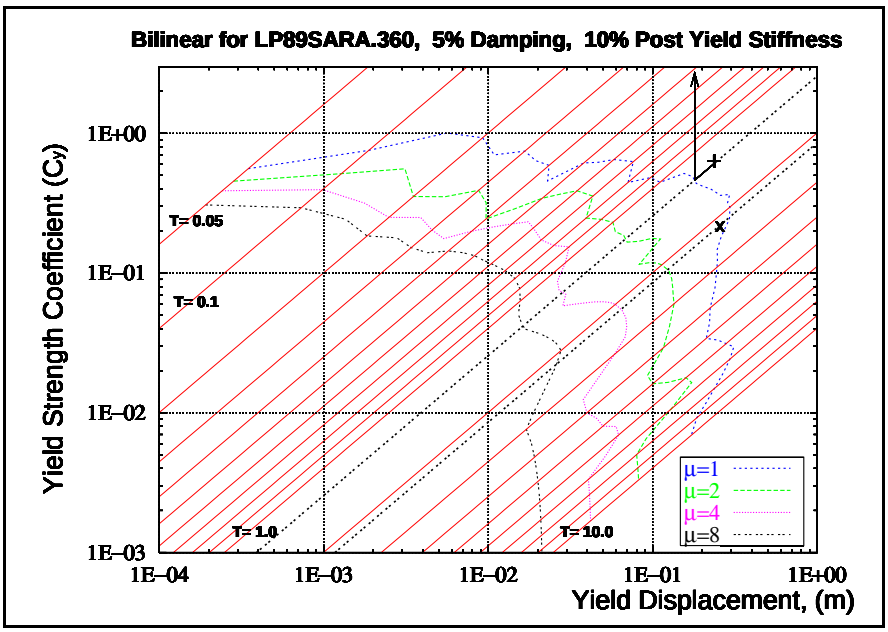

(a)

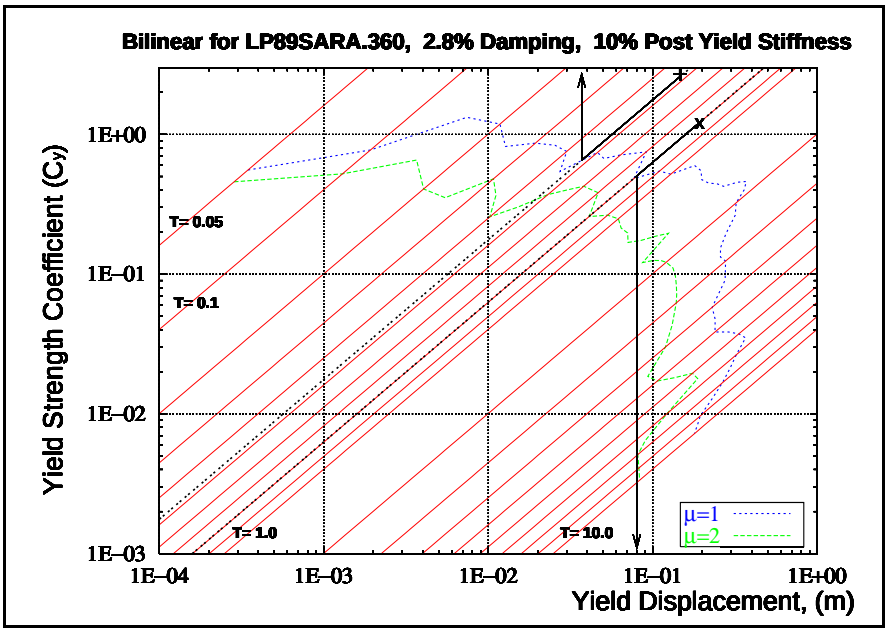

(b)

Figure D.27 YPS For LP89SARA.360 and Yield Points for the 12-Story Frames

'x' indicates Yield Point for the Flexible-12

'+' indicates Yield Point for the Rigid-12

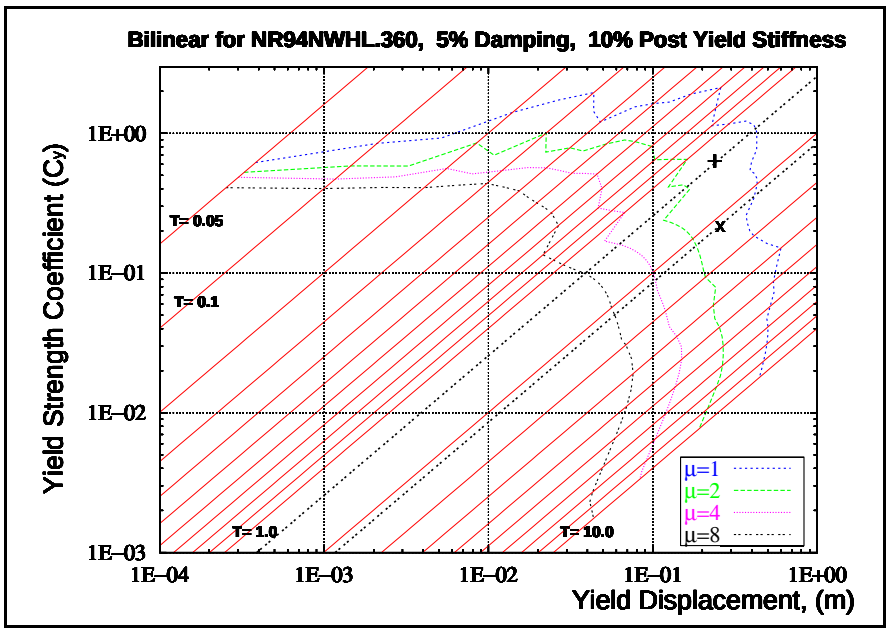

(a)

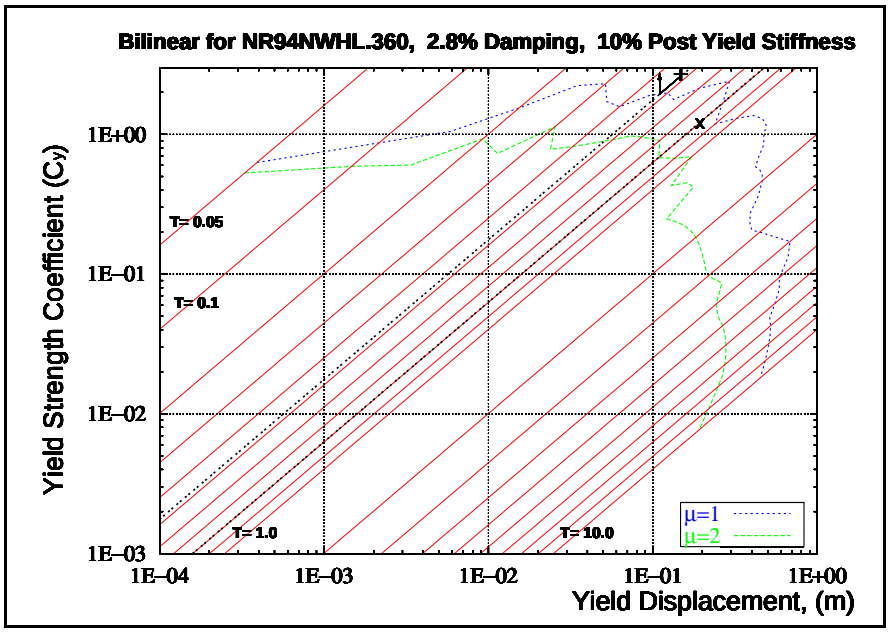

(b)

Figure D.28 YPS For NR94NWHL.360 and Yield Points for the 12-Story Frames

'x' indicates Yield Point for the Flexible-12

'+' indicates Yield Point for the Rigid-12

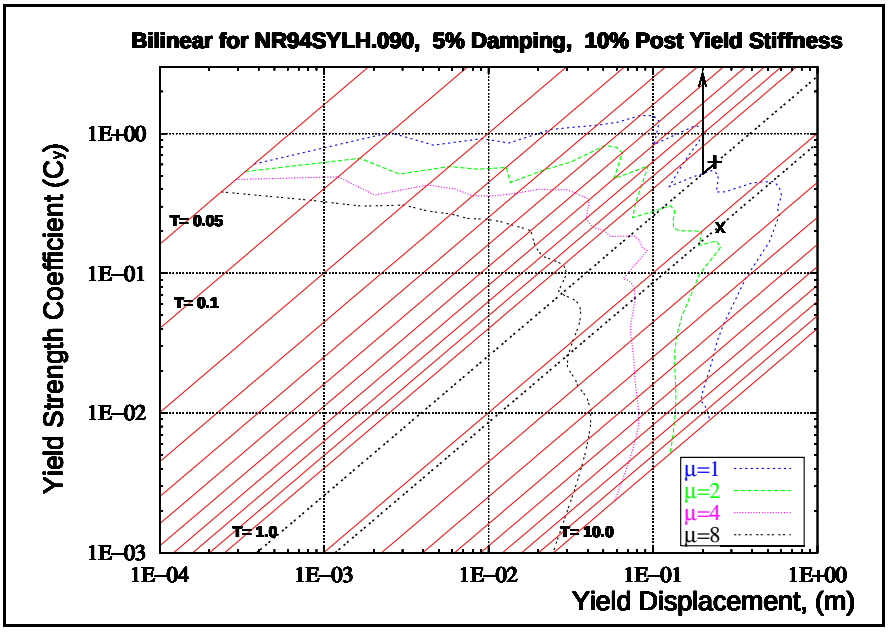

(a)

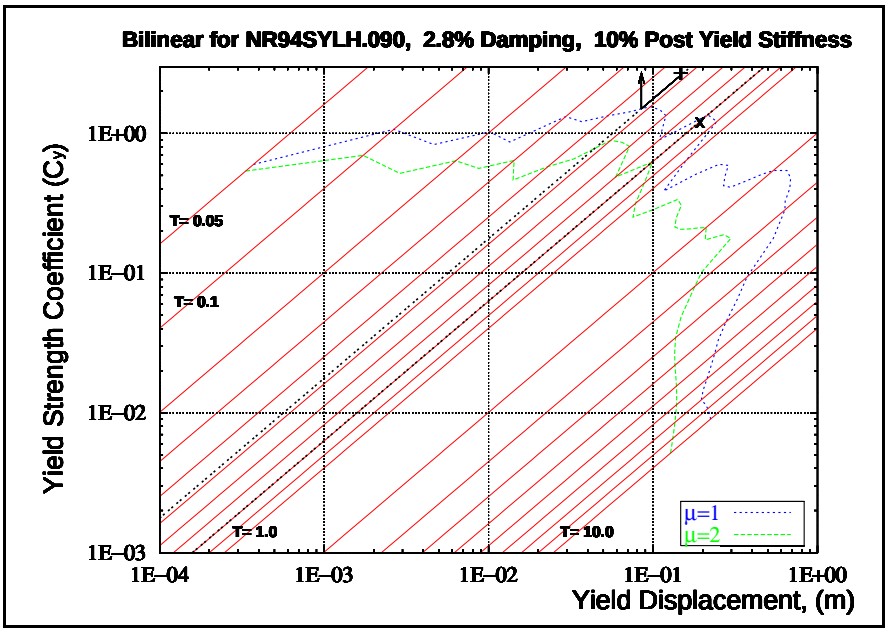

(b)

Figure D.29 YPS For NR94SYLH.090 and Yield Points for the 12-Story Frames

'x' indicates Yield Point for the Flexible-12

'+' indicates Yield Point for the Rigid-12

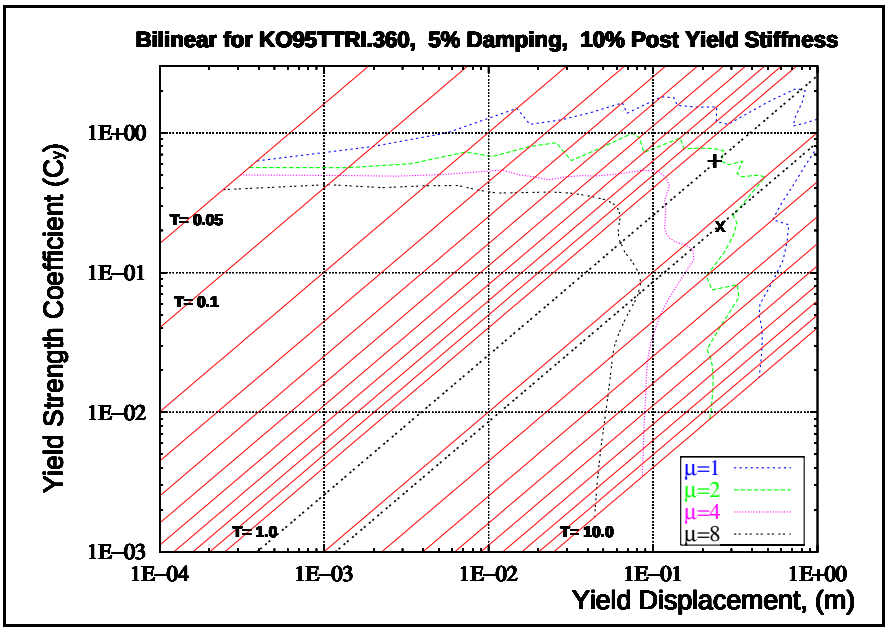

(a)

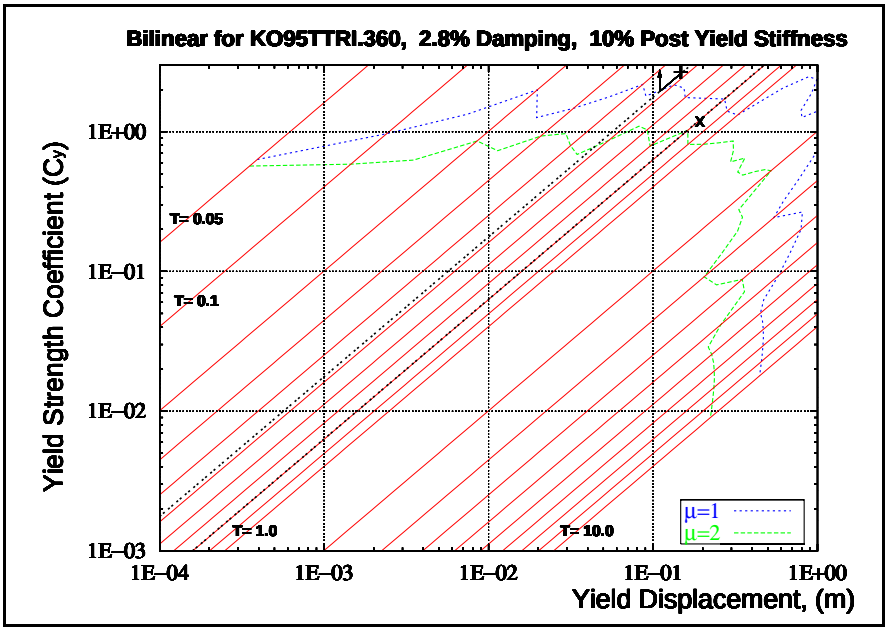

(b)

Figure D.30 YPS For KO95TTRI.360 and Yield Points for the 12-Story Frames

'x' indicates Yield Point for the Flexible-12

'+' indicates Yield Point for the Rigid-12

APPENDIX E

LIST OF THE INPUT FILES USED FOR ANALYSIS OF THE FRAMES DESIGNED WITH THE YPS METHODOLOGY

This appendix provides a listing of the DRAIN-2DX input files for the four frames designed in Chapter 4 using the YPS methodology and analyzed in Chapter 5 using the YPSA method. The program DRAIN-2DX (Powell et al, 1993) was used to perform the static and dynamic analysis of the frames.

```
! 4-Story  Moment Resistant Frame Sytem, Steel
! designed using Yield Point Spectra Methodology.
! for the 1992 Landers at Lucerne G.M.
! Original Design by Edgar F. Black
!
! Units: kN, meters, seconds.
!
!
*STARTXX
  LandDsgn         0 2 0 1              Four STORY FRAME Three Bay
! The frame has a rigid beam and flexible columns.
! Critical vertical load for frame is 200 (based on elastic sidesway buckling).
*NODECOORDS
! Left columns,  from bottom
C        1      0.00      0.00
C        2      8.00      0.00
C        3     16.00      0.00
C        4     24.00      0.00
C        5      0.00      5.00
C        6      8.00      5.00
C        7     16.00      5.00
C        8     24.00      5.00
C       17      0.00     17.00
C       18      8.00     17.00
C       19     16.00     17.00
C       20     24.00     17.00
L        5        17         4
L        6        18         4
L        7        19         4
L        8        20         4
*RESTRAINTS
! fixed supports at foundations
S 111         1         4         1
*SLAVING
!        master     slave     slave
S 100         5         6         8
S 100         9        10        12
S 100        13        14        16
S 100        17        18        20
!
*MASSES
S 100 137.75000       5        20                                  9.807.483541400
!
*ELEMENTGROUP
    2    0    1     1.970724-3          BEAM
    2    0    2
! beam   section
!
!! W18X35
!    1 199.96+06       .056.645148-32.122780-4   4.   4.   2.
! W21X44
    1 199.96+06       .058.387080-33.508831-4   4.   4.   2.
! W21X44
    2 199.96+06       .058.387080-33.508831-4   4.   4.   2.
!
! yield strength
!    1    1 234.294   234.294
    1    1 331.916   331.916
    2    1 331.916   331.916
! beams
! First Floor
    1         5         6         1    2         2    2
    2         6         7         1    2         2    2
    3         7         8         1    2         2    2
! Second Floor
    4         9        10         1    2         2    2
    5        10        11         1    2         2    2
    6        11        12         1    2         2    2
! Third Floor
    7        13        14         1    1         1    1
    8        14        15         1    1         1    1
    9        15        16         1    1         1    1
! Fourth Floor
   10        17        18         1    1         1    1
   11        18        19         1    1         1    1
   12        19        20         1    1         1    1
*ELEMENTGROUP
    2    0    1     1.970724-3          COLUMNS
    2    0    2
! column section
!!
! W14X48
    1 199.96+06       .059.096756-32.018722-4  4.   4.   2.
! W14X74
    2 199.96+06       .051.406449-23.312202-4  4.   4.   2.
!
! yield strength
    1    1 285.952   285.952
    2    1 455.571   455.571
!
! columns
! First  Floor
    1         1         5         1    2         2    2
    2         2         6         1    2         2    2
    3         3         7         1    2         2    2
    4         4         8         1    2         2    2
! Second Floor
    5         5         9         1    2         2    2
    6         6        10         1    2         2    2
    7         7        11         1    2         2    2
    8         8        12         1    2         2    2
! Third Floor
    9         9        13         1    1         1    1
   10        10        14         1    1         1    1
   11        11        15         1    1         1    1
   12        12        16         1    1         1    1
! Fouth Floor
   13        13        17         1    1         1    1
   14        14        18         1    1         1    1
   15        15        19         1    1         1    1
   16        16        20         1    1         1    1

*GENDISP
        5     1  0.20
        1     1 -0.20
*GENDISP
        9     1  0.25
        5     1 -0.25
*GENDISP
       13     1  0.25
        9     1 -0.25
*GENDISP
       17     1  0.25
       13     1 -0.25
*RESULTS
NSD    001        05        17         4
E      001    2    1    4
!GD     001
*ELEMLOAD
 WDLD
G   1    1
    1    0      1.0  0.0      140.928   187.904   0.0       140.928   -187.904
```

```
    1   12    1    1       1.0

!*NODALOAD
! WGTH                                  UNIT HORIZONTAL LOAD
!S       .0-25.706461        0.        05        20        1
!
*NODALOAD
 YPSD                                   1st Mode load pattern
!YPS LOAD PATTERN for lucern design
S   247.45        0.        0.        17        20
S   154.82        0.        0.        13        16
S   107.18        0.        0.         9        12
S    59.55        0.        0.         5         8
!
!
!*NODALOAD
! 1MOD                                   1st Mode load pattern
!! First Mode Pattern
!S  1.00000        0.        0.        17        20
!S  .853552        0.        0.        13        16
!S  .595736        0.        0.         9        12
!S  .313357        0.        0.         5         8
!! Second Mode Pattern
!*NODALOAD
! 2MOD                                   2nd Mode load pattern
!S 1.000000        0.        0.        17        20
!S-0.109690        0.        0.        13        16
!S-1.043150        0.        0.         9        12
!S-0.909288        0.        0.         5         8
!
!*ACCNREC
!
! Short Earthquakes
!
! WNMW   wn87mwln.090 (2E10.3)           Whittier Narrow
! 2000    1    1    1          0.01
! BB92   bb92civc.360 (2E10.3)           Big Bear
! 6001    1    1    1          0.01
! SPGK   sp88guka.360 (2E10.3)           Spitak, Armenia
! 2000    1    1    1          0.01
! LPCO   lp89corr.090 (2E10.3)           Loma Prieta Corralitos
! 2000    1    1    1          0.01
! NRCN   nr94cent.360 (2E10.3)           Nortridge Centenial
! 3000    1    1    1          0.01
!
! Long  Earthquakes
!
! CHLL   ch85lleo.010 (2E10.3)           Chile Llolleo
!23277    1    1    1          0.01
! CHVP   ch85valp.070 (2E10.3)           Chile Valparaiso
!15874    1    1    1          0.01
! ELCN   iv40elcn.180 (2E10.3)           El centro Norte-Sur
! 2688    1    1    1          0.01
! LNJH   ln92josh.360 (2E10.3)           Landers Joshua Tree
! 4000    1    1    1          0.01
! MXST   mx85sct1.270 (2E10.3)           Mexico 85
! 9004    1    1    1          0.01
!
! Near-Forward Earthquakes
!
! LUCN   ln92lucn.250 (2E10.3)           Landers Lucerne
!12321    1    1    1          0.01
! LPSR   lp89sara.360 (2E10.3)           Loma Prieta, Saratoga
! 2001    1    1    1          0.01
! NRNH   nr94nwhl.360 (2E10.3)           El centro Norte-Sur
! 3000    1    1    1          0.01
```

```
! NRSY   nr94sylh.090 (2E10.3)           Northridge, Sylmar
! 3000    1    1    1          0.01
! KOBE   ko95ttri.360 (2E10.3)           Kobi Takatori
! 4096    1    1    1          0.01
!
*PARAMETERS
OS       0    0    1    0    0
!OS       0    0   -1    0    1
DC  1    0    0    0
DT 0.001  0.01      0.01
DA                        0.1                                   5
!OD                                        1  0.0
OD                                       1  0.0                          0
F     1.0      1.0
*MODE                                     Modal Analysis
    4              2
!*GRAV
!N     WGTH  8.0
!*GRAV
!E     WDLD 1.0
!*STAT                                    ADD HORIZONTAL LOAD IN 10 STEPS
!N     YPSD    1.0000
!D       17        01    1 0.0020   0.200
!N     1MOD    1.000
!D       17        01    1 0.0025   0.250
!N     2MOD    1.000
!D       17        01    1 0.0010   0.100
!*STAT                                    ADD HORIZONTAL LOAD IN 10 STEPS
!N     YPSD 0.28500000
!N     1MOD 032.00000
!N     2MOD 150.00000
!L    0.010          1
!*ACCN
!50.00     90000    2
! Short Earthquakes Parameters
!1     WNMW       1.0       1.0
!1     BB92       1.0       1.0
!1     SPGK       1.0       1.0
!1     LPCO      1.00       1.0
!1     NRCN      1.00       1.0
!
! Long  Earthquakes Parameters
!
!1     CHLL      1.00       1.0
!1     CHVP      1.00       1.0
!1     ELCN      1.00       1.0
!1     LNJH      1.00       1.0
!1     MXST      1.00       1.0
!
! Near-Forward Earthquakes Parameters
!
!1     LUCN       1.0       1.0
!1     LPSR       1.0       1.0
!1     NRNH       1.0       1.0
!1     NRSY       1.0       1.0
!1     KOBE       1.0       1.0
*STOP
```

```
! 4-Story  Moment Resistant Frame Sytem, Steel
! designed using Yield Point Spectra Methodology.
! for the 1994 Northridge at Newhall L.A. County Fire Station G.M.
! Original Design by Edgar F. Black
!
! Units: kN, meters, seconds.
!
!
*STARTXX
  NwhlDsgn         0 2 0 1              Four STORY FRAME Three Bay
! The frame has a rigid beam and flexible columns.
! Critical vertical load for frame is 200 (based on elastic sidesway buckling).
*NODECOORDS
! Left columns,  from bottom
C        1      0.00      0.00
C        2      8.00      0.00
C        3     16.00      0.00
C        4     24.00      0.00
C        5      0.00      5.00
C        6      8.00      5.00
C        7     16.00      5.00
C        8     24.00      5.00
C       17      0.00     17.00
C       18      8.00     17.00
C       19     16.00     17.00
C       20     24.00     17.00
L        5        17         4
L        6        18         4
L        7        19         4
L        8        20         4
*RESTRAINTS
! fixed supports at foundations
S 111         1         4         1
*SLAVING
!        master     slave     slave
S 100         5         6         8
S 100         9        10        12
S 100        13        14        16
S 100        17        18        20
!
*MASSES
S 100 137.75000       5        20                                  9.807.785193032
!
*ELEMENTGROUP
    2    0    1     1.239446-3          BEAM
    2    0    2
! beam   section
! W24X55
    1 199.96+06       .051.045159-25.619124-4   4.   4.   2.
! W24X94
    2 199.96+06       .051.787093-21.123825-3   4.   4.   2.
!
! yield strength
    1    1 463.706   463.706
    2    1 903.007   903.007
! beams
! First Floor
    1         5         6         1    2         2    2
    2         6         7         1    2         2    2
    3         7         8         1    2         2    2
! Second Floor
    4         9        10         1    2         2    2
    5        10        11         1    2         2    2
    6        11        12         1    2         2    2
! Third Floor
    7        13        14         1    1         1    1
    8        14        15         1    1         1    1
    9        15        16         1    1         1    1
! Fourth Floor
   10        17        18         1    1         1    1
   11        18        19         1    1         1    1
   12        19        20         1    1         1    1
*ELEMENTGROUP
    2    0    1     1.239446-3          COLUMNS
    2    0    2
! column section
!!
! W14X99
    1 199.96+06       .051.877416-24.620169-4  4.   4.   2.
! W14X176
    2 199.96+06       .053.341929-28.907353-4  4.   4.   2.
!
! yield strength
    1    1 638.613   638.613
    2    1 1143.00   1143.00
!
! columns
! First  Floor
    1         1         5         1    2         2    2
    2         2         6         1    2         2    2
    3         3         7         1    2         2    2
    4         4         8         1    2         2    2
! Second Floor
    5         5         9         1    2         2    2
    6         6        10         1    2         2    2
    7         7        11         1    2         2    2
    8         8        12         1    2         2    2
! Third Floor
    9         9        13         1    1         1    1
   10        10        14         1    1         1    1
   11        11        15         1    1         1    1
   12        12        16         1    1         1    1
! Fouth Floor
   13        13        17         1    1         1    1
   14        14        18         1    1         1    1
   15        15        19         1    1         1    1
   16        16        20         1    1         1    1

*GENDISP
        5     1  0.20
        1     1 -0.20
*GENDISP
        9     1  0.25
        5     1 -0.25
*GENDISP
       13     1  0.25
        9     1 -0.25
*GENDISP
       17     1  0.25
       13     1 -0.25
*RESULTS
NSD    001        05        17         4
E      001    2    1    4
GD     001
*ELEMLOAD
 WDLD
G   1    1
    1    0      1.0  0.0      140.928   187.904   0.0       140.928   -187.904
    1   12    1    1       1.0

!*NODALOAD
! WGTH                                  UNIT HORIZONTAL LOAD
```

```
!S       .0-25.706461        0.        05        20        1
*NODALOAD
 YPSD                                  UNIT HORIZONTAL LOAD
!YPS LOAD PATTERN for kobe design
S   631.14        0.        0.        17        20
S   426.05        0.        0.        13        16
S   294.95        0.        0.         9        12
S   163.86        0.        0.         5         8
!
!
!*NODALOAD
! 1MOD                                  1st Mode load pattern
!! First Mode Pattern
!S  1.00000        0.        0.        17        20
!S  .798888        0.        0.        13        16
!S  .515736        0.        0.         9        12
!S  .274275        0.        0.         5         8
!! Second Mode Pattern
!*NODALOAD
! 2MOD                                  2nd Mode load pattern
!S 1.000000        0.        0.        17        20
!S-0.245730        0.        0.        13        16
!S-1.098929        0.        0.         9        12
!S-0.863847        0.        0.         5         8
!
!*ACCNREC
!
! Short Earthquakes
!
! WNMW   wn87mwln.090 (2E10.3)           Whittier Narrow
! 2000    1    1    1          0.01
! BB92   bb92civc.360 (2E10.3)           Big Bear
! 6001    1    1    1          0.01
! SPGK   sp88guka.360 (2E10.3)           Spitak, Armenia
! 2000    1    1    1          0.01
! LPCO   lp89corr.090 (2E10.3)           Loma Prieta Corralitos
! 2000    1    1    1          0.01
! NRCN   nr94cent.360 (2E10.3)           Nortridge Centenial
! 3000    1    1    1          0.01
!
! Long  Earthquakes
!
! CHLL   ch85lleo.010 (2E10.3)           Chile Llolleo
!23277    1    1    1          0.01
! CHVP   ch85valp.070 (2E10.3)           Chile Valparaiso
!15874    1    1    1          0.01
! ELCN   iv40elcn.180 (2E10.3)           El centro Norte-Sur
! 2688    1    1    1          0.01
! LNJH   ln92josh.360 (2E10.3)           Landers Joshua Tree
! 4000    1    1    1          0.01
! MXST   mx85sct1.270 (2E10.3)           Mexico 85
! 9004    1    1    1          0.01
!
! Near-Forward Earthquakes
!
! LUCN   ln92lucn.250 (2E10.3)           Landers Lucerne
!12321    1    1    1          0.01
! LPSR   lp89sara.360 (2E10.3)           Loma Prieta, Saratoga
! 2001    1    1    1          0.01
! NRNH   nr94nwhl.360 (2E10.3)           El centro Norte-Sur
! 3000    1    1    1          0.01
! NRSY   nr94sylh.090 (2E10.3)           Northridge, Sylmar
! 3000    1    1    1          0.01
! KOBE   ko95ttri.360 (2E10.3)           Kobi Takatori
! 4096    1    1    1          0.01
!
```

```
*PARAMETERS
OS       0    0    1    0    0
!OS       0    0   -1    0    1
DC  1    0    0    0
DT 0.001  0.01      0.01
DA                        0.1                                    5
!OD                                       1  0.0
OD                                      1  0.0                          0
F     1.0      1.0
*MODE                                     Modal Analysis
    4              2
!*GRAV
!N     WGTH  8.0
!*GRAV
!E     WDLD 1.0
!*STAT                                     ADD HORIZONTAL LOAD IN 10 STEPS
!N     UBC7    1.0000
!D       17        01    1 0.0020   0.200
!N     1MOD    1.000
!D       17        01    1 0.0035   0.350
!N     2MOD    1.000
!D       17        01    1 0.0020   0.200
!*STAT                                     ADD HORIZONTAL LOAD IN 10 STEPS
!N     YPSD 0.2900000
!N     1MOD 032.00000
!N     2MOD 150.00000
!L    0.010          1
!*ACCN
!50.00     90000    2
! Short Earthquakes Parameters
!1     WNMW       1.0       1.0
!1     BB92       1.0       1.0
!1     SPGK       1.0       1.0
!1     LPCO      1.00       1.0
!1     NRCN      1.00       1.0
!
! Long  Earthquakes Parameters
!
!1     CHLL      1.00       1.0
!1     CHVP      1.00       1.0
!1     ELCN      1.00       1.0
!1     LNJH      1.00       1.0
!1     MXST      1.00       1.0
!
! Near-Forward Earthquakes Parameters
!
!1     LUCN       1.0       1.0
!1     LPSR       1.0       1.0
!1     NRNH       1.0       1.0
!1     NRSY       1.0       1.0
!1     KOBE       1.0       1.0
*STOP
```

```
! 12-Story  Moment Resistant Frame Sytem, Steel
! designed using Yield Point Spectra Methodology.
! for the 1985 E-W Michoacan at Secretary of Communication G.M.
! Original Design by Edgar F. Black
!
! Units: kN, meters, seconds.
!
!
*STARTXX
  MxcoDsgn         0 2 0 1             12   STORY FRAME Three Bay
! The frame has a rigid beam and flexible columns.
! Critical vertical load for frame is 200 (based on elastic sidesway buckling).
*NODECOORDS
! Left columns,  from bottom
C        1      0.00      0.00
C        2      8.00      0.00
C        3     16.00      0.00
C        4     24.00      0.00
C        5      0.00      5.00
C        6      8.00      5.00
C        7     16.00      5.00
C        8     24.00      5.00
C       49      0.00     49.00
C       50      8.00     49.00
C       51     16.00     49.00
C       52     24.00     49.00
L        5        49         4
L        6        50         4
L        7        51         4
L        8        52         4
*RESTRAINTS
! fixed supports at foundations
S 111         1         4         1
*SLAVING
!     master     slave    slave
S 100         5         6         8
S 100         9        10        12
S 100        13        14        16
S 100        17        18        20
S 100        21        22        24
S 100        25        26        28
S 100        29        30        32
S 100        33        34        36
S 100        37        38        40
S 100        41        42        44
S 100        45        46        48
S 100        49        50        52
!
!
*MASSES
S 100 137.75000       5        52                                  9.807.266848382
*ELEMENTGROUP
    2    1    1     2.731661-3          BEAM
    6    0    6
! beam   section
! W18X46
    1 199.96+06       .058.709660-32.963568-4   4.   4.   2.
! W21X57
    2 199.96+06       .051.077417-24.869908-4   4.   4.   2.
! W21X68
    3 199.96+06       .051.290320-26.160225-4   4.   4.   2.
! W24X68
    4 199.96+06       .051.296772-27.617035-4   4.   4.   2.
! W24X76
    5 199.96+06       .051.445158-28.740860-4   4.   4.   2.
! W24X76
    6 199.96+06       .051.445158-28.740860-4   4.   4.   2.
!! W27X94
!    6 199.96+06       .051.787093-21.361077-3   4.   4.   2.
!
!
! yield strength
    1    1  320.5268 320.5268
    2    1  451.5035 451.5035
    3    1  569.4639 569.4639
    4    1  626.4102 626.4102
    5    1  715.8974 715.8974
    6    1  715.8974 715.8974
!    6    1  988.4266 988.4266
! beams
! 1st Story Beams
    1         5         6         1    6         6    6
    2         6         7         1    6         6    6
    3         7         8         1    6         6    6
!  2nd Story Beams
    4         9        10         1    6         6    6
    5        10        11         1    6         6    6
    6        11        12         1    6         6    6
!  3rd Story Beams
    7        13        14         1    5         5    5
    8        14        15         1    5         5    5
    9        15        16         1    5         5    5
! 4th Story Beams
   10        17        18         1    5         5    5
   11        18        19         1    5         5    5
   12        19        20         1    5         5    5
! 5th Story Beams
   13        21        22         1    4         4    4
   14        22        23         1    4         4    4
   15        23        24         1    4         4    4
! 6th Story Beams
   16        25        26         1    4         4    4
   17        26        27         1    4         4    4
   18        27        28         1    4         4    4
! 7th Story Beams
   19        29        30         1    3         3    3
   20        30        31         1    3         3    3
   21        31        32         1    3         3    3
! 8th Story Beams
   22        33        34         1    3         3    3
   23        34        35         1    3         3    3
   24        35        36         1    3         3    3
! 9th Story Beams
   25        37        38         1    2         2    2
   26        38        39         1    2         2    2
   27        39        40         1    2         2    2
! 10th Story Beams
   28        41        42         1    2         2    2
   29        42        43         1    2         2    2
   30        43        44         1    2         2    2
! 11th Story Beams
   31        45        46         1    1         1    1
   32        46        47         1    1         1    1
   33        47        48         1    1         1    1
! 12thStory Beams
   34        49        50         1    1         1    1
   35        50        51         1    1         1    1
   36        51        52         1    1         1    1
!
*ELEMENTGROUP
    2    1    1     2.731661-3          COLUMNS
    6    0    6
```

```
! column section
! W14X68
    1 199.96+06       .051.290320-23.009353-4   4.   4.   2.
! W14X99
    2 199.96+06       .051.877416-24.620169-4   4.   4.   2.
! W14X120
    3 199.96+06       .052.277415-25.743994-4   4.   4.   2.
! W14X145
    4 199.96+06       .052.754833-27.117557-4   4.   4.   2.
! W14X159
    5 199.96+06       .053.012897-27.908397-4   4.   4.   2.
! W14X193
    6 199.96+06       .053.664509-29.989554-4   4.   4.   2.
! yield strength
    1    1 418.9627  418.9627
    2    1 638.6130  638.6130
    3    1 772.8438  772.8438
    4    1 943.6830  943.6830
    5    1 1033.170  1033.170
    6    1 1260.856  1260.856
! columns
! 1st Story Columns
    1         1         5         1    6         6    6
    2         2         6         1    6         6    6
    3         3         7         1    6         6    6
    4         4         8         1    6         6    6
! 2nd Story Columns
    5         5         9         1    6         6    6
    6         6        10         1    6         6    6
    7         7        11         1    6         6    6
    8         8        12         1    6         6    6
! 3rd Story Columns
    9         9        13         1    5         5    5
   10        10        14         1    5         5    5
   11        11        15         1    5         5    5
   12        12        16         1    5         5    5
! 4th Story Columns
   13        13        17         1    5         5    5
   14        14        18         1    5         5    5
   15        15        19         1    5         5    5
   16        16        20         1    5         5    5
! 5th Story Columns
   17        17        21         1    4         4    4
   18        18        22         1    4         4    4
   19        19        23         1    4         4    4
   20        20        24         1    4         4    4
! 6th Story Columns
   21        21        25         1    4         4    4
   22        22        26         1    4         4    4
   23        23        27         1    4         4    4
   24        24        28         1    4         4    4
! 7th Story Columns
   25        25        29         1    3         3    3
   26        26        30         1    3         3    3
   27        27        31         1    3         3    3
   28        28        32         1    3         3    3
! 8th Story Columns
   29        29        33         1    3         3    3
   30        30        34         1    3         3    3
   31        31        35         1    3         3    3
   32        32        36         1    3         3    3
! 9th Story Columns
   33        33        37         1    2         2    2
   34        34        38         1    2         2    2
   35        35        39         1    2         2    2
   36        36        40         1    2         2    2
! 10th Story Columns
   37        37        41         1    2         2    2
   38        38        42         1    2         2    2
   39        39        43         1    2         2    2
   40        40        44         1    2         2    2
! 11th Story Columns
   41        41        45         1    1         1    1
   42        42        46         1    1         1    1
   43        43        47         1    1         1    1
   44        44        48         1    1         1    1
! 12th Story Columns
   45        45        49         1    1         1    1
   46        46        50         1    1         1    1
   47        47        51         1    1         1    1
   48        48        52         1    1         1    1
*GENDISP
       5     1  0.20
       1     1 -0.20
*GENDISP
       9     1  0.25
       5     1 -0.25
*GENDISP
      13     1  0.25
       9     1 -0.25
*GENDISP
      17     1  0.25
      13     1 -0.25
*GENDISP
      21     1  0.25
      17     1 -0.25
*GENDISP
      25     1  0.25
      21     1 -0.25
*GENDISP
      29     1  0.25
      25     1 -0.25
*GENDISP
      33     1  0.25
      29     1 -0.25
*GENDISP
      37     1  0.25
      33     1 -0.25
*GENDISP
      41     1  0.25
      37     1 -0.25
*GENDISP
      45     1  0.25
      41     1 -0.25
*GENDISP
      49     1  0.25
      45     1 -0.25
*RESULTS
NSD    001        05        49        04
E      001    2    1   04
!GD     001
*ELEMLOAD
 WDLD
G   1    1
    1    0      1.0  0.0      140.928   187.904   0.0       140.928   -187.904
    1   36    1    1       1.0


!*NODALOAD
! WGTH                                  UNIT HORIZONTAL LOAD
!S       .0-70.056553        0.        05        52        1
!
```

```
*NODALOAD
 YPSD                                    UNIT HORIZONTAL LOAD
!YPS LOAD PATTERN for kobe design
S  322.302        0.        0.        49        52
S  135.278        0.        0.        45        48
S  123.253        0.        0.        41        44
S  111.228        0.        0.        37        40
S   99.204        0.        0.        33        36
S   87.179        0.        0.        29        32
S   75.154        0.        0.        25        28
S   63.130        0.        0.        21        24
S   51.105        0.        0.        17        20
S   39.080        0.        0.        13        16
S   27.056        0.        0.         9        12
S   15.031        0.        0.         5         8
!
*NODALOAD
 1MOD                                    UNIT HORIZONTAL LOAD
!FIRST MODE PUSH
S 1.000000        0.        0.        49        52
S .9546110        0.        0.        45        48
S .8867900        0.        0.        41        44
S .8120360        0.        0.        37        40
S .7253710        0.        0.        33        36
S .6356360        0.        0.        29        32
S .5408800        0.        0.        25        28
S .4492150        0.        0.        21        24
S .3556390        0.        0.        17        20
S .2640060        0.        0.        13        16
S .1704100        0.        0.         9        12
S .0828456        0.        0.         5         8
!
*NODALOAD
 2MOD                                    UNIT HORIZONTAL LOAD
!SECOND MODE PUSH
S 1.000000        0.        0.        49        52
S .7108690        0.        0.        45        48
S .3124310        0.        0.        41        44
S-.0489882        0.        0.        37        40
S-.3750510        0.        0.        33        36
S-.6057180        0.        0.        29        32
S-.7437130        0.        0.        25        28
S-.7780060        0.        0.        21        24
S-.7266610        0.        0.        17        20
S-.6034440        0.        0.        13        16
S-.4203220        0.        0.         9        12
S-.2136120        0.        0.         5         8
!*ACCNREC
!
! Short Earthquakes
!
! WNMW   wn87mwln.090 (2E10.3)           Whittier Narrow
! 2000    1    1    1          0.01
! BB92   bb92civc.360 (2E10.3)           Big Bear
! 6001    1    1    1          0.01
! SPGK   sp88guka.360 (2E10.3)           Spitak, Armenia
! 2000    1    1    1          0.01
! LPCO   lp89corr.090 (2E10.3)           Loma Prieta Corralitos
! 2000    1    1    1          0.01
! NRCN   nr94cent.360 (2E10.3)           Nortridge Century
! 3000    1    1    1          0.01
!
! Long  Earthquakes
!
! CHLL   ch85lleo.010 (2E10.3)           Chile Llolleo
!23277    1    1    1          0.01
! CHVP   ch85valp.070 (2E10.3)           Chile Valparaiso
!15874    1    1    1          0.01
! ELCN   iv40elcn.180 (2E10.3)           El centro Norte-Sur
! 2688    1    1    1          0.01
! LNJH   ln92josh.360 (2E10.3)           Landers Joshua Tree
! 4000    1    1    1          0.01
! MXST   mx85sct1.270 (2E10.3)           Mexico 85
! 9004    1    1    1          0.01
!
! Near-Forward Earthquakes
!
! LUCN   ln92lucn.250 (2E10.3)           Landers Lucerne
!12321    1    1    1          0.01
! LPSR   lp89sara.360 (2E10.3)           Loma Prieta, Saratoga
! 2001    1    1    1          0.01
! NRNH   nr94nwhl.360 (2E10.3)           El centro Norte-Sur
! 3000    1    1    1          0.01
! NRSY   nr94sylh.090 (2E10.3)           Northridge, Sylmar
! 3000    1    1    1          0.01
! KOBE   ko95ttri.360 (2E10.3)           Kobi Takatori
! 4096    1    1    1          0.01
!
*PARAMETERS
OS       0    0    1    0    0
!OS       0    0   -1    0    1
DC  1    0    0    0
DT 0.001  0.01      0.01
DA                        0.1                                  5
OD                                        1  0.0                        0
F     1.0      1.0
*MODE                                     Modal Analysis
!   12              2
   06              2
!*GRAV
!N     WGTH  4.0
!*GRAV
!E     WDLD 1.0
!*STAT                                    ADD HORIZONTAL LOAD IN 10 STEPS
!N     YPSD    1.0000
!D       49        01    1 0.0050   0.5
!
!N     1MOD    1.000
!D       49        01    1 0.0072   0.72
!N     2MOD    1.000
!D       49        01    1 0.0025   0.25
!
!*STAT                                    ADD HORIZONTAL LOAD IN 10 STEPS
!N     YPSD 0.025000
!N     1MOD 032.00000
!N     2MOD 150.00000
!L    0.100
!*ACCN
!80.00     90000    2
! Short Earthquakes Parameters
!1     WNMW       1.0       1.0
!1     BB92       1.0       1.0
!1     SPGK       1.0       1.0
!1     LPCO      1.00       1.0
!1     NRCN      1.00       1.0
!
! Long  Earthquakes Parameters
!
!1     CHLL      1.00       1.0
!1     CHVP      1.00       1.0
!1     ELCN      1.00       1.0
!1     LNJH      1.00       1.0
```

```
!1     MXST      1.00       1.0
!
! Near-Forward Earthquakes Parameters
!
!1     LUCN       1.0       1.0
!1     LPSR       1.0       1.0
!1     NRNH       1.0       1.0
!1     NRSY       1.0       1.0
!1     KOBE       1.0       1.0
*STOP
```

```
! 12-Story  Moment Resistant Frame Sytem, Steel
! designed using Yield Point Spectra Methodology.
! for the 1995 Hyogo-Ken Nambu at Takatory-kisu G.M.
! Original Design by Edgar F. Black
!
! Units: kN, meters, seconds.
!
!
*STARTXX
  KobeDsgn         0 2 0 1             12   STORY FRAME Three Bay
! The frame has a rigid beam and flexible columns.
! Critical vertical load for frame is 200 (based on elastic sidesway buckling).
*NODECOORDS
! Left columns,  from bottom
C        1      0.00      0.00
C        2      8.00      0.00
C        3     16.00      0.00
C        4     24.00      0.00
C        5      0.00      5.00
C        6      8.00      5.00
C        7     16.00      5.00
C        8     24.00      5.00
C       49      0.00     49.00
C       50      8.00     49.00
C       51     16.00     49.00
C       52     24.00     49.00
L        5        49         4
L        6        50         4
L        7        51         4
L        8        52         4
*RESTRAINTS
! fixed supports at foundations
S 111         1         4         1
*SLAVING
!     master     slave    slave
S 100         5         6         8
S 100         9        10        12
S 100        13        14        16
S 100        17        18        20
S 100        21        22        24
S 100        25        26        28
S 100        29        30        32
S 100        33        34        36
S 100        37        38        40
S 100        41        42        44
S 100        45        46        48
S 100        49        50        52
!
!
*MASSES
S 100 137.75000       5        52                                  9.807.459956173
*ELEMENTGROUP
    2    1    1     1.662157-3          BEAM
    6    0    6
! beam   section
! W24X68
    1 199.96+06       .051.296772-27.617035-4   4.   4.   2.
! W24X104
    2 199.96+06       .051.974190-21.290317-3   4.   4.   2.
! W27X129
    3 199.96+06       .052.438705-21.981262-3   4.   4.   2.
! W27X146
    4 199.96+06       .052.767736-22.343383-3   4.   4.   2.
! W27X161
    5 199.96+06       .053.058058-22.613933-3   4.   4.   2.
! W27X194
    6 199.96+06       .053.677412-23.254930-3   4.   4.   2.
!
!
! yield strength
    1    1  626.4102 626.4102
    2    1  1049.441 1049.441
    3    1  1403.322 1403.322
    4    1  1671.783 1671.783
    5    1  1850.758 1850.758
    6    1  2261.585 2261.585
! beams
! 1st Story Beams
    1         5         6         1    6         6    6
    2         6         7         1    6         6    6
    3         7         8         1    6         6    6
!  2nd Story Beams
    4         9        10         1    6         6    6
    5        10        11         1    6         6    6
    6        11        12         1    6         6    6
!  3rd Story Beams
    7        13        14         1    5         5    5
    8        14        15         1    5         5    5
    9        15        16         1    5         5    5
! 4th Story Beams
   10        17        18         1    5         5    5
   11        18        19         1    5         5    5
   12        19        20         1    5         5    5
! 5th Story Beams
   13        21        22         1    4         4    4
   14        22        23         1    4         4    4
   15        23        24         1    4         4    4
! 6th Story Beams
   16        25        26         1    4         4    4
   17        26        27         1    4         4    4
   18        27        28         1    4         4    4
! 7th Story Beams
   19        29        30         1    3         3    3
   20        30        31         1    3         3    3
   21        31        32         1    3         3    3
! 8th Story Beams
   22        33        34         1    3         3    3
   23        34        35         1    3         3    3
   24        35        36         1    3         3    3
! 9th Story Beams
   25        37        38         1    2         2    2
   26        38        39         1    2         2    2
   27        39        40         1    2         2    2
! 10th Story Beams
   28        41        42         1    2         2    2
   29        42        43         1    2         2    2
   30        43        44         1    2         2    2
! 11th Story Beams
   31        45        46         1    1         1    1
   32        46        47         1    1         1    1
   33        47        48         1    1         1    1
! 12thStory Beams
   34        49        50         1    1         1    1
   35        50        51         1    1         1    1
   36        51        52         1    1         1    1
!
*ELEMENTGROUP
    2    1    1     1.662157-3          COLUMNS
    6    0    6
! column section
! W14X132
    1 199.96+06       .052.503221-26.368341-4   4.   4.   2.
```

```
! W14X211
    2 199.96+06       .053.999992-21.107176-3   4.   4.   2.
! W14X283
    3 199.96+06       .055.374183-21.598329-3   4.   4.   2.
! W14X342
    4 199.96+06       .056.516116-22.039534-3   4.   4.   2.
! W14X370
    5 199.96+06       .057.032244-22.264299-3   4.   4.   2.
! W14X455
    6 199.96+06       .058.645144-22.992704-3   4.   4.   2.
! yield strength
    1    1 850.1282 850.1282
    2    1 1374.848 1374.848
    3    1 1867.028 1867.028
    4    1 2273.788 2273.788
    5    1 2469.033 2469.033
    6    1 3075.105 3075.105
! columns
! 1st Story Columns
    1         1         5         1    6         6    6
    2         2         6         1    6         6    6
    3         3         7         1    6         6    6
    4         4         8         1    6         6    6
! 2nd Story Columns
    5         5         9         1    6         6    6
    6         6        10         1    6         6    6
    7         7        11         1    6         6    6
    8         8        12         1    6         6    6
! 3rd Story Columns
    9         9        13         1    5         5    5
   10        10        14         1    5         5    5
   11        11        15         1    5         5    5
   12        12        16         1    5         5    5
! 4th Story Columns
   13        13        17         1    5         5    5
   14        14        18         1    5         5    5
   15        15        19         1    5         5    5
   16        16        20         1    5         5    5
! 5th Story Columns
   17        17        21         1    4         4    4
   18        18        22         1    4         4    4
   19        19        23         1    4         4    4
   20        20        24         1    4         4    4
! 6th Story Columns
   21        21        25         1    4         4    4
   22        22        26         1    4         4    4
   23        23        27         1    4         4    4
   24        24        28         1    4         4    4
! 7th Story Columns
   25        25        29         1    3         3    3
   26        26        30         1    3         3    3
   27        27        31         1    3         3    3
   28        28        32         1    3         3    3
! 8th Story Columns
   29        29        33         1    3         3    3
   30        30        34         1    3         3    3
   31        31        35         1    3         3    3
   32        32        36         1    3         3    3
! 9th Story Columns
   33        33        37         1    2         2    2
   34        34        38         1    2         2    2
   35        35        39         1    2         2    2
   36        36        40         1    2         2    2
! 10th Story Columns
   37        37        41         1    2         2    2
   38        38        42         1    2         2    2
   39        39        43         1    2         2    2
   40        40        44         1    2         2    2
! 11th Story Columns
   41        41        45         1    1         1    1
   42        42        46         1    1         1    1
   43        43        47         1    1         1    1
   44        44        48         1    1         1    1
! 12th Story Columns
   45        45        49         1    1         1    1
   46        46        50         1    1         1    1
   47        47        51         1    1         1    1
   48        48        52         1    1         1    1
*GENDISP
       5     1  0.20
       1     1 -0.20
*GENDISP
       9     1  0.25
       5     1 -0.25
*GENDISP
      13     1  0.25
       9     1 -0.25
*GENDISP
      17     1  0.25
      13     1 -0.25
*GENDISP
      21     1  0.25
      17     1 -0.25
*GENDISP
      25     1  0.25
      21     1 -0.25
*GENDISP
      29     1  0.25
      25     1 -0.25
*GENDISP
      33     1  0.25
      29     1 -0.25
*GENDISP
      37     1  0.25
      33     1 -0.25
*GENDISP
      41     1  0.25
      37     1 -0.25
*GENDISP
      45     1  0.25
      41     1 -0.25
*GENDISP
      49     1  0.25
      45     1 -0.25
*RESULTS
NSD    001        05        49        04
E      001    2    1   04
!GD     001
*ELEMLOAD
 WDLD
G   1    1
    1    0      1.0  0.0      140.928   187.904   0.0       140.928   -187.904
    1   36    1    1       1.0


!*NODALOAD
! WGTH                                  UNIT HORIZONTAL LOAD
!S       .0-70.056553        0.        05        52        1
!
*NODALOAD
 YPSD                                   UNIT HORIZONTAL LOAD
!YPS LOAD PATTERN for kobe design
```

```
S   720.11        0.        0.        49        52
S   395.00        0.        0.        45        48
S   359.89        0.        0.        41        44
S   324.78        0.        0.        37        40
S   289.67        0.        0.        33        36
S   254.56        0.        0.        29        32
S   219.44        0.        0.        25        28
S   184.33        0.        0.        21        24
S   149.22        0.        0.        17        20
S   114.11        0.        0.        13        16
S    79.00        0.        0.         9        12
S    43.89        0.        0.         5         8
!
*NODALOAD
 1MOD                                UNIT HORIZONTAL LOAD
!FIRST MODE PUSH
S 1.00000         0.        0.        49        52
S .944162         0.        0.        45        48
S .860514         0.        0.        41        44
S .774660         0.        0.        37        40
S .680582         0.        0.        33        36
S .593192         0.        0.        29        32
S .500775         0.        0.        25        28
S .411749         0.        0.        21        24
S .320539         0.        0.        17        20
S .231726         0.        0.        13        16
S .146490         0.        0.         9        12
S .0728221        0.        0.         5         8
!
*NODALOAD
 2MOD                                UNIT HORIZONTAL LOAD
!SECOND MODE PUSH
S  1.00000        0.        0.        49        52
S  .670265        0.        0.        45        48
S  .221097        0.        0.        41        44
S -.144786        0.        0.        37        40
S -.445975        0.        0.        33        36
S -.621475        0.        0.        29        32
S -.711329        0.        0.        25        28
S -.712876        0.        0.        21        24
S -.641854        0.        0.        17        20
S -.513808        0.        0.        13        16
S -.348675        0.        0.         9        12
S -.180415        0.        0.         5         8
!*ACCNREC
!
! Short Earthquakes
!
! WNMW   wn87mwln.090 (2E10.3)           Whittier Narrow
! 2000    1    1    1          0.01
! BB92   bb92civc.360 (2E10.3)           Big Bear
! 6001    1    1    1          0.01
! SPGK   sp88guka.360 (2E10.3)           Spitak, Armenia
! 2000    1    1    1          0.01
! LPCO   lp89corr.090 (2E10.3)           Loma Prieta Corralitos
! 2000    1    1    1          0.01
! NRCN   nr94cent.360 (2E10.3)           Nortridge Century
! 3000    1    1    1          0.01
!
! Long  Earthquakes
!
! CHLL   ch85lleo.010 (2E10.3)           Chile Llolleo
!23277    1    1    1          0.01
! CHVP   ch85valp.070 (2E10.3)           Chile Valparaiso
!15874    1    1    1          0.01
! ELCN   iv40elcn.180 (2E10.3)           El centro Norte-Sur
! 2688    1    1    1          0.01
! LNJH   ln92josh.360 (2E10.3)           Landers Joshua Tree
! 4000    1    1    1          0.01
! MXST   mx85sct1.270 (2E10.3)           Mexico 85
! 9004    1    1    1          0.01
!
! Near-Forward Earthquakes
!
! LUCN   ln92lucn.250 (2E10.3)           Landers Lucerne
!12321    1    1    1          0.01
! LPSR   lp89sara.360 (2E10.3)           Loma Prieta, Saratoga
! 2001    1    1    1          0.01
! NRNH   nr94nwhl.360 (2E10.3)           El centro Norte-Sur
! 3000    1    1    1          0.01
! NRSY   nr94sylh.090 (2E10.3)           Northridge, Sylmar
! 3000    1    1    1          0.01
! KOBE   ko95ttri.360 (2E10.3)           Kobi Takatori
! 4096    1    1    1          0.01
!
*PARAMETERS
OS       0    0    1    0    0
!OS       0    0   -1    0    1
DC  1    0    0    0
DT 0.001  0.01      0.01
DA                        0.1                                  5
OD                                          1  0.0                          0
F     1.0      1.0
*MODE                                    Modal Analysis
!   12              2
   06              2
!*GRAV
!N     WGTH  4.0
!*GRAV
!E     WDLD 1.0
!*STAT                                   ADD HORIZONTAL LOAD IN 10 STEPS
!N     YPSD    1.0000
!D       49        01    1 0.0050   0.5
!
!N     1MOD    1.000
!D       49        01    1 0.0080   0.80
!N     2MOD    1.000
!D       49        01    1 0.0035   0.35
!
!*STAT                                   ADD HORIZONTAL LOAD IN 10 STEPS
!N     YPSD 0.2850000
!N     1MOD 032.00000
!N     2MOD 150.00000
!L    0.010
!*ACCN
!50.00     90000    2
! Short Earthquakes Parameters
!1     WNMW       1.0       1.0
!1     BB92       1.0       1.0
!1     SPGK       1.0       1.0
!1     LPCO      1.00       1.0
!1     NRCN      1.00       1.0
!
! Long  Earthquakes Parameters
!
!1     CHLL      1.00       1.0
!1     CHVP      1.00       1.0
!1     ELCN      1.00       1.0
!1     LNJH      1.00       1.0
!1     MXST      1.00       1.0
!
! Near-Forward Earthquakes Parameters
```

```
!
!1      LUCN        1.0         1.0
!1      LPSR        1.0         1.0
!1      NRNH        1.0         1.0
!1      NRSY        1.0         1.0
!1      KOBE        1.0         1.0
*STOP
```

LIST OF REFERENCES

Abrams, D. P., 1985, ***Nonlinear Earthquake Analysis of Concrete Buildings Structures***, Final Report on a study to the American Society for Engineering Education.

Algan, B.B., 1982, , Ph.D. Dissertation Submitted to the Graduate College of the University of Illinois, Urbana, Illinois, March.

Applied Technology Council, 1978, ***Tentative Provisions for the Development od Seismic Regulations for Buildings.***, Prepared by Applied Technology Council, Report ATC 3-06,Redwood City, California, June.

Applied Technology Council, 1996, ***Seismic Evaluation and Retrofit of Concrete Buildings***, prepared for the California Seismic Safety Commission (Report SSC 96-01), Report ATC-40, Redwood City, California, November.

Aschheim, M., Maffei, J., and Black, E., 1998, ***Nonlinear Static Procedures and Earthquake Displacement Demands*****,** Proceedings of the Sixth U.S. National Conference on Earthquake Engineering, Earthquake Engineering Research Institute, 31 May - 4 June , Seattle, Washington.

Bertero, V. V., 2000, ***Performance-Based Seismic Engineering: Conventional Vs. Innovative Approaches***, Proceedings of the 12th World Conference on Earthquake Engineering, Auckland, New Zealand, 30 January- 4 February.

Boroschek, R.L. 1991, ***PCNSPEC MANUAL, A Modified Version of NONSPEC*** (Unpublished)**.**

Chopra, A., 1995, ***Dynamics of Structures***. Prentice Hall, Inc., Englewood Cliffs, New Jersey.

Clough, R.W. and Penzien, J., 1993, ***Dynamics of Structures***. Second Edition, McGraw Hill, Inc.

Collins, K.R., Wen, Y.K., and Foutch D.A., 1995, ***Investigation of Alternative Seismic Design Procedures for Standard Buildings.*** Civil Engineering Studies, Structural Research Series No. 600, University of Illinois, Urbana, Illinois, May.

Collins, K.R., 1995, ***A Reliability-based Dual Level Seismic Design Procedure for Building Structures,*** Earthquake Spectra, Earthquake Engineering Research Institute, Volume 11, No. 3, 417-429.

Fajfar, P., and Fischinger, M., 1988, ***N2 - A Method for Non-Linear Seismic Analysis of Regular Buildings***, Proceedings of the Ninth World Conference on Earthquake Engineering, Tokyo-Kyoto, Japan, Volume 5.

FEMA 222A, 1995, ***NEHRP Recommended Provisions for Seismic Regulations for New Buildings, Part 1 - Provisions***, Report No. FEMA-222A, Federal Emergency Management Agency, Washington, D.C., May.

FEMA 223A, 1995, ***NEHRP Recommended Provisions for Seismic Regulations for New Buildings, Part 2 - Commentary***, Report No. FEMA-223A, Federal Emergency Management Agency, Washington, D.C., May.

FEMA 273, 1997, ***NEHRP Guidelines for the Seismic Rehabilitation of Buildings***.,Report No. FEMA-273, Federal Emergency Management Agency, Washington, D.C., October.

FEMA 274, 1997, ***NEHRP Commentary on the Guidelines for the Seismic Rehabilitation of Buildings***, Report No. FEMA-274, Federal Emergency Management Agency, Washington, D.C., October.

FEMA 302, 1998, ***NEHRP Recommended Provisions for Seismic Regulations for New Buildings and Other Structures, Part 1 - Provisions***, Report No. FEMA-302, Federal Emergency Management Agency, Washington, D.C., February.

FEMA 303, 1998, ***NEHRP Recommended Provisions for Seismic Regulations for New Buildings and Other Structures, Part 2 - Commentary***, Report No. FEMA-303, Federal Emergency Management Agency, Washington, D.C., February.

Freeman, S.A., 1978, ***Prediction of Response of Concrete Buildings to Severe Earthquake Motion,*** Douglas McHenry International Symposium on Concrete and Concrete Structures, SP-55, American Concrete Institute, Detroit, Michigan, 589-605.

Hamburger, R., O., 1997, ***Defining Performance Objectives***, Seismic Design Methodologies for the Next Generation of Codes, Fajfar & Krawinkler eds., Balkema, Rotterdam.

Husid, R.,1969, ***The Effect of Gravity On The Collapse Of Yielding Structures with Earthquake Excitation***., Proceeding of the 4th World Conference Earthquake Engineering, Santiago, Chile, II, (A-4), 31-43.

International Conference of Building Officials, ***Uniform Building Code***, Whittier California, 1973,1979,1982,1988,1991,1994, 1997.

Jennings, P.C., and Husid, R., 1968, ***Collapse of Yielding Structures During Earthquakes***, *Journal of the Engineering Mechanics Division*, ASCE, Vol 94, No. EM5, Proc. paper 6154, 1045-1065.

Jirsa, J., O., 1997, ***Opportunities and Challenges - Development of Performance-Sensitive Engineering***, Seismic Design Methodologies for the Next Generation of Codes, Fajfar & Krawinkler eds., Balkema, Rotterdam.

Krawinkler, H. and Nassar, A. A., 1992, ***Seismic Design Based on Ductility and Cumulative Damage Demands and Capacities,*** *Nonlinear Seismic Analysis and Design of Reinforced Concrete Buildings*, P. Fajfar and H. Krawinkler, Eds., Elsevier Applied Science, New York.

Krawinkler, H., 1996, ***Pushover Analysis: Why, How, When, and When Not to Use it***. Proceeding of the 65th Annual Convention, Structural Engineering Association of California, Maui, Hawaii, 1-6 October.

Krawinkler, H., 1997, ***Seismic Design Based on Inelastic Behavior***, The EERC-CUREe Symposium in Honor of Vitelmo V. Bertero, Report UCB/EERC 97-05, Earthquake Engineering Research Center, University of California, Berkeley, CA.

Leelataviwat, S., Goel, S.C., Stojadinovic, B., 1999, ***Toward Performance-Based Seismic Design of Structures***, Earthquake Spectra, Earthquake Engineering Research Institute, Volume 15, No. 3, 435-461.

Lepage, A., 1997, ***A Method for Drift Control in Earthquake-Resistant Design of RC Building Structures***, Doctoral Thesis, Department of Civil Engineering, University of Illinois, Urbana, Illinois.

Mahin, S., and Boroschek, R. 1991, ***Influence of Geometric Nonlinearities on the Seismic Response and Design of Bridge Structures-Background Report***, California Department of Transportation, Division of Structures, October.

Mahin, S.A., and Lin, J. 1983, ***Construction of Inelastic Response Spectra for Single-Degree-of-Freedom Systems - Computer Program and Applications***, Earthquake Engineering Research Center, Report No. UCB/EERC-83/17, University of California, Berkeley, California, June.

Miranda E. 1991, ***Seismic Evaluation and Upgrading of Existing Buildings***, Ph.D. dissertation. Department of Civil Engineering, University of California, Berkeley.

Miranda, E. and Bertero V.V., 1994, ***Evaluation of Strength Reduction Factors for Earthquake-Resistant Design***, Earthquake Spectra, Earthquake Engineering Research Institute,Volume 10, No. 2, 357-379.

Moehle, J.P., 1992, ***Displacement-Based Design of RC Structures Subjected to Earthquakes***, Earthquake Spectra, Earthquake Engineering Research Institute, Vol. 8, No. 3, 403-428.

Nassar, A.A., and Krawinkler, H., 1991, ***Seismic Demands for SDOF and MDOF Systems***, Report No. 95, John A. Blume Earthquake Engineering Center, Stanford University.

Newmark, N.M., and Hall W.J., 1982, ***Earthquake Spectra and Design***, Monograph Series, Earthquake Engineering Research Institute, Berkeley, CA.

Prakash, V., Powell, G.H., and Campbell, S., 1993, ***DRAIN-2DX Base Program Description and User Guide. Version 1.10***, Report No. UCB/SEMM-93/17, Structural Engineering Mechanics and Materials, University of California, Berkeley, November.

Priestley, M., Kowalsky, M., Ranzo, G., and Benzoni, G., 1996, ***Preliminary Development of Direct Displacement-Based Design for Multi-Degree of Freedom Systems***, Structural Engineers Association of California, Proceedings of the 65th Annual Convention, Maui, Hawaii, October 1-6.

Priestley, M., 2000, ***Performance Based Seismic Design.*** Proceedings of the 12th World Conference on Earthquake Engineering, Auckland, New Zealand, 30 January- 4 February.

Powell, G.H., Prakash, V., and Campbell, S., 1993, ***DRAIN-2DX Base Program Description and User Guide - Element Description and User Guide for Elements TYPE01, TYPE02, TYPE04, TYPE06, TYPE09, TYPE15 - Version 1.10,*** Report No. UCB/SEMM-93/18, Structural Engineering Mechanics and Materials, University of California at Berkeley, December.

Qi, X. and Moehle, J.P., 1991, ***Displacement Design Approach for Reinforced Concrete Structures Subjected to Earthquakes***, Report No. UCB/EERC-91/02, Earthquake Engineering Research Center, University of California, Berkeley, January.

Sasaki, K., Freeman, S., and Paret, T., 1998, ***Multi-Mode Pushover Procedure (MMP)-A Method to Identify the Effects of Higher Modes in a Pushover Analysis,*** Proceedings of the Sixth U.S. National Conference on Earthquake Engineering, Earthquake Engineering Research Institute, Seattle, Washington, 31 May - 4 June.

Saiidi, M., and Sozen, M. A., 1981, ***Simple Nonlinear Seismic Analysis of R/C Structures***, American Society of Civil Engineers,Journal of the Structural Engineering Division, New York, New York, Volume 107, No. ST5, 937-951.

Somerville, P.G., Smith, N.F., Graves, R.W., and Abrahamson, N.A., 1997, ***Modification of Empirical Strong Ground Motion Attenuation Relations to Include the Amplitude and Duration Effects of Rupture Directivity***, Seismological Research Letters, Vol. 68, No. 1, January/February.

Shimazaki K., and Sozen, M.A., 1984, ***Seismic Drift of Reinforced Concrete Structures***, Research Reports, Hazama-Gumi Ltd. Tokyo (in Japanese) and draft research report (in English).

Sozen, M. A., and Lepage, A., 1996, ***Earthquake-Resistant Design in Regions of Moderate Seismicity***, Second International Symposium of Civil Engineering Systems, Hong Kong, China, December 9-12.

Vision 2000, 1995, ***Performance Based Seismic Engineering of Buildings***, California Office of Emergency Services, prepared by Vision 2000 Committee, Structural Engineers Association of California, Sacramento, California, April.